IMPERIAL COLLEGE OF SCIENCE TECHNOLOGY AND MEDICINE

University of London

ASPECTS OF THE MECHANICAL BEHAVIOUR OF HELICAL WIRE STRUCTURES

RELATING TO QUASI STATIC AND FATIGUE PROPERTIES

by

James John Evans

A thesis submitted to the University of London

for the degree of Doctor of Philosophy

Department of Mechanical Engineering

Imperial College of Science, Technology and Medicine

London SW7 2BX

May 1999

'That which does not kill us makes us stronger'

Pyramids Beverage Co.*
Egypt

***Also attributed to Friedrich Nietzsche, but in fact taken by him during a pleasure cruise on the Nile.**

i. Abstract

This work examines various aspects of the mechanical behaviour of two types of flexible structure : multiple layer thermoplastic wire reinforced hoses and six strand wire ropes. Whilst one structure is designed to transport highly pressurised fluids and the other to transmit large axial forces they have in common the helical wire structure giving rise to similar basic problems which impact on their fatigue performance.

It is well known that a broken wire in a rope will take up load again after a certain distance from a break, known as the effective length. Strain gauges have been used to measure the effective length and assess the effect of load cycling on it. It has been found that the effective length is influenced by both fatigue cycling and the level of load. The implications of this for rope integrity assessment are discussed. In particular the limitations of using static measurements, such as residual breaking load, to derive the effective length are emphasised.

A significant degree of variation in strain has been measured in the outer wires of the rope during tensile loading both on different wires at the same cross section and, to a lesser extent, along the length of a single wire. The effect of load cycling and overloading on this strain variation has been investigated. Overloading on a rope is seen to give a significant increase in fatigue life and this phenomenon has been correlated with a decrease in the level of wire stain distribution. It is suggested that this variation is an indication of the rope's quality and the normalised standard deviation of the strain distribution is proposed as a suitable parameter for quantifying this characteristic. A stochastic model to predict fatigue life based on wire strain distribution is implemented and used to give an indication of the limits of endurance for a range of assumed and measured strain distributions.

A structural model has been developed for the static pressure deformation response of thermoplastic wire hose. The model is derived from existing models for hose and accommodates the inclusion of a compressible core. It also takes account of the lateral compression of the wires in a layer caused by a shortening of the hose. Comparison of the

theoretical predictions with experimentally data acquired for hose axial strain and wire strain show an encouraging agreement. It is observed that the hose shows a significant level of hysteresis in the pressure / axial strain characteristic and it is suggested that this is likely to provide an indication of the level of inter-wire movement and may therefore be a good predictor of the level of fretting which would occur in extended use.

Finally the contact stresses between wires of different layers are calculated for three possible winding configurations. Based on these calculations a number of changes in the hose design are proposed with a view to improving its endurance characteristics.

ii. Acknowledgements

I am very grateful to my flatmate Dr. Paul Wilcox and my dad Prof. John Evans who have both contributed a considerable amount to the structure and content of this work and have also greatly improved the spelling and grammar within it.

I would also like to thank Prof. Richard Chaplin and Dr. Isobel Ridge of the Reading Rope Research group, for allowing me to use experimental work carried out at the University of Reading within this work and for providing guidance in many helpful discussions during and since my period at Reading.

Thanks to Dr. Rowland Travis for encouraging me to be organised and putting the time in to do some administrative work.

Liz Evans
Mark Evans, Jackie Evans and Clive Orrock have all read sections of this work and made useful comments on it. John Frew, Ian Martin, Chris Washington and Alan Priest all helped me in aspects of my experimental work at Reading. Alex Noorbai, Nick Taylor, Mark Evans and Shi Chi Hos all helped me with my experimental work at Imperial College.

Thanks to Polyflex for financial support towards the hose research and Amerada Hess Ltd, Bridon International Ltd, BP Exploration Operating Co. Ltd, Haggie Rand Ltd and Petrobras CENPES SEMEC for their financial support of the rope research.

Thanks to the members of IC^3 for not disturbing me while I wrote this work up.

Thanks to Dr. D.K. Longmore and Professor J.A.Witz for reading two very different versions of my thesis, making a number of very useful technical suggestions and generally doing more than is usually expected of examiners.

iii. Table of Contents

iv. Table of Figures

v. Table of Tables

1. Background

1.1 Introduction

This thesis is concerned with studying two helical wire structures, stranded wire rope and thermoplastic wire hose. The work has concentrated on analysis to understand the mechanical behaviour of these structures with a view to improving their integrity assessment in service and fatigue properties. The word strand used in this thesis refers to a tensile structure consisting of layers of helical wires around a central core. The word rope generally refers to a tensile structure consisting of a number of strands wound helically around a core unit. The word hose refers to a pressure bearing structure consisting primarily of an inner tube unit reinforced with layers of helical wires.

This chapter begins in Section 1.2 by reviewing a representative sample of the relevant applications of ropes and hoses. The common feature of the ropes and hoses used in these applications is the helical load bearing structure and Section 1.3 describes the reasons why this is the case. It also contains the fundamental mathematical equations which are necessary to define a helix and which will be required in the models which are developed in later chapters. Section 1.4 looks in more detail at the functional requirements which different applications place on ropes and how these requirements are realised in the various techniques of rope construction. Section 1.5 analyses hoses in the same manner. Section 1.6 looks at the process of manufacturing of ropes and hoses as this can have significant effects on the performance and in-service degradation of the final product. The in-service degradation of ropes is the subject of Section 1.7, which reviews and compares the extensive literature on this subject. The discussion in Section 1.7.3 draws together the main points in this chapter and Section 1.9 provides an overview of the remainder of this thesis.

1.2 Applications of ropes and hoses

1.2.1 Rope

Wire rope sees a vast range of applications. To conduct a comprehensive review of all the applications is beyond the scope of this present work and instead four applications have been chosen which are representative of the diversity of the functional requirements of wire ropes. The applications discussed are bridges, mooring, mining and cranes.

1.2.1.1 Bridges

A recent article by Ito [1] discussed the main design considerations relating to cable supported bridges. There are two types of cable supported bridge, the suspension bridge and the cable stayed bridge as shown in Figure 1.1 (a).

For spanning distances of one kilometre or more the suspension bridge is accepted as being the only suitable method and currently the longest suspension span is just under two kilometres. The cable profile is in the form of a catenary curve, usually with a sag:span ratio of between 1:8 and 1:12.

The cable stayed bridge consists of a number of straight guy cables which attached the bridge deck to the supporting towers. This gives a much stiffer structure than the suspension bridge. The use of this type of structure was initially inhibited because the level of indeterminacy made it difficult to calculate the strength and stiffness using theoretical techniques. However, it has seen rising popularity in the last thirty years with the advent of computational means for solving such problems numerically.

The span length of suspension bridges and cable stayed bridges has seen considerable increases in the last century (see Figure 1.1 (b)). The determining factors in developing longer bridge spans which are most related to the suspension ropes themselves are as follows:

- The use of higher grade steel wires in the ropes.

- The improvement in the rope structure and especially the development of parallel wire ropes in recent years.

- Improvements in modelling techniques for providing a better understanding of the mechanical and aerodynamic properties of the bridge structure.

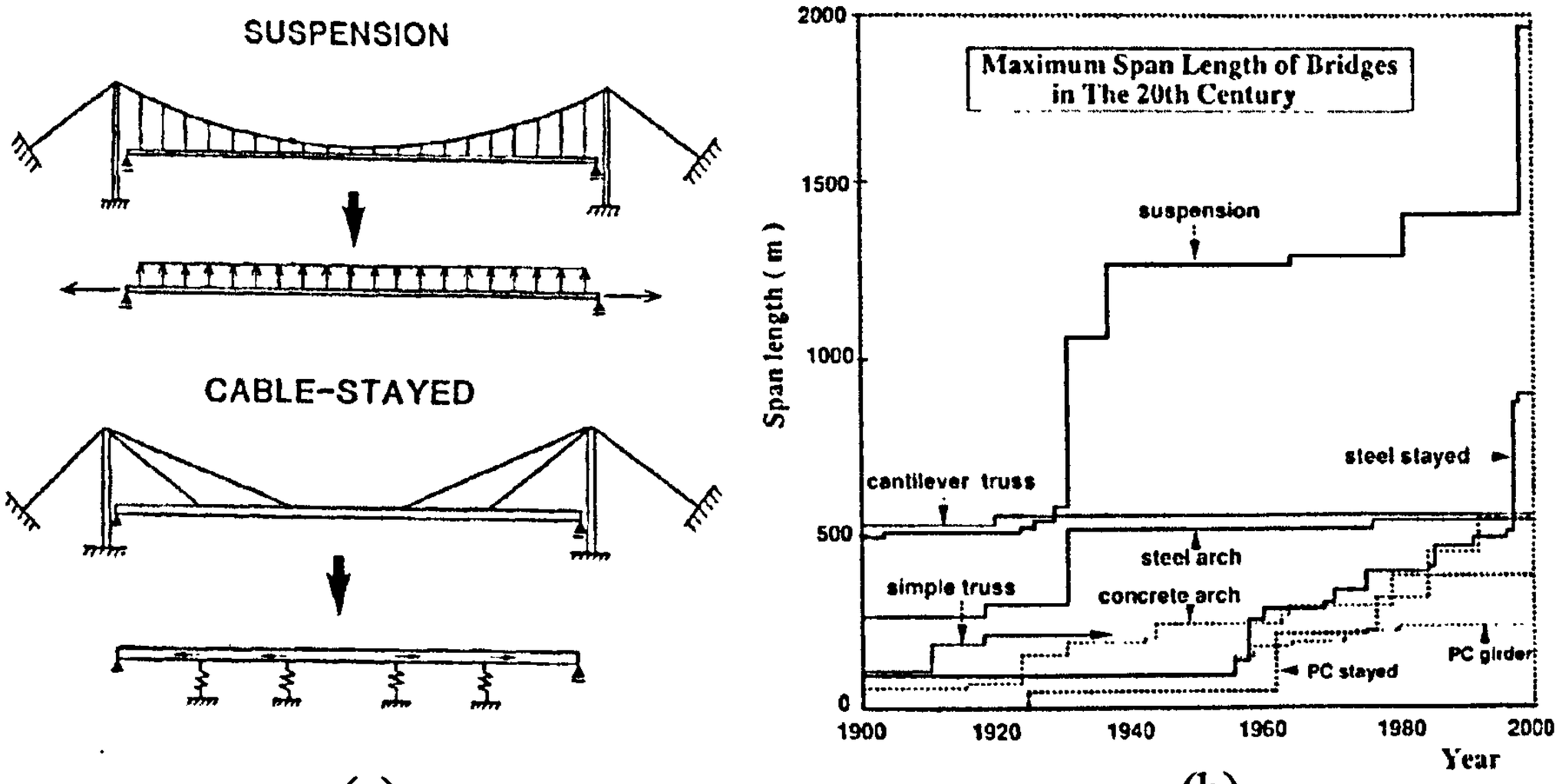

Figure 1.1. (a) The two types of cable bridges (cable stayed and suspension) and (b) the increase in span length over the last century for a number of different bridge constructions (from[1]).

The main requirement of bridge ropes is to maximise tensile strength. The level of fluctuating tensile load and the degree of bending in service will both be very low. The main requirement for flexibility is to enable the rope to be transported to the site. Some modern bridge building techniques involve constructing the ropes on site in order to minimise the flexibility requirements and maximise tensile strength.

1.2.1.2 Mooring

An extensive review of the use of wire ropes in offshore structures has been conducted by Ridge [2]. The first type of offshore platform was a permanent structure which sat on the

sea bed. The 'jack up' platform is the classic example of this (see Figure 1.2) and can generally be used in sea depths of up to around 50 m. As operating depths get greater, however, the 'jack up' structure becomes unsuitable in terms of its stability and a number of intermediate solutions have been designed which give solid structures which may operate in depths of up to around 300 m. The 'guyed tower' is one such solid structure, and comprises a tall and slender tower which relies on guy ropes for its lateral stability.

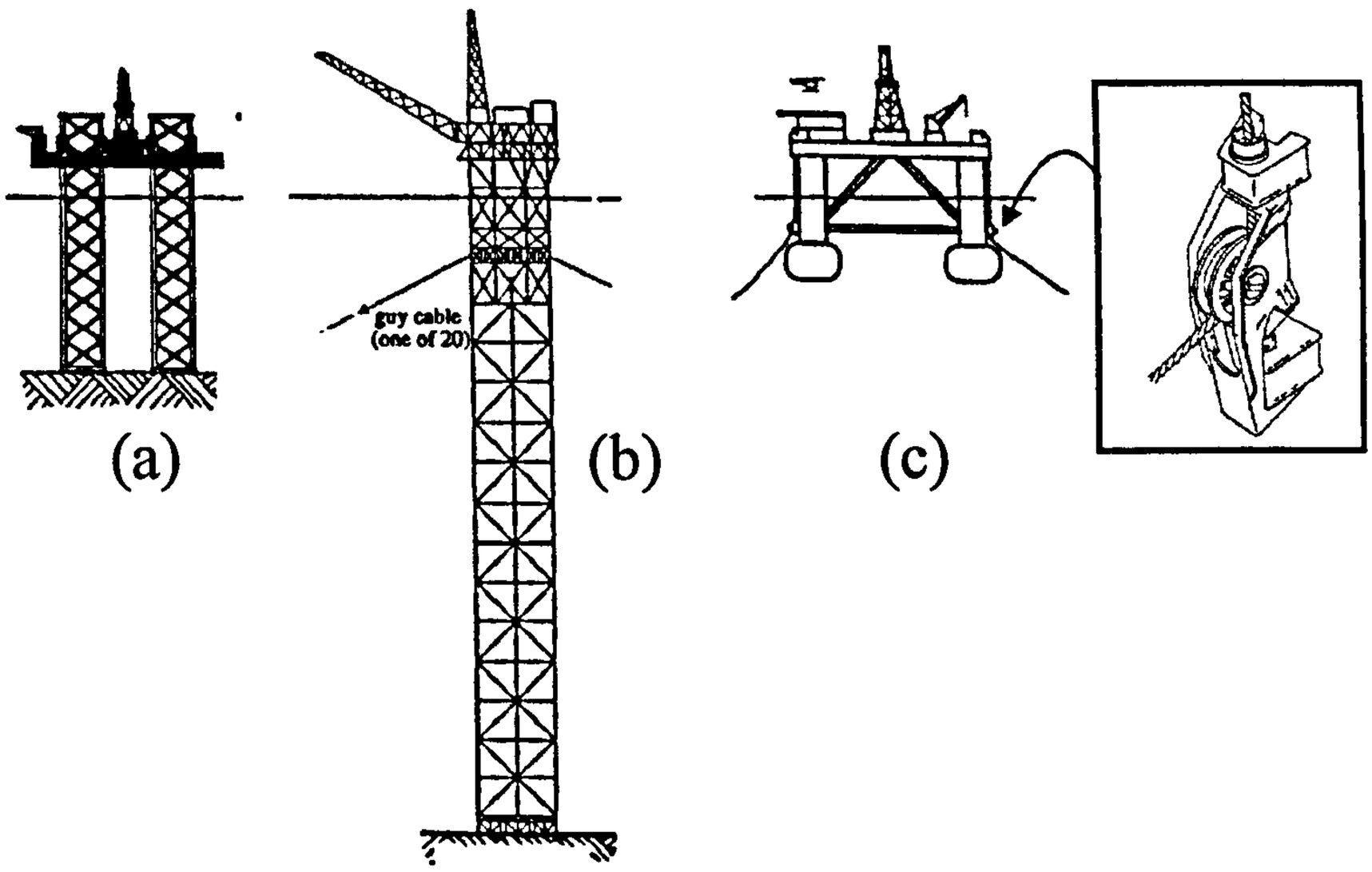

Figure 1.2. Three types of oil platform: (a) jack up platform, (b) guyed tower and (c) floating platform with the insert showing an example of one design of Fairlead pulley (from Ridge [2]).

Large oil reserves found in the North Sea at depths significantly greater than those which could be exploited using solid structures has led to the development of the floating platform with a spread mooring system. The basic structure of a spread mooring system is a number of ropes radiating out in different directions from the platform, with each rope being attached to the sea bed by means of a chain and an anchor. There are two types of floating platform, the mobile drilling unit and the floating production platform (FPP).

A mobile unit, which may be moved regularly, has different mooring requirements from an FPP which may remain in one location for the duration of its working life (up to twenty five years). In the case of the mooring ropes on a mobile unit, the most important factor is ease of installation and de-installation, whereas in the case of an FPP the most important factor is their overall life, as the need for replacement is highly undesirable.

1.2.1.3 Mining

There are two basic types of hoisting techniques used in mine shafts: drum hoists and friction hoists (also known as Koepe hoists) [3]. In the case of drum hoists, one end of the hoist rope is attached to the drum, while the other is attached to the cage or skip being hoisted. Two ropes are usually used, one being over wound on the drum whilst the other being under wound, thus enabling one conveyance to be lowered while the other is being raised. The general configuration of this type of system is to have a ground mounted drum leading up to a tower mounted sheave directly above the mine shaft. Drum winding is the favoured technique for very deep shafts where the drum will usually have multiple layers of rope coiled on it.

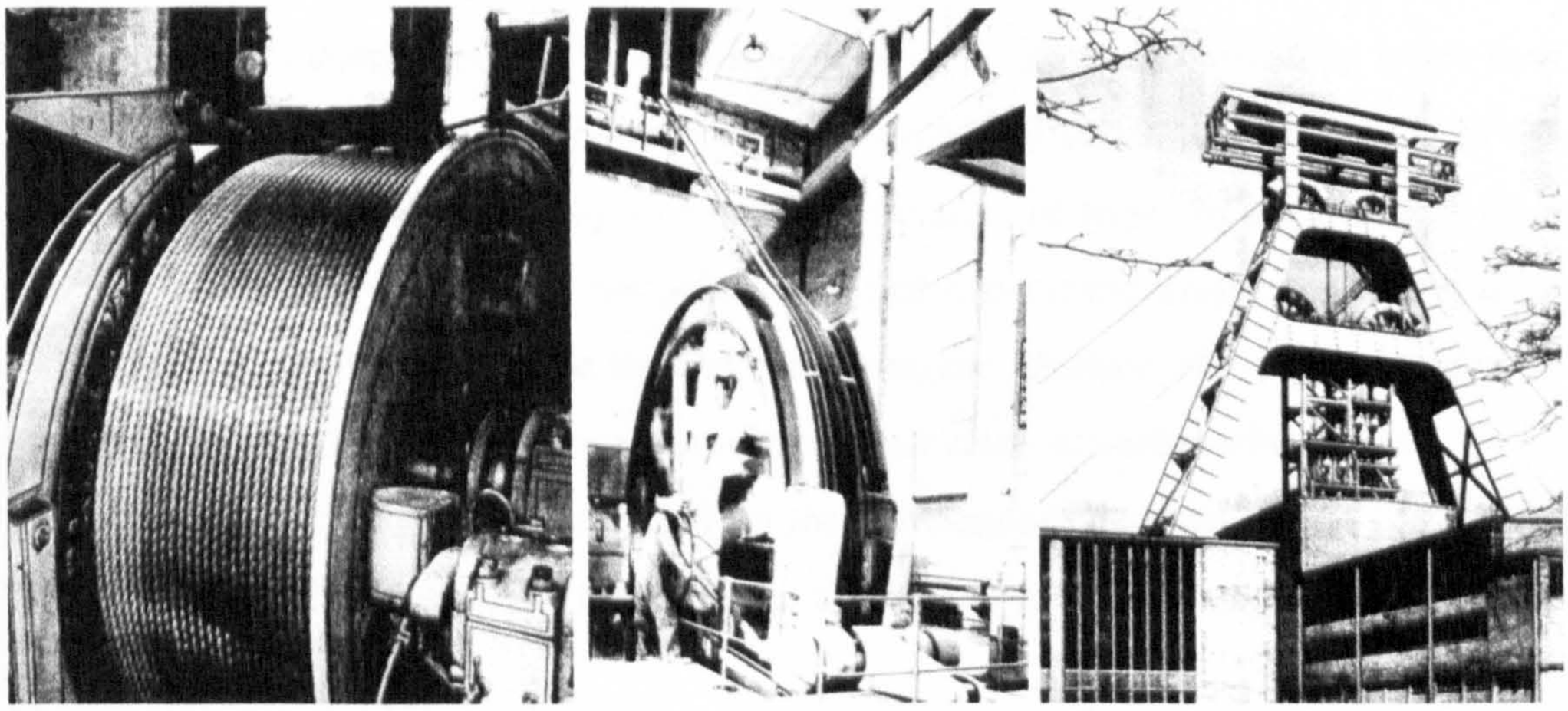

(a) (b) (c)

Figure 1.3. (a) an example of a drum winder(b) an example of a friction drive sheave (c) an example of a pitch head structure with pulleys (all from[3])

The alternative technique to drum winding is friction winding. Friction winding has a driving sheave which can be ground mounted with a towered pulley (like a drum winder) or may be mounted directly above the mine shaft. Each end of the rope is attached to a conveyance and the rope is driven by the friction sheave which is lined with a suitable material, such as plastic. Balance or 'tail' ropes are required to hang under the conveyances which should be of equal weight per unit length as the hoist ropes.

Bending stresses are kept low in hoisting applications. The ratio of the curvature diameter, D, to the rope diameter, d, which is known as the D/d ratio, is generally kept above 100.

Because drum diameters are large in comparison to the rope diameter the bending loads are not a major factor in this application. The main loading these ropes will experience is a fluctuating tension when off the drum and high transverse loads when on it.

1.2.1.4 Cranes

The two main classes of crane used in industrial applications are mobile cranes and tower cranes. Both mobile cranes and tower cranes are driven by drum winders and the ropes go through a number of pulleys during operation (see Figure 1.4). As it is not practical to have very large diameter pulleys in such situations, D/d ratios are commonly lower than 20:1. Because of this ropes must be carefully selected taking account of the amount of use and the number of pulleys in an applications. Predictions for rope life can be made from empirical equations [4]. Verret [5] has pointed out that some crane standards [6] have failed to recognise the importance of the level of use during the selection of ropes and pulleys in design, and this has led to a suppression of the tower crane manufacturing industry in the USA, since the recommended practice from the US standard leads to a rope life of only two weeks. Hence almost all the tower cranes used in the USA are imported from Europe or Japan.

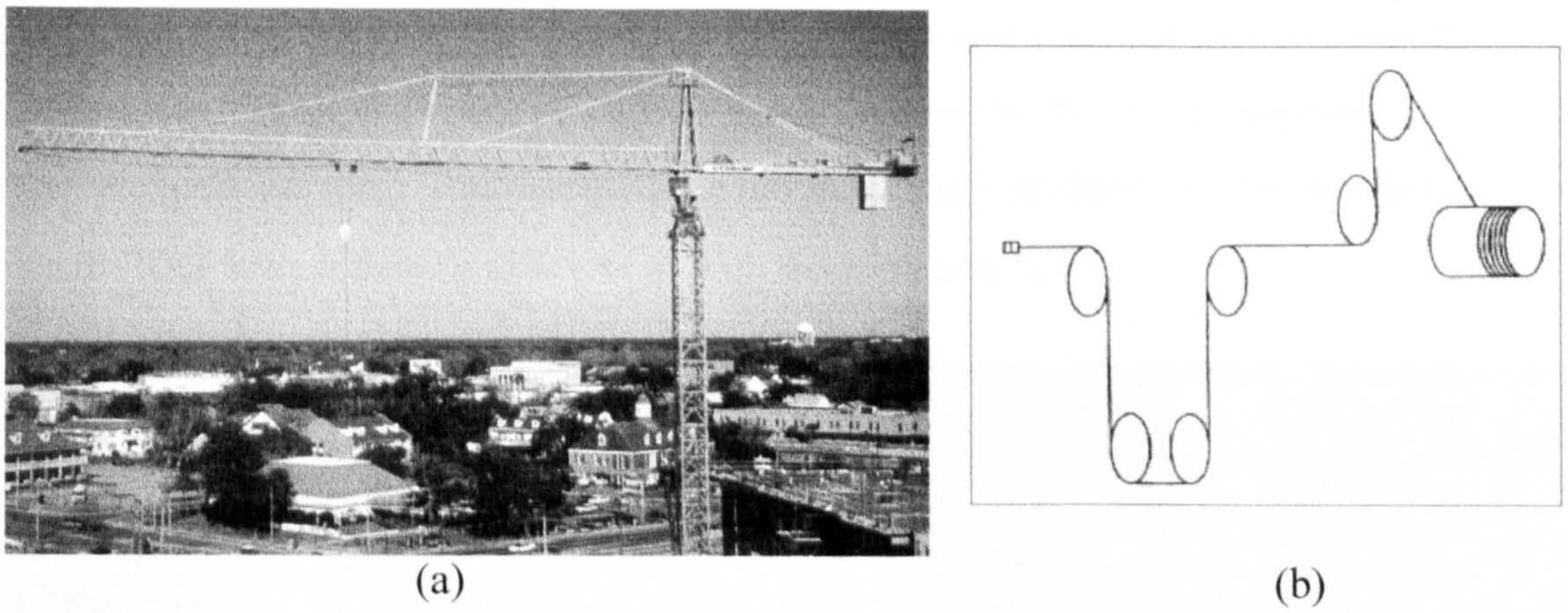

(a) (b)

Figure 1.4. (a) an example of a tower crane (b)simplified diagram (from [7]) of the rope and pulley configuration.

1.2.2 Hose

Hoses have widespread applications in many fields of industry, but broadly speaking they can be divided into two groups [8]: fluid conveyance and power transmission.

1.2.2.1 Fluid conveyance

Hoses are commonly employed in the transportation of a medium, for example water, oil or air and generally these hoses work at pressures below 10 bar. Common examples of fluid conveyance hoses are fire hoses and petrol hoses at petrol stations. A relatively recent development in this field is the large diameter flexible pipes such as those which are used for transportation of crude oil from well heads to floating oil platforms, and those which are used for transporting fluids from oil platforms to oil tankers using the single point mooring technique [9]. Often gaining a high flow rate will be an important factor for fluid conveyance applications and the main factors influencing this are the inner bore diameter and the surface roughness. Although generally fluid conveyance hoses work at low pressures, there are some exceptions to this and one which is at the other end of the pressure spectrum is the use of water as a tool. This is a relatively new and fast growing area, in which water at high pressure is used for cleaning, blasting or cutting as shown in Figure 1.5(a). In the case of cutting it is possible to have a very accurate cut without

raising the temperature of the material. However, progress in this field is limited by the maximum pressure which can be carried by the system. With the development of reliable high pressure pumping equipment the main remaining problem is the development of flexible hose with suitable endurance at high working pressures.

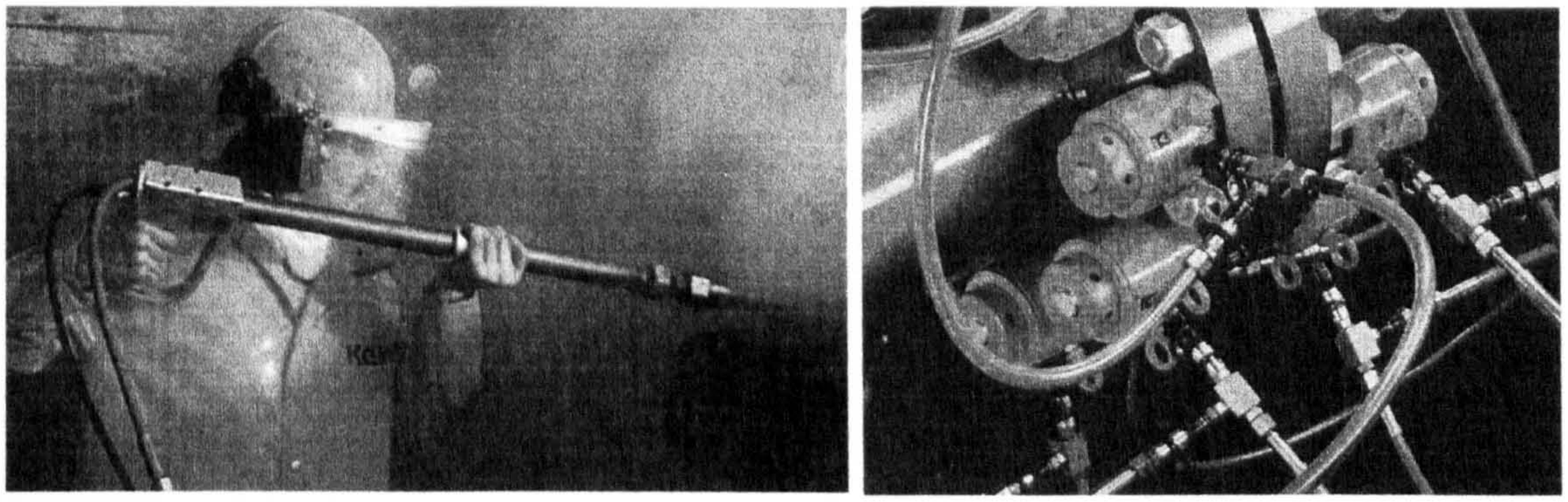

(a) (b)

Figure 1.5. Examples of high pressure hose application: (a) an operator carrying out water jet blasting and (b) a flange held where a specific tension is kept on the bolts by means of a bolt tensioning device (from Polyflex [10]).

1.2.2.2 Power transmission

Hoses are used to transmit power within a system and usually use an incompressible fluid to convey high power, although pneumatic lines are also common for lower power applications. Generally power transmission applications work at much higher pressures than fluid conveyance applications with pressures up to about 350 bar. In certain situations pressures up to 4000 bar can be used. A common use of power transmission hoses is for hydraulic controls and motors used in robots and earth moving machines. Two ultra-high pressure examples of power transmission hoses are the control of devices to prevent blow-out of a well head (called blow-out preventers) and devices which keep tension on flange bolts used for high pressure piping and pressure vessels (see Figure 1.5 (b)).In some situations hydraulic hoses are used to transfer power to hydraulic controls over relatively long distances. In these situations, it is important that the pressure signal is not dissipated and hence the volumetric expansion of the hose becomes an important factor.

1.2.3 General functional requirements of ropes and hoses

The functional requirements of rope and hose are broadly similar, they must perform a load bearing function while remaining flexible . In the case of rope the load bearing is tensile whereas in the case of hose it is pressure containment. When comparing the geometrical structure of rope and hose it is apparent that in both cases the load bearing element is based on a helical structure. Helical structures have a number of aspects which make them ideal flexible load bearing members. The next section will discuss helical structures in more detail.

1.3 Properties of helical structures

The nature of load which a structure must bear is a critical factor in its design. Structural design is an extensive topic and a number of books cover the subject in general (e.g. Gordon [11]). A brief summary will be given in this section as an introduction to helical fibre structures as they form the bases of all the ropes and hoses examined in this thesis.

1.3.1 Flexibility of helical structures

The key features of a helical structure are that it has a high axial strength and a low bending stiffness. An understanding of how this is achieved gives an insight into why ropes and hoses have the structures which they do.

The bending properties of a component are dependant on the distribution of cross sectional area resisting the bending. Bending results in the highest stresses furthest from the neutral plane of bending and resistance of an area, A, to bending is given by the familiar equation for second moment of area, I, [12]:

$$I = A\int_A y^2 dA \qquad \ldots(1.1)$$

where y is the distance from the bending axis. The second moment of area, I, of a solid circular cross section about a line through its centre is related to its radius, r, as follows:

$$I_c = \frac{\pi \cdot r^4}{4} \qquad \ldots(1.2)$$

If a solid circular fibre is subjected to bending about an axis which is offset from its own centre line by a distance d_i then its second moment of area, I_i, is:

$$I_i = I_c + Ad_i^2 \qquad \ldots(1.3)$$

Consider a bundle of fibres which is held together in such a way that the fibres cannot move relative to one another. The second moment of area of the bundle, I_B, will then be the sum of the individual second moments of areas of each of the fibres about the centreline of the bundle:

$$I_B = \sum_i I_c + Ad_i^2 \qquad \ldots(1.4)$$

If calculated in this manner, the second moment of area for a circular bundle of fibres, will be little different from that of a circular bar of the same overall radius.

On the other hand, if the fibres can slide freely past each other and they are wound in a helical fashion then the Ad_i^2 term in Equation 1.4 disappears, resulting in a massively reduced second moment of area. The reason for this is that the net change in length which a helical individual fibre experiences when the bundle is bent is zero, hence the only remaining contribution to the overall bending stiffness if the bending stiffness of the fibre about its own centre line, I_C.

The above theory assumed no friction between fibres within the helix. However, in practice there will be friction between wires, which makes the structure stiffer than the above theory suggests. The theoretical derivation of bending stiffness, including friction, is much more complex and poorly understood phenomenon, most theoretical derivations do the two boundaries to this case, i.e. full slip and no slip, rather than tackle the problem directly.

1.3.2 Helical fibre structures and crack propagation

In a fibre structure, the structure itself offers an extremely useful mechanism for preventing crack propagation, which was first quantified by Cook and Gordon [13] in relation to composite materials. The general mechanism of fatigue failure is that a crack grows slowly throughout the component until eventually the remaining cross sectional area of the component is insufficiently strong to support the applied load and it fails due to rapid crack propagation through the remainder of the material. For a fibre composite component to fail, a crack must move from within a fibre, across a substrate interface, through the substrate and then into the next fibre to propagate.

It can be shown that if the interface is sufficiently weak, the highly concentrated region of tensile stress which exists just ahead of the crack tip will cause a separation of the fibre interface and this separation will cause a blunting of the crack which is an effective crack stopping mechanism. It was calculated that the strength of the interface must be less than one fifth of the general strength of the material for this mechanism to work. In the case of helical wire structures such as rope and hose, there is no substrate and the mechanism of load transfer between neighbouring wires is purely through frictional forces caused by the contact load between them. This frictional adhesion is only effective in shear across the interface. Hence the tensile stress region ahead of an advancing crack will cause a separation of the wires and the crack will be arrested and will not continue into the neighbouring wire.

A closely related and very important attribute of a spiral structure is the existence of frictional forces between the fibres caused by the helix structure pulling itself together. If a fibre breaks within the structure then clearly at the actual location of the break it will be carrying none of the axial load on the structure. However, moving away from the break, the fibre gradually takes up the load until at some distance from the break it regains its full share again. The axial length over which this occurs is of great importance in the understanding of rope and hose behaviour and it is known as the effective length. This will be discussed in more detail in Chapter 2

1.3.3 Structural hierarchy of helical structures

Neglecting the offset term in the bending calculation (i.e. Ad_l^2 in Equation 1.4)a helical wire effectively assumes that there is no friction. Although it is not easy to calculate exactly what the effect of friction will be a rough qualitative analysis can be made as follows: if it is assumed that the friction between wires does not change depending on the layer within a spiral strand (in practice there will be some variation) then it is not difficult to see that as the winding radius of a particular helical layer increases so the length of the spiral of that wire increases. For the same level of friction per unit length there will therefore be a greater force resisting slipping the further out the layer is. Consequently the first layer in a spiral strand will be the closest to the full slip approximation and the assumption will get progressively worse until at some layer the wires will have so much frictional force restricting it that it will virtually behave like a solid tube. It would therefore be an advantage if a flexible structure were composed of spiral units with only a limited number of layers (ideally one layer). At the same time it is advantageous to make a structure out of many very thin elements. These two requirements seem to be mutually exclusive, but the solution is to build up units within units. Once a helical unit has one layer on it then instead of building it up with more layers to increase the diameter a number of these single layer units are wound together in the same structure as the original helix. Once this helix of helices has one layer then again to build up further it is used as a single element in a helical structure. The advantage is that flexibility is introduced at a number of levels and at no level are the helices built up to such a level which would greatly effect the flexibility because of the frictional effect.

1.3.4 Helical structures in ropes

The fundamental requirements of a rope are to carry tensile load while remaining flexible. These two requirements have conflicting demands on the rope structure since generally increasing flexibility will decrease the tensile strength. The optimum design for tensile strength is parallel wires and whereas flexibility requires helical wires. This leads to the

concept of tensile strength efficiency as a measure of the loss in strength due to the wires not being axially aligned The tensile strength efficiency of a rope, η, is defined as:

$$\eta = \frac{P_r}{P_p} \qquad \ldots(1.5)$$

where P_r is the tensile strength of the rope and P_p is the tensile strength of an equivalent bundle of straight, parallel wires.

The stress, σ_{wire}, in a wire in a stranded wire rope is given by [14]:

$$\sigma_{wire} = \frac{P_r}{A\cos\alpha_{rope}\cos\alpha_{strand}} \qquad \ldots(1.6)$$

Where P_r is the rope load, A is the cross sectional area of the wires in the rope and α_{rope} and α_{strand} are the rope and strand lay angles respectively. For the equivalent bundle of straight, parallel wires, the stress in a wire will be simple:

$$\sigma_{wire} = \frac{P_p}{A} \qquad \ldots(1.7)$$

Hence by setting the stress equal to the yield stress in equations 1.6 and 1.7, the following expression for strength efficiency can be deduced:

$$\eta = \cos\alpha_{rope}\cos\alpha_{strand} \qquad \ldots(1.8)$$

1.3.5 Helical structures in hoses

When considering a hose, the loads acting on the helical wire reinforcement are more complex than the simple axial case of ropes.

Consider a helical hose reinforcement wire wound at a lay angle, α, which is purely in tension. Then the axial and circumferential forces, F_a and F_c respectively must be related to the lay angle by the following relationship:

$$\tan\alpha = \frac{F_c}{F_a} \qquad \ldots(1.9)$$

where the axial force, F_a can be calculated from the pressure, P and the cross sectional area of the end of the hose as follows:

$$F_a = P\pi R^2 \qquad \ldots(1.10)$$

and the circumferential force F_c can be calculated [15] for a pitch, S:

$$F_c = PRS \qquad \ldots(1.11)$$

The pitch can be calculated from the reinforcement geometry in terms of the winding radius and lay angle:

$$S = \frac{2\pi R}{\tan\alpha} \qquad \ldots(1.12)$$

combining these equations and solving for the lay angle, α, gives the well known result for the 'neutral angle' as $\alpha = 54.736^o$. If wires are wound at this angle, then the wires will be completely in tension and a single layer design will be optimised. If a wire is wound at any other angle, then when the hose is pressurised it will tend to get either longer or shorter as the wires move towards the neutral angle.

1.3.6 Mathematical description of a helix

The mathematical description of a helix is fundamental to many complex theories for the mechanical behaviour of rope and hose and so a brief derivation of it is given in this section. A circular helix is a special instance of the family of spirals with a constant, but non-zero, curvature and torsion (note that this is torsion in the geometric rather than the engineering sense[16]) The helix is generally represented by the vector function, **h**, shown in Equation 1.13 as a function of the parameters ϕ, which represents the angle of rotation

about the central axis, and b, which represents the length moved along the central axis (as shown in Figure 1.6).

$$\mathbf{h} = \begin{bmatrix} R\cos\phi \\ R\sin\phi \\ b\phi \end{bmatrix} \qquad \ldots(1.13)$$

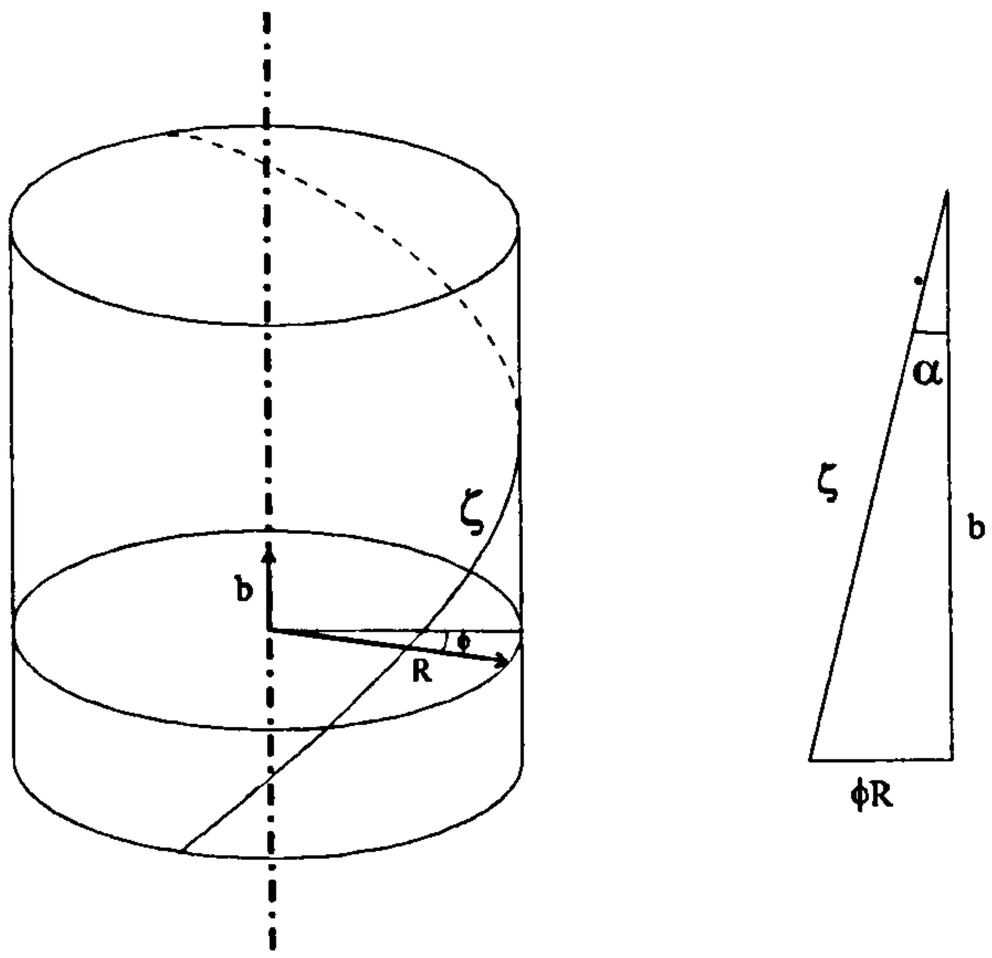

Figure 1.6. The geometry of a right hand helix (defined in the same way as a right hand screw thread).

A more useful form of **h** is in terms of the arc length, ζ:

$$\mathbf{h} = \begin{bmatrix} R\cos\phi \\ R\sin\phi \\ \zeta\cos\alpha \end{bmatrix} \text{ with } \phi = \frac{\zeta}{R}\sin\alpha \qquad \ldots(1.14)$$

The new variable, α, is (in hose and rope terminology) referred to as the lay angle and is the complimentary of the helix angle (β). Expressing **h** in this form enables the calculation of the radius of curvature and torsion to be performed using simple identities involving the principle unit normal vector, $\mathbf{n}(\zeta)$, the unit tangent vector, $\mathbf{T}(\zeta)$, and the unit binormal

vector, $\mathbf{B}(\zeta)$. These relationships are usually referred to as the Serret-Frenet equations [16].

The unit tangent vector can be calculated as the first derivative of $\mathbf{h}$ with respect to ζ to give:

$$\mathbf{T}(\zeta) = \frac{d\mathbf{h}}{d\zeta} = \frac{d\mathbf{h}}{d\phi}\frac{d\phi}{d\zeta} = \begin{bmatrix} -\sin\phi\sin\alpha \\ \cos\phi\sin\alpha \\ \cos\alpha \end{bmatrix} \qquad \ldots(1.15)$$

The curvature, $\kappa(\zeta)$, is then calculated as the modulus of the derivative of $\mathbf{T}(\zeta)$ with respect to ζ as follows:

$$\kappa(\zeta) = \left|\frac{d\mathbf{T}(\zeta)}{d\zeta}\right| = \sqrt{(\sin^2\phi + \cos^2\phi)\frac{\sin^4\alpha}{R^2}} \qquad \ldots(1.16)$$

This reduces to the expressions for the curvature, $\kappa(\zeta)$, and its reciprocal, the radius of curvature, $\rho(\zeta)$, as follows:

$$\kappa(\zeta) = \frac{\sin^2\alpha}{R},\ \rho(\zeta) = \frac{R}{\sin^2\alpha} \qquad \ldots(1.17)$$

The unit normal vector, $\mathbf{n}(\zeta)$, is calculated as:

$$\mathbf{n}(\zeta) = \frac{d^2\mathbf{h}/d\zeta^2}{\kappa(\zeta)} \qquad \ldots(1.18)$$

and the unit binormal vector is the cross product of the unit normal vector and the tangent vector:

$$\mathbf{B}(\zeta) = \mathbf{T}(\zeta)\mathrm{X}\,\mathbf{n}(\zeta) \qquad \ldots(1.19)$$

The torsion, $\tau(\zeta)$, is given by:

$$\tau = -\frac{d\mathbf{B}(\zeta)}{d\zeta}\mathbf{n}(\zeta) \qquad \ldots(1.20)$$

which following some algebraic manipulation reduces to the following expression:

$$\tau(\zeta) = \frac{\cos\alpha \sin\alpha}{R} \qquad \ldots(1.21)$$

Similar calculations can be performed for a left hand circular helix, the parametric equation for which is shown in Equation 1.22

$$\mathbf{h} = \begin{bmatrix} R\sin\phi \\ R\cos\phi \\ b\phi \end{bmatrix} \qquad \ldots(1.22)$$

The resulting curvature and torsion expressions are given then:

$$\kappa(\zeta) = \frac{\sin^2\alpha}{R} \text{ and } \tau(\zeta) = -\frac{\cos\alpha \sin\alpha}{R} \qquad \ldots(1.23)$$

It can be seen that the curvature is unchanged but the torsion is the negative of the right hand case.

These expressions for curvature and torsion are purely representations of the three dimensional curve and are not to be confused with their meaning in elasticity (they clearly have a geometric similarity). The change in these values during deformation can however be used as a technique for calculating fibre stresses within a structure and they are commonly utilised in the form shown in Equations 1.17 and 1.21. A comprehensive study has been carried out by Lee [17], in order to derive expressions for curvature and torsion of wire ropes in a range of configurations of bending and for single and double helix configurations with a view to improved stress analysis of these configurations.

1.4 Structure of ropes

This section gives an overview of the wide range of wire rope designs available. Initially Section 1.4.1 gives a classification of rope based on the level of twist imposed on the wires within it. Section 1.4.2 then discusses the various types of mechanical environment in which a rope might have to function and the design implications from this. Section 1.4.3 discusses the helical strand, which may be a structural unit in its own right, but also forms the basic unit of a stranded rope. Finally 1.4.4 discusses the defining characteristics of stranded rope constructions.

1.4.1 Classification of ropes

Wire ropes can be classified into four categories, according to the amount of twist imposed on the wires. These are:

1. **Parallel wire ropes -** manufactured with parallel wires.

2. **Spiral strands -** concentric layers of wires wound helically around a central wire.

3. **Stranded ropes -** a number of spiral strands wound helically around a core which may be either another strand, a smaller stranded rope or a cylinder of a solid material (for example a thermoplastic).

4. **Cable laid ropes -** a number of stranded ropes wound helically around a central stranded rope.

The classification can be divided into straight ropes (i.e. type 1) and twisted ropes (i.e. types 2, 3 and 4). Other classifications exist (e.g in the mining industry [3]) which are useful in practical situations, but these are governed more by application than structure and are therefore beyond the scope of this discussion.

Straight ropes are in many ways unrelated to all other wire rope constructions, mainly because they are purely tension members and flexibility is not an issue. They will not be considered further here.

The relationship between the three types of twisted ropes, (i.e. strands, stranded ropes and cable ropes) is evident in Figure 1.7. Each construction is the next level up in terms of a structural hierarchy, a spiral strand being the basic unit of a stranded rope, and a stranded rope being the basic unit of a cable laid rope.

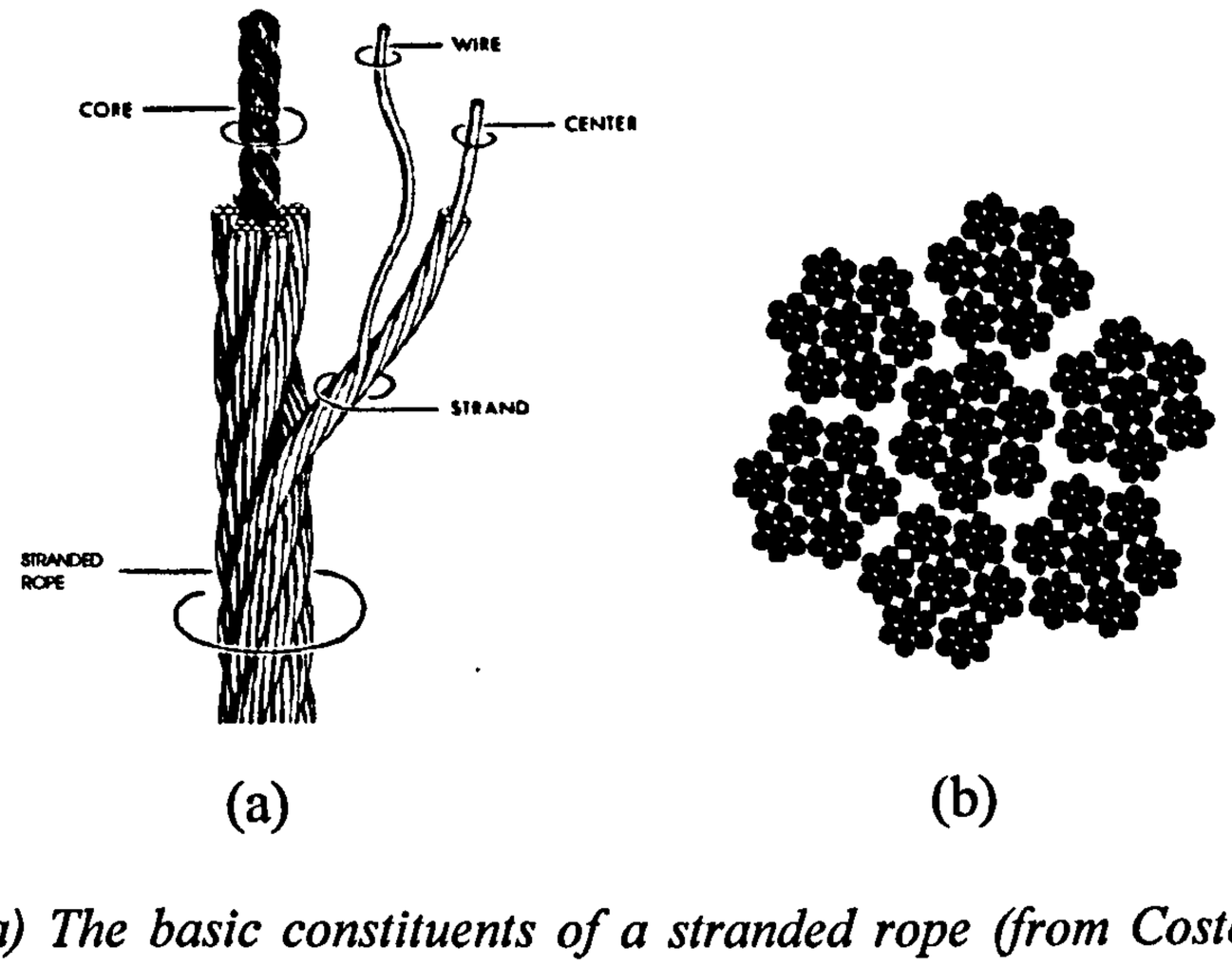

Figure 1.7. (a) The basic constituents of a stranded rope (from Costello [18]) (b) A cross section of a cable laid rope.

1.4.2 Functional requirements of rope

There are a number of factors which influence rope construction. Often improving the properties of a rope in one respect will worsen it in other respects. Hence rope design becomes a careful balancing act. The most important factors influencing design are summarised below:

- **Flexibility** - as has been mentioned above, the main factor influencing the flexibility of a helical structure such as wire rope is the amount of twist. The larger the diameter of a rope the more difficult it is to retain flexibility, and hence the use of hierarchical helical structures for large diameter ropes.

- **Contact forces** - if a rope is subjected to high lateral forces then it is important that the cross section, has a suitable resistance to deformation. One of the most

important factors influencing a stranded ropes behaviour in this respect is the stiffness of the core. Different core designs are discussed later in this section.

- **Wear properties -** clearly the external profile of the rope will be the most important factor determining the resistance to wear of a particular construction of rope. The more circular the exterior of a rope is, the better its wear properties will be (because of the size of the contact area). The size of the wires in the outer layer and their configuration is also important.

- **Twist under tensile load -** some applications require that a rope will not twist when tensile load is applied and ropes which satisfy this requirement are termed 'torque balanced'.

- **Tensile strength per unit cross sectional area -** in some applications the ultimate tensile strength per unit area of the rope is most important. One way to achieve this is to reduce the twist, which of course decreases the flexibility of the rope. Alternatively, the packing density of wires can be increased by various means.

- **Fatigue properties -** fatigue of a rope is an extremely complex process and it is difficult to identify simple rope design rules for fatigue. For example increasing the number of wires within a particular cross sectional area (by reducing wire diameter) will have benefits to fatigue because of the greater number of wire to wire interfaces to resist to fatigue crack propagation. On the other hand a greater number of wires will mean more wire to wire contact points and hence a greater level of fretting fatigue within the rope. Also, the geometry and nature of wire crossing points strongly influences the fatigue life, hence certain rope constructions are more suited to ropes where a long fatigue life is required.

1.4.3 Structure of strands

The basic definition of a strand is one or more helical layers of wires wound around a central wire which is known as the king wire. The simplest of all strands is the seven wire

strand, with six wires wound around one (i.e. 6/1). On a particular layer of a strand the wire lay angle is defined as the angle it makes with the rope axis and the wire lay length (also called the pitch, *S*) is defined as the axial length in which a wire does one complete cycle of the helix. If the strand is to have more than one layer of wires then there are a number of options for the construction. Firstly as a layer can be wound either in a left hand or right hand helix, there is a choice of whether to have some degree of symmetry, by winding each layer in alternate directions or to have all layers in the strand wound in the same direction; these have been defined here as bi-directional lay and uni-directional lay and are discussed below. Additionally for the case of uni-directional lay there is the choice of whether the wire lay lengths is allowed to vary or kept the same between layers.

1.4.3.1 Bi-directional lay

The intuitively obvious way to construct a wire strand is to have each layer wound in opposite directions, giving the strand some degree of symmetry and therefore minimising the level of twist on tensioning. This type of construction however has the inherent disadvantage of stress concentrations caused by point contacts between wires in alternate lays. Additionally rotational movements at the point of contact between wires causes accelerated degradation as a result of fretting fatigue. Consequently bi-directional lay construction is never used in strands which are used within stranded ropes, where fatigue performance is of critical importance. Bi-directional lay is however used in large structural strands, where cyclic loading frequencies are low, fatigue is not a critical factor, and torque balanced strands are required. Often such constructions will have a change in direction every second layer (i.e. left hand, left hand, right hand, right hand, etc) to minimise the number of cross lay layer interfaces, while still achieving a reasonably torque balanced construction.

1.4.3.2 Uni-directional lay

The accepted wisdom for strands which make up stranded rope is to lay all layers in the same direction, either all left or all right. There are two groups of uni-directional strand construction, varying and equal lay length (i.e. cross and equal lay) as discussed below.

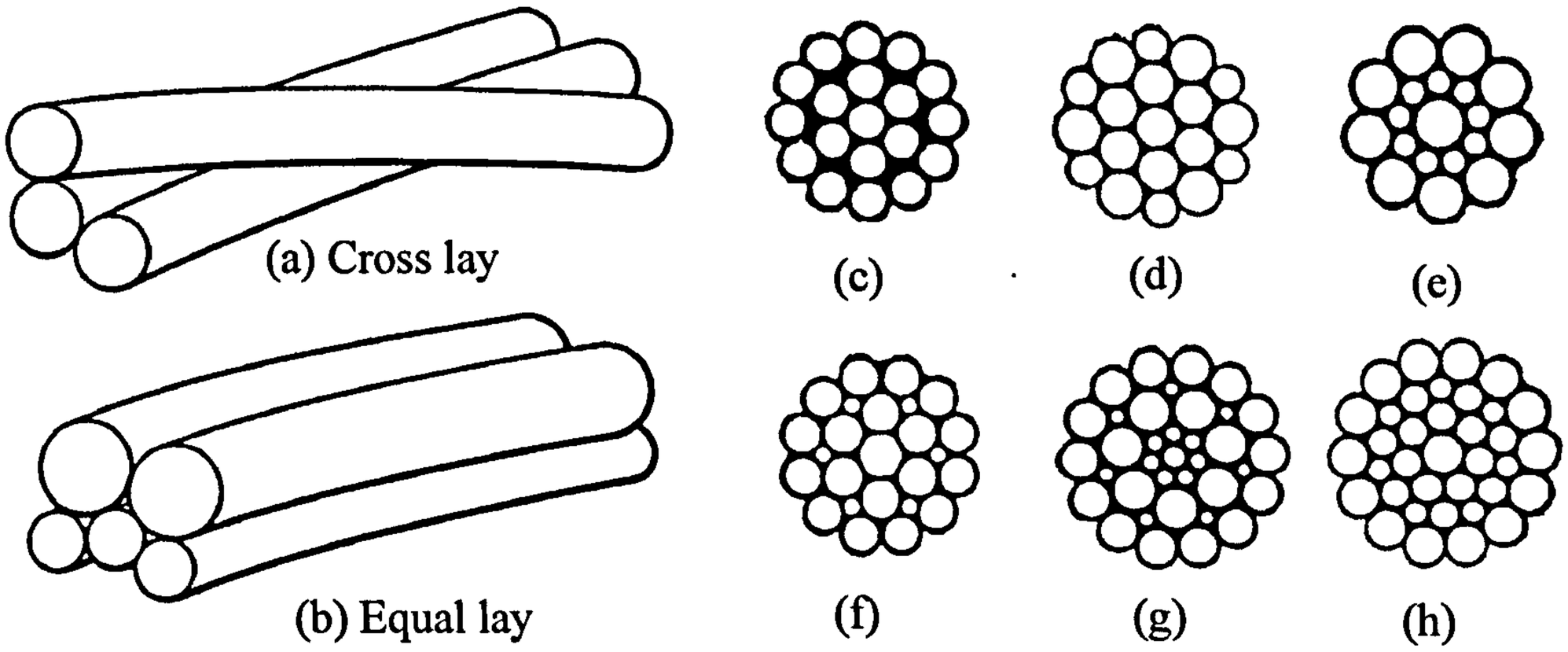

Figure 1.8. *(a) and (b) are basic types of contact between the wires in different layers in a strand as described in the next sections (from [3]). Also shown are a number of common strand constructions used in stranded rope applications (from Ridge [2]) as follows: (c) simple strand (12/6/1) cross lay. (d) Warrington (6+6/6/1) equal lay, (e) Seale (9/9/1) equal lay, (f) Filler wire (12/6+6F/1) Equal Lay (g) Filler-Seale (14/7+7F/7/1) Equal Lay and (h) Warrington Seale (14/7+7F/7/1) equal lay.*

If wires in concentric layers have the same winding angle, then they will share an equal part in bearing the axial load on the rope. This was the basis for the first strands used in stranded rope and the most common construction used is the 1/6/12 built up of equal diameter wires as shown in Figure 1.8 (c). Having the same winding angle in two concentric layers, however, will necessarily mean that the two layers have different lay lengths and this configuration is known as cross lay. The result of this is that the inter-layer contact will be the result of discrete cross wire contact points as shown in Figure 1.8 (a), as in the case of bi-directional layer but less frequently. Any advantages that a cross lay construction has from equal load sharing is outweighed by the stress concentration caused by the point contacts. Equal lay construction as described in the next section is preferred.

The equal lay length type of construction is now by far the most commonly used, and comes from the assumption that the most important factors in the strand construction is

the inter-layer contact and seating configuration between wires. If wires in concentric layers have equal lay length then the contact between the layers will be a single line contact along the length of the wire as shown in Figure 1.8 (b). If outer layer wires can be arranged to sit in the groove between two wires of the inner layer, the contact configuration will be even better. It turns out that the way to achieve this type of seating is by constructing strands with different wire diameters. Improving the seating between wires and having equal lay construction has the additional benefit of increasing the wire packing density. There are three common constructions of two layer equal lay strands: Seale, Warrington and Filler wire which are described briefly:

The Seale construction was patented in 1885 by Thomas Seale [19]. This construction consists of a number of large wires laid around an equal number of smaller wires, in such a way that each outer wire lies in the valley of the two underlying wires, as shown in Figure 1.8 (e). Consequently this construction has a very good packing density and, because of the large diameter of the outer wires, excellent wear properties. The larger outer wire diameters do, however, cause a reduction in rope flexibility. This is considered the best equal lay construction, where flexibility is not a major issue [3]. The Filler wire construction was patented in 1894 by W. B. Brown [20]. This construction consists of an even number of wires laid around an inner layer of half that number, and each valley is filled with a small wire (see Figure 1.8 (f)). The number of valleys is thus doubled and each outer wire beds in the valley formed by one main wire and one of the filler wires. This construction is more flexible than the Seale construction, but has not such a good packing density [3]. The Warrington construction was patented by R. Dixon in 1888 [20]. This construction has an outer layer of wires with twice as many as the inner layer, but the outer layer of wires consists of alternate wires of two diameters (see Figure 1.8 (d)). Consequently the large diameter external wires sit in the valleys of the inner layer, and the smaller wires sit on the crowns of the inner layer wires. This construction has very good flexibility, but not a good wear resistance [2]. For equal lay strand construction of three layers generally some combination of Warrington, Seale or Filler wire is used, for example the Warrington-Seale and Filler-Seale as shown in Figure 1.8 (g) and (h).

1.4.3.3 Shaped wire constructions

Shaped wires may be used within a rope for a number of reasons. The most common reason for using shaped wires is to give the outside of a spiral strand a more circular cross section, and consequently better wear properties (as the increased area reduces contact stresses). Two common examples of this are the half lock and full lock spiral strands as shown in Figure 1.9.

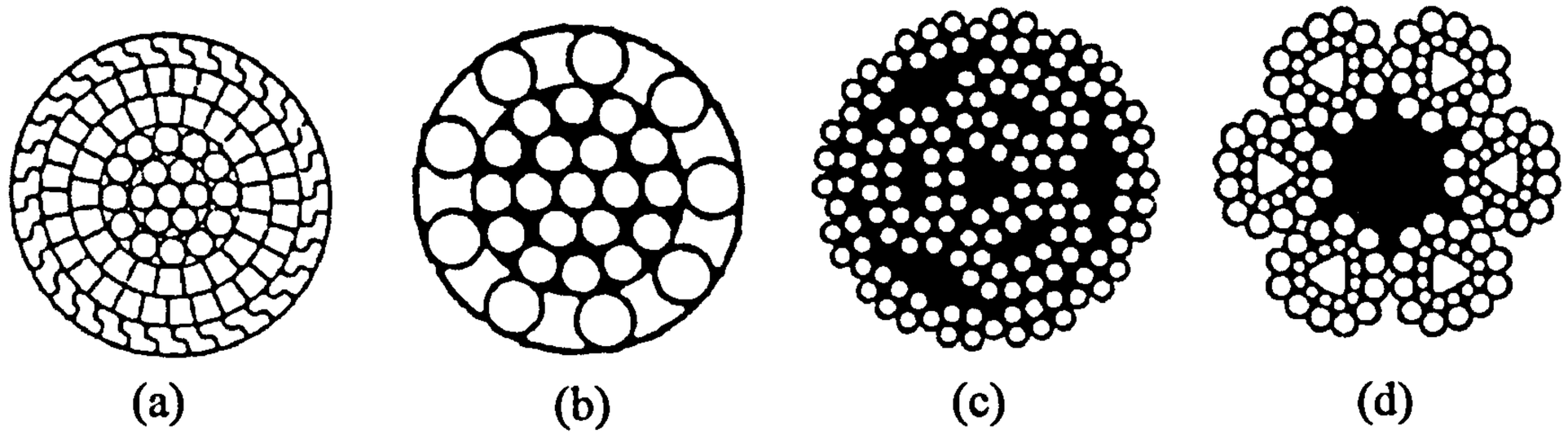

Figure 1.9. Four examples of constructions with shaped wires or strands (from Ridge[2]): (a) full lock structural strand (32Z/28T/20T/12/6/1), (b) a half lock strand (9H/12/6/1), (c) Paragon multistrand (12x6/3x24) and (d) triangular six strand (6x25(12/12/V) +Fibre Core (FC).

Better rope performance can also be obtained from stranded ropes with a more cylindrical cross section and this can be achieved by the use of triangular shaped centres to strands (see Figure 1.9 (d)). Triangular strands consist of a triangular shaped king wire which is then wound up in the usual way with standard circular wires. Generally triangular strands have a Seale construction.

1.4.4 Structure of stranded rope

A stranded wire rope consists of a number of individual strands wound around a central core. There are a number of cores and the relationship between the strand lay and wire lay within the strand have an important influence on the properties of the rope. Because of the wide diversity of applications and resulting conditions in which stranded wire ropes are used, there is a wide spread of rope constructions each with its specific advantages (and

disadvantages). This section concludes with a description of some of the more common constructions.

1.4.4.1 Types of cores

The main function of the core within a stranded rope is to provide support for the outer strands. The three types of core which are generally used in stranded rope are shown in Figure 1.10. The fibre core (FC) consists of a bundle of thermoplastic fibres although original designs based on this concept used hemp fibres. This construction has an excellent flexibility and also has the added advantage that the core can be charged with lubricant, which will subsequently be released slowly into the outer strands. The disadvantage with this type of core is that the construction may not be sufficiently rigid to prevent cross sectional distortions as a result of lateral loading. Where a more rigid cross section is required, the core is made from stranded wires. Two wire constructions of core are used. The simpler of the two wire cores is another strand similar to the outer strands and this construction is known logically as wire strand core (WSC). WSC construction gives an inherently stiff rope and is therefore used in applications which require such properties, for example a boom stay rope[2]. If more flexibility is required then the core can itself be constructed of a mini wire rope, thus giving another level of structural hierarchy. This core construction is known as independent wire rope core (IWRC). Of course, the question of core construction can be extended down to what is the core of the IWRC, which is invariably a mini strand. An IWRC core gives a rope good flexibility while providing a stiff seating for the outer strands against lateral forces. IWRC also gives a much better contact with the outer strands because of its more circular profile.

1.4.4.2 Types of strand lay

Strands can either be wound in a left hand or right hand helix within the rope and consequently stranded ropes are known as left hand or right hand respectively depending on this. There is nominally no difference between a left hand or right hand rope, except the direction of any residual twist effect during loading. Sometimes a left and right had rope are used together in parallel, to cancel out any twisting effects.

The relationship between the strand lay direction and the wire lay direction is critically important to the rope properties. There are two categories with most common construction being that of Ordinary Lay where the strands are laid in the opposite direction to the wires within the strand (see Figure 1.10 (d)). The other possible configuration is that wires are laid in the same direction as the strands and this construction is know as Lang's Lay, (see Figure 1.10), This construction was first patented by John Lang in 1879, although it was originally used by Albert[20]when he invented the wire rope .

Ordinary lay ropes have the advantage that they exhibit reduced twisting under load because of the opposite lay directions between wires and strands. Lang's lay rope on the other hand, will untwist indefinitely if the ends are allowed to rotate and consequently should only be used where the ends are prevented from rotating. The main advantage of Lang's lay rope is its increased resistance to wear caused by having a longer length of individual wire exposed at the crown. In fact there are many more subtle differences between the fatigue characteristics of Lang's and Ordinary Lay ropes and these are discussed in later chapters as well as being part of the overall investigation of this thesis.

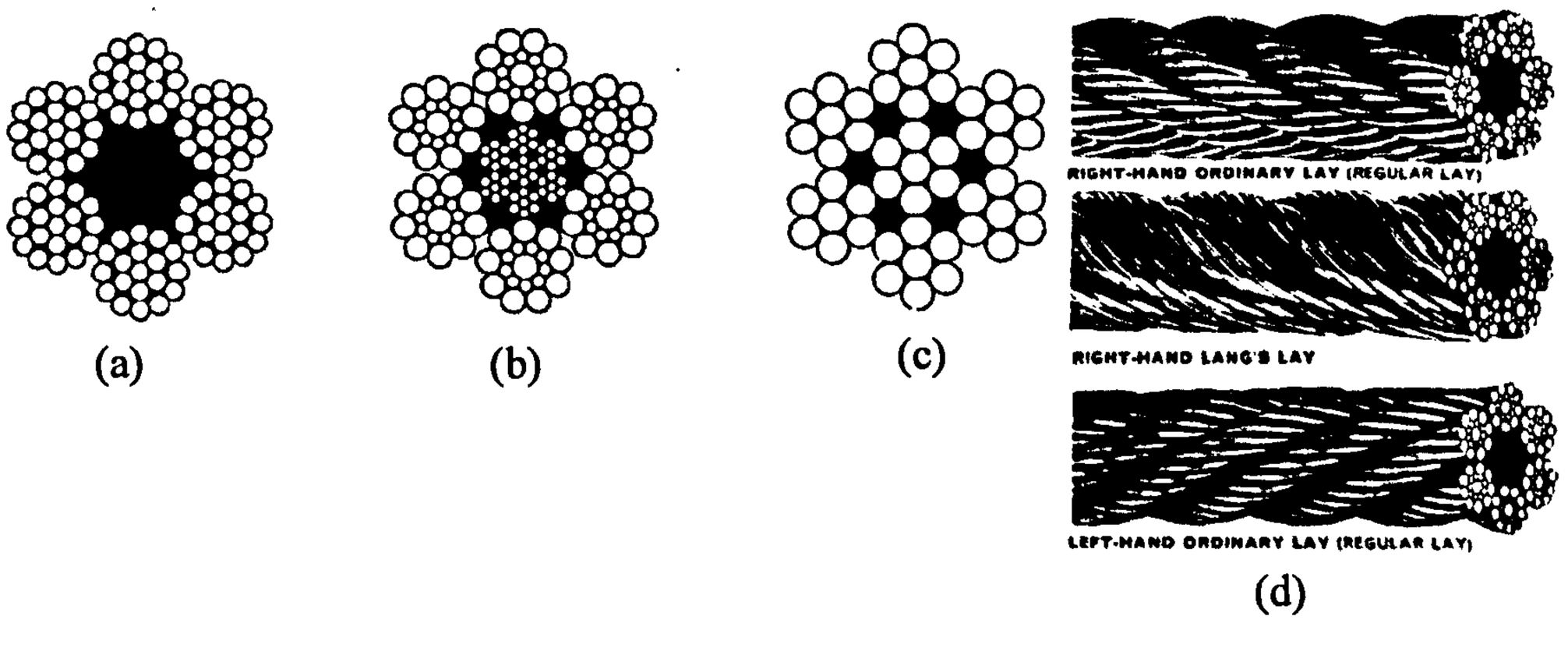

Figure 1.10. Three different kinds of cores used in stranded rope as follows: (a) Fibre Core (FC) so the rope is 6x(12/6/1) with FC (b) Independent Wire Rope Core (IWRC), the rope is 6x(9/9/1) Seale with IWRC (c) Strand Core (SC) the rope is 6x(6/1)SC. (d) shows three types of lay (from [3]) as follows

from top to bottom) right hand ordinary lay (RHOL), right hand Lang's lay (RHLL) and left hand ordinary lay (LHOL).

1.4.4.3 Common rope types

The basic and most common stranded ropes consist of a single layer of strands wound around a core and of these constructions the six strand rope is the most prolific, while eight stranded rope provides a more flexible alternative. There are numerous constructions of six and eight strand ropes resulting from different combinations of the variables previously discussed, i.e. strand construction, lay directions and types of core.

A more complex variation of the stranded rope consists of two or more layers of strands and is generally categorised as multi-strand ropes. The main advantage of multi-strand ropes is that almost perfect torque balance can be achieved by varying the lay directions of different layer of strands a rope. One distinct disadvantage of many of these types of ropes is the high contact stress between concentric wire layers and the resulting disproportionately high level of wire breaks occurring inside the rope.

1.5 Structure of hoses

This section discusses the structure of hose, initially the basic components are introduced: the inner core and outer cover, the reinforcement and the endfittings. Subsequently variations of these components are discussed. Finally the construction of flexible pipes and umbilicals, which share many common elements to hose, are discussed.

1.5.1 General terminology

Hose is a generic term for a family of flexible pipes which are reinforced by either wires or fibres. All hoses consist of a number of fundamental components as follows (see Figure 1.11 and [15]):

- The inner core which is a tube the main function of which is to contain the hydraulic or pneumatic medium. The inner core is made from either polymer or elastomer.

- Reinforcement which is one or more layers of helically wound wires or fibres.

- An outer cover which is concerned mainly with protecting the reinforcement from wear and corrosive attack. Like the inner core it is made from either polymer or elastomer.

- A hose must be capable of facilitating some form of attachment within its operating environment and this attachment is known as the end fitting.

These components will be considered in more detail in the following sections.

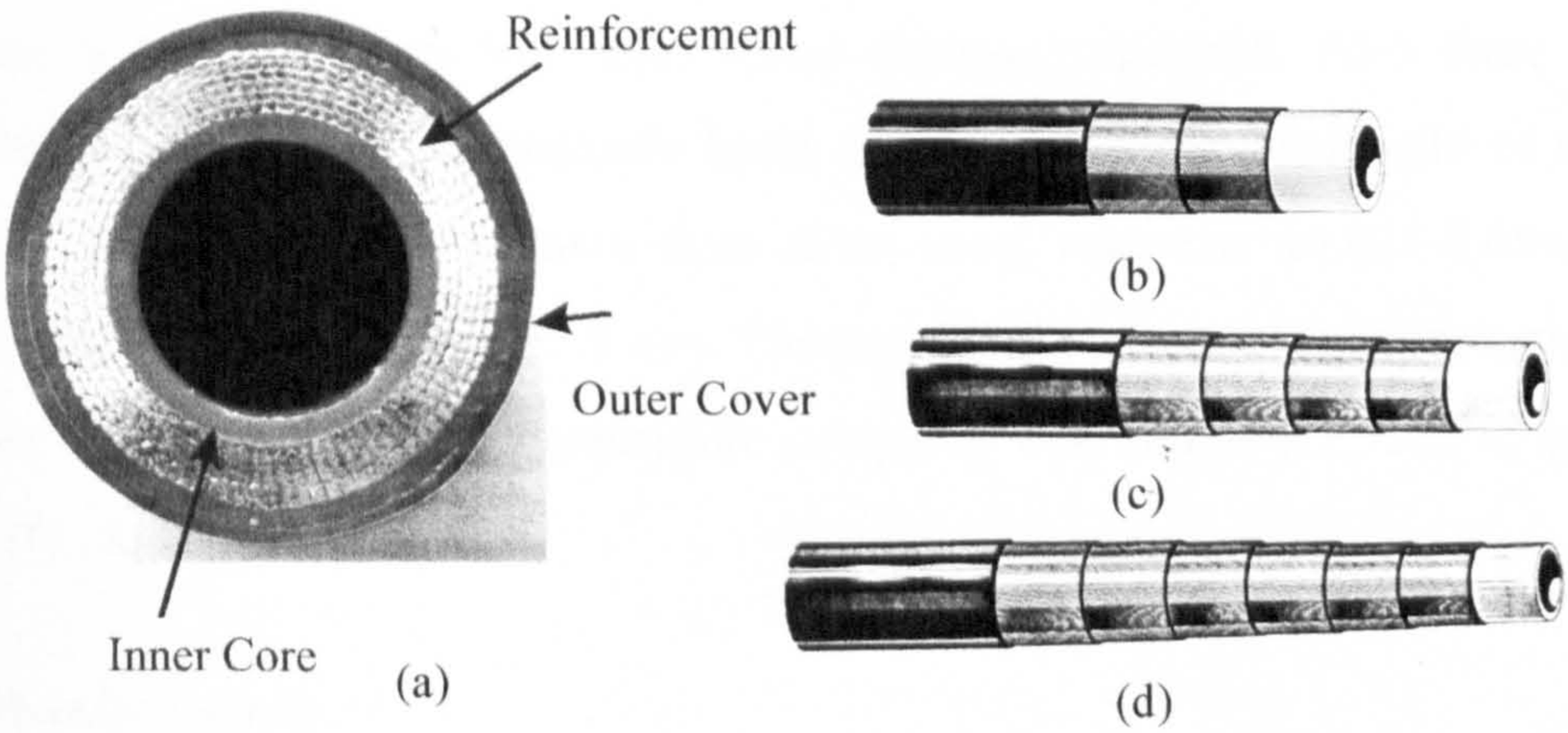

Figure 1.11. (a) Shows the cross section of a six layer Polyflex hose, indicating the basic components of the hose. (b) Shows two layer spiral hose, (c) four layer spiral hose, (d) six layer spiral hose, all figures from Polyflex [10].

1.5.2 The inner core and outer cover

Since the inner core and outer cover tend to have a similar construction they will be discussed together. The inner core prevents leakage of the fluid and it is loaded in almost hydrostatic conditions, since its outer diameter is constrained by the reinforcement layers.

The inner core can be made of elastomer (rubber like substances) or polymer (thermoplastic substances). The outer cover protects the reinforcement from damage, wear and corrosion. It contributes little to the strength or stiffness of the hose structure. Similar materials are used for the outer cover as are used for the inner core.

The traditional material used for the inner core and outer cover of hoses is rubber. A number of types of rubber can be used depending the hose requirements (e.g. chemical resistance). Some common types of rubber used are Latex, Butyl and Natural Rubber, Hypalon and Neoprene [15].

Since the early 1960's thermoplastic materials have been tried as an alternative to rubber. Some common thermoplastics which are used are Nylon, Polyester and PVC [21]. Thermoplastics have a number of distinct advantages over rubbers [22]. Thermoplastic hose is up to 50% lighter than an equivalent rubber hose, it has superior chemical resistance and it has up to 500 times better abrasion resistance. Also there are less processes to manufacture thermoplastic hoses and longer continuous lengths of hose can be made. Thermoplastic hose has a finer dimensional tolerance ±0.025-0.05 mm than rubber which is of the order of ±0.8 mm. The main disadvantage of thermoplastic hose is the lower maximum operating temperature compared with rubber (i.e. 120°C compared with 150°C for rubbers).

1.5.3 Reinforcement

This is the load bearing component and consists of layers of fibres or wires wound around the inner core. The reinforcement can be either braided or spiral wound. Braiding involves inter-knitting both left and right hand helical fibres on the same layer (see Figure 1.12 (b)) and consequently a single layer will not twist on pressurisation. Spiral winding involves the wires or fibres on a single layer being wound in the same direction. Layers are wound in pairs, one pair left hand and then the next right hand in order to achieve some level of torsional stability. A number of companies manufacture spiral hose with up to eight layers of reinforcement, for example Polyflex GmbH [10] and Flow Inc. [23]. There seems to be

no general consensus as to the best configuration of wire diameter and often new designs are not released into the public literature. Polyflex tends to use increasingly small diameter wires for the further out layers (based qualitatively on the Lamé stress distribution for a thick walled cyclinder [24]). Flow Inc. have experimented with hose with a range of winding angles, varying from the innermost layer wound at 39° to the outermost (eighth) layer wound at 83.5° and they claim to have achieved a burst pressure of 7000 Bar with this construction. Although there are standard hose designs for low pressure hoses (e.g [25]) multiple layer high pressure hose configurations tend to be specific to a particular company and detailed configurations for the hoses analysed in this thesis are given in the Appendix.

1.5.4 End fittings

For high pressure hoses the end fitting consists of three parts. These are the nipple or insert, the ferule or sleeve and the swivel nut as shown in Figure 1.12(a). The nipple fits into the hose, the ferule fits over the outside of the hose and both are squeezed together in a crimping process to form a tight seal and mechanical interlock with the hose. The ferule and nipple interlock by means of a shoulder on the nipple. The sealed connection between the hose and the system is made by the end of the nipple which is in the form of a cone (for high pressure ratings). This interlocks with an adjacent cone in the system to produce a line seal: this type of fitting is known as autoclave, after the company which first marketed it. The connection is then held together with the swivel nut.

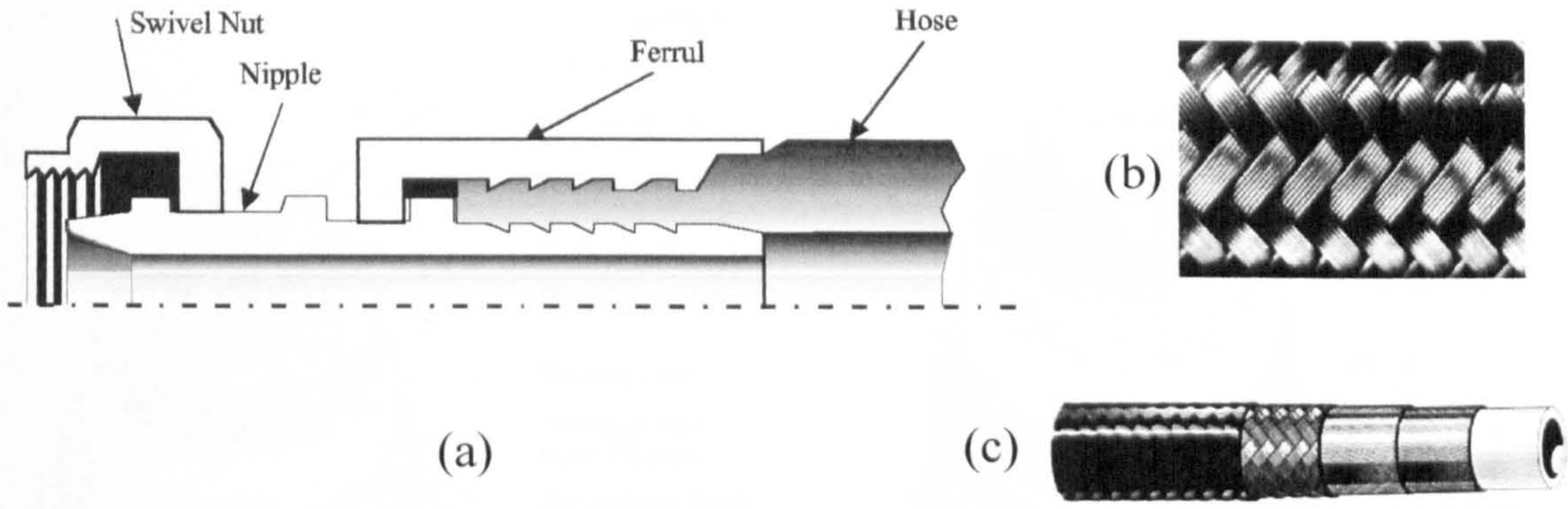

Figure 1.12. (a) the cross section of an endfitting showing the basic components, (b) Braided construction and (c) a hose with both braided and spiral layers (from Polyflex [10]).

1.5.5 Related structures

The use of floating oil platforms for deep see oil production has resulted in the development of a number of hose related structures.

Oil must be transported from the sea bed to the platform by pipes known as risers. A floating platform requires a flexible riser, the most common type of which is known as a non-bonded flexible pipe (for example see Figure 1.13). These pipes are a much larger diameter than hoses and one of the most important considerations is to prevent collapse from the external sea water pressure while retaining flexibility. Consequently such structures have unusual layers such as locked coils (which are also used in ropes to improve crushing behaviour) and corrugated carcasses to prevent internal collapse as well as wire layers for hoop and longitudinal strength.

Another requirement of flexible platforms is to control the well head on the sea bed remotely from the platform. This is enabled by umbilicals (see Figure 1.13) which are basically a number of hoses and electrical cables, generally wound together inside a hose structure. The large external hose functions mainly to protect the hydraulic and electrical flexible sub-units from external pressures while maintaining adequate flexibility to allow for platform movements.

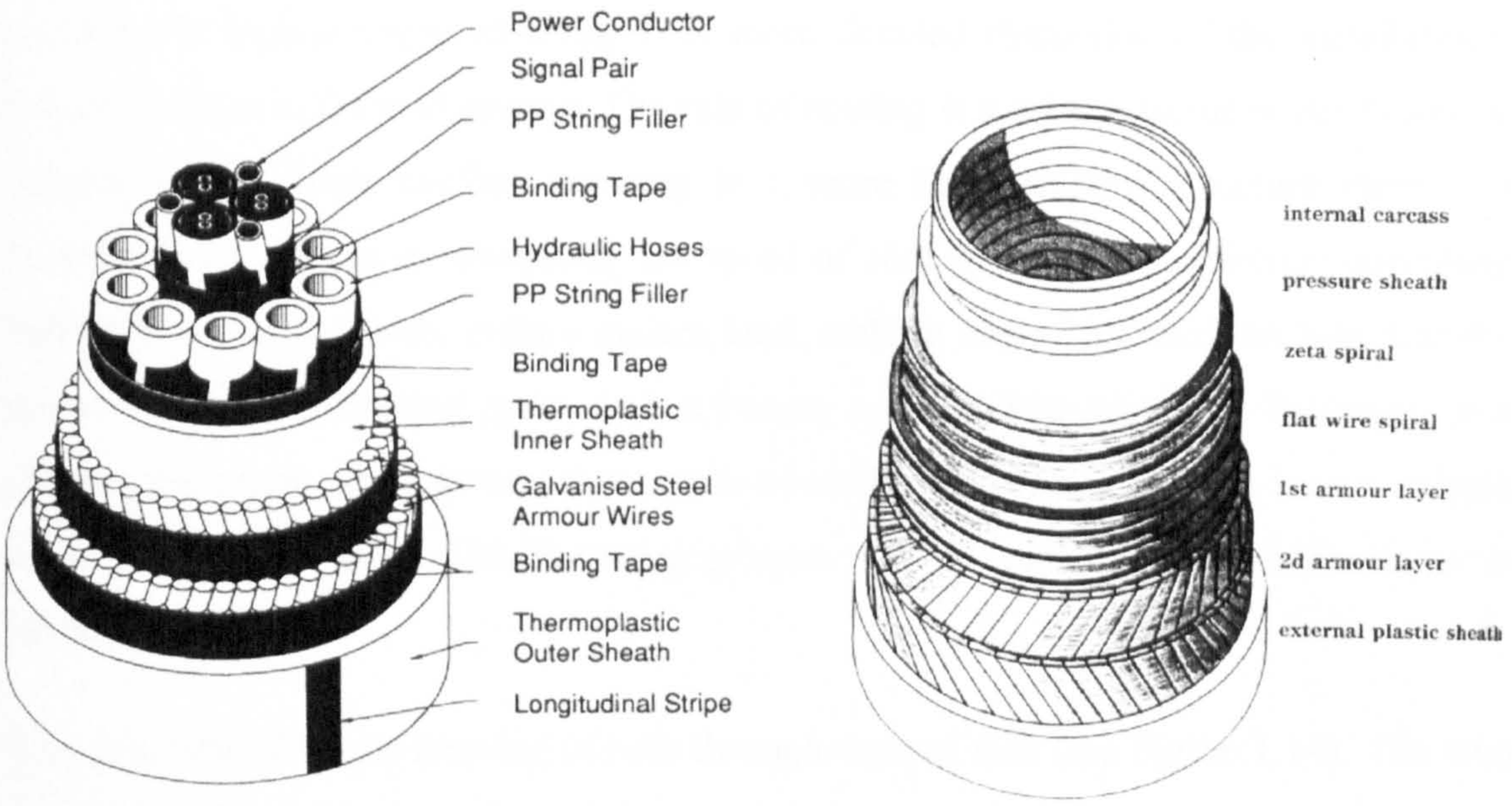

Figure 1.13. An example of an umbilical manufactured by Dunlop-Coflexip (from [26]), and an example of a flexible pipe manufactured by Coflexip (from [27]).

1.6 Manufacturing techniques

The machines currently used for productions of ropes and hose, were derived originally from the weaving industry. The basic spiral winding technique is broadly the same procedure used for producing all ropes and spiral wound hoses, these are discussed together. The procedure used to produce braiding, which is used in some hose constructions, is a more complex one and is not discussed here. This section begins by discussing the special process used to manufacture the high tensile wires which are the main constituents of the rope and hose in this work. This includes some discussion about the metallurgical process involved and the resulting metallurgy of the wires.

1.6.1 Wire

1.6.1.1 Manufacturing processes

The heat treatment process known as Patenting is a crucial part of the manufacture of medium and high carbon wires, giving them sufficient ductility to be drawn, while

retaining the high strength advantages. A more detailed discussion of the metallurgical process is given in the next section. The rate of cooling is a critical factor in the Patenting process, with a faster cooling resulting in a more homogeneous structure there is a considerable benefit from maximising the speed of cooling. The most effective quenching technique currently known utilises molten lead, making use of its excellent heat transfer properties and low melting point, and is known as Lead Patenting. Air Patenting, is a cheaper alternative which gives a slower rate of cooling and consequently a lower strength in the final wire product. This Patenting process may be carried out continuously, or in batches of coils [28].

Wire is produced by the drawing of rods through tapered dies (see Figure 1.14). The wire is deformed plastically in a die because of the pull exerted on it and the taper of the die. There is consequently a limit to the reduction in diameter that can be achieved at one die, according to the amount of tension the wire can stand without breaking. Because of this the wire drawing process is usually conducted in a number of stages. It is also important that the wire does not get too hot during the drawing process and this is a consideration when deciding on the amount of reduction at each stage. The amount of reduction in cross sectional area per stage for patented wire is usually around 25 % [29]. Detailed wire drawing programs seem to rely on the experience of the manufacture.

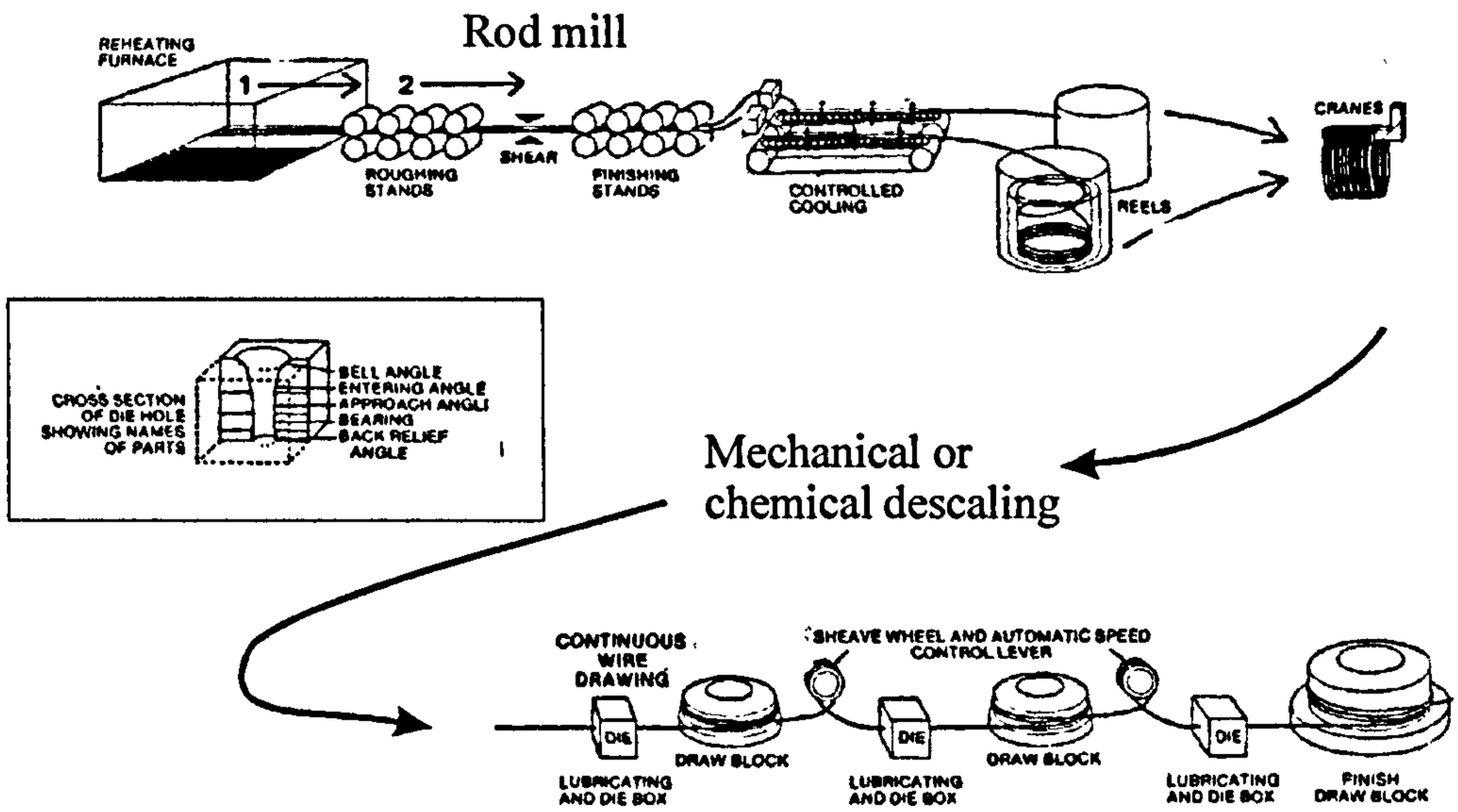

Figure 1.14. The rod rolling and multiple stage wire drawing processes- schematic (from [30])

Wires are lubricated before each drawing stage and the lubricant may be one of a number of substances such as dry soap powder, grease, oil or graphite. The lubricant is placed in a container in front of the die and picked up by the moving wire as it passes through.

Wire drawing machines are basically a number of power driven capstans which draw the wire through the dies. These are arranged in sequence with speeds to suit the elongation of the wire at each diameter reduction. There are three basic types of wire drawing machine. Firstly there are non-slip machines where the capstans run at exactly the same speed as the wire. Secondly, there are slip machines where the capstans run faster than the wire and the wire slips over them. Thirdly, accumulation machines which collect more wire at each stage than is necessary [28]. The non-slip process requires feedback control for the speed of the capstan and is therefore the most expensive technique, but is the most common method for high tensile wire manufacture because of the quality of product and speed of manufacture (enabled by continuous running).

1.6.1.2 Microstructure and mechanical properties of wire

The Patenting process involves an austenization of the wire at high temperature followed by an extremely rapid cooling to temperature below the transformation temperature of 723°C. This results in an almost isothermal transformation of the Austenite structure into a Pearlite with a very fine laminate structure. The idealised transformation and the Patenting cooling curve are both shown on a time temperature transformation curve in Figure 1.15.

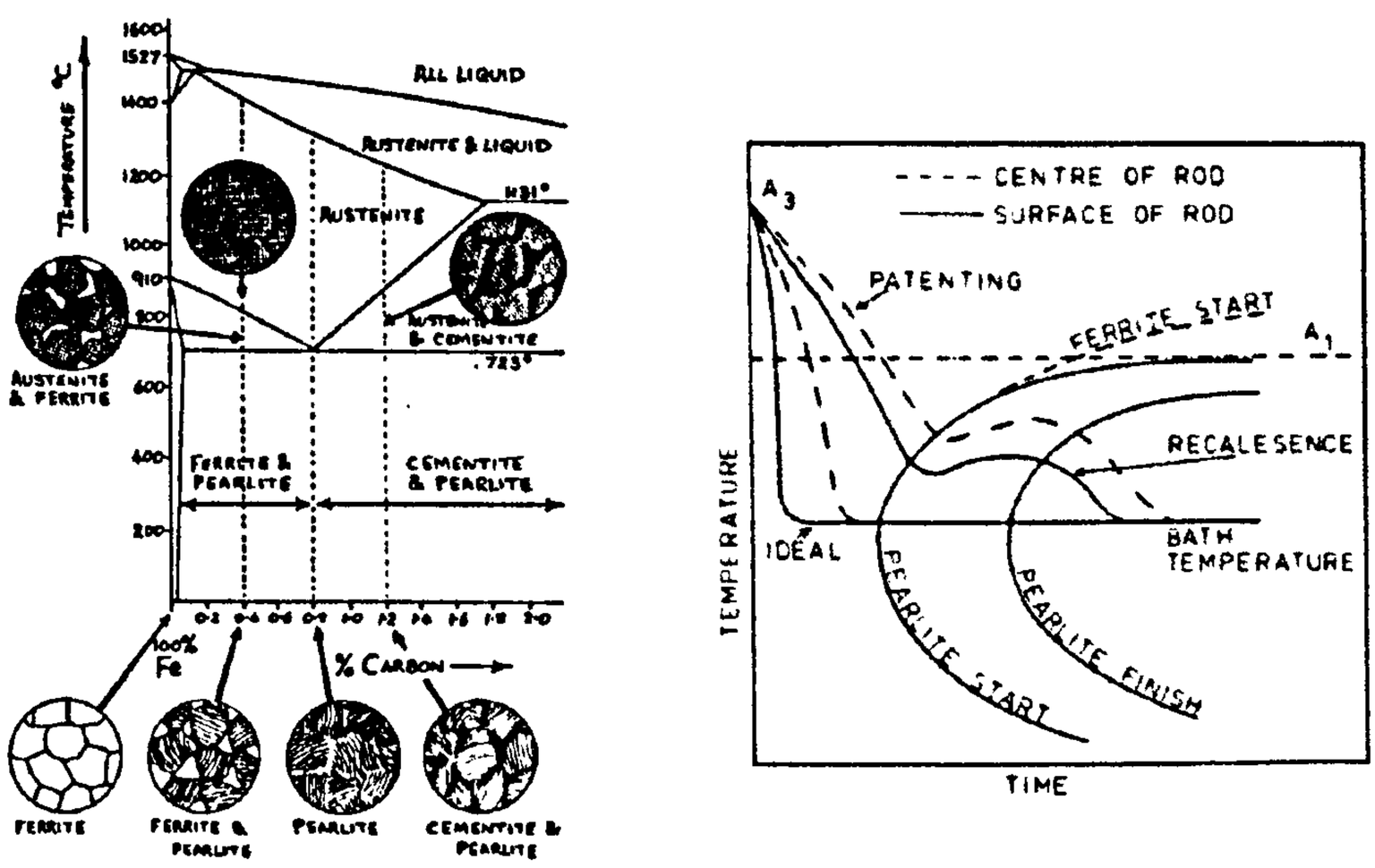

Figure 1.15. (a) The phase diagram for plain carbon steel in equilibrium conditions (from [31]), (b) A time temperature diagram showing ideal and actual patenting lines for microstructure transformation (from Franklin [32])

The Patenting process results in a consistent Pearlite structure for steels with carbon contents other that the Eutectoid 0.8%, and in practice carbon contents from 0.7 to 0.85 can be used satisfactorily for high strength Patented steel wires. The inter-laminar spacing of the Pearlite layers depends on the carbon and the exact details of the heat treatment process. It usually ranges from 0.005-0.1μm with the thickness of the Cementite layer being approximately one tenth of this [33]. This is a minimum of an order of magnitude finer than the course Pearlite structure found in plain carbon eutectoid steel. It is the ability of this material to bear large amounts of cold working without the brittle failure of

the Cementite layers which make it ideally suited to the high levels of cold working involved in multistage wire drawing (standard plain carbon steels with this level of carbon cannot be cold drawn to any significant level). The exact nature of the deformation of the Pearlite during drawing is not completely understood but it is thought to either be inter-laminar slip, or homogeneous deformation [34]. Plastic deformation of the brittle Cementite layers has been observed indirectly from drawn wires [34] and a number of reasons for this unusual apparent behaviour have been proposed [34],[35]. The microstructure can be likened to a fibre composite, with the high strength, but brittle Cementite layers acting as the fibre reinforcement and the ductile ferrite as the weaker aggregate. The undrawn Patented wire has a tensile strength of between 800 and 1300 N/mm^2 depending on the inter-laminar spacing of the Pearlite [32] (a finer spacing giving a higher strength). The drawing process is capable of more than doubling this strength mainly because of the effect of work hardening which causes an increase in the number of dislocations and their entanglement is accompanied by a decrease in ductility [36].

Another reason why the cold drawing process increases the axial strength is the resulting alignment of the grain structure along the wire axis. Because of the non-uniformity of deformation across the wire cross section, the outside of the wire exists in a state of residual tension, while the inside resides in a state of residual compression. This is however a generalisation and much work has been carried out to measure and assess the effect of drawing on the specific residual stress pattern within a wire (e.g. [37, 38]). The wire has a fibrous microstructure when viewed in a longitudinal cross section with an electron microscope, but a wavy cross section when viewed in the cross section [33].

The selection of the level of carbon content for the highest strength wire is not a simple choice and in practice the many variables in the production of wires mean that there may be a number of subtle methods for producing similar properties of wire. This can be illustrated by two patented wires with different carbon contents, 0.7 % and 0.85 %, as shown in Table 1.1). As can be seen the higher carbon steel has a higher patented tensile strength as would be expected. However, once the wires have been drawn to a

point just before any significant loss in ductility, the lower carbon steel, with the better drawability has the strength advantage. In practice it has been found that the higher carbon steels (i.e. 0.85 %) are better for larger diameter wires which are drawn less, but the lower carbon content steel (i.e. 0.7 %) is more appropriate for wires with diameters of less than 2 mm [32].

Table 1.1. The effect of carbon content on the mechanical properties of drawn steel wire, (from Franklin [32]).

Carbon Content	0.69%	0.84 %
Property		
Patented Tensile Strength (N/mm^2)	1028	1235
Reduction of area by wire drawing (%)	91.97	86.7
Wire diameter	3.48	2.92
Final Ultimate Tensile Strength(N/mm^2)	2119	2098
Reduction of area at fracture (%)	43	24

1.6.2 Spiral winding

The route to the development of spiral winding was the invention of the Cordelier, by Edmund Cartright in 1786, which was patented 100 years later [20]. Although the Cordelier (see Figure 1.16 (a)) was designed for yarns in the weaving industry it incorporates the essential feature of removing any twist in the yarns as they are wound together.

An additional manufacturing process which has been found to be beneficial to the final mechanical properties of rope and hose is that of pre-forming of the wires into a helix before they are wound into the final component. This has the result of reducing contact stresses within the component and also reduces the level to which an un-terminated end will try to unwind.

1.6.2.1 Rope

The Cordelier is the basic principle employed in manufacture of the wire rope, which was invented by W.A.J. Albert in 1831, in the Harz Mountains of Germany, for use in mines.

His rope consisted of three strands, each of four wires with no core. Modern ropes and stands however have a core (or 'king' wire in the case of a strand) around which the other elements are wound. To accommodate this modern winders have a hollow axis enabling the core unit to pass through from a spool behind the Cordelier. A stranded rope is the product of two separate winding processes. Firstly wires are wound together into a strand as shown in Figure 1.16 (b) and then the strands are subsequently (in a completely separate process) wound together around a core as shown in Figure 1.17 (b). This latter procedure is known as 'closing' a rope.

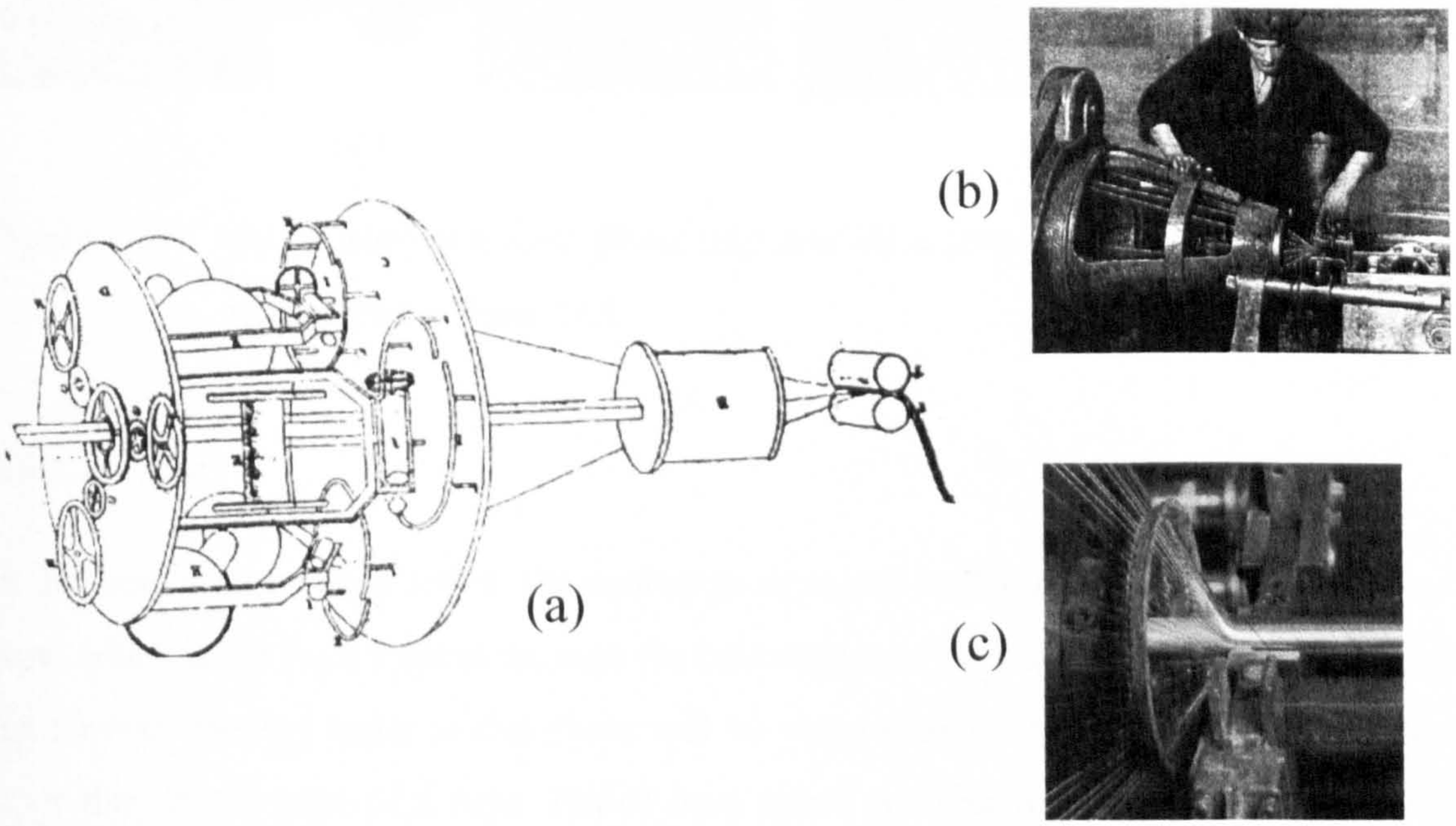

Figure 1.16. (a) The Cartright Cordelier (from [20]) (b) winding of a rope strand (from[20]) (c) hose winding (from[10])

An essential element to the wire rope construction is the lubricant. This has two purposes: Firstly, and primarily, it is to reduce the friction between contacting wires and therefore reduce the effects of fretting fatigue during use. Secondly the lubricant has the added benefit of acting as coating to prevent corrosion. Once a rope has been assembled it is extremely difficult to lubricate the interior, consequently the rope must be thoroughly lubricated at all stages of manufacture. During the making of a strand hot grease is applied to the wires just before they enter the guide (or 'nips'), and grease is applied again to the

strand as it emerges from the nips (see Figure 1.17(b)). Grease is again applied in the second winding stage when a stranded rope is closed.

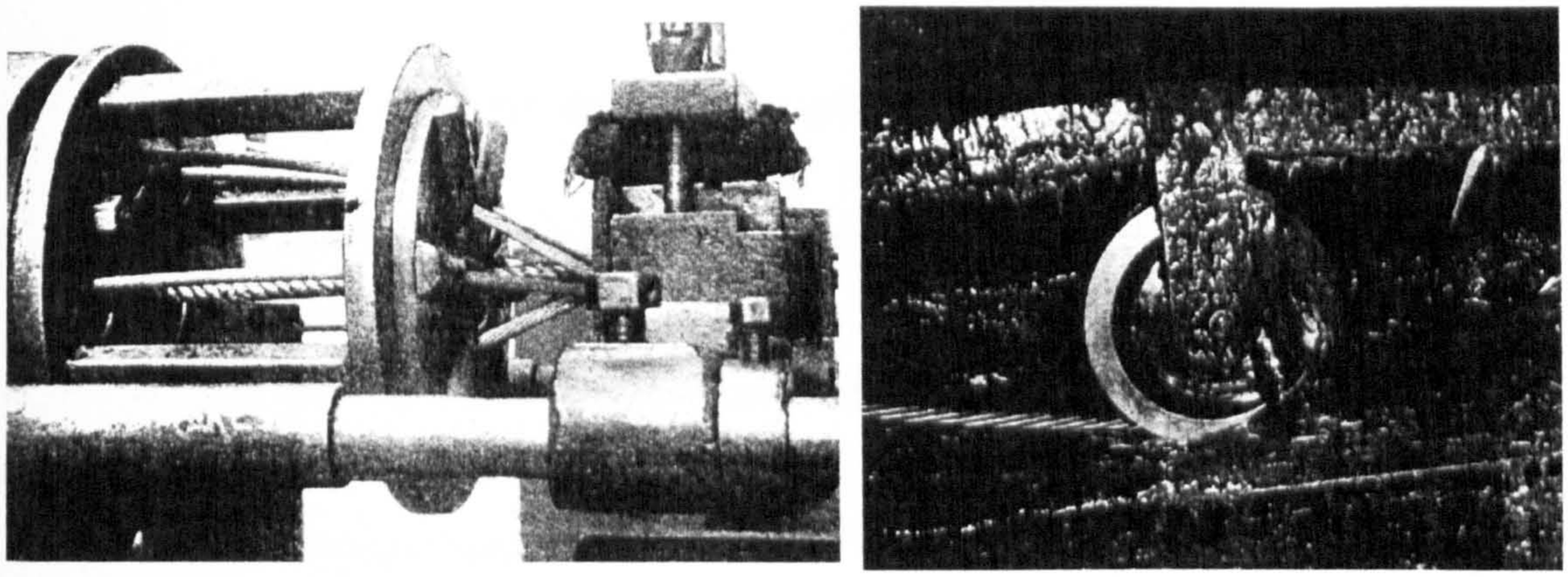

(a) (b)

Figure 1.17. (a) Closing of a rope (from [20]) and (b) a strand being lubricated during manufacture (from [20]).

1.6.2.2 Hose

In the case of hose construction, the equivalent core unit to that of a rope is the hose inner core, which is fed from a spool through the hollow axis of the winder. The consequence of the steeper winding angle is that there will be proportionally much more wires in each layer than in the case of a rope. Hence hose spiral winding machines have many more rotating bobbins of wires on each winding wheel, and do not incorporate the 'Cordilier' principle. This is because of the much steeper angle at which a layer of hose wire is wound, the problem of introducing twist along the axis of the wire is not significant.

One complication in the hose winding process is that often the bobbins have a friction brake incorporated so that wires are wound onto the hose with a residual tension. This has been found to be beneficial to the properties of the hose and it thought to give a more even load share between the wires when the hose is pressurised, although the reasons are not fully understood. The constant friction brake, however, will result in varying tension within the wire because of the change in effective diameter of the bobbin as the amount of

wire on the bobbin reduces, causing varying properties of hose from one end of a reel to the other. Recently a variable friction brake has been developed which allows for this, and a moderate level of success has been reported [39].

1.7 Degradation of rope and hose while in service

This section discusses the many ways that a rope may degrade in service, divided into two types of degradation. Firstly degradation caused by environmental factors not directly related to load bearing and secondly failure relating to load bearing, i.e. mechanical fatigue. An understanding of how ropes behave in service helps put laboratory fatigue tests covered in chapters 2 and 3 into context.

1.7.1 Non load bearing degradation of rope.

1.7.1.1 Corrosion

Looking at wire rope failures in British mines in the twelve year period 1938-49, McClelland [40] found that a high proportion of rope failures were due to corrosion and corrosion fatigue. 63 % of the 32 failures in winding ropes and 33 % (of 27 failures) in man riding haulage ropes were due to this mechanism of failure. McClelland pointed out that most of these failures could have been avoided with the use of zinc coatings in conjunction with careful lubrication. Unfortunately, many collieries at the time did not use galvanised ropes until an accident or near accident had drawn attention to the need. Only one of the corrosion fatigue failures mentioned above had galvanised protection and this was a locked coil strand. Unfortunately, the close fitting trapezoid shaped wires left no voids for the retention of internal lubricant and the unsuitability of the strand type for the application was cited as the reason for failure. Modern day users of ropes in corrosive environments are more aware of the benefits of galvanised well greased ropes. The harsh corrosive environments of offshore platforms however means that additional measures are required in the battle against corrosion. In the case of offshore crane ropes, the rope is in the highly corrosive sea water spray region. Chaplin [41] suggests a regular re-lubrication

programme employing a pressure re-lubricator to reduce corrosion. Other possible methods of increasing resistance against corrosion are by means of a thicker coat of zinc and thicker greases [2]. For applications which have no contact loading, such as mooring lines, another possible means of protection is by 'jacketing' [2]. A polymer material such as polyethylene can be used as an outer cover, similar to the outer cover used in thermoplastic hose. In such cases zinc coatings are generally still used as a secondary line of defence, in case of damage caused by handling or shark bites.

1.7.1.2 Surface embrittlement

Surface embrittlement is a mechanism of degradation which was first identified by Stead [42] in mine haulage ropes and has been studied in detail by Trent [43]. During rubbing the rope may frequently seize or weld locally to the object against which it is in contact due to frictional effects will cause a very high temperature locally which will rapidly cool after contact. This heating causes a phase change of the carbon steel to austenite and the effective quenching causes a thin layer of brittle martensite to form on the outside of the rope. These layers are easily cracked and lead to the rapid failure of wires through fatigue. McCelland [40] has stated that this can often be a serious problem in situations of wear. Mine ropemen may judge a rope based on the loss of metal, but a rope with a brittle layer of martensite on its surface may show little loss of metal. McCelland cites an accident when a man haulage rope failed while lowering 80 men down a 1 in 9 slope, one man was killed. He states 'The ropeman in this case was intelligent and alert but knew nothing of this type of deterioration, thus ropemen must be given the requisite information if they are to be held responsible for their ropes'. Since this survey was carried out, the Ropemans' Handbook [44] has been changed to give guidelines for recognising and minimising the incidence of surface embrittlement, as well as other degradation factors in the mining industry.

Another application of rope which is at risk of surface embritlement is the spread mooring ropes of floating oil platforms as identified by Chaplin [41]. This type of mooring ropes lie in a catenary shape (similar to a suspension bridge strand) and are attached to an anchor

by a length of chain. During deployment an anchor handling vessel will locate the anchor in the appropriate place using short line (anchor pendant) and then a buoy will be attached to this line to allow the anchor to be raised so that the rope can be reeled in during redeployment or inspection. In bad weather conditions however the anchor pendant may be lost and another technique known as 'chasing' will be used. A large steel hook is used to fish out the rope: once the rope has been hooked by the anchor handling vessel it moves towards the anchor paying out line but maintaining tension on the line. By this process the chaser will slide down the line until it hits the anchor at which point the anchor can be pulled out. As the chaser moves down the rope it tends to move in a slip stick mechanism and this has been shown to cause martensite formation on the surface. Chaplin [41] has suggested that the solution to this problem is to avoid chasing by locating the point of anchoring with a device such as a global positioning system. If a piece of chain is left on the anchor, the anchor can be retrieved by grappling.

1.7.1.3 Plastic wear

The mechanism of 'plastic wear' is a common phenomenon on drum winder mine hoist ropes and is described by Chaplin [41]. This is in fact not a wear process but a process of plastic deformation within the surface layers of the wire which leads to wires having a flattened cross section. The effect of plastic wear can be seen in Figure 1.18.

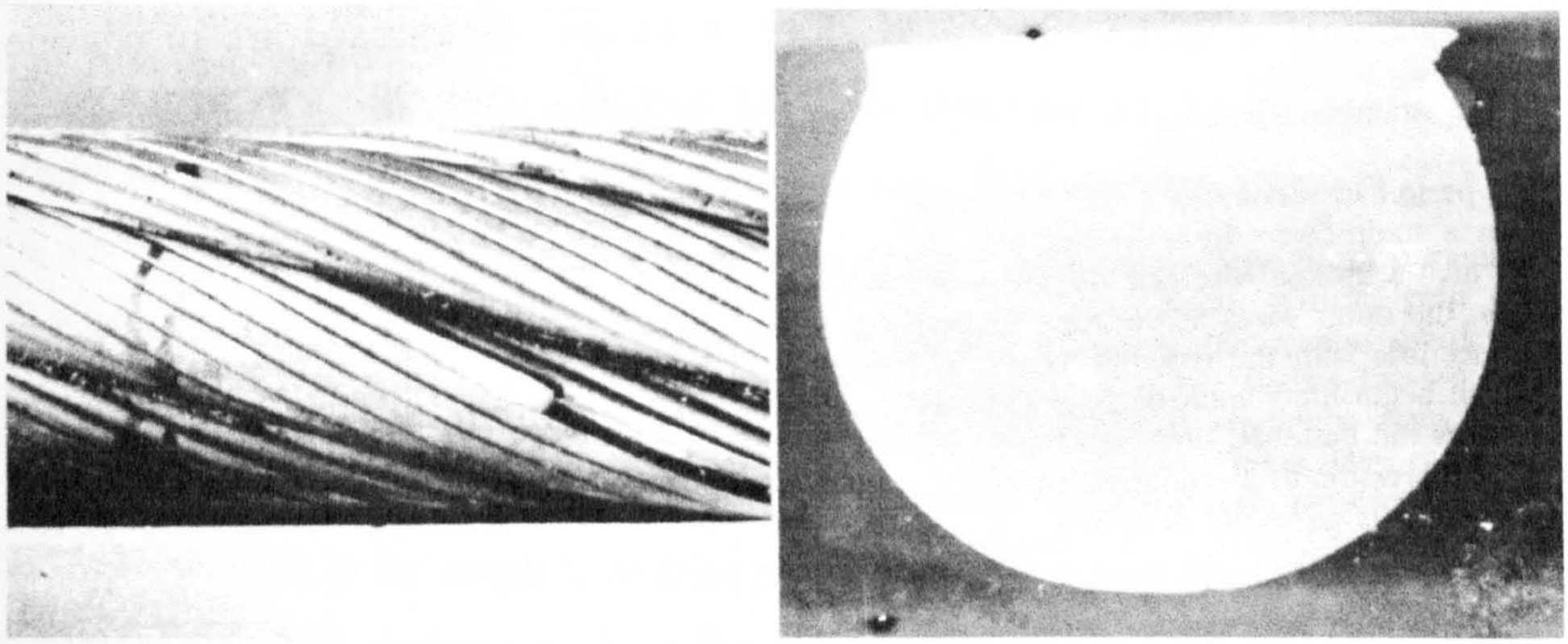

(a) (b)

Figure 1.18. (a)The manifestation of plastic wear within a mine hoist rope (with a wire break clearly visible), and (b) the effect of plastic wear on the cross section of an individual wire both pictures from Chaplin [41].

Plastic wear is caused by rope being wound onto a drum with residual tension while a container full of minerals is hoisted out of the shaft. When the empty container is wound down the shaft the rope will go through a sudden drop in tension as it comes off the drum which causes a 'backslip'. The rope generally shows sufficient variations in the its rotational position on the drum so that this plastic wear is manifested on the full circumference of the rope and on the full length of the rope except for a short region near the end of the rope which never gets wound onto the drum. The plastic displacement disrupts the axially orientated grain structure of the wire and makes them more susceptible to fatigue crack initiation. There is considerable incentive for a greater understanding of this phenomenon in the push for single drop mine hoisting systems in the deep gold mines of South Africa. At present mines use a split level mine shaft, mainly because of uncertainties in the capacity of the rope.

1.7.1.4 Gross geometric distortions

Twist build up in sections of a rope can cause problems. Vereet [45] demonstrated how this can occur behind a sheave if a non-torque balanced rope is used with a swivel.

Another example of twist building up in a rope is that of a triangular strand rope on a drum winder of a deep mine shaft [46]. The mine shafts are fitted with steel guides and therefore there will be no overall twist within the rope. However, this construction of rope is not torque balanced and the weight of the rope will mean that there will be a considerably higher torque acting on the rope at the top of the shaft compared with the rope at the bottom. This will mean that the rope at the top will effectively unwind and, as there must be no overall twist, the rope at the bottom of the shaft will wind up. Seventy percent increases in lay length have been seen in the sheave end of such systems with a corresponding 20% decrease at the splice end. Such behaviour makes it is necessary to understand the properties of these ropes under different conditions of twist and lay length. A recent study by Rebel [46] has investigated this phenomenon.

Built up twist within a rope can make it more susceptible to localised distortions in rope such as kinks as shown in Figure 1.19(b). Often kinks occur when sudden slack is introduced into a system.. McClelland [40] discusses nine incidences of kinking which occurred in haulage ropes on steeply inclined roadways in the South Wales coal fields. On further investigation it was found that these roadways showed numerous changes in gradient and direction and were thus particularly conducive to kinking of the rope.

Bird caging as shown in Figure 1.19(a), may occur when a rope sees a compressive or torsional shock loading [47] which travels along a rope until its effects are concentrated into a localised region such as the point when a rope goes onto a drum.

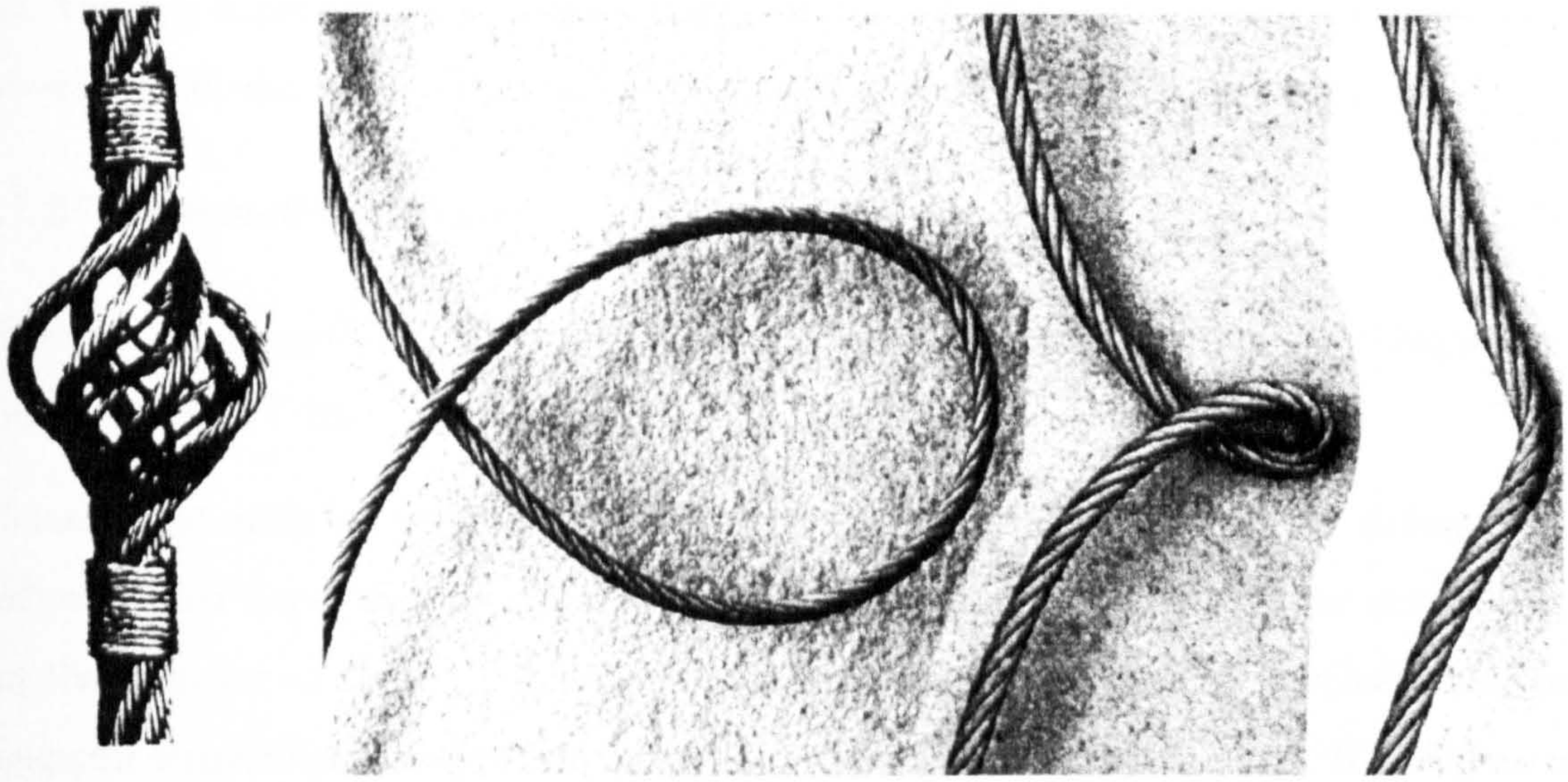

(a) (b)

Figure 1.19. (a) An example of bird caging in a rope from Costello[47] and (b) the three stages of genesis of a true kink from McClelland [40].

1.7.1.5 Wear

Ropes which rub during service will experience a simple wear mechanism. Haulage ropes are very susceptible to this type of degradation. It can also occur in crane and cable car ropes. This phenomenon can simply be measured by a loss in cross sectional area of a rope, but should not be confused with surface embrittlement. Standards will often specify a maximum allowable loss in cross sectional area of a rope at which point the rope must be discarded.

1.7.1.6 Crushing

If a rope winch is being operated in conditions of high tension, contact forces between adjacent wraps on the pulley can be sufficient to cause plastic deformation and crushing of a rope [41]. This can lead to an imbalance of stresses within a rope and premature failure. The rope may show no difference in the breaking load during a static tensile test (because stresses are evened out before failure) but it will experience a considerable loss in fatigue

life. This has happened for example during the proof load to set an anchor in a mooring system. It can also happen if a crane rope is used beyond its specified loading.

1.7.1.7 Termination problems

There are many methods of terminating a wire rope, the most common techniques are shown in Figure 1.20.

Matanzo [48] made a comparison of various rope terminations in terms of strength and endurance and found that the type of rope did not effect the efficiency of the terminations but the diameter of the rope is important. The most efficient type of termination is the cone cast terminations (referred to as 'spelter socket' in the diagram) [49]. If constructed properly these ends will transfer the rope breaking and fatigue properties (i.e. the rope will not necessarily fail at the end). All other termination types will fail prematurely in quasi-static breaking and tensile fatigue conditions. A rope which sees high tensile loading in service will therefore generally be terminated using the spelter socket method. These end fittings involve the brushed out end of the rope being cast into a medium (details of this process is described in Chapter 2). Although the traditional media for casting are zinc, spelter or white metal, resin has become a popular socketing medium in recent years [50, 51].

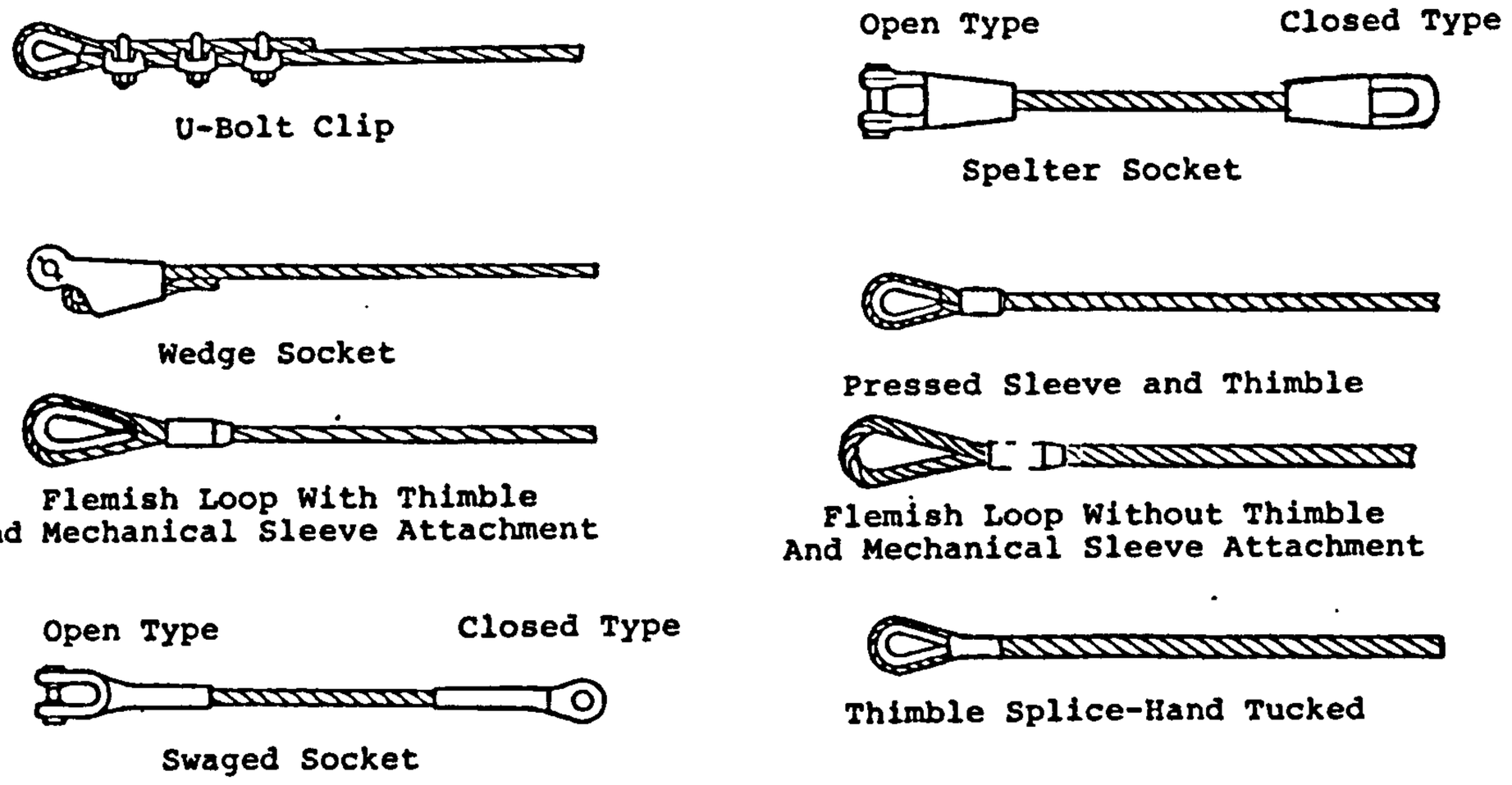

Figure 1.20. Different types of termination as tested by Matanzo [48]

Spelter socketing is a relatively complicated process which requires accurate alignment of the rope with the socket and a thorough degreasing of the splayed wire ends. Failures have occurred in service on occasions, usually as a consequence of bad termination practice. McClelland [40] found that 28% of the breakages in mine hoisting ropes could be attributed to termination failure, all of which were caused by bad techniques. On two occasions for example it was found that the wires were not degreased before zinc was poured into the sockets. Vereet [49] describes problems which can occur because of the over heating of spelter socket because of the molten zinc. He also describes corrosion problems which may occur if a region beyond the socket is accidentally degreased while the rope brush is degreased.

1.7.2 Degradation of rope due to load bearing - mechanical fatigue

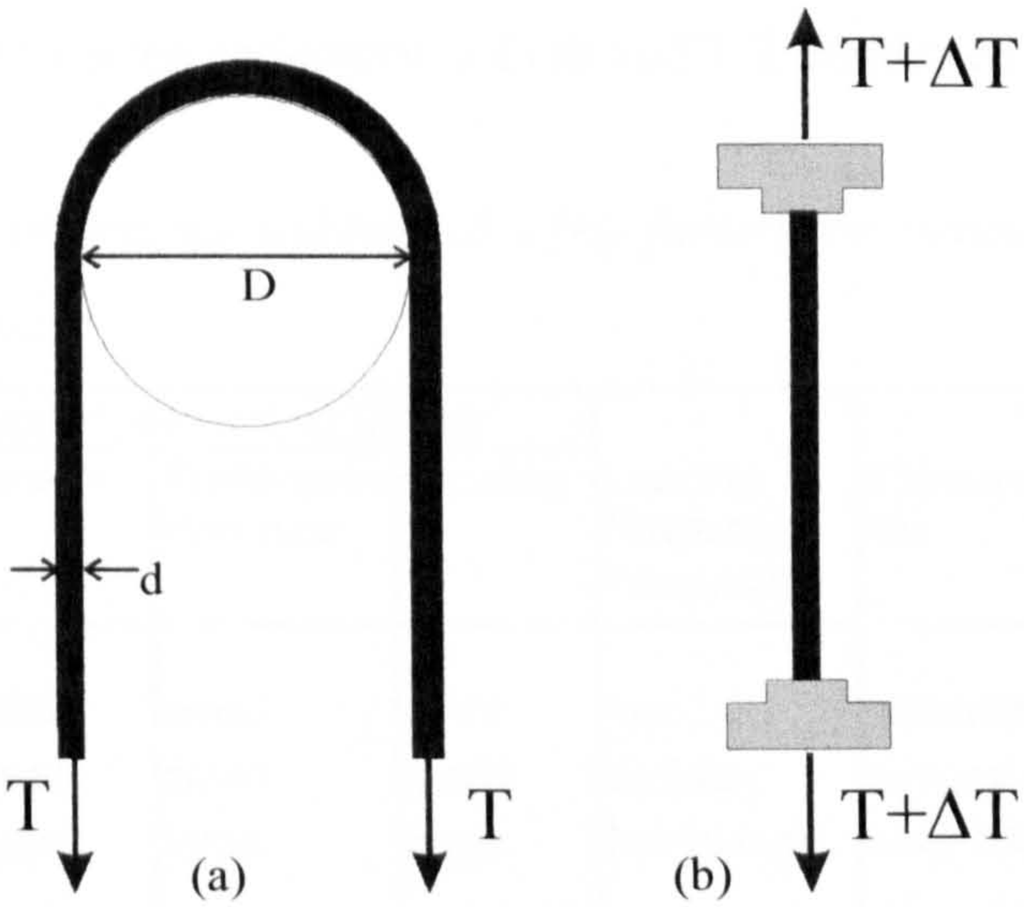

Figure 1.21. The two most common types of rope loading: (a) bending over sheave with constant tension (BOS) defined by the ratio of the sheave diameter, D, to the rope diameter, d and (b) Tension-tension fatigue (T-T) which is fluctuating tension.

The mechanical loading which a rope experiences in a particular application is the major factor in the selection of the rope and the level of safety factor used. The safety factor is defined as the ultimate breaking load divided by the tensile load in service. Other types of loading on a rope are not included in the calculation and therefore the size of the safety factor will reflect the level of other types of loading which exist in service.

The main types of fatigue loading a rope can experience are tension-tension (T-T) and bending over a sheave with constant tension (BOS) as shown in Figure 1.21. Müller [52] discusses what factors influence the level of safety factor for a particular application. He states that there will be low safety factors if there are only small alternating stresses, a short working life is expected or only a few stress reversals take place over unit time. There will be a high safety factor however if there are a large alternating stresses, a long working life is required or there are a large number of stress reversals in unit time. For a number of common applications he lists the type of alternating stresses experienced, the

expected working life and the safety factor usually chosen for the application. These are given in Table 1.2. The rest of this section goes through the specific factors which are most influential in determining endurance in BOS and T-T conditions.

Table 1.2. Types of stresses and typical safety factors for common rope applications, from [52].

Type of Rope	Type of Alternating Stress			Loading Reversal Frequency	Expected Working life	Safety Coefficient
	Tension	Transverse Pressure	Bending			
Bridge Ropes	small	small	small	low	unlimited	2-2.5
Cable Car Ropes	small	small	small	ordinary	several decades	3.5
Crane and Haulage Ropes	large	large	large	low to high	weeks to years	3.5-10
Pit Hoisting Ropes	large	small	small	high	years	6-9.5
Elevator ropes	small	large	small	high	years	11-24

1.7.2.1 Bending over sheave fatigue

1.7.2.1.1 Influence of the *D/d* ratio

A very important factor in the fatigue life of a rope bent over a sheave is the ratio of the sheave diameter, *D*, to the rope diameter, *d*, which is commonly referred to as the *D/d* ratio. Müller [52] carried out extensive tests with *D/d* ratios ranging from 7.3 to 59.3 for a 6x19 Lang's lay rope. The relationship between load and cycles to failure can be seen in Figure 1.22 for seven different values of *D/d*. The curves are not the result of a statistical analysis but are merely indicating the general trend taking place. It can be seen that the bending cycles to failure at *D/d*=60 for a typical working load of 30 % Ultimate Breaking Load (UBL) is around 2 million cycles and from the trend a sheave of say a *D/d* of 70 is likely to have a fatigue life a factor of 10 higher than this, thus the bending effect is becoming increasingly less important after a *D/d* of 60. Within realistic loading levels three distinct mechanisms of degradation have been identified by Gibson and others [53]: At low loads and small *D/d* ratios the primary cause of failure will be from bending stress, at medium loads with medium *D/d* ratios the main cause of degradation will be from pulley

contact forces, at high loads and high *D/d* ratios the main failure mechanism will be contact stresses within wires in the rope. A minimum *D/d* ratio of 18 is recommended for crane rope applications [2].

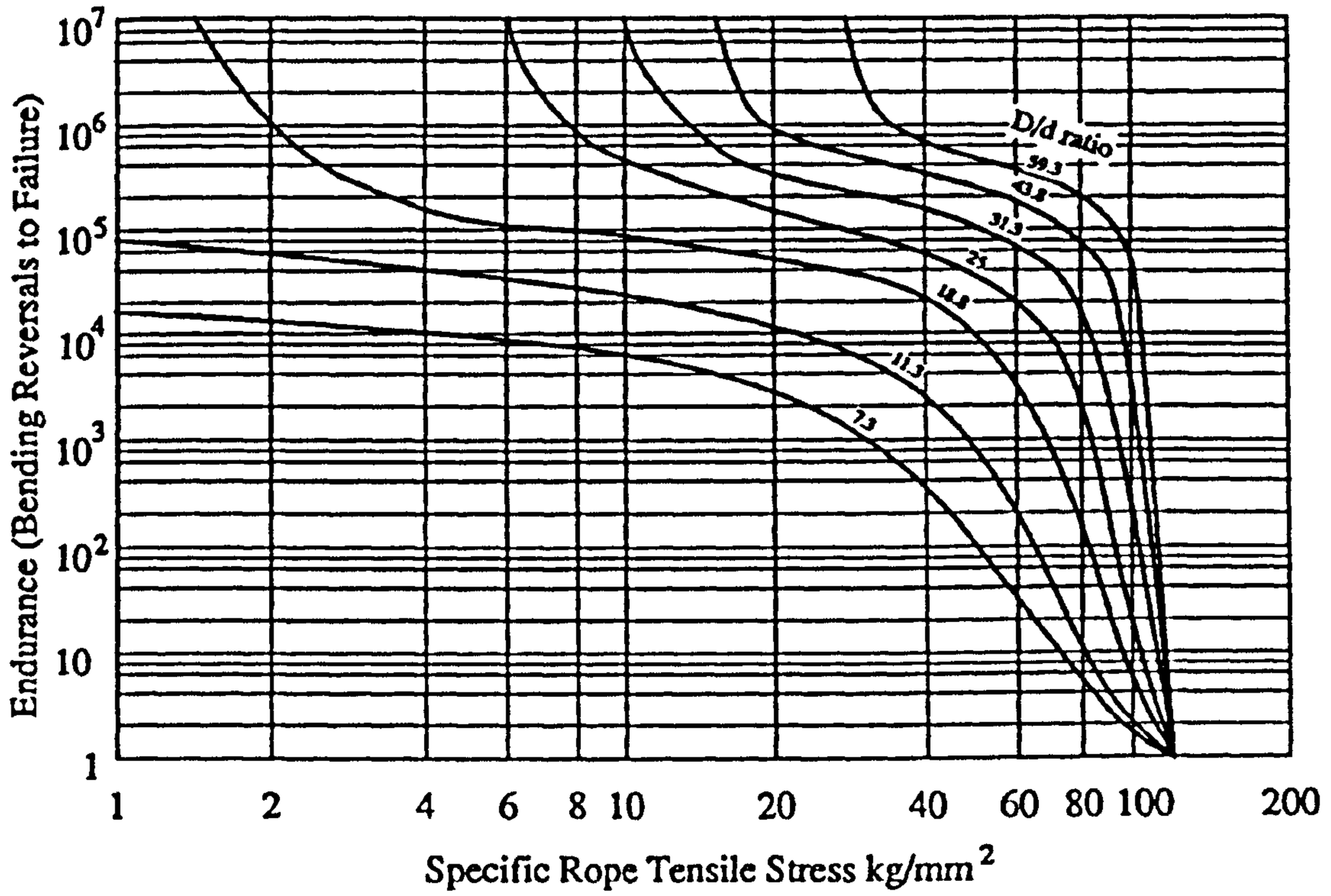

Figure 1.22. Effect of rope tensile stress on reversals to failure in bending over sheave tests for various D/d ratios of 7.3 to 59.3 from Müller[52], diagram translated by Ridge [2].

1.7.2.1.2 Applied load

The general relationship between the applied load and the endurance can be seen from Figure 1.22. Müller [52] states that the most significant cause of fatigue from tensile load is due to the contact stresses between the wires and between the rope and the sheave. He proves this by testing individual wires with varying tension and bending, showing that there is very little variation between tensile load and fatigue life for the individual wires

when compared with the overall rope and this is explained by the fact that a wire will have negligible alternating compressive stresses compared with a rope.

1.7.2.1.3 Sheave material and profile

Muller [52] investigated the effect of six different sheave profiles on the endurance of the rope (Figure 1.23). He demonstrated that the best profile is the 60° groove type because it gave the greatest contact area. He also discussed the effect of sheave lining material, stating that the contact pressures according to Hertzian theory will be proportional to the square root of the average of the rope and lining stiffness. Thus linings with only slightly lower stiffness than the rope such as iron bronze or aluminium, will have negligible effect on the contact stresses. Materials such as wood, rubber or plastics will have a considerable effect on the contact stresses and have in practice been shown to be beneficial to rope endurance.

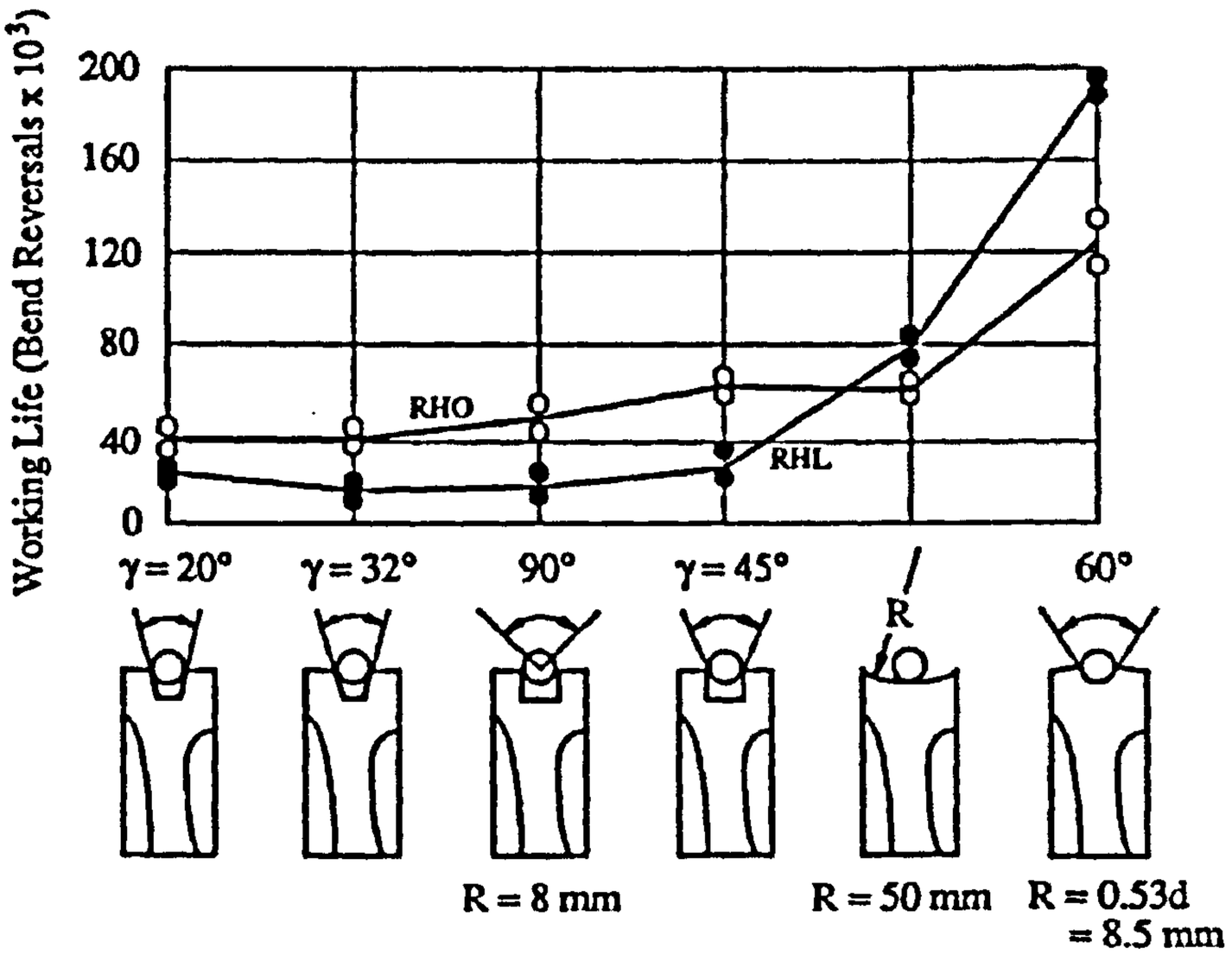

Figure 1.23. The effect of various sheave profiles on endurance for right hand ordinary (RHO) and right hand Lang's (RHL) lay ropes from Müller[52], diagram translated by Ridge [2].

1.7.2.1.4 Bending Length and Angle of Contact

The length of rope which goes through a full bending cycle is defined as the bending length. Rope fatigue life is independent of the bending length, until the bending length goes below one rope lay length at which point the endurance increases exponentially with reducing bending length (Figure 1.24). This increase in fatigue life is explained [52] by the fact that a reduced number of strands will see alternating compressive stresses and an increased number will only see alternating bending stresses (which will not on their own cause wire failures) as the bending length falls below one lay length.

The angle of contact is the angle of the sheave which is contacted by the pulley. In a similar manner to bending length the rope endurance has been shown to be independent of angle of contact until the angle reduces to a level where the amount of rope touching the sheave is less than one lay length. Below a contact length of one lay length the endurance will drop slightly down to about 0.3 lay lengths at which point it will rise steeply (It can be safely assumed that a rope with an angle of contact of zero will have an infinite fatigue life as this is effectively a straight rope in constant tension).

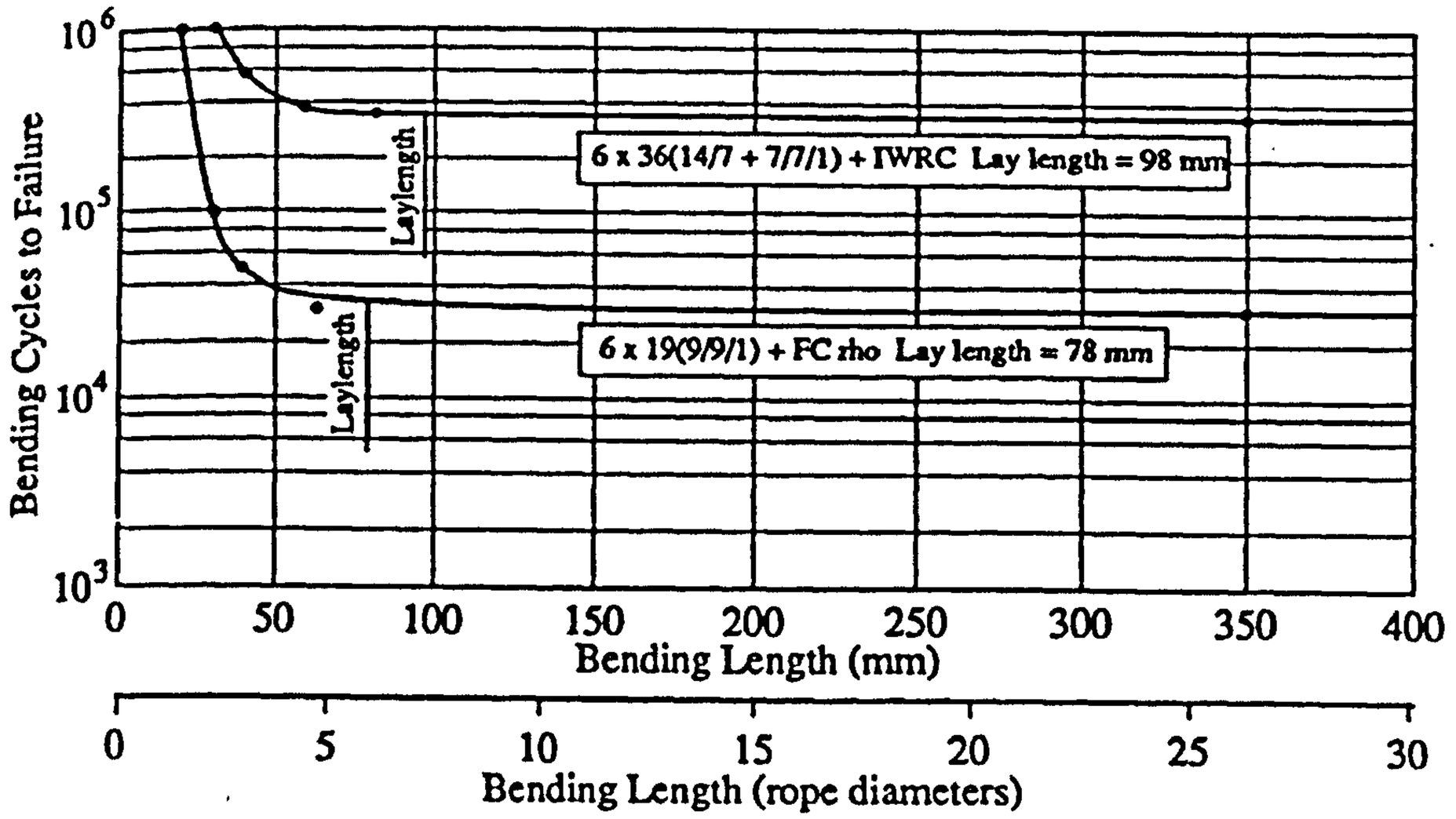

Figure 1.24. The effect of bending length on rope endurance from Müller[52], diagram translated by Ridge [2].

It is very important that the effect of bending length and angle of contact is taken into consideration when designing a representative bending fatigue test set-up. Most applications will be working above one lay length for both parameters and so they must be kept above one lay length in testing conditions.

1.7.2.2 Tension-tension fatigue

There are a few common applications where fluctuating tension loads are the predominant loading factor in a ropes fatigue life, three examples of which are mine hoisting ropes, offshore mooring ropes and ropes used in static structural applications such as suspension bridges or tension stayed bridges [54]. Until recently little experimental data was available for this form of fatigue, but over the last few years there has been a considerable amount of experimental data built up [55-58]. This has given a reasonable understanding of rope endurance under these conditions and the factors which affect it. It is well established [54]

that the characteristic curve of a wire rope in tension-tension fatigue fits to a power law relationship (e.g. Figure 1.22) where the number of cycles to failure, *N*, can be equated to the load range, *S*, by the following formula:

$$N = AS^B \qquad \ldots(1.24)$$

where *S* is the normalised range as a percentage of the ultimate breaking load and A and B are constants. The rope does not show the endurance limit as seen with many alloys including steel, i.e. there is no minimum useful load range below which there will be an unlimited endurance. Unlike in the case of BOS fatigue, where similar ropes display very consistent behaviour, T-T fatigue characteristics are much more sensitive to slight variations in rope construction or geometry as will be discussed in the following sections.

1.7.2.2.1 Effect of mean load

Yeung and Walton [59] have suggested that a variation of the original Goodman diagram [60] for dealing in variations in mean load for purely tensile bearing structures. Chaplin [61] has found that there is some evidence to show that the mean load has little effect on the fatigue life. He suggests that this may be due to a reduced fretting effect caused by increased friction between wires, or equally a decrease in the load take up from a wire break (also caused by increased friction between wires) requiring more breaks before failure. In any case with a realistic maximum load of 55 % of the ultimate breaking load and a range of 15-20 % there is not much scope for variation in the mean load. It would seem sensible, in the absence of data for a specific rope, to use the Goodman diagram to give a conservative prediction for this effect.

1.7.2.2.2 End effects and specimen length

The importance of end terminations in T-T fatigue has already been emphasized. For a short test specimen to behave representatively of a much longer in service length it must be long enough to give a section of a rope in the middle which is unaffected by the end terminations (i.e. free field). As the course of a rope fatigue test will result in multiple wire

breaks along the length, the specimen length must be long enough for these wire breaks to develop and interact. The effect of specimen length on the endurance of spiral strands has been assessed experimentally by Esslinger [62] who gave a strong indication of a decrease in wire axial fatigue life with increases in the length of test specimens from 150 mm to 10410 mm. Chaplin [63] found little end effects during a series of fatigue tests on a six strand rope with specimen lengths varying between one and four lay lengths. This may just reflect the small length range (and very small lengths) tested and the efficiency of the end terminations. Chaplin [63] suggested that a minimum specimen length of 10 lay lengths from experience would give a representative behaviour of free field fatigue. Raoof and Hobbs [64] suggest that there should be a free field length of two times the effective length, plus a termination zone of influence also twice the effective length giving a desirable specimen length of four times the effective length. From previous theoretical work Raoof [65] had calculated an upper bound effective length of 2.5 rope lay lengths, and thus a specimen length of ten rope lay lengths was suggested, agreeing with the suggestion by Chaplin.

1.7.2.2.3 Scale effects

All available data for 19 mm diameter ropes and above [54] shows a reasonably consistent slope on an alternating stress vs. number of cycles (S-N) curve ranging from 4 to 5.5 when plotting percentage of breaking load against cycles on a log-log scale. For rope diameters smaller than this however it has been found that the slope is considerably higher. Ridge [57] found a power of 8.8 for a 13 mm diameter six strand rope and Husain *et al.* [66] found a power of 8.8 for an 8 mm diameter rope. These differences between large and small diameter ropes do not appear to be connected with different failure modes. The stepped scale effect may be a result of differing wire properties. The wire diameter in the smaller size ropes are 0.7 mm or less and in the larger ropes are 0.8 mm or larger. The smaller diameter wires must go through more cold drawing stages as all wires are produced from the same original size of rod. Chaplin [54] suggests that the effect may be caused by residual compressive stresses on the outsides of the wires and their proportion to the overall cross sectional area of the wire. He also makes it clear that more

experimental work is needed if this phenomenon is to be properly understood. From his results it is clear that any scaled down model of a large rope in service (which is impractical to test in a laboratory) must be at least 19 mm in diameter to give a reasonable representation of the S-N characteristics.

1.7.3 Degradation of hose

If a hose fails in service an investigation can be made in order to determine the mode of failure. Failure mode analysis procedures have been developed by Miller [67] for free hose failure (defined as being when the failure is more than 2 inches from the end fitting). These procedures involve the gradual stripping down of the hose, layer by layer, taking a number of measurements and using the information to piece together a hypothesis for the cause of failure. Chermak [68], Buzzelli [69] and Briggs [70] in three separate articles discuss the causes of failure in hydraulic hose as seen in service. From their discussions it is possible to make the following summary: there are three ways in which a hose can ultimately fail, by bursting, by end blow-off or by leakage. The various forms of these failures are summarised in Table 1.3, Table 1.4, Table 1.5 respectively. In many ways, what is more interesting is the cause of these failures and in this respect the following classification is proposed:

1. Mechanical factors - the hose has failed as a direct result of pressures and bending which are within its specified operating conditions, i.e. it has failed in fatigue. Such failures can be modelled in the laboratory with mechanical fatigue tests as discussed in Chapter 5.

2. Environmental factors - the hose has failed due to environmental factors such as outer wear or high temperatures accelerating a fatigue failure. These effects can be investigated in advance and appropriate material selection can minimise the effects of chemical or abrasive degradation.

3. Inappropriate installation or use - the wrong hose has been selected for the application, the end fitting or assembly has been fitted badly or the hose has been

abused in service. Failures due to inappropriate installation can be reduced by clear guidelines for hose selection, installation and use. Trying to eliminate these types of failure by design is inappropriate.

The 'Type' columns in the tables refer to which of the above classifications of failure mode the item falls under.

Table 1.3. Different reasons for hose burst, compiled from Chermak's [68] Buzzelli [69] and Briggs [70] reports.

Observations	Detailed cause of failure	Type
Randomly broken wires seen when cover removed	Fatigue failure: probably a high loading frequency application	1
No wire breaks seen	Excessive pressure	2
Wires are rusted, breaks in outer cover	Damage to outer cover, e.g. from abrasion	3
Burst at outer bend of hose- elliptical hole	Excessive bend	2
Hose flattened and kinked at burst	Accidental twisting	2
6-8 inches from end- wires show rusting	Improper end fitting installation allowing moisture to seep in	2
Laterally split open	Hose too short- causing tensile loads spiral hose	2
Flattened at burst area	Kinking	2
Cover and inner core is crazed	Old age (elastomeric hose phenomenon)	3

Table 1.4. Different reasons for end blow off, compiled from Chermak's [68] Buzzelli [69] and Briggs [70] reports.

Observations	Detailed cause of failure	Type
Hose end not distorted	Badly fitted or inappropriate end fitting	2
Hose has been stretched	Insufficient support of hose in long vertical applications	2
End fitting correctly installed, outer cover is nylon	Excessive heat thermoplastic hose	2

Table 1.5. Different reasons for hose leaking compiled from Chermak's [68] Buzzelli[69] and Briggs [70] reports.

Observations	Detailed cause of failure	Type
Teflon material- fluid moving at high velocity, pin hole cracks in inner core	Causes static electricity in fluid and local welding of inner core with wires.	1
Inner layer broken loose from reinforcement	vacuum condition	2
Blisters seen in outer cover- found to be oil	Pin hole cracks in inner core	1
Leaking at end	Hose too short- causing tensile loads	2
Inner core worn and gouged through braid	Caused by abrasive hydraulic medium	3
Hose cracked internally and externally	Combination of low temperature and bending (elastomeric hose phenomenon)	3
Inner layer very hard and cracking	High temperature and aerated hydraulic medium (elastomeric hose phenomenon)	3

It can be seen from the tables that there is a large range of failures which may be caused by abuse of the hose in some way (8 listed). A lower number of failure types are associated with fatigue (3 listed) or environmental factors (3 listed). No estimates of the frequency of any type of failure are given by the reports, but as the reports are written by hose manufacturing personnel in magazines which will be read by hose users it seems that they are aimed at reducing the amount of hose failures through misappropriate use.

Some failures are specific to a particular type of hose, for example elastomeric materials have a tendency to craze after a long period in service, this type of behaviour can be characterised by standards (e.g. [71]). Spiral hoses are more susceptible to damage from over bending or twisting and some thermoplastic materials can show a pin hole crack phenomenon-at the inner core.

Fatigue failures have been identified mainly with relatively high frequency pressure cycling in the hydraulic hose applications. One example cited was the hoses used on injection moulding machines which are continuously subjected to pressurisation several times a minute. In the case of ultra high pressure hoses fatigue has been identified as a significant problem and details of these failures seen in Polyflex hose will be discussed later in the thesis. Fatigue failures have been characterised by a break up of wires attributed to fretting or in some cases to pin hole cracks developing in the inner core.

The end fitting serves a number of purposes. Firstly it must have enough grip on the hose so that it doesn't get 'blown off' from the pressure loading in the axial direction. Secondly it must have reasonable sealing to prevent leakage from the hose/fitting interface. Finally it should not damage the hose significantly near the swaging (where the end fitting is squeezed onto the hose) so as to cause stress concentrations and premature failure of the hose close to the end fitting. These three factors often give conflicting demands on the end fitting design, making it something of a hit and miss affair reliant on experience from trial and error testing. Although a number of failures can be attributed to badly assembled end fittings, properly assembled end fittings may still fail prematurely. End fitting design and development is a critical part of the job of a hose designer. Although standards exist for low pressure hose terminations (e.g. [72]), ultra high pressure hoses have custom made non-standard end fittings. Test methods for assessing the hose coupling interface have been developed by Eleftherakis [73] who lists common interface problems as: inner lining separation bulge or crack, oil pocket formation, hose/coupling separation, hose tearing and hose/coupling leakage. The crimping process is critical in many of these problems and an attempt to model the plastic behaviour of crimping of a rubber hose with its coupling has been made by Haisler [74] although few practical implications have been discussed in this work

1.8 Discussion

The word flexible has developed a much broader meaning than the simple mechanical 'able to bend without breaking' sense from which it stems. The dictionary describes one of its meanings as being adaptable, versatile or variable in relation to an object or a concept, for example 'flexible manufacturing system' or 'flexible working hours'. These terms provide a convenient form of categorisation of the advantages and reasons for use of mechanically flexible structures such as rope and hose:

- **Adaptability:** The ability to adapt within a particular mechanical environment which may be transient - not just in terms of fluctuating loads but in terms of gross movements between bodies in the structure. One example of this is the ability of

mooring ropes, flexible pipes and umbilicals to adapt to the movements of a floating platform relative to a sea bed. Another example is the hydraulic hoses which power robotic arms or diggers, which must adapt to the particular orientation of the arms they are controlling.

- **Versatility:** A structure may be applied easily to a number of different environments. For example the cable car designer does not have to do a detailed study of the contours of the mountain to design his system, whereas a railway engineer must literally move mountains to lay his rigid track. Similar advantages exist for sub-sea and overhead electrical cables.

- **Variability:** The structure can exist easily in a number of different forms depending on whether it is in use or not, i.e. it is portable. The rope or hose can be completely wound onto a drum (or coiled up is some form) when it is not being used, or it can be partially unwound if only a small amount of it is needed. This type of advantage occurs in a wide range of situations, a few examples are on cranes, mountaineering ropes and the fireman's hose.

One problem that most helical structures must deal with is the tendency a single helix direction has to untwist during loading. A braided structure solves this problem by interweaving both left and right helical fibres in a single layer. However for high load bearing applications this technique is not feasible and broadly there are two techniques open to the designer to reduce the level of twisting within a structure as follows:

- **Alternating lay within the same level of hierarchy:** This is the technique used for spiral hoses, each layer of wires is laid in the opposite direction of the previous one. This technique is also used by spiral strands although often in this case there may be two layers in one direction and then a pair in the opposite direction. This technique is never used in the winding of strands within a stranded rope (all wires are wound in the same direction) but it is used if a stranded rope has multiple layers of strands (i.e. a multi-strand rope) in which case the first layer of strands

will be wound in the opposite direction to the second (multi-strand ropes rarely have more than two layers of strands)

- **Alternating lay between different level of hierarchy:** Stranded ropes often use this technique, if the wires in a strand are wound in opposite direction to the strands in the rope, this is known as Ordinary lay. If both are laid in the same direction it is known as Lang's lay, and this type of rope should never be used without fixed ends, as it will completely unwind itself.

The general mechanism of degradation due to loading within a rope or hose can be simply described as a growing number of wire breaks accumulating within the structure until the wire breaks eventually cause complete failure of the structure. There are two aspects here which must be further investigated in order understand and model the process of fatigue, they are:

- **Cause of wire breaks:** What causes the initiation of the wire break? For example contact stress, fretting, corrosion some combination of these phenomenon. How does the crack grow within the wire? The wires have a unique microstructure which may have unusual fatigue properties.

- **Effect of wire breaks:** What effects the take up of tension in a broken wire? For example the level of lubrication or other broken wires in the same region. How does the broken wire effect other wires at the same cross section? For example are adjacent wires more effected than distant wires or is the distribution of wire breaks important?

On top of the above complexities how does the type of loading and precise construction of rope effect the above questions? Clearly there are a lot of factors which must be understood before any unified theory based on fundamental principle can be developed. Any researcher must consider exactly what they aim to achieve before embarking on any program of work. Experimental research which has been carried out generally has one of two objectives:

- Measuring a particular rope or hoses behaviour for a specific loading regime (or group of loading regimes) and then developing empirical formulas to describe the behaviour (for example based on load level or ratio of pulley to rope diameter).

- Developing subtle experimental techniques in order to understand a more fundamental aspect of the structures behaviour, for example using strain gauges to measure individual wire strains or studying the fretting fatigue of a wire.

Because of a traditional emphasis on the first type of experimental research there is a general lack of understanding of the basic fatigue phenomena. Fatigue models have generally been simple extensions of a static model with little attempt to incorporate some of the fundamental process. This thesis is mainly concerned with understanding the fatigue process in rope and hose, but is also concerned with demonstrating that assuming endurance properties are a simple extension of static breaking properties is generally inappropriate and can at times can be highly misleading.

1.9 Overview of thesis

This thesis begins in Chapter 2 by describing an experimental investigation into the take up of load beyond a break in a single wire in a rope and the influence of fatigue cycling on this behaviour. The experimental technique used multiple strain gauges to measure the strain in individual wires. Results from these experiments reveal the transience of the effective length under load cycling conditions as well as its dependence on the load in some circumstances.

The same experimental technique is used in the work described in Chapter 3 which looks at wire strain distributions between wires in a rope in fatigue and overloading conditions. The strain distribution is then correlated with the endurance of a rope. A simple numerical model is implemented to assess the effect of strain distribution on endurance for a number of different strain distributions. The implications which the results from the model have on the manufacturing quality of rope are then discussed.

Attention is then turned to hose. Chapter 4 describes a series of tests to measure the strains in the reinforcement wires and the axial deformation of a number of helical wound thermoplastic wire hoses. The results are then compared to predictions from a structural model which is derived in the same chapter. The simultaneous non-linear equations for equilibrium and compatibility from the model are solved using a minimising Newton Raphson technique.

Chapter 5 continues the analysis on hose and moves on to its fatigue performance. Experience has shown that the fatigue of the type of hose studied here results from a break up of wires which is caused by high contact stresses and fretting between adjacent layers. Because of the lack of research of this phenomenon in hose, a review of related research in the rope field is presented. Theoretical calculations of the stress environment of three different wire contact configurations are then made. Based on the review of related work and the stress calculations a number of improvements to the hose design are proposed in order to improve its endurance.

Chapter 6 summarises all the major conclusions and implications from the previous chapters. A number of aspects of hose and rope behaviour are then compared and discussed. Finally a number of areas where the work of this thesis could be continued are outlined.

1.10 References

1. Ito, M., *Cable-Supported Bridges: Design Problems and Solutions.* Journal of Construction Steel Research, 1996. **39**(1): p. 69-84.

2. Ridge, I.M.L., *Bending Tension Fatigue of Wire Rope (PhD Thesis)*, in *Engineering Department*. 1992, University of Reading: Reading. p. 321.

3. British_Ropes, *Ropes for the Mining Industry*. 1970, Doncaster.

4. Feyrer, K., *Wire Ropes Under Fluctuating Tension and Bending.* Wire, 1993. **43**(1): p. 48-52.

5. Verreet. *The Influence of Wire Rope Fatiigue Research on Crane Standards and Crane Performance.* in *OIPEEC Round Table Conference.* 1997. Reading, UK: OIPEEC.

6. ANSI/ASME_B30.3, *Hammehead Tower Cranes.* 1984.

7. Liebherr_Tower_Cranes, *http://www.cokerequipment.com/liebherr.html*, . 1998.

8. Teerling, H.L.J., *Strength and Stiffness of High Pressure Hoses (PhD Thesis in English)*, in *Wiskunde en Natuurwetenschappen.* 1994, Rijksuniversiteit Groningen: Groningen. p. 150.

9. Gostick, G.H. *Flexible Hose- The Vital Link for the Offshore Industry.* in *Rubber in Offshore Engineering.* 1983. London.

10. Anon, *Polyflex High Pressure Hoses-Product Catalogue*, . 1992, Polyflex Gmbh: Huttenfeld, Germany.

11. Gordon, J.E., *Structures: or why things dont fall down.* 1978, London: Penguin Science.

12. Benham, P.P., R.J. Crawford, and C.G. Armstrong, *Mechanics of Engineering Materials.* 2nd ed. 1996, Essex: Longman.

13. Cook, J. and J.E. Gordon, *A Mechanism for the Control of Cracks in Brittle Systems.* Proceedings of the Royal Society, 1964. **A282**: p. 508.

14. Hruska, F.H., *Calculation of Stresses in Wire Ropes.* Wire, 1951(September): p. 766-801.

15. Evans, C.W., *Hose Technology.* 1974: Applied Science Publishers.

16. Grossman, S. and W. Derrick, *Advanced Engineering Mathematics.* 1988, New York: Harper and Row.

17. Lee, W.K., *An Insight into Wire Rope Geometry.* International Journal of Solids and Structures, 1991. **28**(4): p. 471-490.

18. Costello, G.A., *Analytical Investigation of Wire Rope.* Applied Mechanics Reviews, 1978. **31**(7): p. 897-900.

19. Seale, T., *Wire Rope or Cable*, . 1885: USA.

20. Davies, T.H. *Steel Wire Ropes Used in Mining Practice.* in *Wire Ropes in Mines.* 1950. Leamington Spa, Warickshire: The Institute of Mining and Metallurgy.

21. Searle, K., *Thermoplastic Hose- Selection and Use.* Power, 1981. **1981**(April): p. 170-174.

22. Beercheck, R.C., *New Thermoplastic Hose Thrives in Harsh Service.* Machine Design, 1984. **1994**(April): p. 78-83.

23. Raghaven, C. and J. Olsen. *Development of a 7000 Bar Hose.* in *5th American Water Jet Conference.* 1989. Toronto: USWJTA.

24. Manning, W.R.D. and S. Labrow, *High Pressure Engineering.* Chemical and Proccess Engineering Series, ed. I.L. Hepner. 1974, London: Leanard Hill.

25. SAE, *Test and Procedures for SAE 100R Series Hose and Hose Assemblies,* . 1991, Society of Automative Engineers.

26. Stratfold, M. and L. Legallais. *Design of Umbilicals for Maximum Flex Fatigue Performance of Electrical Conductors.* in *Marinflex.* 1992. London: BPP Ltd.

27. Estrier, P. *Updated Method for the Determination of the Service Life of Flexible Risers.* in *Marinflex 92.* 1992. London: BPP.

28. Clayton, P.A., *The Encyclopaedia of Wire.* 1980: Wire Industry. 120.

29. Adam, A.T., *Wire Drawing and Cold Working of Steel.* 1925, London: H.F. and G. Witherby.

30. Anon, *Steel Wire: Review of a Versatile Design Material.* Design News, 1983. **March**: p. 94-97.

31. Orrock, C.M., *Hooked on Heavy Metal?* ICCC Newsletter, 1993. **17**: p. 17-23.

32. Franklin, J.R., R.P. Preston, and C. Allen, *Heat Treatment and Alloying of Drawn Wires.* Wire Industry, 1980. **November**: p. 967-972.

33. Langford, G., *A Study of the Deformation of Patented Steel Wire.* Metallurgical Transaction, 1970. **1**(February): p. 465-477.

34. Langford, G., *Deformation of Pearlite.* Metallurgical Transactions, 1977. **8A**(June): p. 861-875.

35. Franklin, J.R. and C. Allen, *Patenting of Steel Rod and Wire.* Wire Industry, 1980. **47**(563): p. 958-966.

36. Walker, P.M.B.E., *Material Science and Technology Dictionary.* 1993, Edinburgh: Chambers.

37. Entwistle, K.M. and P. Myerscough, *The Measurement of Axial Internal Stress in Steel Wire.* International Journal of Mechanical Science, 1983. **25**(11): p. 823-831.

38. Willemse, P.F., B.P. Naughton, and C.A. Verbraak, *X-Ray Residual Stress Measurements on Cold Drawn Steel Wire.* Material Science and Engineering, 1982. **56**: p. 25-37.

39. Hutchinson, J.M. and J.C. Hamer, *Design and Testing of a Pneumatic Friction Brake*, . 1991, PCS: The Technology Transfer Centre, Imperial College.: London.

40. McClelland, A.E. *Failure in Wire Ropes in British Colliery Practice.* in *Wire Ropes in Mines*. 1950. Leamington Spa, Warrickshire: The Institute of Mining and Metallurgy.

41. Chaplin, C.R., *Failure Mechanisms in Wire Ropes.* Engineering Failure Analysis, 1995. **2**(1): p. 45-57.

42. Stead, J.E., Journal of the West of Scotland Iron and Steel Institute, 1912. **19**: p. 169.

43. Trent, E.M., *The Formation and Properties of Martensite on the Surface of Rope Wire.* Journal of the Iron and Steel Institute, 1941. **143**: p. 401-419.

44. NCB, *Ropeman's Handbook.* 1983.

45. Vereet, R., *The Rotational Characteristics of Steel Wire Ropes.* 1997: Casar Special Wire Ropes.

46. Rebel, G. *The Torsional Behaviour of Triangular Strand Ropes for Drum Winders.* in *OIPEEC Round Table Conference*. 1997. Reading.

47. Costello, G.A., *Theory of Wire Rope*. 1st ed. Mechanical Engineering. 1990, New York: Springer-Verlag. 106.

48. Matanzo, F. and J.T. Metcalf. *Efficiency of Wire Rope Terminations Used in the Mining Industry.* in *OIPEEC Round Table Conference*. 1977. Luxenburg: OIPEEC.

49. Verreet, *Wire Rope End Connectors*, . 1997, Casar Special Wire Ropes: Aachen, Germany.

50. Dodd, J.M., *Resin as a Socketing Medium.* Wire Industry, 1981. **48**: p. 343-344.

51. Ganthman, D.W., *Resin Socketing for Wire Rope Attachments.* Wire Journal, 1979. **12**(6): p. 82-85.

52. Müller, H., *The Properties of Wire rope under Alternating Stresses.* Wire World, 1961. **3**(5): p. 249-258.

53. Gibson, P.T., C.H. Larsen, and H.A. Cress, *Determination of the Effect of Various Parameters on Wear and Fatigue of Wire Ropes used in Navy Rigging Systems*, . 1972, Batelle's Columbus Laboratories.

54. Chaplin, C.R., *Prediction of the Fatigue Endurance of Ropes Subject to Fluctuating Tension.* OIPEEC Bulletin, 1995. **70**: p. 31-39.

55. Casey, N.F. *The Fatigue Endurance of Wire Rope for Mooring Offshore Structures.* in *OIPEEC Round Tablee Conference*. 1993. Delft, Holland.

56. Chaplin, C.R. *Prediction of Endurance of Offshore Mooring Ropes.* in *OIPEEC Round Table Conference*. 1993. Delft, Holland.

57. Ridge, I.M.L., *Bending Tension Fatigue.* OIPEEC Bulletin, 1993. **66**: p. 31-50.

58. Tilly, G.P., *Long Term Serviceability of Bridge Cables*, in *Strait Crossings*, J. Krokeborg, Editor. 1990, Balkema: Rotterdam. p. 347-354.

59. Yeung, Y.C.T. and J.M. Walton. *Accelerated Block Tension Fatigue Testing of Wire Ropes for Offshore Use.* in *OIPEEC Round Table Conference*. 1985. Glasgow.

60. Goodman, J., *Mechanics Applied to Engineering*. 1899: Longman, Green and Co.

61. Chaplin, C.R., *Tension-Tension Fatigue in Mooring Ropes for Offshore Structures.* OIPEEC Bulletin, 1988. **56**: p. 9-22.

62. Esslinger, V. . in *Workshop on Length Effects on Fatigue of Wires and Strands*. 1992. El Paular, Madrid.

63. Chaplin, C.R. *Tensile Fatigue of Very Short Samples of Stranded Wire Rope.* in *Workshop on Length Effects on Fatigue of Wires and Strands*. 1992. El Paular, Madrid.

64. Raoof, M. and R.E. Hobbs, *Analysis of Axial Fatigue Data for Wire Ropes.* Fatigue, 1994d. **16**: p. 493-501.

65. Raoof, M. and I. Kraincanic, *Recovery Length in Sheathed Spiral Strands in Deep-Water Platform Applications.* International Journal of Fatigue, 1993. **15**(6): p. 485-492.

66. Husain, Z., Z.A. Siddique, and R.A. Cottis, *Corrosion Fatigue of Mooring Rope*, . 1988, Corrosion and Protection Centre, UMIST: Manchester.

67. Miller, S.N., *Systematic Techniques of Hose Failure Mode Analysis.* SAE Technical Paper Series, 1991. **910577**: p. 1-17.

68. Cherimak, M.A., *Diagnosing Hydraulic Hose Failure.* Heavy Duty Equipment Maintenance, 1973. **March/April**: p. 62.

69. Buzzelli, G., *Troubleshooting Hose Failures.* Plant Engineering, 1993. **October**: p. 64-68.

70. Briggs, J., *Causes and Prevention of Hose Failures.* Quality Management and Engineering, 1975. **May**: p. 16-19.

71. ASTM-D518-86, *Standard tests method for rubber deterioration- surface cracking.* 1986.

72. NCB, *Two-Wire-Braid Reinforced Rubber Hose, End Fittings, Hose Assemblies and Machine Outlets.*, 1973, National Coal Board: London.

73. Eleftherakis, J.G. and E.C. Fitch, *Assessing Hydraulic Hose/ Coupling Integrity.* SAE Technical Paper Series, 1987. **870260**: p. 1.1052-1.1061.

74. Haisler, W.E., N. Chandrasekaren, and L. Oliver, *A Finite Element analysis of hydraulic hose couplings.* SAE Technical paper series, 1986.

2. Wire failures in ropes and their influence on local wire strain behaviour in tension-tension fatigue

2.1 Summary

This chapter is concerned with the take up of load by a wire at either side of a break, over a length known as 'effective length', and how this is affected by fatigue cycling. Additionally the effect of a wire break on other wires at the same cross section is investigated. A review of previous work reveals that although a number of researchers have investigated wire breaks and effective length, none have looked at how fatigue loading will influence the effective length of a wire break.

A new experimental set-up is described utilising twelve individual strain gauges placed on wires and monitored simultaneously via a custom built amplifier and specially written software. The test procedure also uses a method of artificially breaking wires without damaging other wires locally.

The results indicated that a considerable amount of slippage can occur for up to 20,000 cycles after a wire break causing the effective length to change from two rope lay lengths to around three. The effective length was found to be much lower for Lang's Lay rope than Ordinary Lay and this was attributed to the higher interlayer forces in Lang's Lay ropes.

With respect to the effect of broken wires on wires at the same cross section it was found that the strains in wires in the same strand will be primarily increased although wires strains in adjacent strands will also increase to some extent. Wires on the opposite side of the rope were found to actually decrease in strain after the break and this was attributed to local bending effects.

2.2 Review of related research

2.2.1 Correlation of wire breaks and strength with fatigue life

One obvious method of characterising the behaviour of a rope in fatigue is to correlate a measurable attribute of the rope with the fatigue life. A number of researchers have conducted experimental work to correlate the number of wire breaks and the static breaking load with the percentage of expected life completed at various points throughout the life of the rope. Only the tension-tension (T-T) fatigue cases will be discussed here.

Stonsifer and Smith [1-3] carried out a series of experiments in T-T fatigue on five different constructions of 6 strand rope (all Seale with IWRC) and one multi-strand rope (19x7) with IWRC.

By using the fairly unusual technique of testing two nominally identical ropes in parallel, they were able to stop different tests at various discreet fractions of the rope endurance and then strip one rope down to the wires to count wire breaks and use the other rope to find the residual static strength. In this way they were able to see how the two parameters were related and also to see how other factors such as cyclic load levels affected them.

With respect to the multistrand rope, they separated the site of wire breaks into core, inner layer of strands and outer layer of strands and found that the most breaks occurred in the core (e.g. 130 breaks/m cycling at 50 % of ultimate breaking load (UBL)), the inner layer of strands saw significantly less (e.g. 30 breaks for the same region) and the outer strands saw very few (around 3 for the same region). Looking at the various six strand ropes they found the majority of wire breaks to occur at the location where the outer strand contacted the core, the so called 'E' location as shown in Figure 2.1 (a), and the analysis of wire breaks against cyclic load level was conducted for this location of break (Figure 2.1 (b)).

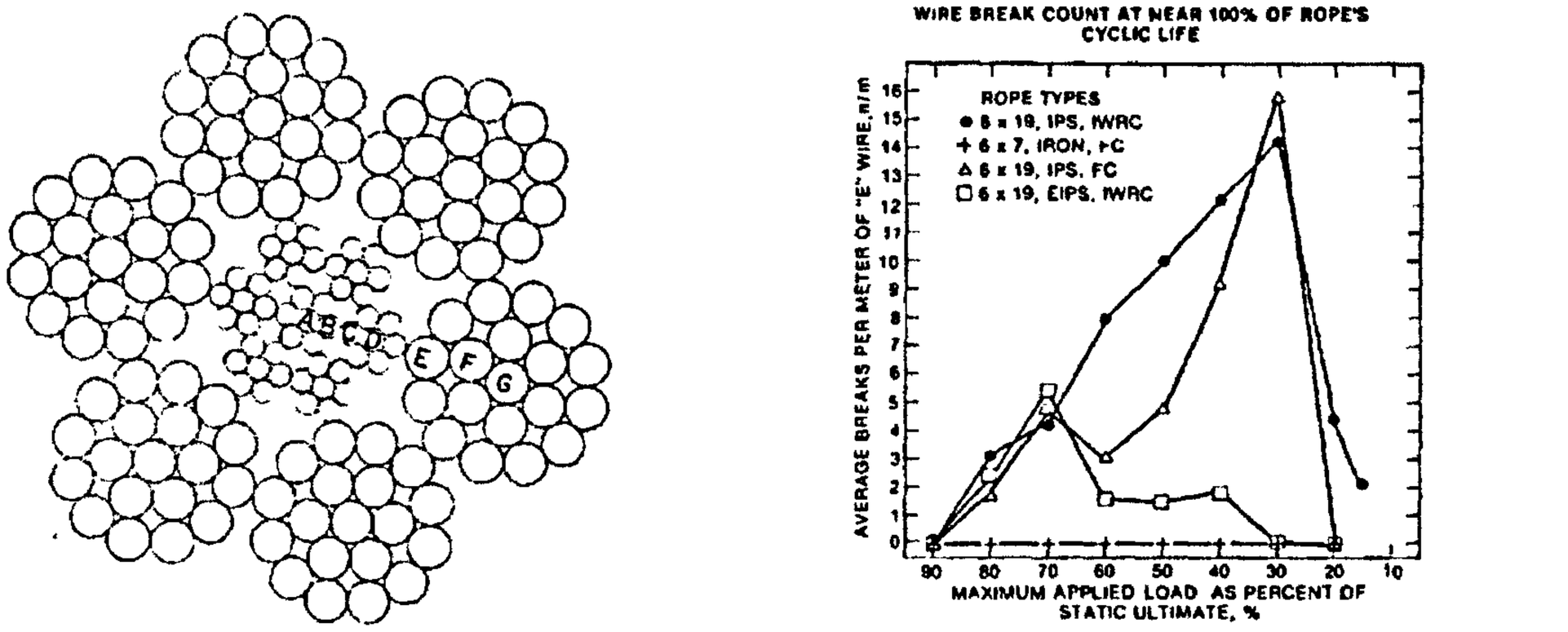

(a) (b)

Figure 2.1. (a) The most common location of wire break within a six strand rope is shown to be the 'E' wire. (b) The frequency of 'E' wire breaks for four types of six strand rope at varying load level, from [2].

They found that there was no direct correlation between fatigue load level and number of wire breaks at the end of life of a rope.

However the number of wire breaks just before failure was found to exhibit a peak at a particular cyclic load level and tail off at loads greater or less than this. Unfortunately the cyclic load at the peak (as a fraction of ultimate breaking load - UBL) was found to be highly dependant on the exact construction of the rope(see Figure 2.1 (b)).

Looking at the effect of cyclic load level on wire break density, they found a consistent deterioration of breaking strength throughout fatigue life for three levels of cyclic load (see Figure 2.2 (b)). They also found a relationship between the number of wire breaks and the percentage of fatigue life for a particular cyclic load level (Figure 2.2 (a)), but they could not find any correlation between the two (i.e. between strength and wire breaks).

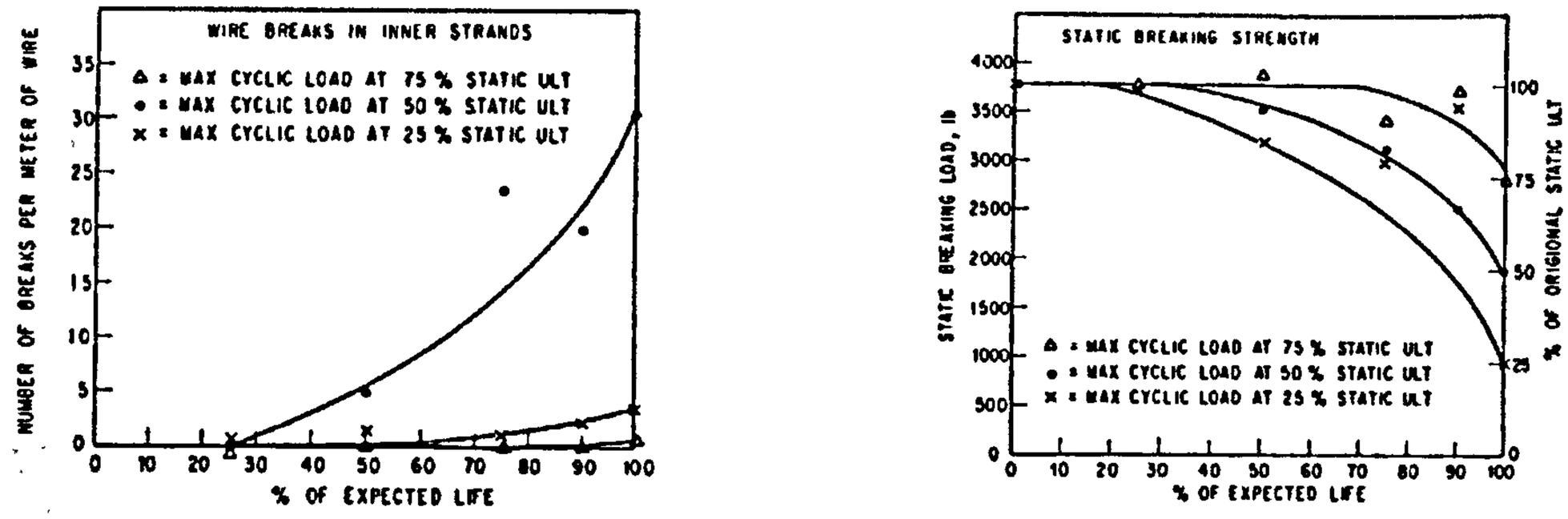

(a) (b)

Figure 2.2. *(a) The relationship between wire breaks and life for three levels of cyclic load (b) The relationship between static strength against percentage of expected life for three levels of cyclic load (19x7 multistrand rope) from [2].*

2.2.2 The effects of multiple wire breaks on rope integrity

2.2.2.1 The effect of radial distribution of wire breaks on rope breaking strength

Chaplin, Potts and Tantrum [4, 5] examined the effect of the distribution of wire breaks around a rope cross section on the breaking load of the rope, by introducing deliberate wire breaks in the rope. For example they found that, for a normal well greased rope, four adjacent wire breaks gave a three times greater decrease in static strength than four breaks distributed more equally about the circumference of the rope. For a degreased rope, however, the effect of the wire breaks on the strength loss was decreased. They concluded that the effect of wire breaks on rope strength in tension is not always directly proportional to the equivalent loss of cross sectional area but is also dependent on the concentration of wire breaks around the cross section (asymmetry), the distribution of wire breaks axially and the state of lubrication of the rope.

An attempt to quantify this asymmetric effect was made by Oplatka and Roth [6] after an accidental rope failure in a cable car application initiated a test series. The asymmetric effect was quantified in terms of factor '*k*' where (1-*k*) multiplied by the remaining cross

sectional area gives the strength ratio (before and after wire breaks). They found that k tended to be from 0-0.1 for symmetric wire breaks but as high as 0.5 for asymmetric wire breaks. It was also found that Lang's lay ropes had considerably higher sensitivity to asymmetric wire breaks than ordinary lay ropes and this was attributed to the lower torque generated in the ordinary lay ropes.

2.2.2.2 Derivation of effective length from strength

In an attempt to determine the effective length of a broken wire in tension, Davidsson [7] used the following logic: for a given break density he assumed the break distribution was even and so the average distance between wire breaks could be used in calculations (this break distribution value was termed a). He then went on to discuss how the weakening effect will be related to the effective length l_e, of the wire break and the break distribution, a, so that it would be proportional to l_e/a. Measuring the loss in strength and knowing the break density it was possible to derive a value for the effective length (see Figure 2.3). For a variety of ropes (Seale, Filler and equal gauge/cross lay) the effective length was calculated and values recorded ranged from one to two lay lengths. It was found that internal wires tended to have an effective length roughly half that of the external wires and that the state of lubrication within the rope would affect the value to some extent.

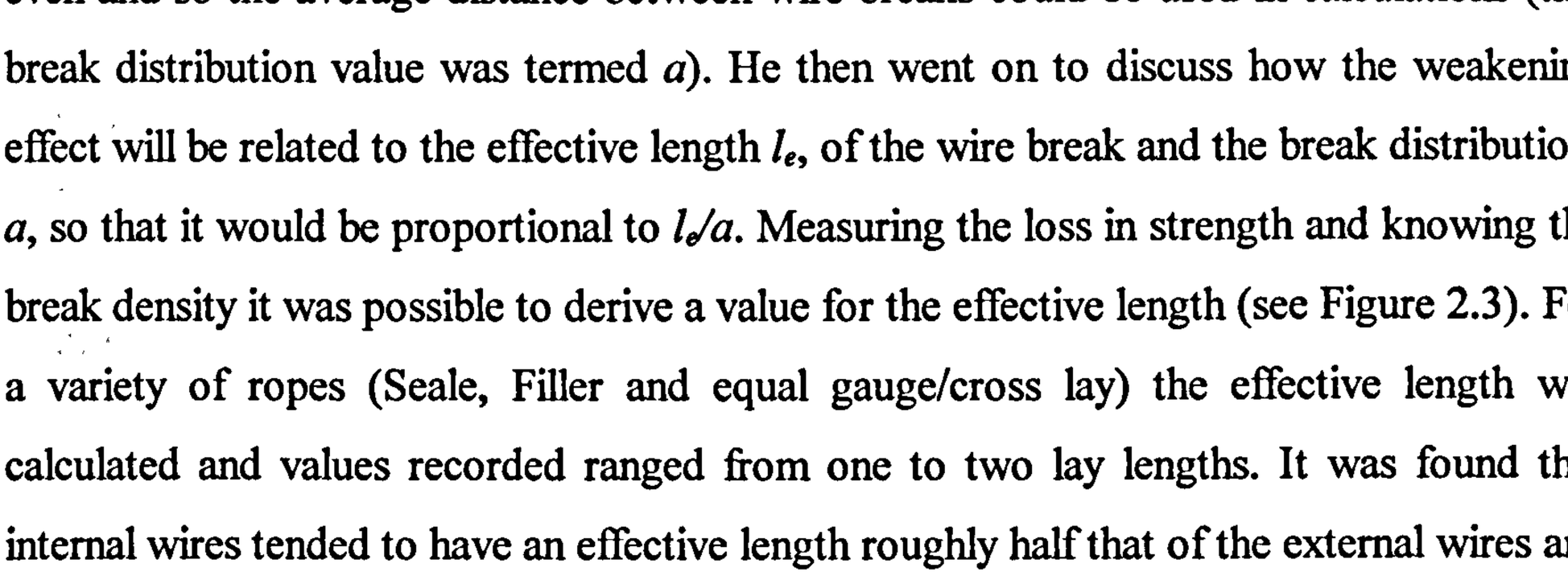

Figure 2.3. Method of dealing with cumulative wire breaks, assumes uniform distribution of wire breaks, separated by axial distance 'a', from [7].

Cholewa [8], considered the length along a rope in which a broken wire regains its full share of the load. Laboratory tests were made on both new and used ropes with artificial wire breaks. Results showed that, for practical purposes, the recovery length of a broken wire in a six strand ordinary lay rope with a triangular strand was around two rope diameters (i.e. around 0.4 rope lay lengths). Some difference was observed in the recovery length between new ropes and those which had been in service. In another work [9], tests were carried out on a 36 mm triangular strand Lang's lay rope. A number of wire breaks were made over a range of test lengths between zero (all on same cross section) and 40 rope diameters. Graphs are presented showing the relationship between actual loss of strength and the loss determined using information from magnetic testing equipment. Later, Cholewa [10] conducted a series of tests on 18 mm 6x19 Seale construction ropes in T-T fatigue. He used a simple technique for summing the cumulative wire breaks (similar to that used by Davidsson [7]) by the summation of 'rope weakening triangles' but not necessarily assuming a constant distribution of wire breaks (see Figure 2.4). Three hypothetical relationships for the load take up of the wire between the break and the recovery length were used (see Figure 2.4). The weakening effect of multiple wire breaks is calculated for a number of ropes with broken wires, some with deliberate breaks and others with breaks arising in service. The effective length was then varied in the summation until the strength loss fitted with that actually seen by breaking the rope. In this way Cholewa was able to calculate an effective length for wire breaks, which they found to be in the region of 4 to 8 rope diameters (i.e. between 0.65 and 1.25 times the rope lay length).

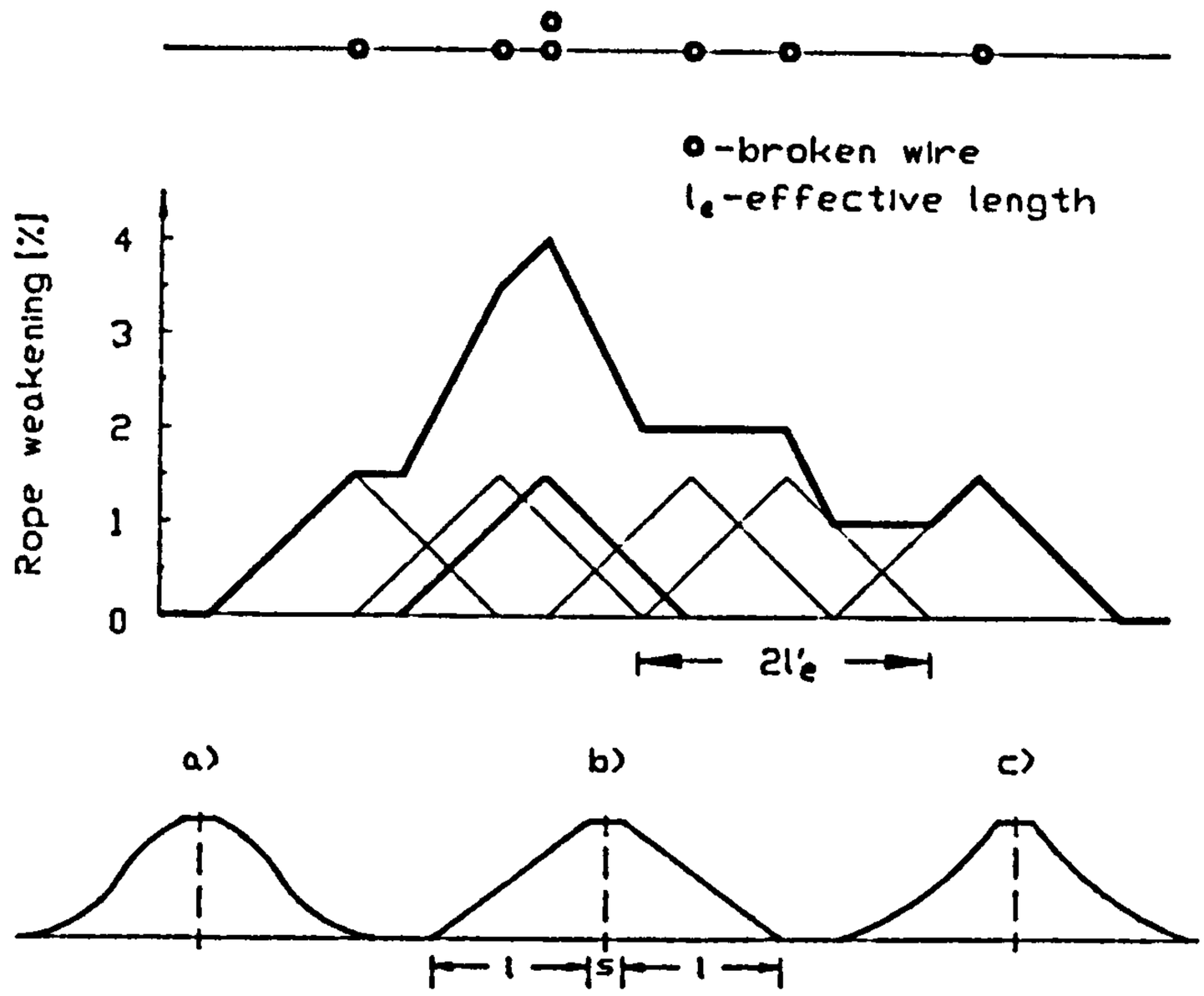

Figure 2.4. Method a summing wire break weakening effect for unevenly distributed wire breaks (above) and three hypothetical relationships of wire load take up at increasing distance from a break as used by Cholewa, from [9].

Chaplin and Tantrum [11], used break load tests to investigate the effect of wire breaks and lubrication on the effective length. By putting artificial wire breaks at various axial separations they could then assess their interactive effect during a break test. It was seen that there seemed to be a considerable degree of scatter in break load results for deliberately damaged ropes and this was attributed to manufacturing inconsistencies. However they were able to derive an effective length and found it to be up to approximately 1.5 rope lay lengths for a well lubricated rope but only about 0.75 lay lengths for a degreased rope. The implications from this work are that a break load test will not necessarily give a good indication of the fatigue endurance, since a badly lubricated rope with breaks will have a higher breaking strength, but is likely to have a shorter fatigue life because of fretting problems.

2.2.2.3 Derivation of effective length from pull out force

Shitkow [12] noticed that individual wires often had more than one break in them and he was the first to suggest the idea of effective length. He attempted to measure the effective length by the use of two tensile testing machines, the first was used to pull the rope at a given tension, the second was used to try and pull a broken wire from the rope which had a second break at varying distances from the pulling positions. By this means he found that the pulling force was dependent on the load on the rope, the rope diameter and the construction of the rope (i.e. the lay type and length). He estimated that the recovery length could be anything from one to six lay lengths depending on these factors.

Working on a 19 mm Ordinary Lay Seale rope with IWRC, Chaplin and Tantrum [11] investigated the frictional forces acting on a wire which allow it to take up its full load. Using a technique similar to Shitkow [12] a broken wire was unwound from the rope slightly and then pulled axially with an instrumented device until the wire slipped. This was repeated for various rope loads and rope conditions. It was concluded that the frictional force acting on a broken wire was linearly related to the rope load and could vary by a factor of 5 depending on whether the rope was well lubricated or corroded and badly lubricated. These findings tied in with other tribological studies from Marguetts and Spikes [13].

2.2.2.4 Strain gauge measurements on wires with breaks

Wiek's work on wire breaks [14] used strain gauges to investigate the effective length on six strand ropes in tension. He carried out static tensile tests on an Ordinary Lay six strand rope with Seale construction and IWRC. Six gauges were placed on a single wire, each separated by one wire lay length. The wire was then broken twelve wire lay lengths from the first gauge, loaded to assess the strains and then subsequently broken eleven, ten, nine wire lay lengths away and so on, each time loading the rope to measure the effect on the wire strains. He found that a wire has regained 67 % of its original load within one wire lay length and 100 % after one rope lay length.

Molinari [15] used strain gauges to measure the take up of load in a broken wire within a single six wire strand. He used axially mounted strain gauges on the crowns of one wire at half lay intervals and also on the crowns of the other five wires at a cross section half a lay length from a deliberate break made in the first wire. By comparing the strain at each gauge position before and after the break, he showed that load sharing between the other wires is such as to maintain torsional and bending equilibrium of the strand. It was observed that by a distance of 2.5 lays from the break, the broken wires take about 20 % of the load they had before the break.

2.2.3 Models of the effective length

Chien and Costello [16] conducted a theoretical analysis of the load take up within a wire after a break. They used the frictionless assumptions based on 'curved rod' model from Costello [17]. They consider friction to be of little importance in analyzing the stresses in a straight rope providing the strands are not in contact with each other (this is the case for independent wire rope core). Using Saint Venant's principle they considered the rope and break analysis separately and assumed that the overall rope stress analysis would be unchanged by the wire break. Friction is essential for the take up of load after a wire break and this was considered for the wire in question and superimposed onto the original model.

Friction was modelled using Amontons' first and second laws of friction (i.e. that friction is independent of the contact area and proportional to the normal force [18]) using an assumed friction coefficient. They showed how this could be applied to two cases: the central wire of a 7 wire strand (6/1) and the outer wire of 6x19 (9/9/1) Seale rope with IWRC. With an assumed friction coefficient of 0.1, for the strand they calculated an effective length of 1.25 times the pitch whereas for the Seale rope they calculated an effective length of 1.18 times the rope lay length. This work did not attempt to measure the effective length experimentally or compare the result with any experimental data.

Raoof and Kraincanic [19] extended the theories developed by Costello and applied them to multilayer spiral strands. They also assumed Saint Venants' Principle for the calculation

of the inter-wire normal contact forces and used the first and second laws of friction to model the frictional forces. In the case of the multilayer strand the contact forces from wires on adjacent layers, which are wound in opposite directions, will often create a multi-contact point problem. They also took into account hoop contact stresses caused by adjacent wires in the same layer. All contact forces were calculated using the general model of Costello's [17]. Raoof and Kraincanic considered that wire within the effective length region would be in one of two states, full slip and no slip, and from previous work had calculated that the full slip condition existed for 90 % of the recovery length. The theory was used to calculate the recovery length in an extensive analysis. Four common strand constructions, two five layer, a six layer and an eight layer were modelled. Two of these strands were wound right hand (RH), left hand (LH), RH etc while the other two were wound RH, RH, LH, LH etc. The recovery length was calculated for every wire at varying helix angles(10-30°) and varying strand strains (up to 0.4 % strain). It was seen that the effective length in general varied between around 0.5 and 1.5 pitch lengths although on a few occasions it went as high as 2.75 and as low as 0.25. In some cases large variations were seen between the recovery length and the strand strain, however this was claimed to be of little significance and an upper bound value was taken for the comparison of recovery length with helix angle. There seemed to be a general decrease in recovery length with increasing lay angle which levelled out at around 25°. No attempt was made to measure the effective length experimentally or compare any predictions with existing experimental work.

2.2.4 Discussion

The results of Stonsifer and Smith [1-3] are very interesting and raise many doubts about the validity of using visible wire breaks as a discard criteria in tensile loading conditions. There are two major reasons for this. Firstly a large amount of wire breaks seem to occur at the strand to core contact point and are therefore very difficult to see. Secondly, a huge difference was found in the number of wire breaks at comparable load ranges for a number of types of very similar ropes (all Seale constructions). It seems that for a particular construction of rope there will be a specific fatigue load which will result in significant

levels of wire breaks before failure (but the fatigue load at which point this peak occurs will vary depending on the construction). A useful continuation of this work could try and focus on the mechanism which causes such a large break up, a combination of experimental and theoretical work may help to clarify this.

Table 2.1 Comparison of the effective length in various six strand rope constructions found through a variety of techniques.

Source of data	Effective length (rope lay lengths)	Rope types	Derived from	Break types
Shitkow [12]	1 to 6	various six strand	pull out force	external
Davidsson [7]	1-2 for external 0.5-1 for internal	Seale/filler and (12/6/1)	breaking strength	internal and external
Cholewa [8]	0.4	Triangular six strand (6x32)	breaking strength	external
Cholewa [10]	0.65-1	Seale OL FC	breaking strength	internal and external
Chaplin and Tantrum [4]	0.75-1.5	Seale OL IWRC	breaking strength	external
Wiek [14]	1	Seale OL IWRC	strain gauge	external
Chien and Costello [16]	1.18	Seale OL IWRC	theory	external

Much experimental work has concentrated on the effect of cumulative wire breaks on rope integrity, in particular for determining the effective length of a particular rope. There are many considerations and questions which still need to be answered: the effect of lubrication on the effective length is not clear, Davidsson [7] sees no significant difference in effective length between the ropes he tested with varying levels of lubrication. Chaplin and Tantrum [4] however, have shown how the effective length can be halved if a rope is poorly lubricated. As the state of lubrication is only ever described in a qualitative sense perhaps the answer to this is to define a more quantitative scale for state of lubrication, possibly involving stripping a small section of the rope and measuring the friction coefficient of the wires within the rope.

All measurements of effective length have been based on a static measurement and not measured the effect of cyclic loading. It is not known how the effective length will vary in

cyclic loading conditions. Many individual measurements of effective length have been made but there has been no real attempt to make a comparison with various measurements giving the rope constructions and method of measurement.

No investigation has been carried out to look at the relationship between wire load fraction as a function of distance along the wire from the break. It seems likely that the contact point with the core, or the strand to strand contact points (depending on the rope construction) will be a point which is critical to the effective length. There are high contact forces, and consequently high frictional forces at this location. In theory there should be a step up in the tension carried by a broken wire as it passes through one of these contact points.

Wiek [14] has demonstrated that the effective length of external wires in bending is approximately twice that of the equivalent configuration in tension. This has been attributed to the bending causing the broken wire to work itself looser from the rope. There are many unanswered questions in this respect, such as: is the effective length so dramatically increased from tension on internal wires or wire contacting the pulley? If Wiek's hypotheses is correct then it would seem unlikely. Are there any changes to the effective length with further cycling? Further experimental work could clarify these points.

Looking at the summary of various research findings in Table 2.1 it can be seen that there seems to be a considerable range of values for the effective length from 0.4 to 6. The smallest value seen, 0.4 by Cholewa, seems to make some sense since this is a large stranded rope and so the external wires are likely to take up tension quicker, since they have more contacting length per lay length. No researcher has attempted to monitor the effect of fatigue cycling on the effective length or look at whether there will be any variation in effective length between Ordinary and Lang's Lay ropes.

2.3 Experimental techniques

2.3.1 Preparation of rope specimens

2.3.1.1 Rope termination technique

There are many different methods of rope termination. For testing purposes if the properties of the rope are to be measured it is important that the termination does not cause a premature failure. The most suitable termination technique is the cast cone socket technique. The traditional method of this type of rope termination is by means of zinc casting. However this is generally unsuitable for tests in a laboratory environment because of the expense and difficulty in reusing end connectors. Resin socketing, where resin is poured into a mould has been suggested and tried by Gantham [20] and showed to work well in comparison to other methods by Dodd [21]. Chaplin and Sharman [22] investigated the mechanisms involved in resin socketing and found that although the wires initially adhered to the resin, the main gripping action on the wires is caused by a wedging action between the resin and the wires. Over a number of years resin socketing has been optimised at the University of Reading. Significant improvements include de-gasing and injecting rather than pouring resin to eliminate air bubbles in the socket. Additionally using a technique as shown in Figure 2.5 and Figure 2.6 allows convenient reuse of the endfittings without any of the traditional problems of having to remove a failed sample.

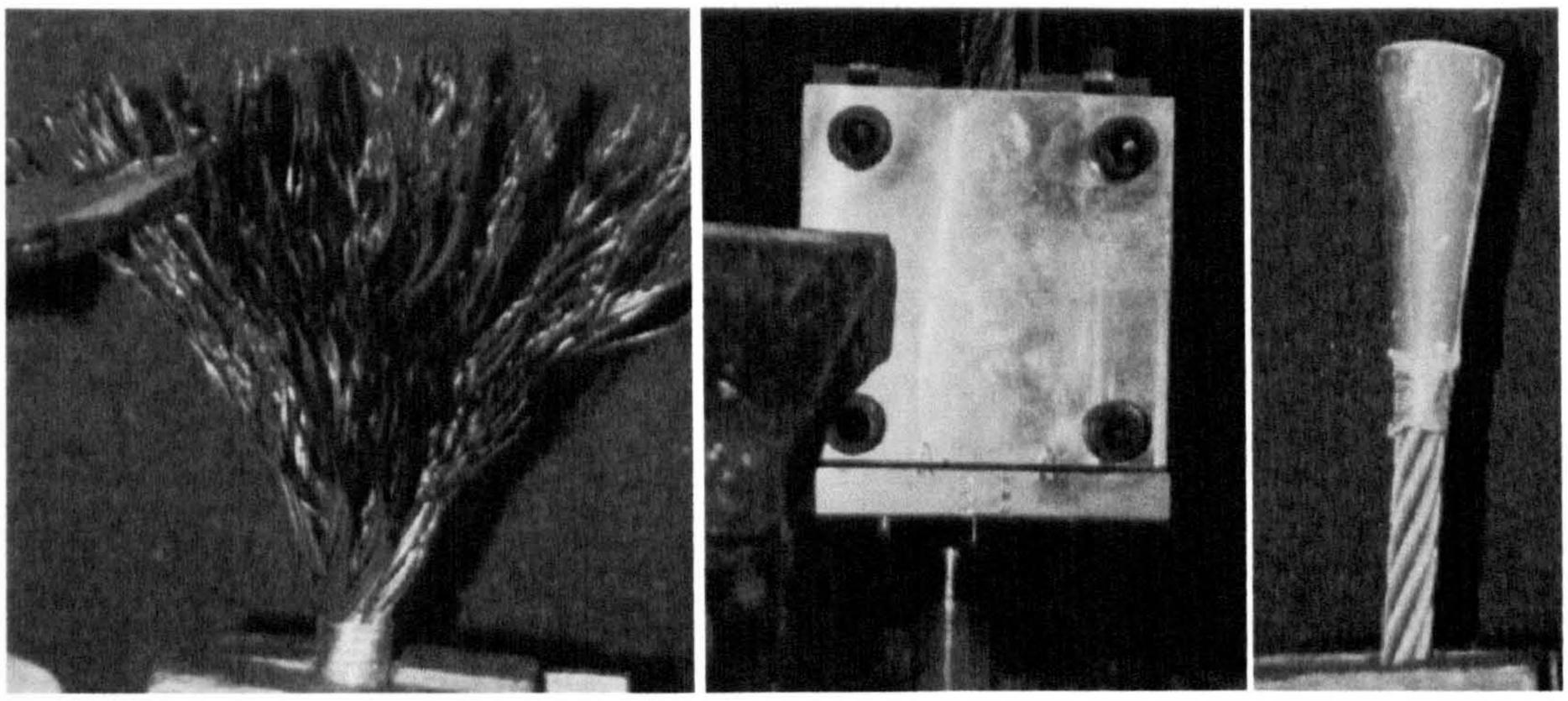

Figure 2.5. The stages in the preparation in a rope end, using polyester resin.

The wire rope specimen is taken from reels of rope and cut to length. Prior to cutting a thin flexible wire, called a serving, is wrapped around the rope at either end to prevent the wires from splaying out once the cut has been made. At a specified distance from the end of the rope (80-120 mm depending on the specific termination) a further serving is placed which marks the start of the termination. Once the rope is cut, the serving closest to the end is removed and the strands are separated and unwound causing a wide brush of exposed wires. Then the ends of the rope was cleaned using a water based degreaser (Gunk, AEC Ltd, Stafford) and allowed to dry. One end of the rope is then placed in a tapered mould, secured in place and held straight with a Vee guide and clamps. The mixture of resin (Polyester resin in styrene 'Strand', Scott-Bader Ltd), the talc filler (calcium carbonate filler from 'Strand') and a catalyst (Methyl Ethyl Keton peroxide from 'Strand') is then prepared in a flask. For the experiments described here the ratio of resin/filler/catalyst was approximately 1/1.5/0.05 by weight. The mixture was then placed in a vacuum chamber to remove air bubbles and subsequently injected into the mould. The termination was then allowed to cure overnight. Once the resin has hardened, the mould is removed and the process repeated for the other end of the rope. The rope terminations are held in fixtures, which are shown in Figure 2.6. Each fixture consists of two parts, the 'top hat' and the collets. The top hats are bolted directly to the testing machine flanges. Each 'top hat' has a tapered bore with the same angle as that of the rope termination, but

the internal diameter is larger than the rope end so as to allow the rope end to be inserted. Two collets are then positioned between these two tapered surfaces (the termination and the bore of the 'top hat') prior to testing as shown in Figure 2.6 (stage 5).

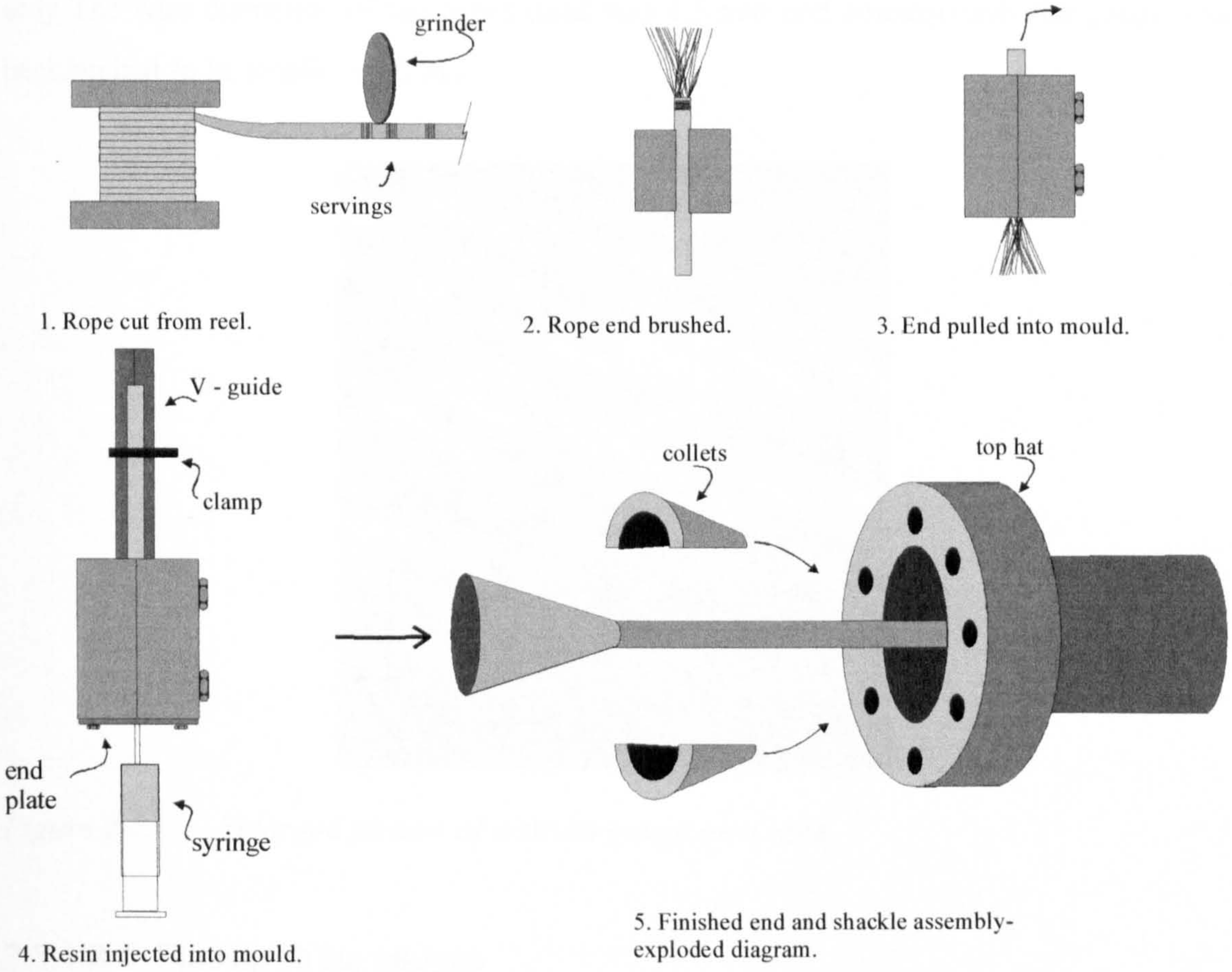

Figure 2.6. The various stages involved in terminating a specimen.

For static break tests the termination used was different from the normal fatigue test set-up owing to the significantly higher loads involved. For the 19 mm diameter Seale ropes used in this research the breaking loads were around 250 kN but the normal terminations tend to cause a failure at the rope termination interface beyond 230 kN. Therefore a longer resin cone and corresponding shackle was used for these tests which eliminated the end effects even at these critically high loads. As only a relatively small number of break tests were required a much simpler termination method was used, where the ends were moulded directly into the sockets.

2.3.1.2 Strain gauging of specimens

The strain measurements were made using surface mounted, metal foil strain gauges. In order to measure the strain of individual wires each gauge had to be attached to one wire only The wire diameters of the ropes used was 1.5 mm and consequently the gauge and backing had to be smaller than this.

Figure 2.7. Enlarged picture of a strain gauge on a rope.

2.3.1.2.1 Placing strain gauges

The attachment and wiring of the strain gauges was a difficult and time consuming task. Even with practice, 25 % of the gauges were damaged or badly aligned and needed to be refitted. The type of gauges used were marketed by Micro Measurement [23] type EA-06-031DE-120. Two versions of this model of gauge were used, one with pre-attached electrical leads and one without. Although the gauges which had leads were more expensive, they were preferred because they proved more reliable. The process of attaching the gauges onto the wire surfaces is described below.

Initially the specific wires to be gauged were marked with a felt pen. The wire surfaces where the gauge was to be located were then cleaned thoroughly and all the grease was

removed using a degreasing solvent, (isopropyl alcohol, (GC-6 [24]). Subsequently the surfaces were treated with a conditioning fluid, (a mild phosphoric acid compound (MCA-1[24])), and a fine emery paper to roughen the surface and improve the adhesion of the gauge. Finally the surface was wiped with a neutralising fluid, (an ammonia based fluid (MN5A-1 [24])), and allowed to dry for a few minutes. The sides of strain gauge were then trimmed off with a razor blade, making the trimmed gauge slightly smaller than the diameter of the wire (1 mm compared with a wire diameter of 1.5 mm). As discussed by Utting [25] experiments have shown that this trimming of backing has little or no effect on the functionality of the gauge, provided that the measured resistance of the gauge does not change significantly after trimming. The gauge was then attached to a piece of clear adhesive tape, the width of the tape being less than the length of the gauge as this made it easier to peel the tape off once the gauge cement has cured. The gauge was then aligned longitudinally along the axis of the wire and the tape pressed into contact. Once aligned, the gauge was pulled off the wire, but one end of the tape was left adherent to the rope to enable the gauge to be easily and accurately re-positioned at a later stage. The wire surface was then coated thinly with a catalyst for the glue. The back of the gauge itself was coated with a fast setting adhesive, epoxy-phenolic (M-Bond 610[23]). The strain gauge was then pressed firmly onto the wire with a soft material, such as an eraser, and held down. After removing pressure from the gauge it was left for ten minutes before attempting to remove the tape, to be sure the adhesive had cured. Finally the resistance was checked and the gauge replaced if there is no resistance reading or any value significantly different from the nominal 120 Ω.

2.3.1.2.2 Wiring of the specimen

The tiny tabs on the strain gauge are connected by fine wires to tabs which are glued on to the wire rope at either end of the gauge. It is very important to have an adequate length of connecting wire from the gauge to the tab to allow for relative movements of the wires in the rope during the loading cycle. From the small tabs at the end of the gauge a wire was connected to a fixed point, which was generally a strip of thick cardboard wrapped around

the specimen (see Figure 2.8) and taped or cable tied firmly in place. The wires were labelled during installation to avoid confusion.

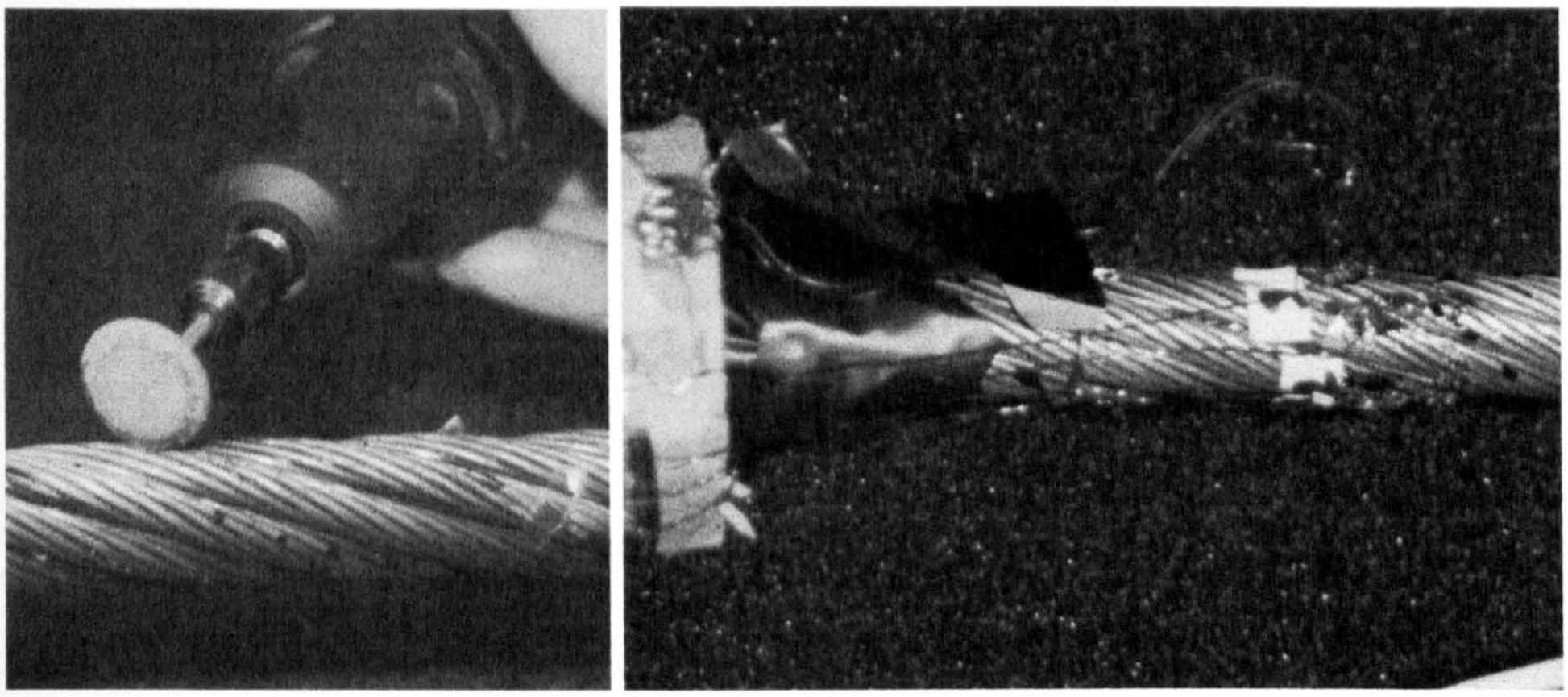

(a) (b)

Figure 2.8. (a) The technique for introducing wire breaks (b)The wiring of the strain gauges.

2.3.1.3 Artificial wire breaks

A technique had previously been developed [4] whereby a screwdriver was used to wedge a single wire out far enough so that it could be partially cut with a hacksaw. Once the wire was sufficiently damaged the rope was loaded up to a pre-determined maximum level (not more than the maximum fatigue load) to try and break the damaged wire. If the wire did not break the rope was unloaded and the wire was damaged further. This process was continued until the wire finally broke. This technique was found to be unsatisfactory for the current research as it resulted in some damage to adjacent wires and distortion of the sample. Additionally it was very difficult to use this technique without damaging the delicate strain gauge wiring. A hand held grinder was used to carefully remove material from a single wire. In order to prevent damage to adjacent wires a very small (1 mm wide) grinding wheel was used . Similarly to the previous technique, the rope was then loaded to

try to break the wire, and if this did not occur, the rope was unloaded and the wire was ground further.

With care it was possible to use this technique to break a wire with little or no damage to the wires around it and no distortion of the sample.

2.3.2 Wire rope experimental set-up

2.3.2.1 Strain gauge amplifier

Initially a series of tests were carried out on a wire rope in static tension with four strain gauges to assess the feasibility of the proposed experiments. These experiments were used to confirm that the strain gauges could be attached successfully to individual wires and useful strain measurements could be made. Each gauge was connected into a quarter bridge circuit. They were attached to four different wires at the centre of the rope. A Micro Measurements four channel 2120 strain gauge amplifier and conditioner was used to process the strain signal which was then displayed by a Laptop PC fitted with analogue to digital (A/D) converter. In each test the rope was loaded to a specific level and then unloaded. These preliminary tests demonstrated the importance of load history for understanding some of the aspects of wire strain behaviour. It was therefore decided that all strains must be measured simultaneously. An experimental set-up was designed with a greater number of strain gauges to give a more statistically meaningful indication of the distribution of wire strains within a rope. The only strain gauge amplifier available in the laboratory had four channels which limited tests to four quarter bridges (four strain gauges). However a greater number of channels were needed in order to measure the desired number of strain gauges.

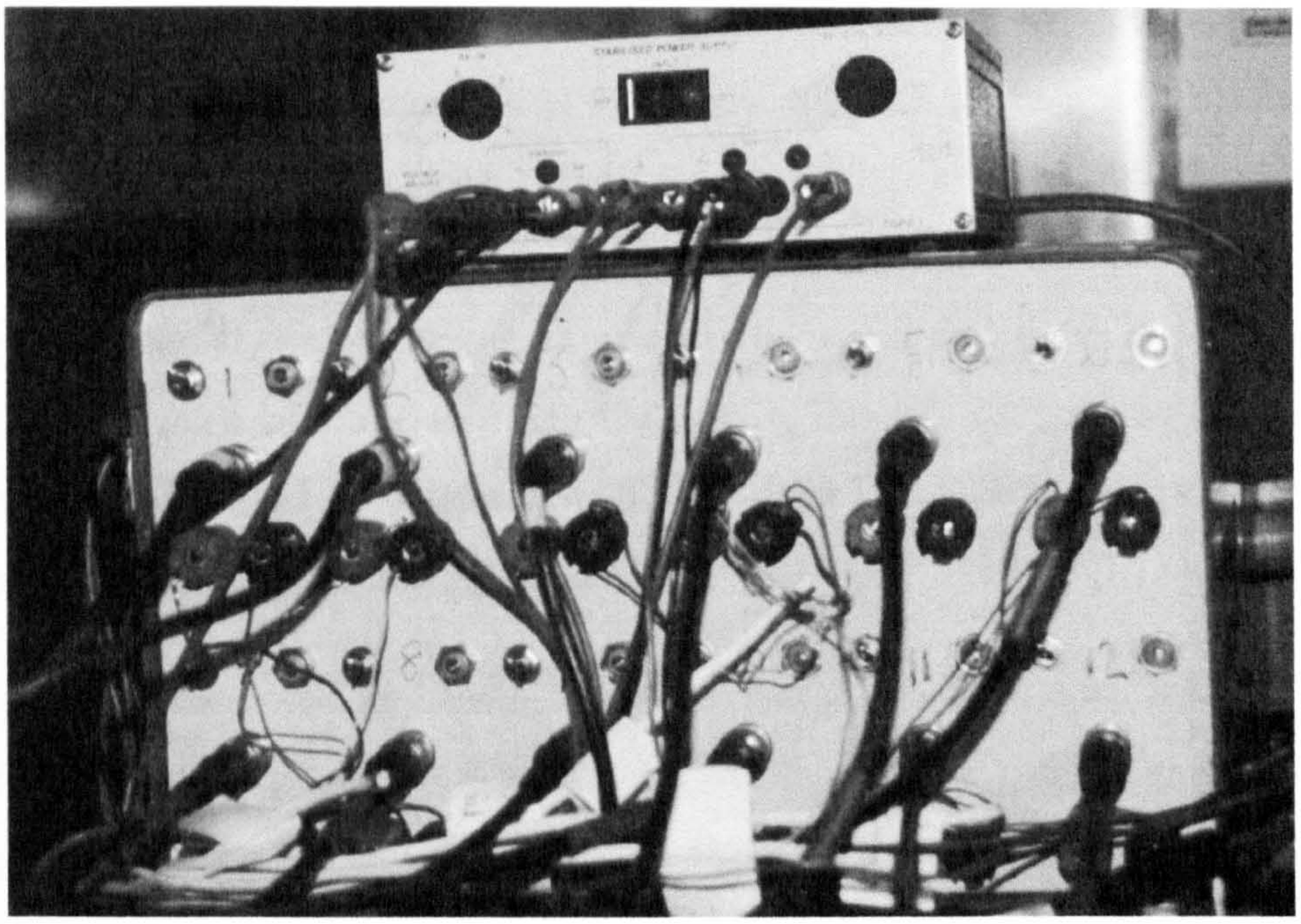

Figure 2.9. The custom built strain gauge amplifier.

A twelve channel amplifier (shown in Figure 2.9) using twelve discrete single channel amplifiers was built for the experimental work. When tested the device was found to have zero drift properties within a range of 1.5 % over one day and had no measurable gain changes with time. Each channel of the amplifier incorporated three dummy 120 Ω resistors to make up a full Wheatstone bridge. Calibration was achieved by wiring in a switch to a high resistor in parallel to one of the legs of the bridge, the resistance was calculated so as to simulate a 0.5 % strain.

2.3.2.2 Overall test set-up

The test set-up is shown in Figure 2.10. The tensile testing machine used was a Dartec with servo hydraulic drive rated at a maximum capacity of 250 kN and the capability of delivering a load fluctuation between 20 and 100 kN at a frequency around 1 Hz. The actual speed of fatigue cycling was kept at 0.8 Hz by a standard digital feedback controller built into the machine.

The control mechanism for the tests involved specifying the maximum load and minimum loads in the cyclic range and the desired frequency of cyclic loading. The machine then attempts to deliver these requirements using a feedback control based on the magnitude of the load. The danger of this load control mechanism is that when a sample starts to break the machine will rapidly accelerate out of control, to try and deliver the desired load. For this reason a trip must be introduced into the system. This will turn off the machine once the cross head has passed a predetermined limit, which is calculated to be equivalent to slightly more than the ropes breaking strain.

Twelve gauges were monitored using the strain gauge amplifier with built in bridges. Signals from the strain gauge amplifier, along with the load and stroke signals from the Dartec controller were fed into a laptop with an A/D PCMCIA card. These 14 voltage signals were connected to A/D card as single ended inputs, all sharing a common earth.

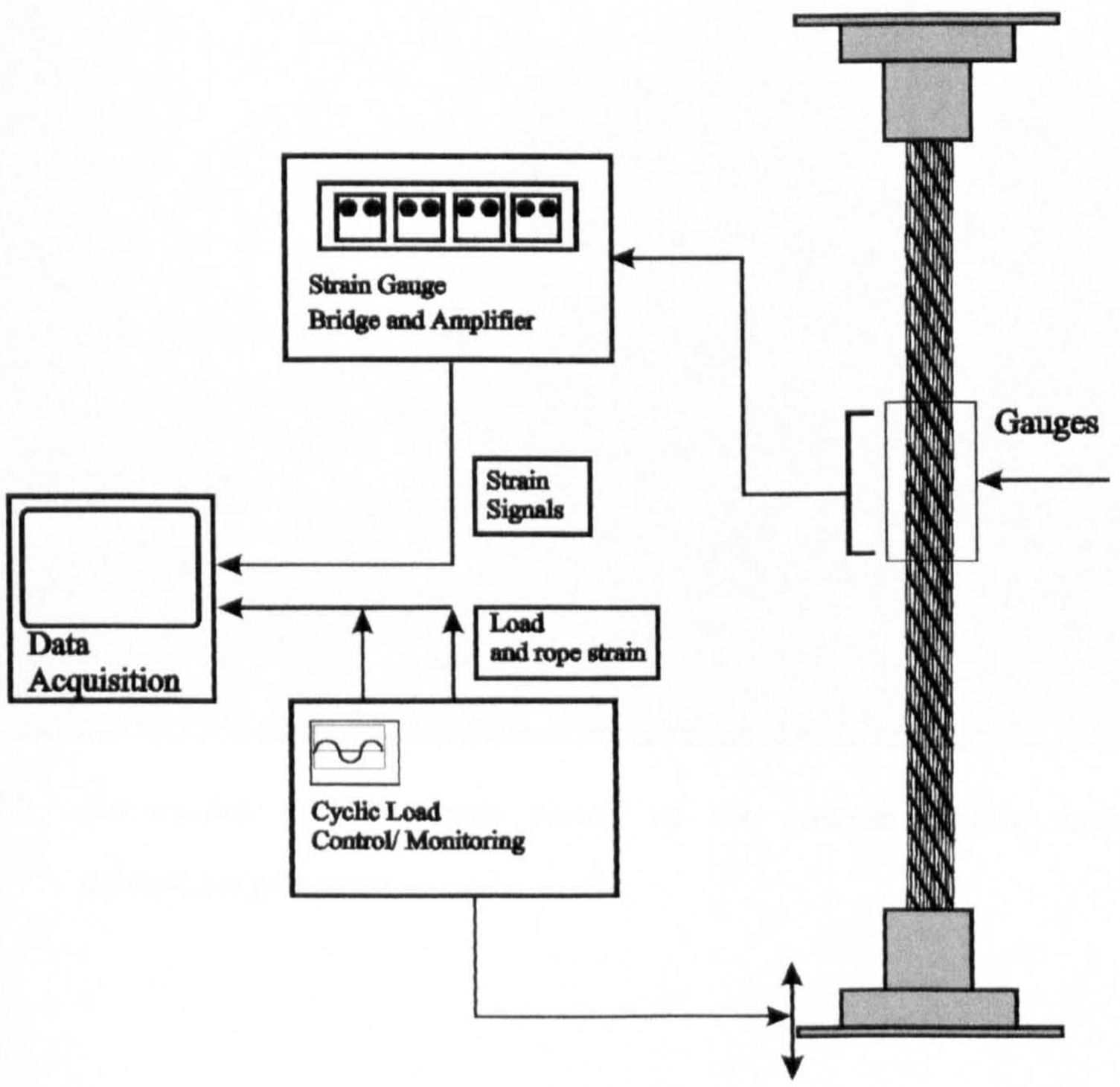

Figure 2.10. The overall test set-up schematically.

2.3.2.3 Rope data acquisition and analysis techniques

The data acquisition program was written using Labview, a graphical programming language specifically designed for data acquisition and reduction .The program was written specifically for this test series and allowed continuous data acquisition and the strains measured by each strain gauge to be plotted against the load on the rope. Once the data acquisition is complete the data can be exported as an ASCII text file for further processing.

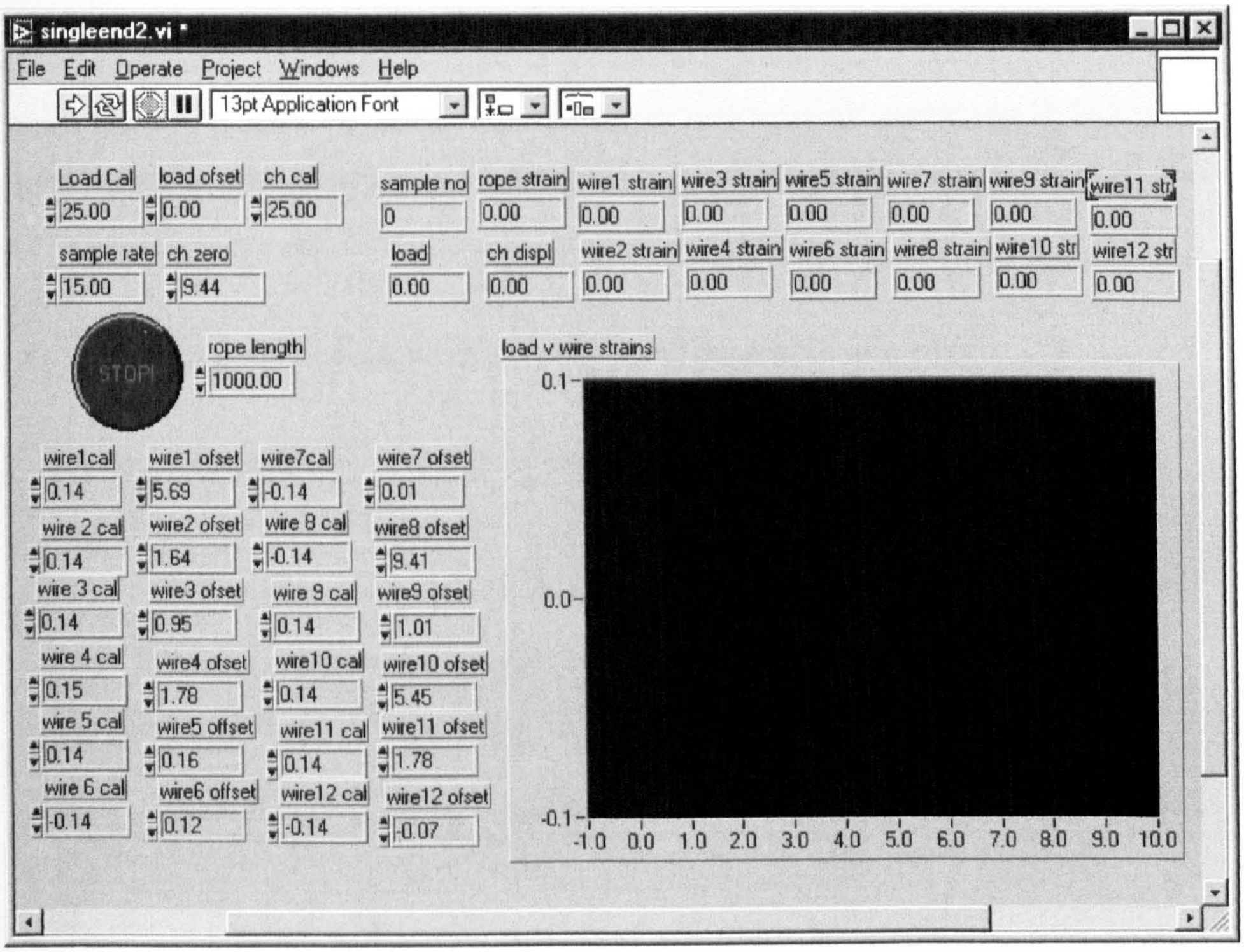

Figure 2.11. Screenshot of the 'front panel' of the custom written Labview data aquisition program.

2.4 Results

This section details tests carried out on two types of rope: a 19 mm Seale 6x19(9/9/1) right hand Ordinary Lay rope with IWRC and the same rope in Lang's lay.* All the wires used in the rope had a breaking stress of 1770 MPa. The exact specifications of the rope are given in the Appendix. Both ropes came from reels which were manufactured consecutively on the same machine, the only difference being that the direction of rotation of the closing process was one way for the Lang's lay rope and reversed for the Ordinary Lay rope. The reason for obtaining a 'pair' of ropes in this way was that it eliminated as many unpredictable variables as possible so that actual difference between Ordinary and Lang's Lay ropes could be identified. The fatigue tests were all carried out in T-T fatigue with a minimum load of 26 kN and a maximum load of 99 kN. As the ropes have an UBL of 250 kN this represents a fatigue range of 10-25 % of the UBL.

2.4.1 Effect of a wire break on the strain along the length of a wire

2.4.1.1 Ordinary lay

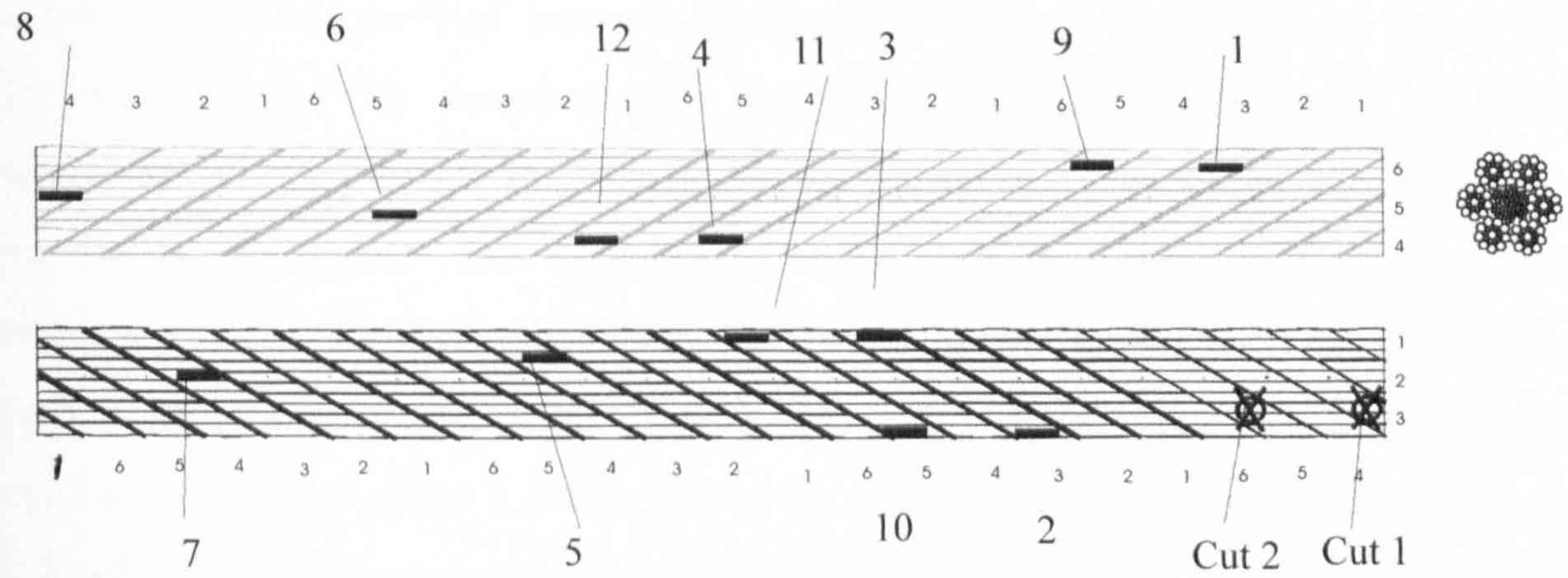

Figure 2.12. The configuration of strain gauges, 6 on each wire, one at each available location beyond breaks 1 and 2.

* both in a well lubricated condition

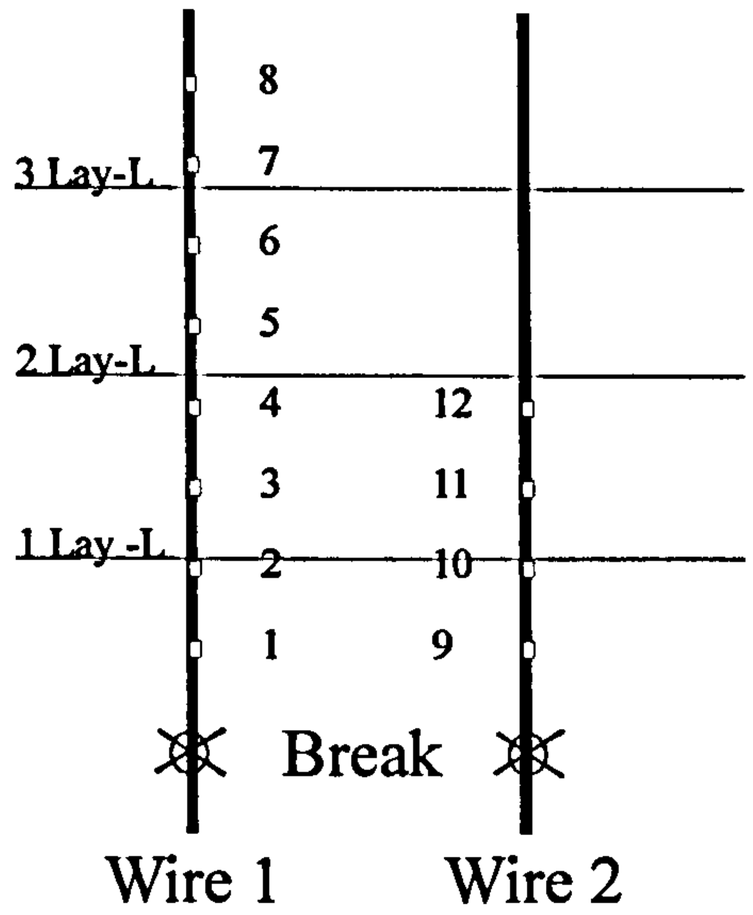

Figure 2.13. Simplified diagram of the strain gauge locations on the two wires.

The effect of 'breaking' the wires in the locations shown in Figure 2.13 on immediate wire strains can be seen between Figure 2.14 and Figure 2.15. Before being cut, gauges 3 and 5 show a linear wire behaviour. A few cycles after being cut gauge 3 reverts to a non-linear behaviour. Looking at the behaviour (Figure 2.14) it appears that at low load there is a very low strain gradient with a negative strain gradient (implying compressive strains) at the lowest loads. As the load increases the gradient becomes very similar to before the wire was broken. This would suggest that this flattening of the curve and wire compression is probably due to the wire having slipped along its length from the break since the time of failure. The compression would then be a result of the subsequent unloading. Wire 5 seems to be initially unaffected by the break. After 20,000 cycles however, gauge 5 has started to slip slightly before gripping (Figure 2.15). It can be seen from Figure 2.13 that gauge 5 is over 2 rope lay lengths which is larger than the 1.5 rope lay lengths previously suggested from static testing. It is not known if the wire was slipping beyond gauge 5, as gauges 6, 7 and 8 had all failed by this time. A further 60,000 cycles did not change the behaviour from that seen for gauges 3 and 5 in Figure 2.15. Figure 2.16 shows how the take up of load beyond a break varies from immediately after the break to 20,000 cycles after the break. It can be seen that initially the effective length

seems to be around 2.25 rope lay lengths but after 20,000 cycles it has extended to around 3 rope lay lengths.

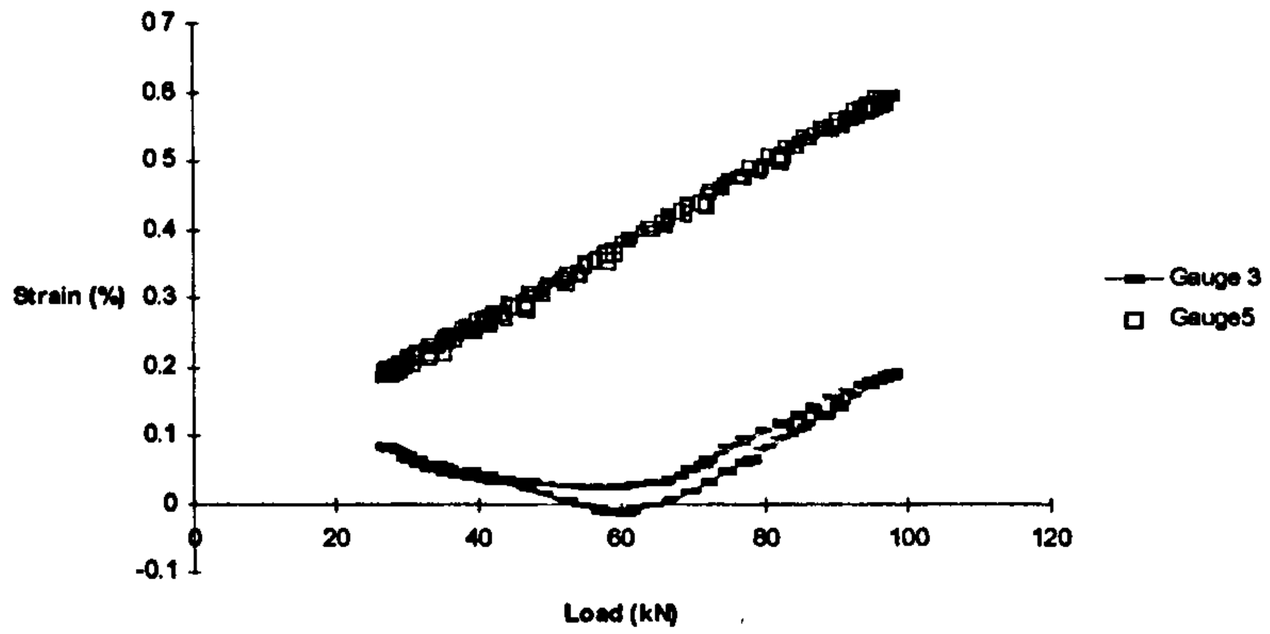

Figure 2.14. Wire strains a few cycles after wire 1 is cut at location shown in Figure 2.23.

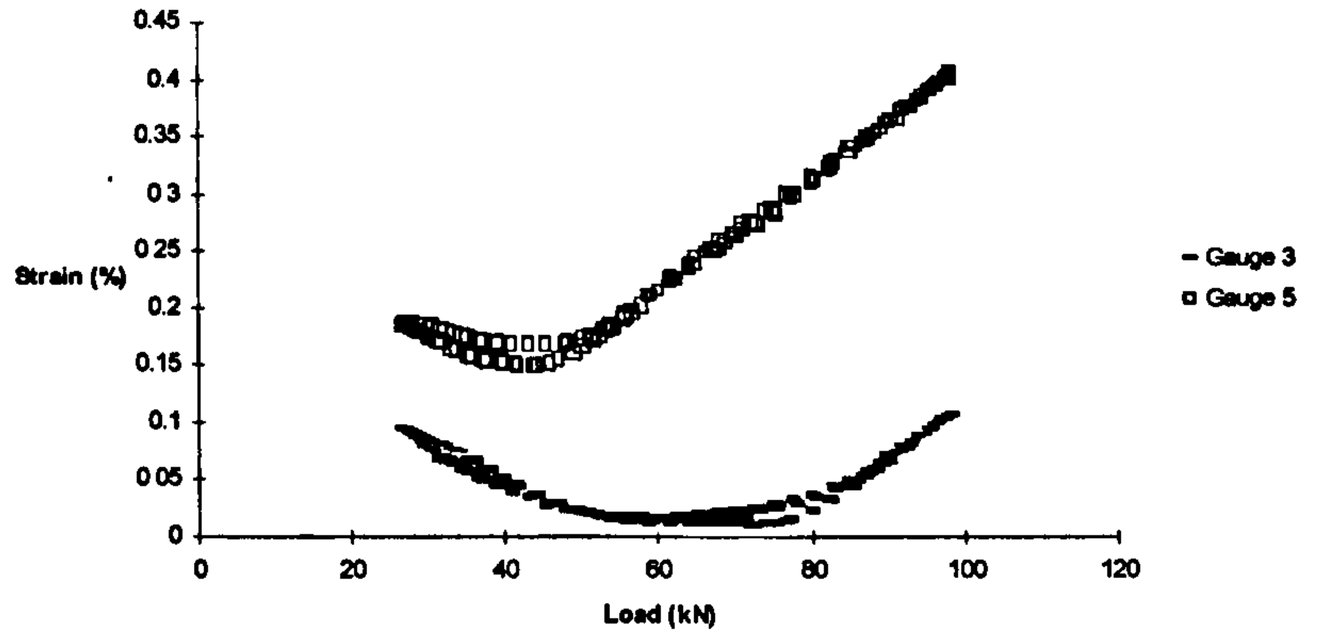

Figure 2.15. Wire strains 20,000 cycles after the wire is cut.

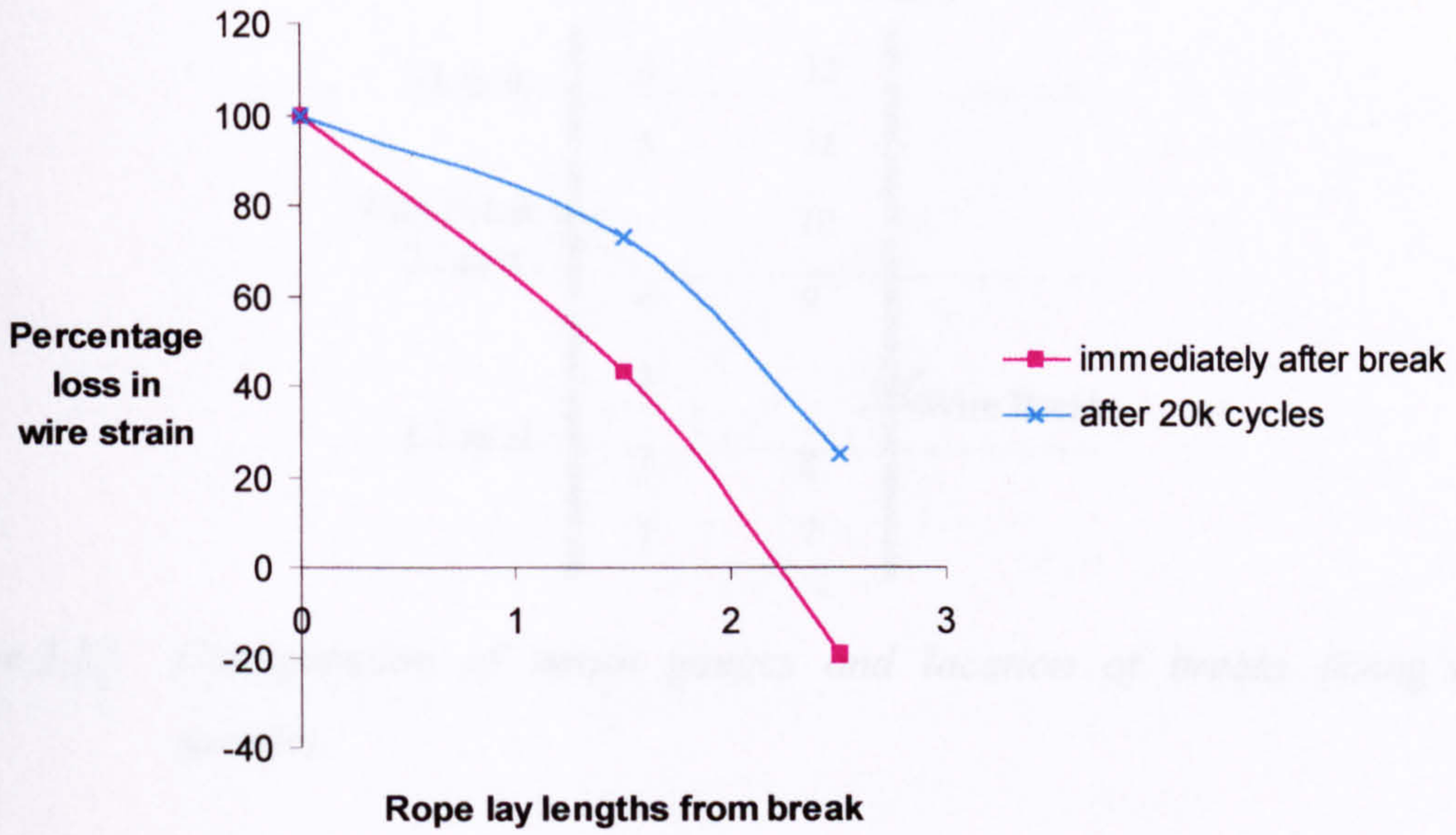

Figure 2.16. The effective length properties immediately after a wire break and how it has changes after 20,000 cycles.

2.4.1.2 Lang's lay

The configuration of strain gauges and wire breaks for the Lang's lay test is shown in Figure 2.17. To try and increase the chances of having 12 working gauges at the time of rope breaking, 14 gauges were originally placed on the rope. Two gauges failed early in the test and so these locations were adopted as the wire break positions (as there was no available location beyond the gauged wires on the samples).

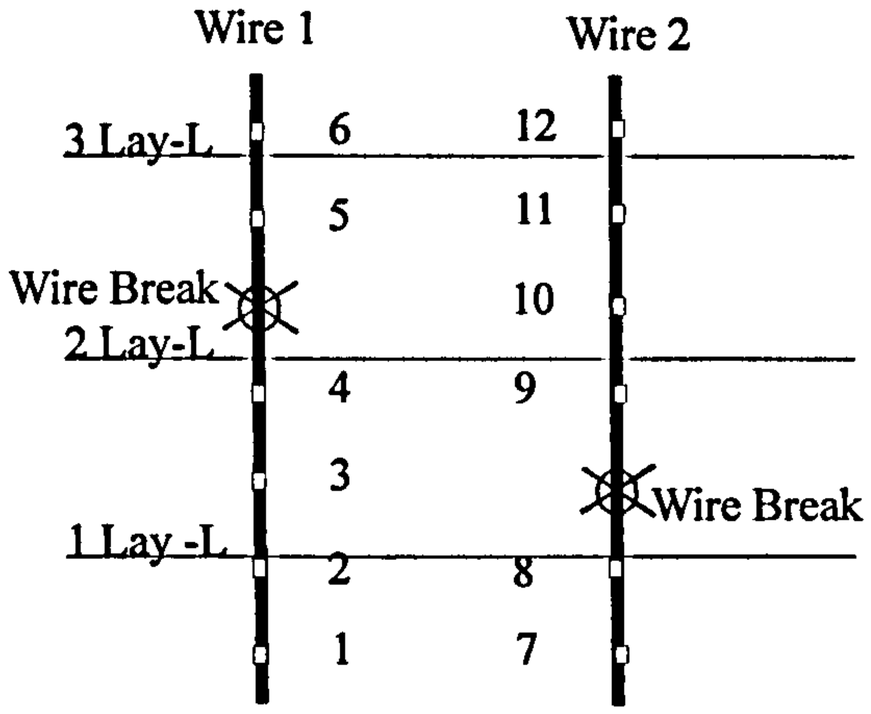

Figure 2.17. Configuration of strain gauges and location of breaks (Lang's Lay sample).

The wire behaviour before the cut was made in the first wire is linear as shown in Figure 2.18. Continuous monitoring during the cycles immediately after the induced damage enabled the slippage from two locations adjacent to the break (gauge 4 and 5) to be monitored as shown in Figure 2.19 and Figure 2.20

It was noted that no change in the behaviour of gauge 2, 2 lay lengths from the break, was observed at any stage after the break. Within about ten cycles the wires have settled down to a steady state response and this remains unchanged during the rest of the subsequent rope life. Figure 2.22 and Figure 2.23 give two examples of the wire strain response, one at 1,500 cycles and the other at 18,000 cycles, This show that there is no difference between the two. Figure 2.21 shows the take up of load immediately after the wire break. It can be seen that the effective length of this break is around 1 rope lay length, which should be compared with the much higher value of between 2 and 3 rope lay lengths in the case of the Ordinary Lay rope (Figure 2.24).

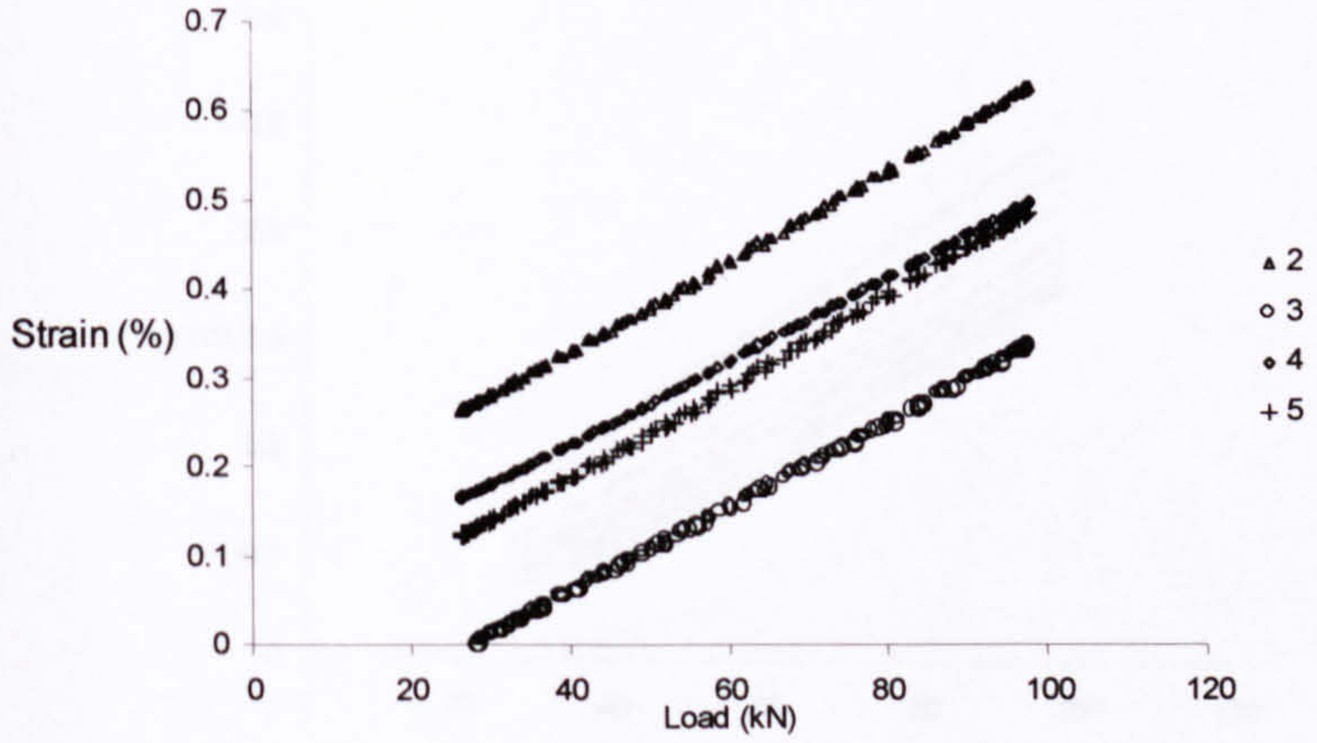

Figure 2.18. Wire behaviour before first wire break.

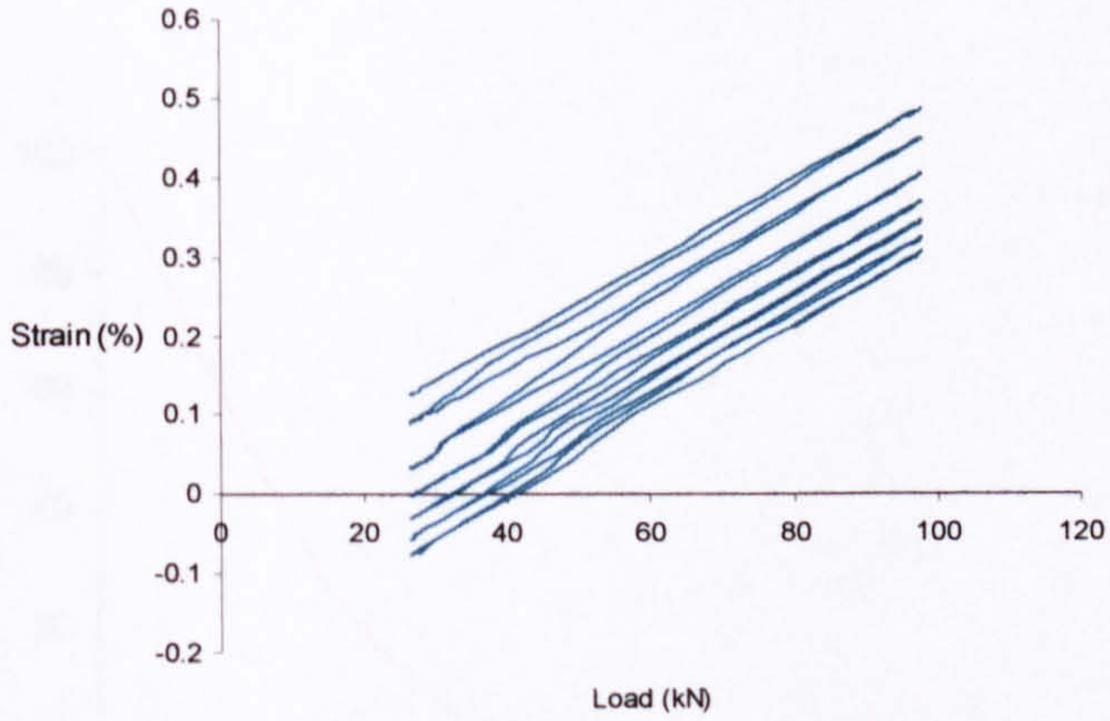

Figure 2.19. Slippage of a wire which is one strand lay length from the break during six load cycles immediately after break occurred (gauge 5).

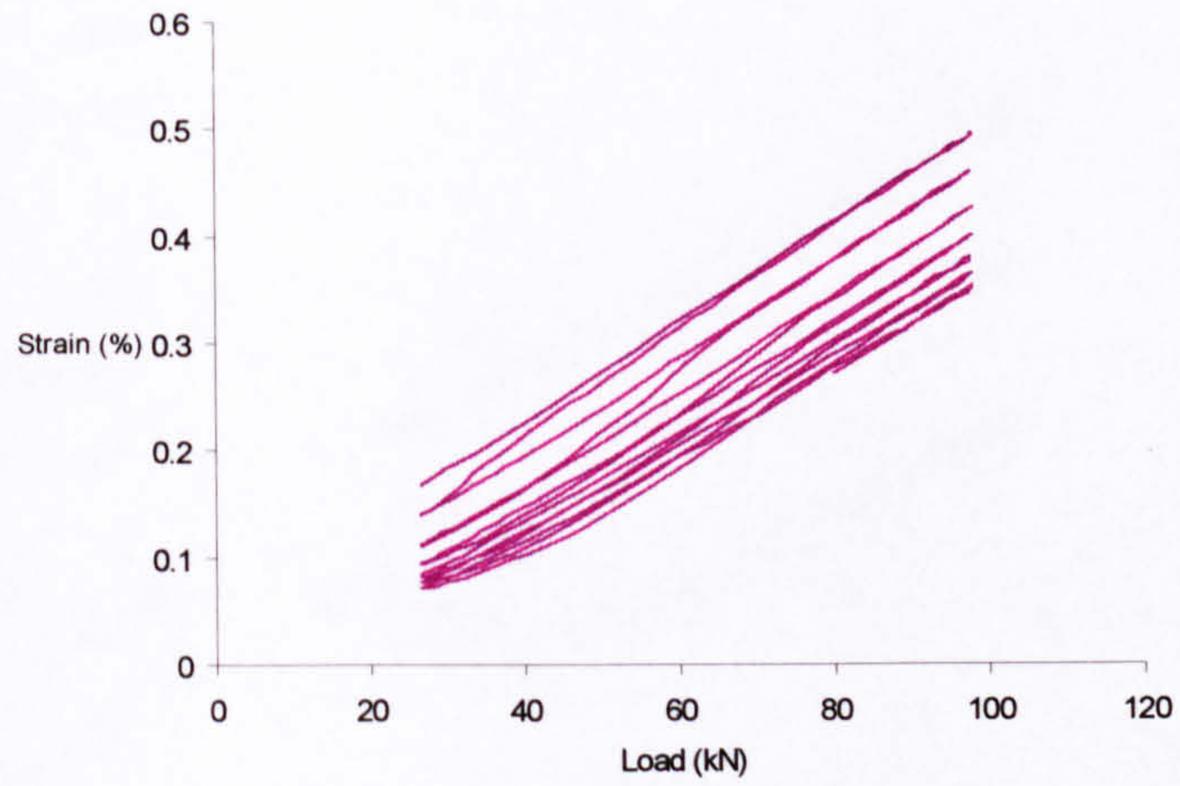

Figure 2.20. Slippage of a wire which is one strand lay length from break during six load cycles immediately after break occurred (gauge 4).

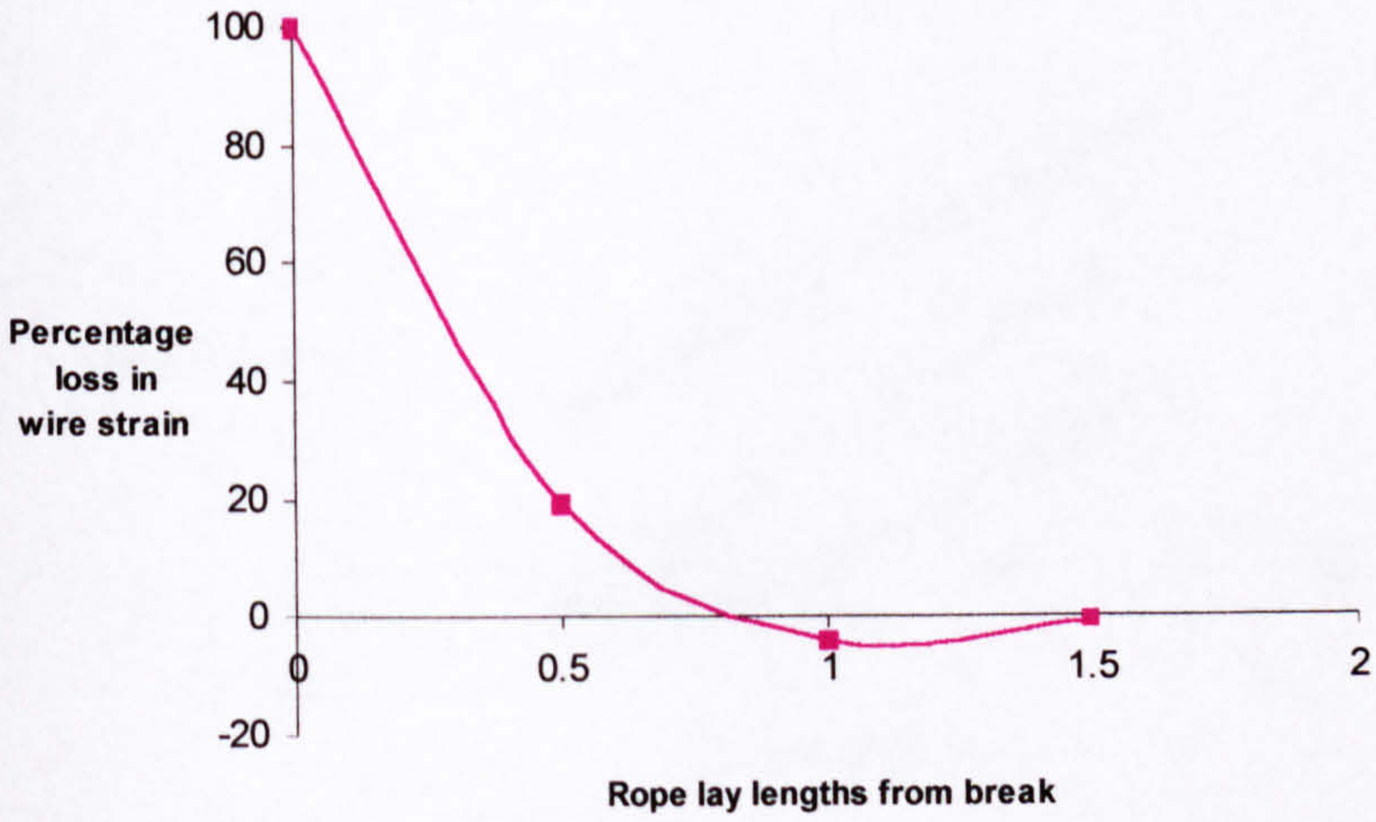

Figure 2.21. The effective length properties immediately after a wire break - Lang's lay rope.

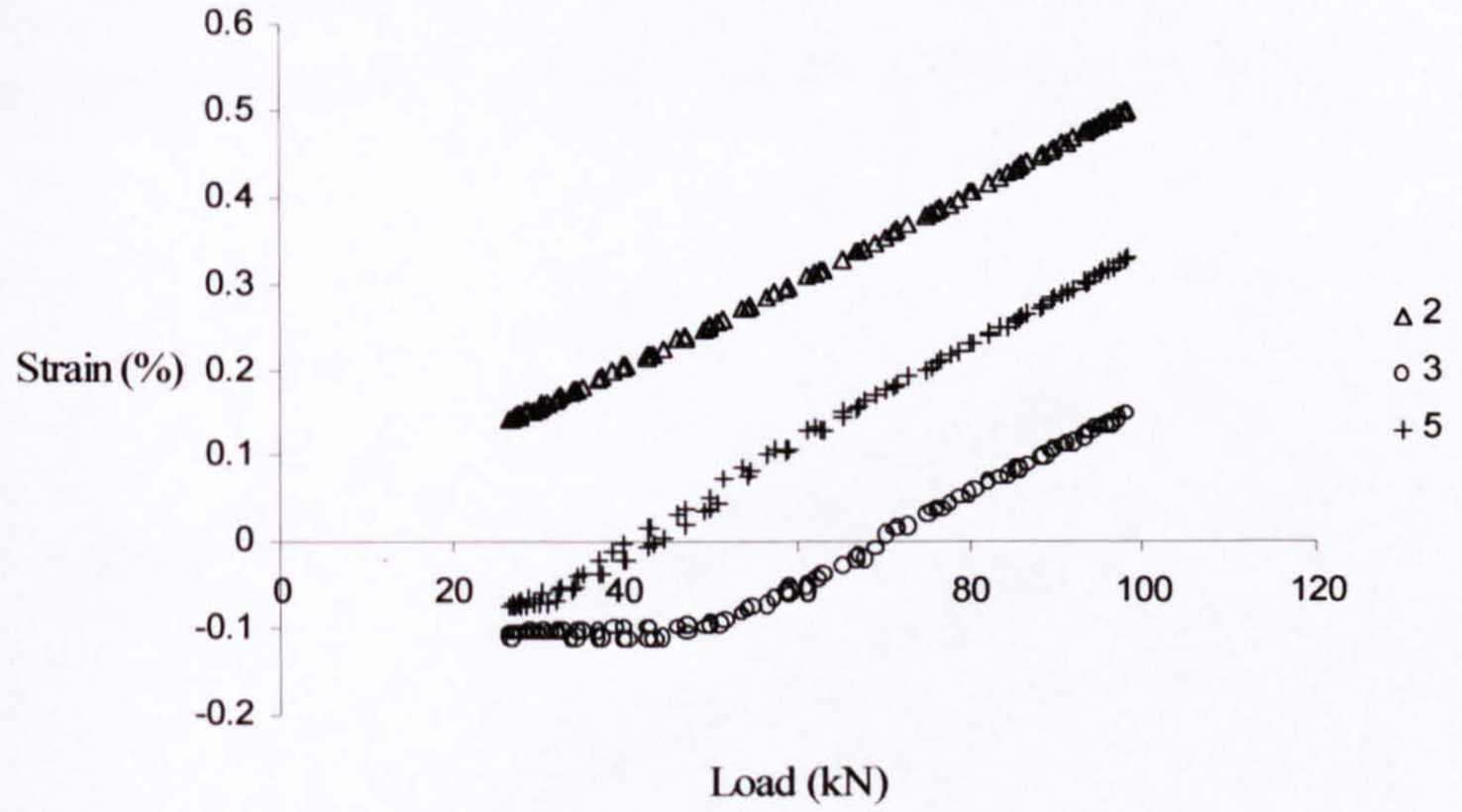

Figure 2.22. Strains after 1,500 cycles.

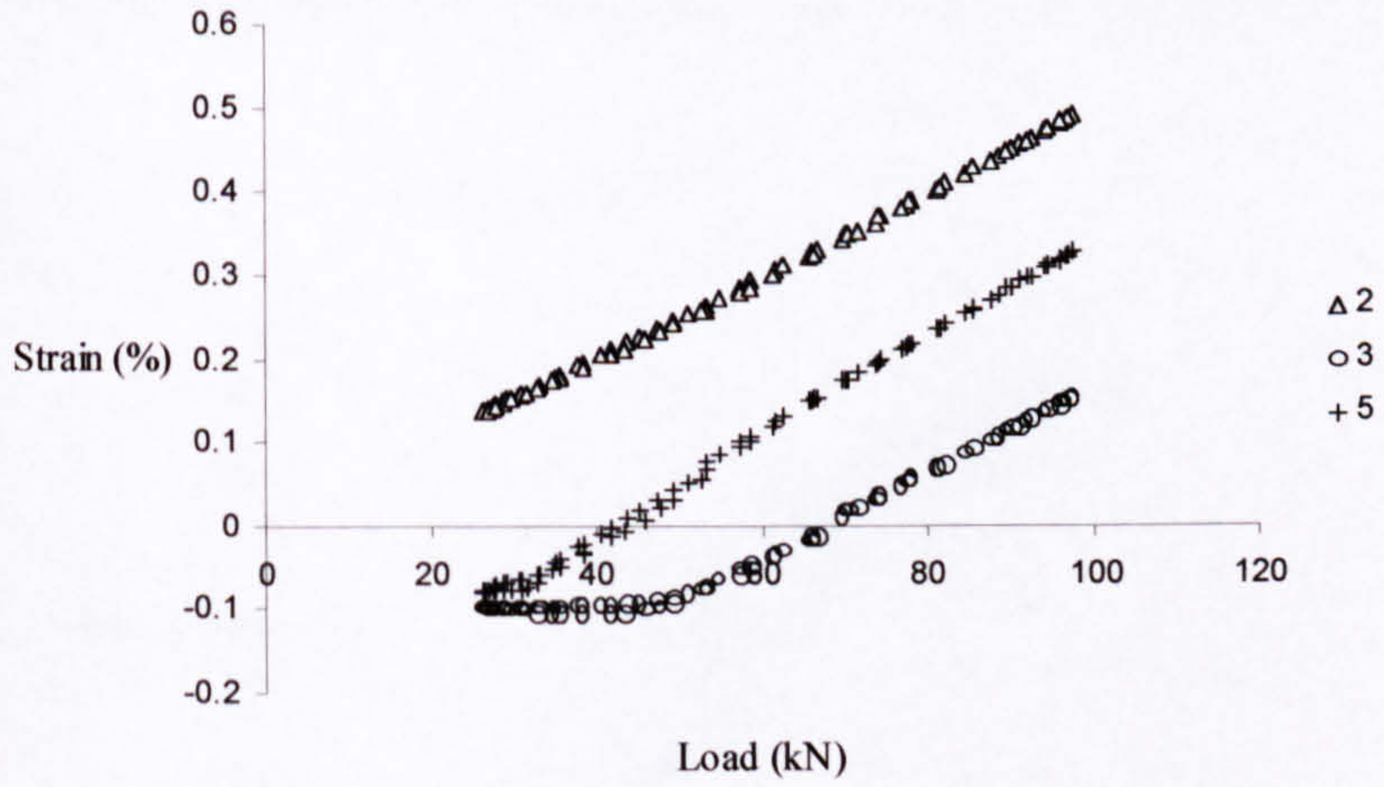

Figure 2.23. Strains after 18,000 cycles.

The strain response of the remaining working gauges on the second wire before the breakage is shown in Figure 2.24 and again a linear response is observed. Figure 2.25 shows the slippage immediately after the break of the gauge one strand lay length from the break, and Figure 2.26 shows the effect on a gauge 2 strand lay lengths from the break, which in contrast with the first wire breakage, is affected. Again like the first wire breakage within ten to twenty cycles the strain readings have settled down to a steady state condition and do not change for the remainder of the fatigue life. Figure 2.27 and

Figure 2.28 give two examples of this response at two different points in the rope life, one at 1,500 cycles after the break and the other 18,000 cycles after the break.

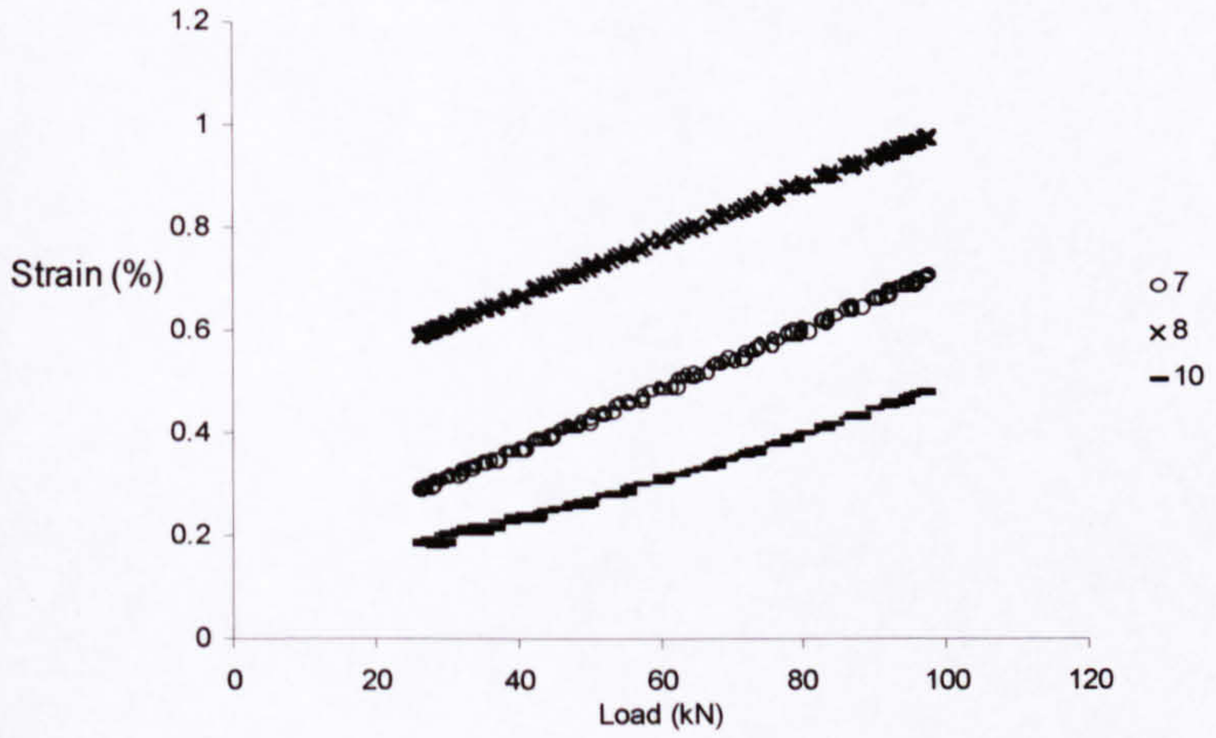

Figure 2.24. Strains readings from the gauges on the second wire before the break.

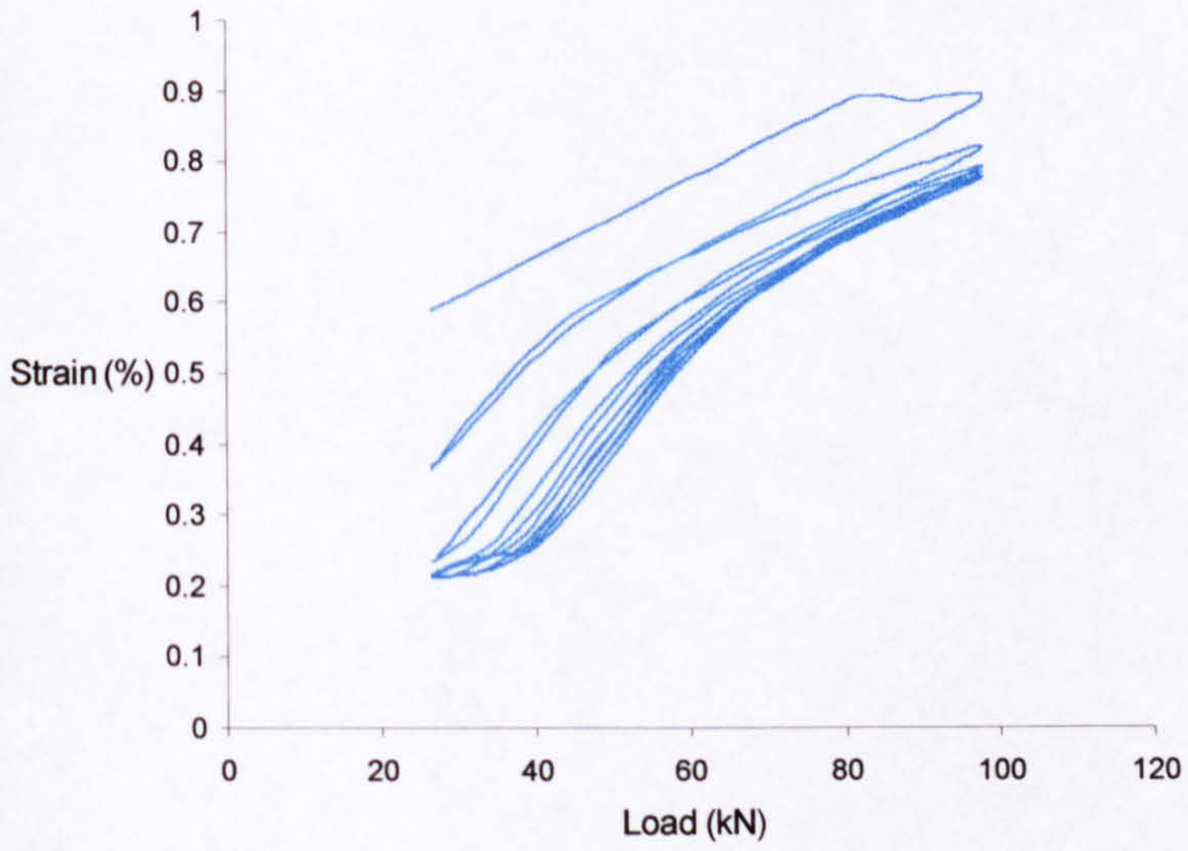

Figure 2.25. Wire strains during load cycling on a gauge one strand lay length from the break, slippage of wire occurred immediately after the break occurred- during six cycles (gauge 8).

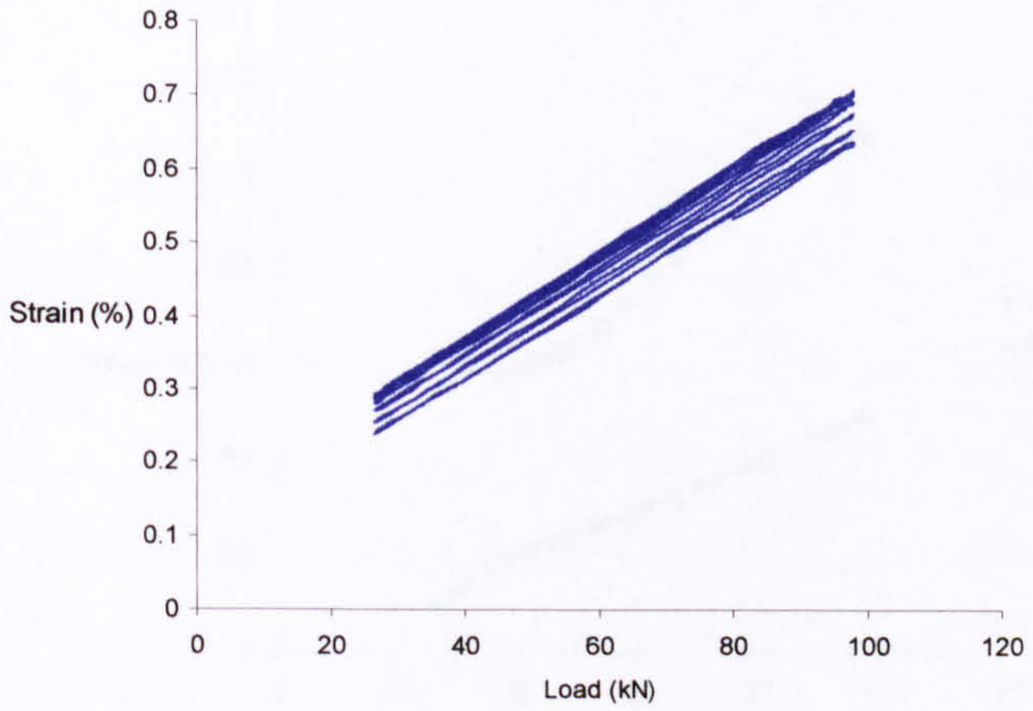

Figure 2.26. Slippage of wire two strand lay lengths from break immediately after the break occurred (gauge 7).

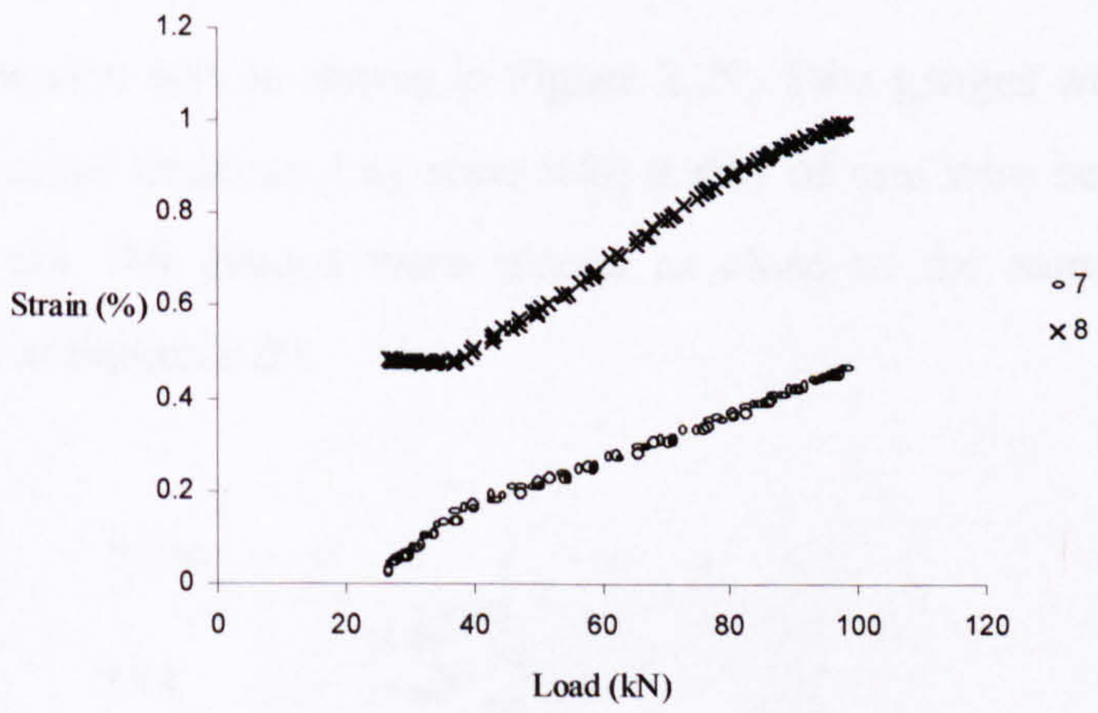

Figure 2.27. Wire strains after 1,500 cycles.

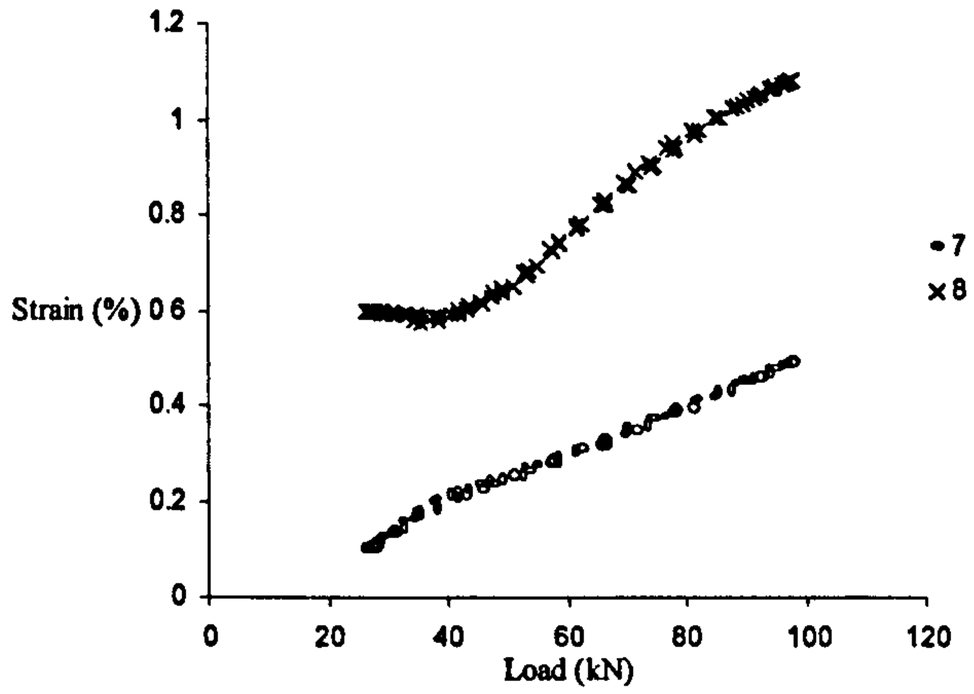

Figure 2.28. Wire strains after 18,000 cycles - no change.

2.4.2 The effect of wire breaks in strains on adjacent wires

The gauge configuration was as shown in Figure 2.29. Two gauges were placed on each of the six strands of an Ordinary Lay rope with a gap of one wire between them, these wires later being cut. All gauges were placed as close to the same cross section as possible, as shown in Figure 2.29.

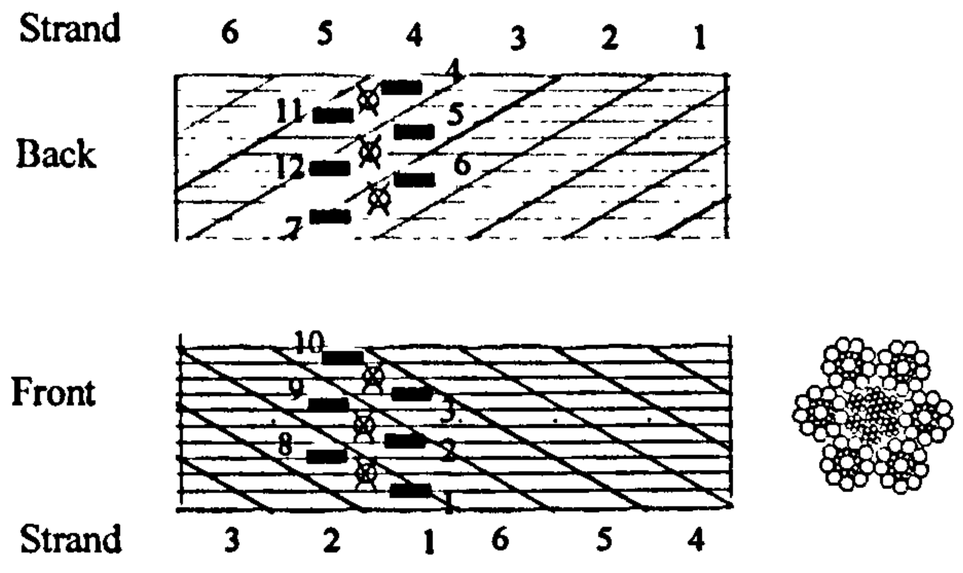

Figure 2.29. Locations of gauges and wire cuts showing rope cross section.

Table 2.2 shows the effect of a wire break on the normalised strain range in adjacent wires and strands. The normalised strain range is the range of strain divided by the fatigue load range and is discussed and justified in more detail in Chapter 3.3.1.

When the wire between gauges 4 and 11 had been cut it can be seen that there is an increase in the normalised strain range (defined as the change in strain divided by the change in load) in these two adjacent gauged wires (4 and 11). Likewise wires in the adjacent strand (5 and 12) show a corresponding increase in their load sharing. The same phenomenon can be seen when other wires are broken as shown in Table 2.2. The data in Table 2.3 demonstrates an interesting phenomenon in that although the wire break between gauges 5 and 12 causes wires 5 and 12 to have an increase in load share, it seems to cause almost all other gauged wires to decrease their load share. This could be an effect of previously broken wires causing an asymmetry within the rope and hence causing large bending stresses in the same wires. Breaking another wire redressed the balance and reduced this effect. This phenomenon may be connected with the observations discussed [4] that wire breaks which are asymmetric cause a higher strength loss, it seems that wires on the opposite side from the breaks have a compressive load on them from the consequent rope bending. When superimposed on top of the tensile stress this reduces the net load, but places a disproportionately higher burden on the wires adjacent to the break.

Table 2.2. The effect on the normalised strain range (%/MN) of breaking the wire between gauges 4 and 11.

	1	2	3	4	5	6	7	8	9	10	11	12
before		4.98	4.82	3.51	6.22	5.78	5.71	5.71	5.18	5.12	4.87	6.25
after		4.49	5.21	5.62	6.71	5.95	5.89	5.90	4.74	4.91	5.94	6.85

Table 2.3. The effect on the normalised strain range (%/MN) of breaking the wire between gauges 6 and 7.

	1	2	3	4	5	6	7	8	9	10	11	12
before	0.00	4.97	4.96	5.34	6.30	5.71	5.69	5.64	5.14	5.46	5.96	6.44
after	0.00	4.72	5.07	5.35	6.65	6.26	6.76	6.18	4.85	4.89	5.04	6.61

Table 2.4. The effect on the normalised strain range (%/MN) of breaking the wire between gauges 5 and 12.

	1	2	3	4	5	6	7	8	9	10	11	12
before	0.00	5.26	4.75	5.19	6.19	6.23	6.73	0.00	5.15	5.54	5.45	6.48
after	0.00	3.00	2.95	3.43	7.06	5.45	6.97	0.00	4.47	4.05	2.22	8.21

2.5 Discussion and conclusions

The results from the Ordinary Lay rope fatigue test indicate that a broken wire takes up its full load around two rope lay lengths from the break immediately after the break occurs but this changes to around three rope lay lengths after 20,000 cycles. This change in effective length is attributed to significant slipping which is seen up to 20,000 cycles after the initial break After this a steady state condition exists. This value of effective length is considerably higher than the majority of results previously seen and emphasises the importance of taking transient factors into consideration.

For the Lang's Lay rope it appears that there is considerable slippage of wires one and two strand lay lengths from a break, but this settles down within a few cycles and after this no changes are noted. Also in contrast to the Ordinary Lay rope the take up in load beyond a break seems to occur over a much shorter region of around one rope lay length. In one of the tests on one wire only the nearest strain gauge indicated slip after the break (i.e. half a rope lay length away) whereas on the other broken wire a gauge one rope lay length from the break was affected.

For both Ordinary and Lang's Lay rope it seems clear from the slippage and the shape of the curve that the effective length will not be constant over the full load range. At low loads a slipped wire will probably give a much longer effective length than at higher loads, probably because the higher wire to wire frictional forces caused during the rope loading will result in a more rapid take up of strain. This would suggest that a technique to calculate the effective length based on the residual breaking load will only give a lower bound value. This is the reason why the effective length derived in this section is higher than the effective length as derived from breaking strength in previous research (see Table 2.1 for summary).

The slippage seen in the strain measurements beyond a break ties in with casual observations that a wire break gradually separates with fatigue loading leaving a slight gap between the wires. A further study would be to try and measure this wire separation and correlate it with fatigue cycles.

As strain measurements can only be made once every strand lay length (when the wire comes to the surface) it is not clear how the strain varies between these discrete locations. It may be that the strain in the wire is fairly constant until it gets to the strand core contact point at which point there is a sudden change depending on the precise geometry of the specific wind. It may be of interest to take individual strands before it is wound into a rope and carry out similar break tests, with strain gauges, to investigate the importance of the strand to core contact.

The difference seen between Lang's and Ordinary lay effective length may be caused by the higher intralayer tangential forces between wires of the same layer. This may be an indication that interlayer wire forces are more critical in determining the effective length than layer to layer radial forces.

From the tests on an Ordinary Lay rope examining the effect of broken wires on the strains of adjacent wires and wires in adjacent strands it appears that a broken wire will affect primarily wires in the same strand and in adjacent strands to a lesser extent. This is in accordance with previous observations that concentrated wire breaks have a bigger proportional effect than symmetrically distributed ones [4]. It was seen that breaks in wires may sometimes cause a decrease in strain of wires on the opposite side of the rope. This may be caused by localised bending of the rope resulting from the wire break and, if so, this effect is likely to be most significant in the external wires.

2.6 References

1. Stonesifer, F.R. and H.L. Smith. *Tensile Fatigue in Wire Ropes*. in *Offshore Technology Conference*. 1979. Housten, Texas.

2. Smith, H.L., F.R. Stonesifer, and E.R. Seibert. *Increased Fatigue Life of Wire Rope through Periodic Overloads*. in *Offshore Technology Conference*. 1978. Housten.

3. Kies, J.A., *Overload Effects on Fatigue Damage of Wire Rope Pendants*. Journal of Engineering Materials Technology, 1977. **July**: p. 277-278.

4. Chaplin, C.R. and N.R.H. Tantrum. *The influence of wire break distribution on strength*. in *OIPEEC Round Table Conference*. 1985. Glasgow: OIPEEC.

5. Chaplin, C.R. and A.E. Potts, *Wire Rope Offshore- a critical review of wire rope endurance research affecting offshore applications*. 1991: Health and Safety Executive. 335.

6. Oplatka, G. and M. Roth. *Relation between Number and Distribution of wire breaks and residual breaking force.* in *Wire Rope Discard Criteria, OIPEEC Round Table Coference*. 1989. Zuric, Switzerland: OIPEEC.

7. Davidsson, W., *Investigation and Calculation of the Remaining Tensile Strength in Wire Ropes with Broken Wires.* Ingeniörsvetenskapsakademien, Handliger, 1955. **214**.

8. Cholewa, W. and J. Hansel. *The Influence of the Distribution of Wire Rope Faults on the Actual Breaking Load.* in *OIPEEC. Round Table Conference,*. 1981. Krakow: OIPEEC.

9. Cholewa, W. *A study of the Decay Zone Length and Course of the Defect Influence of Doubly Twisted Steel Ropes.* in *OIPEEC Round Table Conference,*. 1981. Krakow: OIPEEC.

10. Cholewa, W. *Wire Fractures and Weakening of Wire Ropes.* in *OIPEEC Round Table Conference, 'Wire Rope Discard Criteria'*. 1989. ETH, Zurich, Switzerland: OIPEEC.

11. Chaplin, C.R. and N.R.H. Tantrum, *Influence of Wire Breaks and Distortion on Strength*, . 1986, University of Reading: Reading.

12. Shitkow, *Drahtseile*. 1957.

13. Marguetts, R.G. and H.A. Spikes. *Single Contact Testing and the Lubrication of Wire Ropes.* in *Proceedings of the International Wire and Machinery Conference.* 1983.

14. Wiek, L. *The Influence of Broken Wires on Wire Rope Strength and Discard.* in *OIPEEC Round Table Conference*. 1977. Luxembourg: OIPEEC.

15. Molinari, G., *On the Strain Distribution in the Wires of a Single Spiral Strand under Tensile Loading during the Breaking of one of them (in Italian).* Elevatorti, 1980. **6**: p. 30-39.

16. Chien, C.H. and G.A. Costello, *Effective Length of a Fractured Wire in Wire Rope.* Journal of Engineering Mechanics, 1985. **111**(7): p. 952-961.

17. Costello, G.A., *Theory of Wire Rope*. 1st ed. Mechanical Engineering. 1990, New York: Springer-Verlag. 106.

18. Teer, D.G. and R.D. Arnell, *Friction Theories*, in *Principles of Tribology*, J. Halling, Editor. 1978.

19. Raoof, M. and I. Kraincanic, *Recovery Length in Multilayered Spiral Strands.* Journal of Engineering Mechanics, 1995. **121**(7): p. 795.

20. Ganthman, D.W., *Resin Socketing for Wire Rope Attachments.* Wire Journal, 1979. **12**(6): p. 82-85.

21. Dodd, J.M., *Resin as a Socketing Medium.* Wire Industry, 1981. **48**: p. 343-344.

22. Chaplin, C.R. and P.C. Sharman, *Load Transfer Mechanics in Resin Socketed Terminations.* Wire Industry, 1984(October 1984).

23. Micro_Measurements, *Catalogue 500- Precision Strain Gauges*. 1993.

24. Micro_Measurements, *Transducer-Class, Strain Gauges, Bondable Resistors, Installation Accessories*. 1992.

25. Utting, W.S. and N. Jones, *Tensile Testing of a Wire Rope Strand.* Journal of Strain Analysis, 1985. **20**(3): p. 151-163.

3. Wire strain variations in normal and overloaded ropes in tension-tension fatigue conditions and their effect on endurance

3.1 Summary

This chapter investigates wire strain variations in ropes in tension-tension (T-T) fatigue. Wire strain distributions have been investigated along the length of a single wire and on a number of wires at the same cross section.

It has been found on the rope samples tested that there is a considerable variation in wire strains both on different wires at the same cross section and to a lesser extent along the length of the same wire. It has also been found that a Lang's Lay rope has a wider strain distribution than the equivalent Ordinary Lay rope. Load cycling has been found to reduce the distribution slightly for an initial period, around 20,000 cycles at which point the variation in wire strains does not change significantly for the rest of the life of the rope. These observations agree with results obtained by Wiek, but the actual level of variation seen by Wiek is much higher, around double, and it is suggested that this may be an indication of a difference in quality of the ropes used in the two investigations.

Tests overloading ropes have shown a considerable reduction in wire strain variation. As an example for an Ordinary Lay rope the standard deviation reduced from 22 % of mean to 11 % of mean and this overload resulted in an increase in endurance by a factor of 2.4. A simple statistical model has been used to predict the fatigue life of a rope using strain variations seen in experimental work to extrapolate a complete rope strain distribution based on a Gaussian probability prediction. Predictions show reasonable correlation with endurance data and a number of possible improvements to the model have been suggested.

3.2 Review of related research

3.2.1 Statistical distribution of tensile fatigue data

Chaplin [1] has found that Tension-Tension fatigue tests carried out on rope samples from the same batch conform to a simple power law relationship within remarkable small scatter bands (Figure 3.1 (a)).

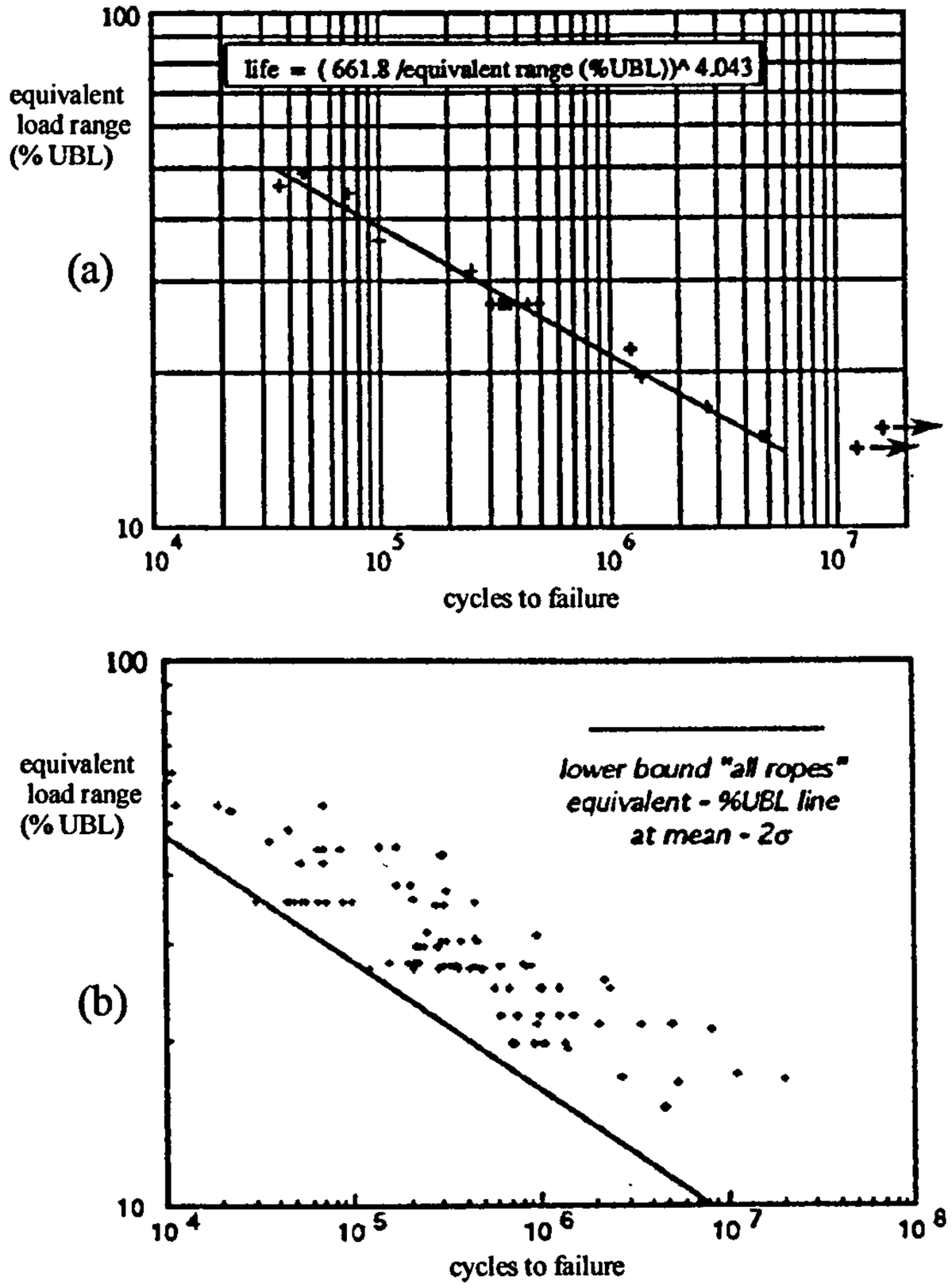

Figure 3.1. (a) The scatter from one specific rope reel showing remarkably little scatter (b) Data for a number of nominally identical ropes (from different manufacturing runs) which show a wide range of scatter, from Chaplin [1].

Different ropes however, or even similar ropes with the same size and constructions and possibly even the same manufacturer, show considerably more scatter. The scatter has been attributed to differences between ropes rather than differences within a particular rope batch and is likely to be related to slight differences in the machine set-up causing slight variations in the rope geometry. Because of its nature, T-T fatigue appears to be very sensitive to these slight variations (whereas bending over sheave (BOS) fatigue is not because the loading is dominated by the distortions imposed on the rope externally by the pulley). This phenomenon raises questions about the validity of predicting the T-T endurance of a specific rope based on a generic curve for a given construction and loading regime. A lower bound based on two standard deviations as shown in Figure 3.1 (b) still gives a number of points on the lower bound line. All these lower bound points represent not a lower bound behaviour but a lower bound rope. Chaplin [1] has suggested that there will be considerable benefit in testing a section of an actual rope to be used in service. The prediction in endurance can then be given within much tighter bounds and a lower bound curve can be predicted without the need to be over conservative. It was suggested [1] that this wide scatter in rope endurance between ropes gives an indication of the ropes 'quality' and is likely to be related to the statistical distribution of the wire strains within a rope.

3.2.2 Effect of overload on tensile fatigue life

Kies [2] and later Smith, Stonesifer and Seibert [3] investigated the effect of overload on rope fatigue behaviour in tension-tension conditions. They were initially driven by the phenomenon of improved fatigue life of overloaded metal specimens caused by the crack closure mechanism. T-T fatigue tests were carried out on a 3/16 inch multistrand rope (19x7 +IWRC) and various constructions of six strand rope (all ¼ inch six strand RHOL ropes with a variety of strand and core constructions [4]). It was found that periodic overloads increased the life of ropes and the optimum overload seemed to be the point of 'rope yield' (where the rope exhibits permanent stretch). It was found that for the majority of ropes there was a significant increase in fatigue life (i.e. around five times) when the rope was periodically overloaded to 75 % of its static breaking load, the exception to this

was the 6x7 iron wire rope which saw a peak in life at an overload of 50 % of static breaking load. It was concluded that the main mechanism of increased endurance was due to crack closure (some retarded slow crack growth was shown in SEM images) but could also be due to a readjustment in strains in the wires. One or both of these factors was also said to be likely to have caused the decrease in the concentration of wire breaks throughout the life of the rope.

In their subsequent work, Stonesifer and Smith [3] discovered that a single overload at the start of a test gave almost as much increase in endurance as periodic overloading throughout the test. This led them to conclude that the main mechanism for increased fatigue life was the redistribution of wire strains caused by the 'rope yielding'. Another significant discovery was that pre-cycling a rope at low loads before the test made no difference to the rope life, as it had been previously thought to. Additionally it was found that the whole rope assembly (i.e. rope plus terminations) must be overloaded to gain the fatigue life improvement, if a rope was overloaded and then the terminations removed and the rope re-terminated then there would be only very marginal increase in fatigue life. This suggests that the re-termination introduces stress variations which cancel out the benefit of the original overload. It should be mentioned that the termination technique used in this test series was the 'thimble splice' which has been shown to be a less efficient technique than the wedge socket method more generally used in experimental work[5].

The overload is most effective when it reaches a permanent stretch or 'rope yield' at which point there is a decrease in the compliance of the rope caused by the strain equalisation. This increase in stiffness gives an increase in fatigue life for load controlled configurations. An important point is that under fixed displacement controlled loading, the increased stiffness will effectively mean an increased loading and a decrease in the fatigue life under these conditions. There are some situations where ropes do come under a fixed displacement loading, such as mooring, where it may also be inevitable that at some time during the rope life, due to extreme weather or wave conditions, the ropes will experience some kind of overload. All work carried out on the effect on overload on fatigue life was

concerned with T-T fatigue and it is not known how it would effect a rope loaded in the BOS fatigue regime.

3.2.3 Wire strain variations in tension

Wiek carried out tensile tests on a six strand Ordinary Lay rope [6, 7]. The results of which can be seen in Figure 3.2. The measured wire strains display considerable scatter and a number of wires showed compression in the initial stage of the rope loading. Tensile testing was also carried out on the equivalent Lang's lay construction [8] (see Figure 3.3) and again a number of wires seem to go into compression. For both types of ropes two groups of wire behaviour are identified by Wiek: those with compression at low loads, and those with high tensile strains at low loads. For the two types of rope it was noticed that the offset between these two groups seems to be different, 11.6 for Ordinary Lay and 36 for Lang's Lay (in Kgf/mm^2). Additionally the scatter within the two regions seems to be greater for Lang's lay. The differences were thought to be due to the strand winding being opposite from wire winding (i.e. Ordinary Lay) which would correct for winding inconsistencies to some extent. Whereas strand winding in the same direction as wires in the strand (i.e. Lang's Lay) could exaggerate winding inconsistencies.

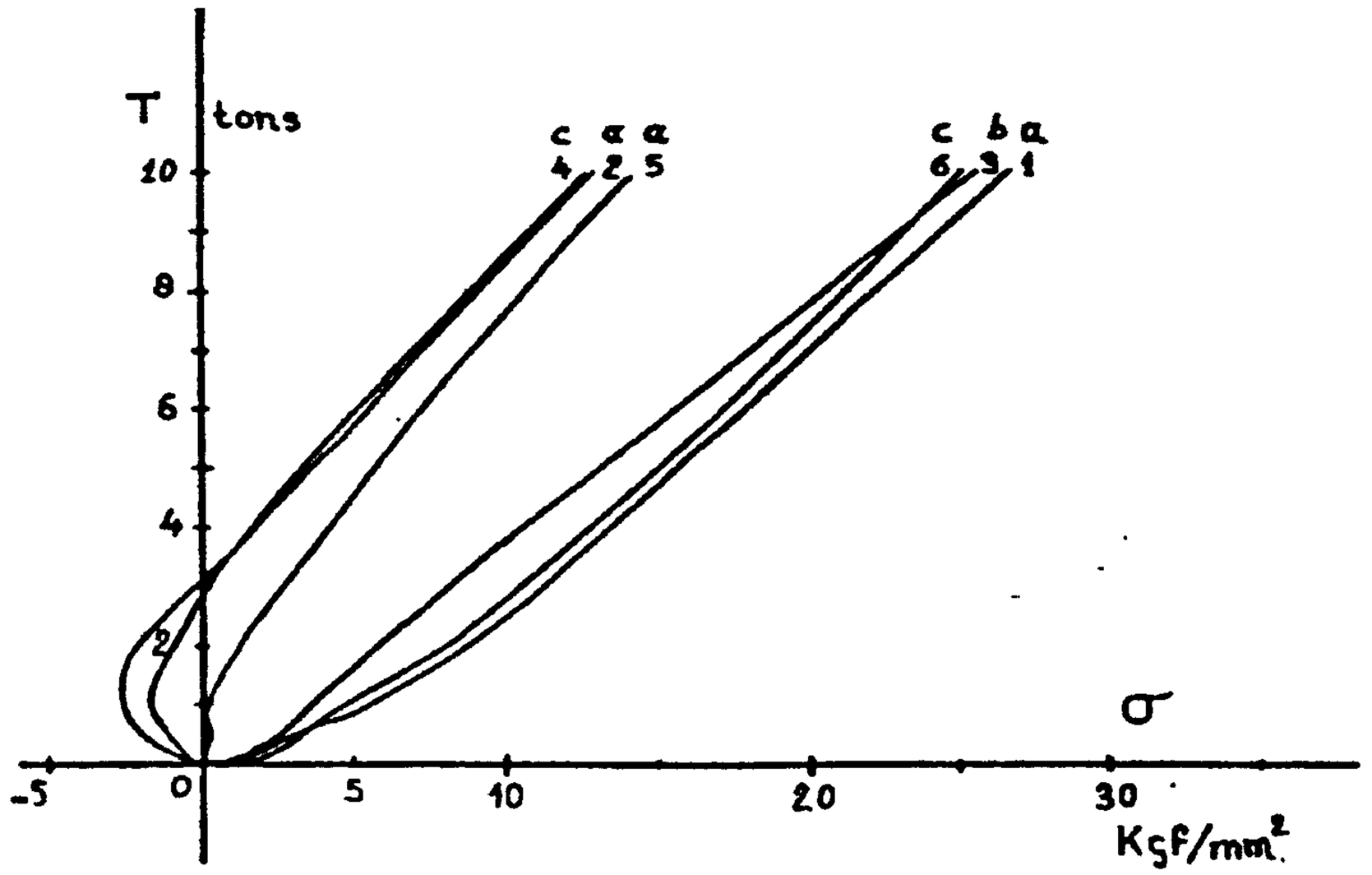

Figure 3.2. *Wire stresses in tension for a six strand Ordinary Lay rope, Warrington-Seale with IWRC, from [7].*

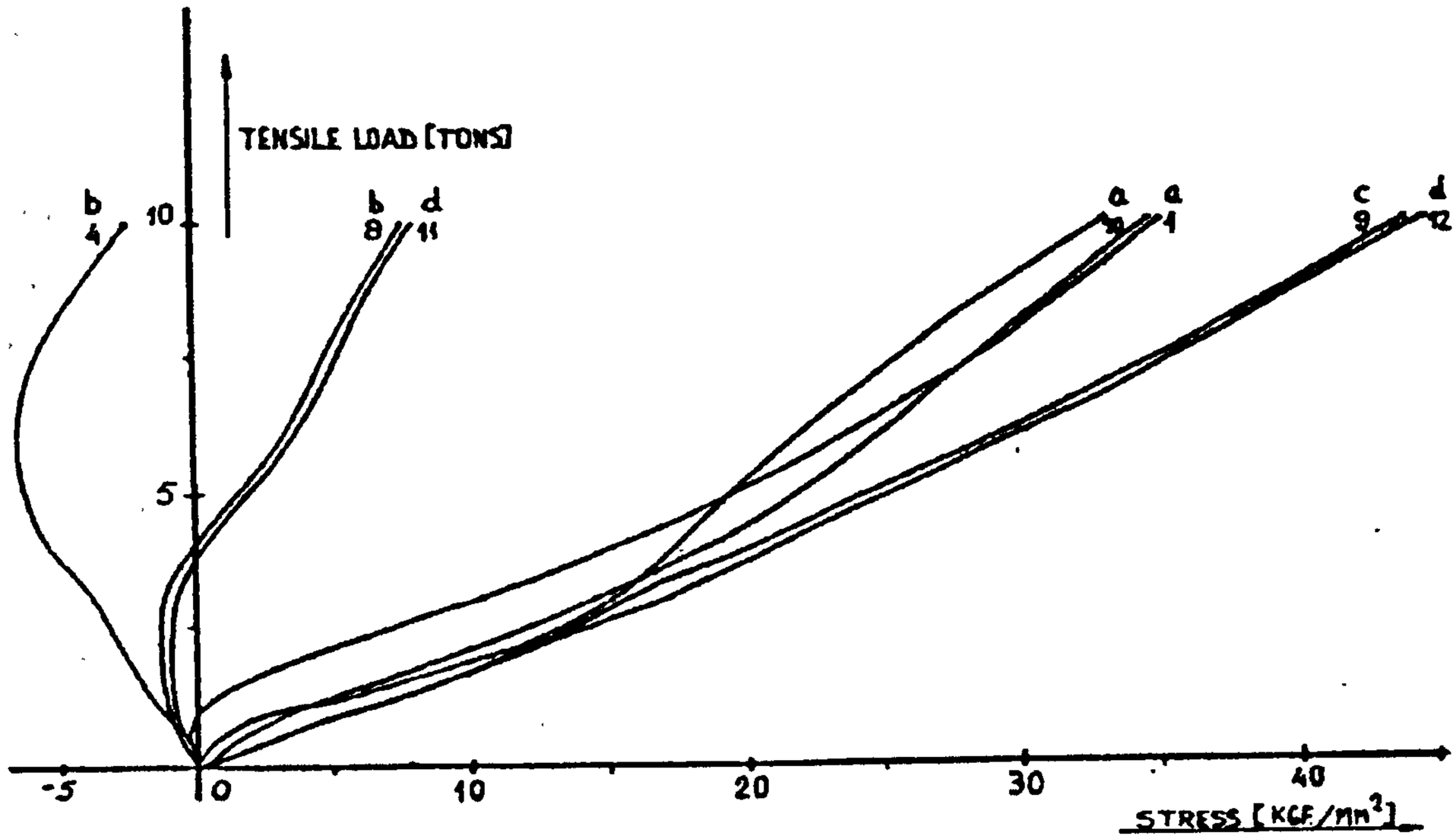

Figure 3.3. *Wire stresses in tension for a six strand Lang's Lay rope, Warrington-Seale with IWRC, from[8].*

When Wiek carried out tensile tests on Multi Strand rope [9] he found considerable distribution on nominally identically outside wires. A Gaussian distribution fitted these results and yielded a standard deviation of 60 % of mean for fixed end conditions and 80 % of mean for free end conditions. It was suggested that this distribution could be an indication of rope quality. A calculation of the stress using Hruskas' theory [10] gave a value close to the mean value measured (calculated 253 kN/mm^2, measured 263 kN/mm^2). Hysteresis was seen in the wire behaviour which was attributed to inter-wire frictions. When the rope end was free to rotate the outer wire strains went down by an average of 40 %, the two inner wire strains measured increased by 53 % and 93 %. Wiek suggested that this is probably one reason why inner wire failures are common in this construction.

In his static tests to characterise the strain distribution within a six strand rope [11], Wiek found a standard deviation of 65 % from mean between the wires and 50 % of mean for variations in a single wire along its length. When fatigue i loaded between 60 and 110 kN for 2 million cycles, measuring the strains periodically there seemed to be a decrease in mean wire stress in rope after a 'breaking in' period of about 3,000 cycles. Initially the mean stress was 315 N/mm^2 with a standard deviation of 237 (75 % of this value). After the break in period this decreased to a mean stress of 281 kN/mm^2 with a standard deviation of 158 (56 % of mean), possibly due to some sort of evening out of the stresses in the initial stages of the test. It was found that the standard deviation varied between 71 % and 46 % throughout the fatigue test. The statically determined distribution can be compared with the distribution previously determined for a multi-strand rope, and also for other ropes. Wiek considered the possible reasons for the strain distribution between the wires and concluded that the differences are likely to be either variation of the strand geometry within the rope or variation in the wire geometry within the strand.

During bending tests of the same 6x26 Warrington Seale rope he found considerably less scatter in the strain results. For example he found that 2.5 % of wires in bending will have stress over 25 % of the mean value as compared with in tension, where 2.5 % of wires in tension will have stresses over 100 % of mean.

The strain measurements of Durelli [12, 13] on a strand in tension were mainly carried out as a verification of the model he presents. The results showed good agreement with theory developed within the paper. It was noted however that there was variation in strains of wires at the same cross section, the same phenomenon was also noted in the tests on oversized strand models made of epoxy[12, 13]. Again Paolini [14] noted variations in the wire strain for different wires at the same axial location.

Utting and Jones [15, 16] also demonstrated considerable wire strain differences at the same axial location on a seven wire strand. The free end condition showed a lower mean stress in the wires and considerably more scatter.

Raoof [17]used a log normal distribution to model the scatter seen in a multilayer 39 mm spiral strand. Mean values showed good agreement with the theory of Hruska for stress [10]. Raoof found little difference between strain distribution near and far from the termination. It was pointed out by Raoof that wire breaks tend to be more frequent close to the terminations in this type of construction, so strain distribution would therefore not be a good method for predicting degradation in axial fatigue in this case.

3.2.4 Discussion

The suggestion has been made that, because of the variations among ropes, fatigue testing each rope batch to be used in service could result in a major increase in the ropes allowable working loads without compromising safety factors. In high expense situations, the savings may offset the cost of testing, but in many other situations the high cost of testing would not make this procedure economically viable. If the rope quality could be quantified and measured in some indirect and simpler way then this factor could be more universally applied in predicting the behaviour of a specific batch of rope for T-T fatigue.

Overload has been shown to give a significant improvement in fatigue life in tension-tension fatigue. As a single overload at the beginning of the test gives almost as much benefit as periodic overloads, it has been suggested that the improvement in behaviour is the effect of a redistribution in strains rather than the more familiar mechanism of crack closure. It was also observed that the overloading effect was associated with a decrease in

the rope compliance, so it seems possible that there may be some form of relationship between wire strain distribution and rope compliance within a rope.

Other than the large degree of scatter in wire strains measured in ropes in tension, the first obvious aspect of note is that some of the wires appear to go into compression initially, and then gradually go into tension as the load increases. Although this phenomenon is not discussed within the article by Wiek, it seems very unlikely that these compressive strains are caused by an overall axial compression within the wire and more likely that it is the result of some degree of wire bending. Given this then the large scatter seen in the results, with varying degrees of compressive, and steeply rising tensile loads in wires at low loads suggests that there is some variation in the relative curvature, (i.e. relative to the mean curvature), of the wires (see Figure 3.4). If the relative curvature is such that the outside of the wire is on the outside of a bend, then the gauge will measure a compressive strain until the overall tensile stress in the wire has risen sufficiently to reverse this. On the other hand if the outside wire is on the inside of a relative bend then the strain measured will be a combination of a tensile load in the wire and the effect of tension caused by the bending, thus the wire strain measured will be higher than the mean (see Figure 3.4).

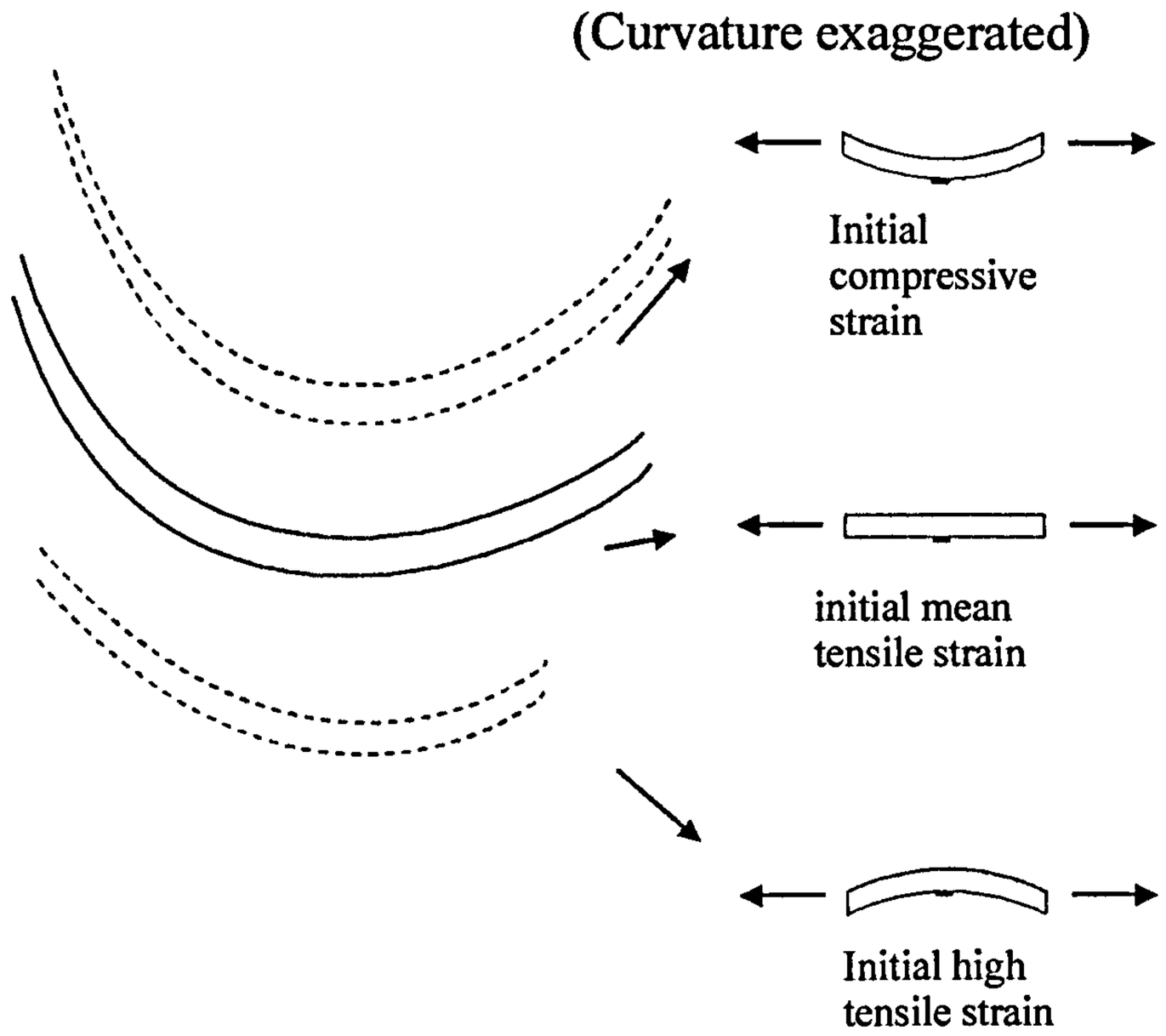

Figure 3.4. Possible mechanism for wire strain variations and compressive strains in some wire showing the relative curvatures of different types of distortion.

In his tests on six strand ropes Wiek identifies two separate groups of behaviours for the Lang's and Ordinary Lay ropes- the wires that go into compression and the wires that go steeply into tension.

There seems no obvious reason why the wire behaviour should be split into two groups like this and reasons for this are not discussed. The observation seems valid looking at the results, however it may just be an anomaly of the tests (only one test was carried out on each rope). No such grouping is seen on the multi-strand ropes which Wiek tests in a later work[9]. Wiek attributes wire strain variations to variations in the rope geometry caused by two stages in manufacture: the laying of the strand and the laying of the rope. It seems that the influence of each of these factors could be assessed by measuring the strain variation in a single strand component before it is closed into a rope and then comparing this to the strain variation once it is twisted into a rope construction. This has not been done, but some comparisons in strain variations can be made among ropes and strands from unrelated work. This may give some indication of the contribution of the two

manufacturing procedures to the strain scatter. If strand twisting is the predominant cause of strain variation, then this may be a reason why there seems to be two groups of wire strain behaviour for six strand ropes as previously mentioned- as changes in curvature would tend to happen to groups of wires at a time and it is quite likely that if three strands are slightly curved one way at a particular cross section, then the other three may curved slightly the other, in order to maintain some sort of symmetry. Wiek suggests that variations in wire strains within a rope may be a good indication of rope manufacturing quality. It would seems that identifying the root cause of the variation, whether strand lay, wire lay or some other phenomenon, would give a useful indication to a rope manufacturer of where they could improve their manufacturing procedure. Of course strain variations may be caused by different factors in different circumstances, the construction of the rope, the manufacturing process and possibly even the individual machine that a rope is constructed on may influence this.

The strain measurement of wire on a multi-strand rope (18x7) test gave an insight into why wire breaks are so common on inner wires as observed for example by Chaplin [1]. The wire strains on the outer wires decreased while the strains measured on the inner wires increased when the end conditions went from fixed to free to rotate. The free end condition is common for this type of rope because of its torque balanced construction. Another contributing factor to wire break up on inner strands in this type of rope is that the inner layer of strands is wound in the opposite direction to outer ones, this type of cross lay construction will give greater contact stresses in the wire, especially in free end conditions when the outer strands wind tightly onto the inner ones.

One final comment about wire strain measurements in wires in a rope is that, the wire diameters on the ropes used in almost all testing conditions have been small, in the region of 1 mm, (because of the impracticalities and high cost of testing large specimens). Consequently, because of limitations in the minimum sizes of gauges, it is only possible to attach wires axially, and the only types of strain measurable with this configuration is tensile and bending (or some combination of the two).

A number of researchers have carried out strain gauge tests on spiral strands and observed considerable scatter in the data. Utting and Jones found a greater scatter of strains for free end conditions as compared with fixed ends for a seven wire strand. This is possibly because under fixed end conditions the strand is fixed in a particular geometry whereas when one end is free to rotate the strand will unwind and any geometrical inconsistencies will be emphasised and be reflected in the wire strains. In practice this type of construction is invariably fixed and the free end condition was purely to give data to validate various modelling conditions. When Raoof investigated the strain variation close to and a long way from a strand termination, he found considerable scatter in both cases but no significant difference between the two as had been expected. He concluded that as fatigue failures in these strands generally happen at the terminations, strain variation was not a good indication of fatigue life. This seems a reasonable conclusion, however if terminations were improved to such a level that they did not induce premature failure, the strain variation may then be an important factor in the strands fatigue life. It seems that whatever mechanism causes increased wire breaks and ultimately premature failure at these strand terminations cannot be deduced by strain gauges placed on the wires.

3.3 Experimental results

This section details tests and modelling carried out on two types of rope: a 19 mm Seale 6x19(9/9/1) right hand Ordinary Lay rope with IWRC and the same rope in Lang's Lay. The specifications for the ropes and the fatigue loading regime are exactly the same as that used in Chapter 2.

A number of tests have been carried out to investigate the variation in wire strains measured in individual wires during quasi static loading and in fatigue under normal and overloading conditions. An initial series of plots of experimental wire strain against rope load helped identify the strain range within the fatigue loading range as a single parameter which will allow statistical monitoring of variations between wires in cycling conditions.

The first fatigue test examined the effect of fatigue cycling up to 100,000 cycles on the strain ranges of twelve wires at the same cross section. The test was carried out on an Ordinary Lay rope but unfortunately no equivalent Lang's lay results are available.

The second test series looked at the strain distribution along the length of a wire and the effect of fatigue cycling on this. This test was carried out on one Ordinary Lay specimen and a Lang's lay specimen.

The following series of tests examined the effect of overload on the strain range distribution at a single cross section. Test were carried out on both Ordinary and Lang's Lay ropes and once the rope had been overloaded the effect of further fatigue cycling on the strain range distribution was also investigated.

Finally results are presented for the effect of overload on the strain range distribution along the length of a wire in a Lang's Lay rope. The effect of further fatigue cycling on the strain distribution has also been investigated and is included.

3.3.1 Wire strains in quasi static conditions- effect of overload

Figure 3.5 shows the four wire strain readings when the rope is loaded up to 70 kN (28 % rope breaking load). It can be seen that one wire has a significantly higher strain than the rest (approximately 0.5 % compared with 0.3 % for the others). Figure 3.6 shows the rope strain during the same test and it can be seen that this is closer to the more highly strained wire (although 'rope strain' does include termination movement). If we look at the approximate equation for calculating wire strain from rope strain [10]:

$$\varepsilon_{wire} = \frac{\varepsilon_{rope}}{\cos\alpha_{wire}\cos\alpha_{strand}} \qquad \ldots(3.1)$$

with the wire and strand angles both around 16° this predicts that the wire strain should be slightly higher than the rope strain which is the case with the wire with the higher strain. However on the basis that the linear section of the unloading behaviour of the rope is more representative of rope behaviour (through excluding resin cone draw in the

termination) the group of three wire strains appear more 'normal' and the higher strain more exceptional.

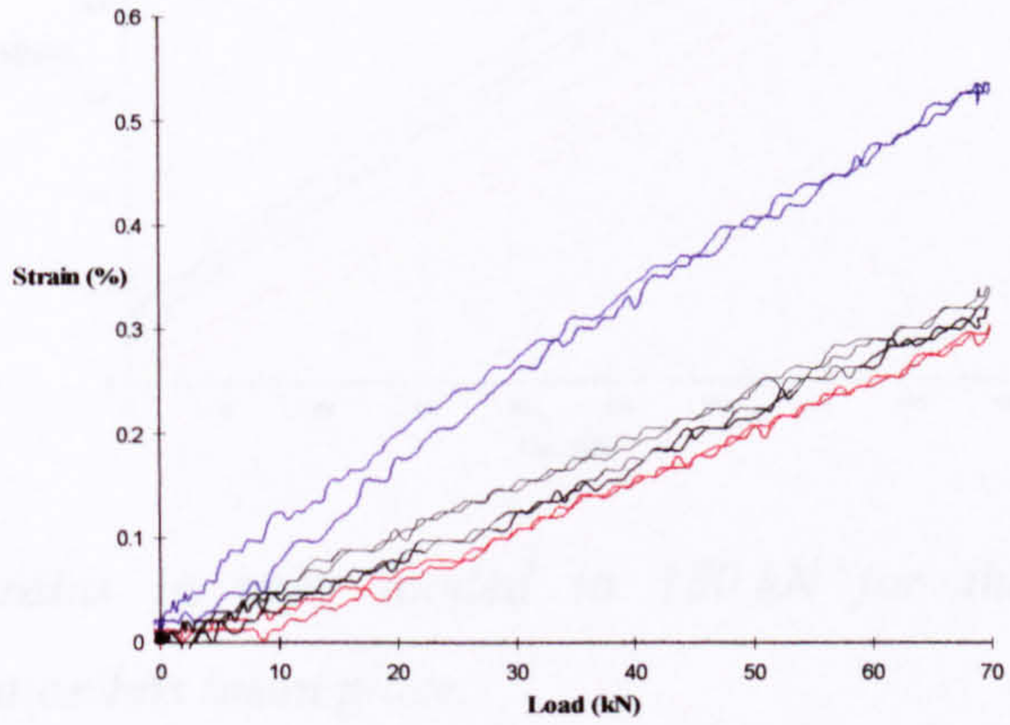

Figure 3.5. Rope loaded up to 70 kN showing variations in wire strains.

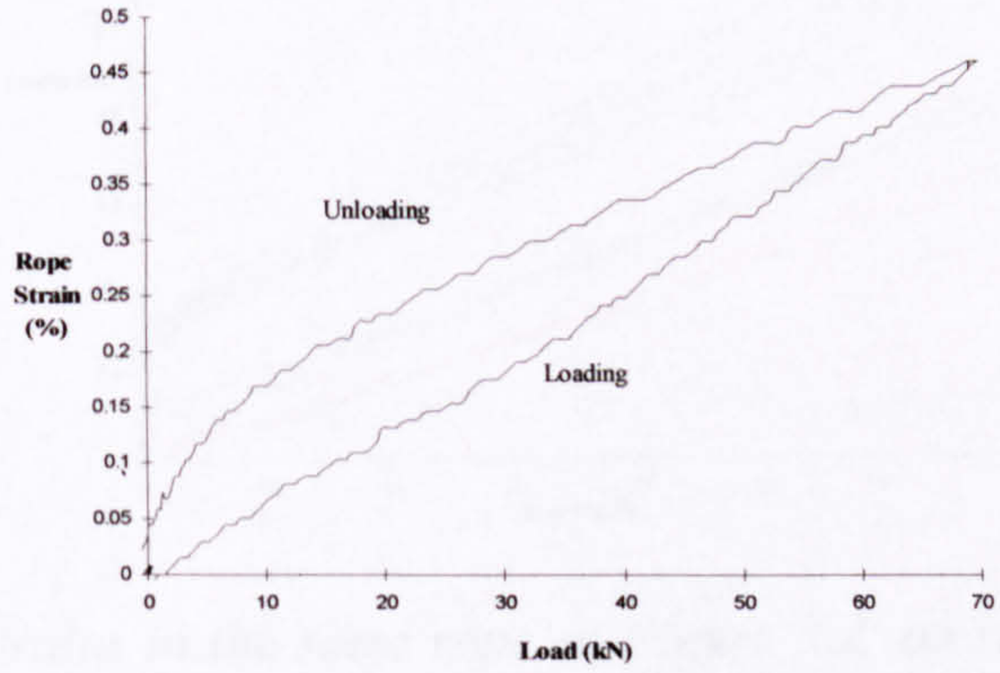

Figure 3.6. Rope strain (including terminations) during the same loading period as Figure 3.5.

Figure 3.7 and Figure 3.8 show the effect of overloading the rope to 72 % rope breaking load. It can be seen that two of the wires have undergone permanent deformation. Once unloaded, on subsequent loading all wires behave elastically with a uniform elastic strain range and the strain in the initially more highly strained wire is brought closer to the common level.

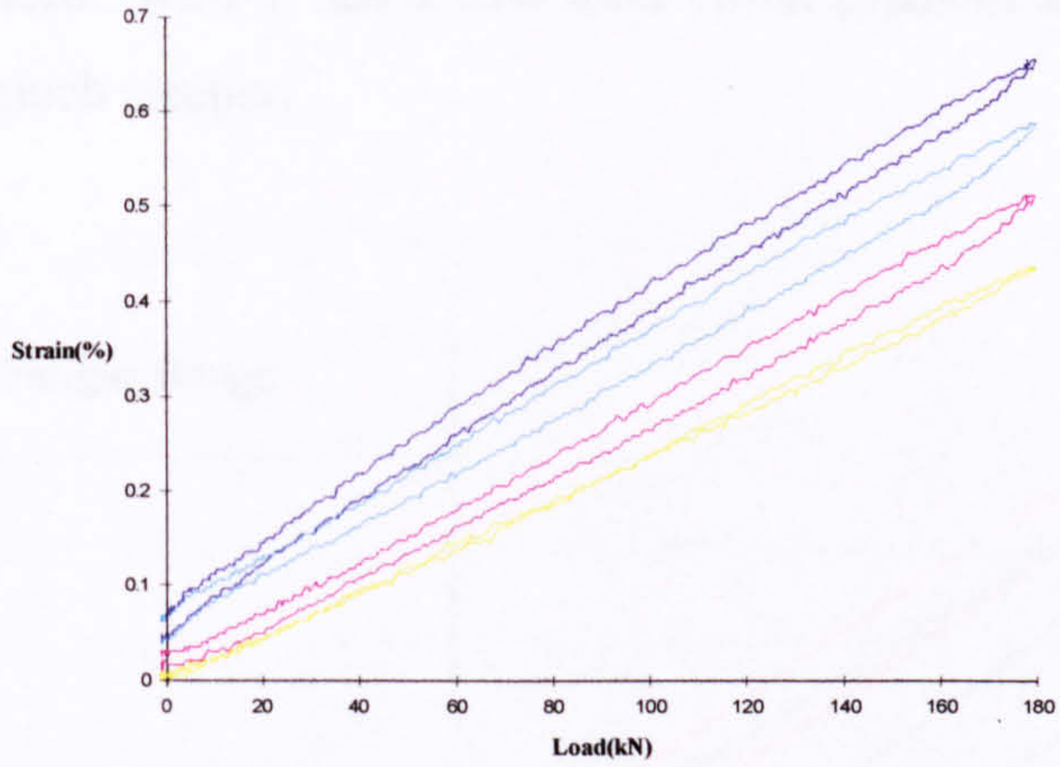

Figure 3.7. Wire strains in rope loaded to 180 kN for the first time. Plastic deformation has taken place.

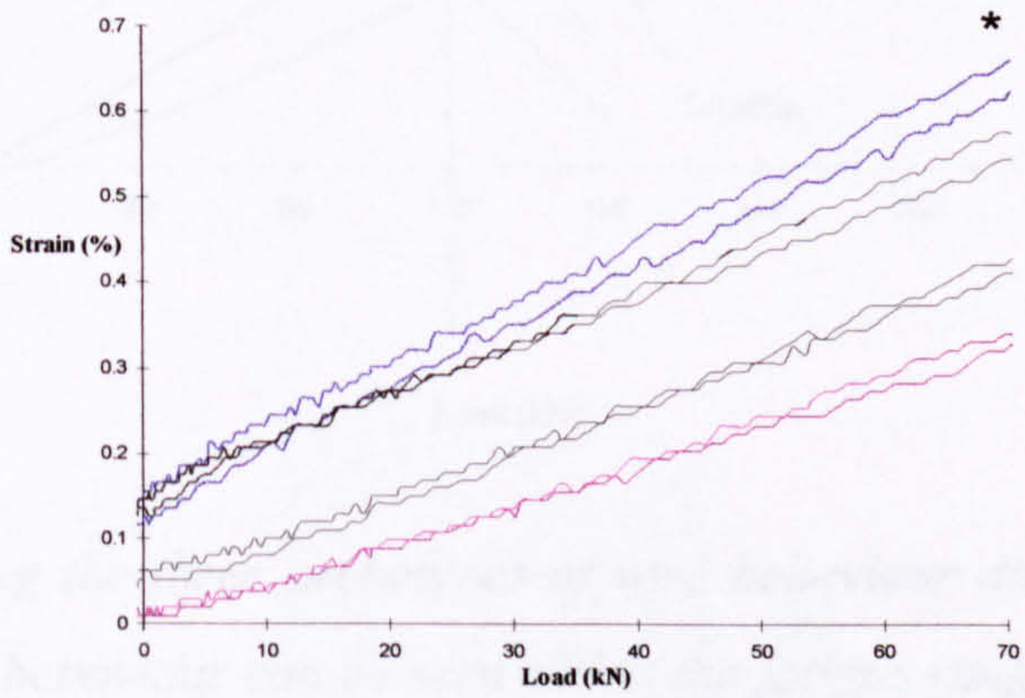

Figure 3.8. Wire strains in the same rope as Figure 3.3, on reloading to 70 kN after overload to 180 kN,for comparison with Figure 3.5. This is actually a partial plot of a test to a higher load, hence the discontinuity location marked (*).

The three types of wire behaviour which were observed during overload are shown in Figure 3.9. By way of examples wire 2 has an average load/strain gradient and appears to be unaffected by overload, wire 12 originally had a high load/strain gradient and clearly becomes plastic at high loads and on unloading the wire load strain gradient within the

fatigue region is reduced. Wire 7 had a low load strain gradient and on unloading the gradient has become much steeper.

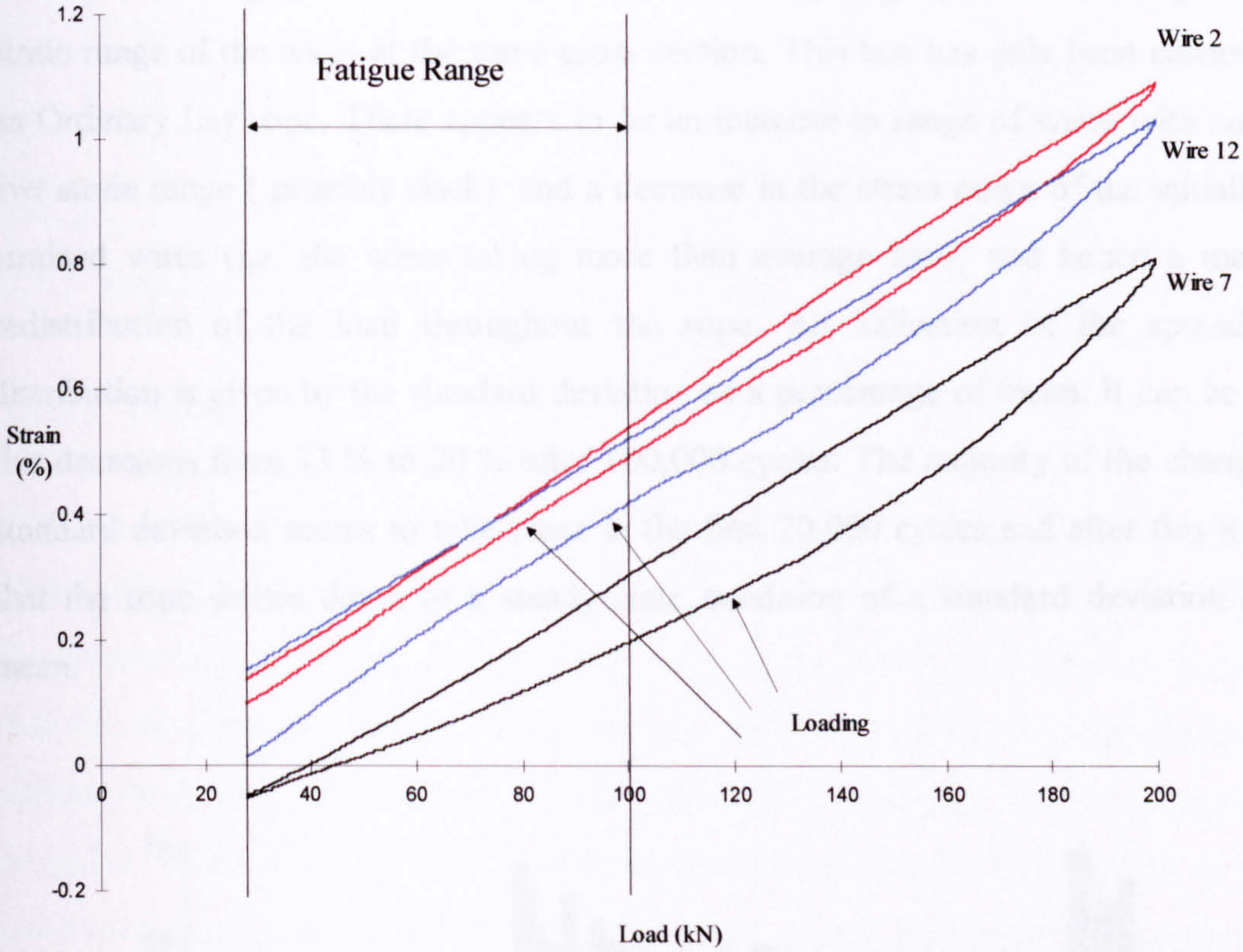

Figure 3.9. Showing the three archetypes of wire behaviour during rope overload. A linear behaviour can be seen within the fatigue range.

A parameter, 'strain range', defined as the average slope of the strain load plot within the fatigue region can be used as a single value to define the strain within a wire for subsequent statistical analysis. All analysis of the strain distributions as described in the following sections of this chapter have utilised this parameter which has been normalised by dividing it by the load range, since the load range is constant for all tests carried out (70 kN) the parameter has still been called 'strain range' despite the fact its units imply stiffness.

3.3.2 Effect of load cycling on the strains of wires measured at the same cross section

Table 3.1 and Figure 3.10 show the effect of load cycling up to 100,000 cycles on the strain range of the wires at the same cross section. This test has only been carried out on an Ordinary Lay rope. There appears to be an increase in range of wires with an initially low strain range (possibly slack), and a decrease in the strain range of the initially highly strained wires (i.e. the wires taking more than average load) and hence a more even redistribution of the load throughout the rope. An indication of the spread of the distribution is given by the standard deviation as a percentage of mean. It can be see that this decreases from 33 % to 20 % after 100,000 cycles. The majority of the change in the standard deviation seems to take place in the first 20,000 cycles and after this it appears that the rope settles down to a steady state condition of a standard deviation 20 % of mean.

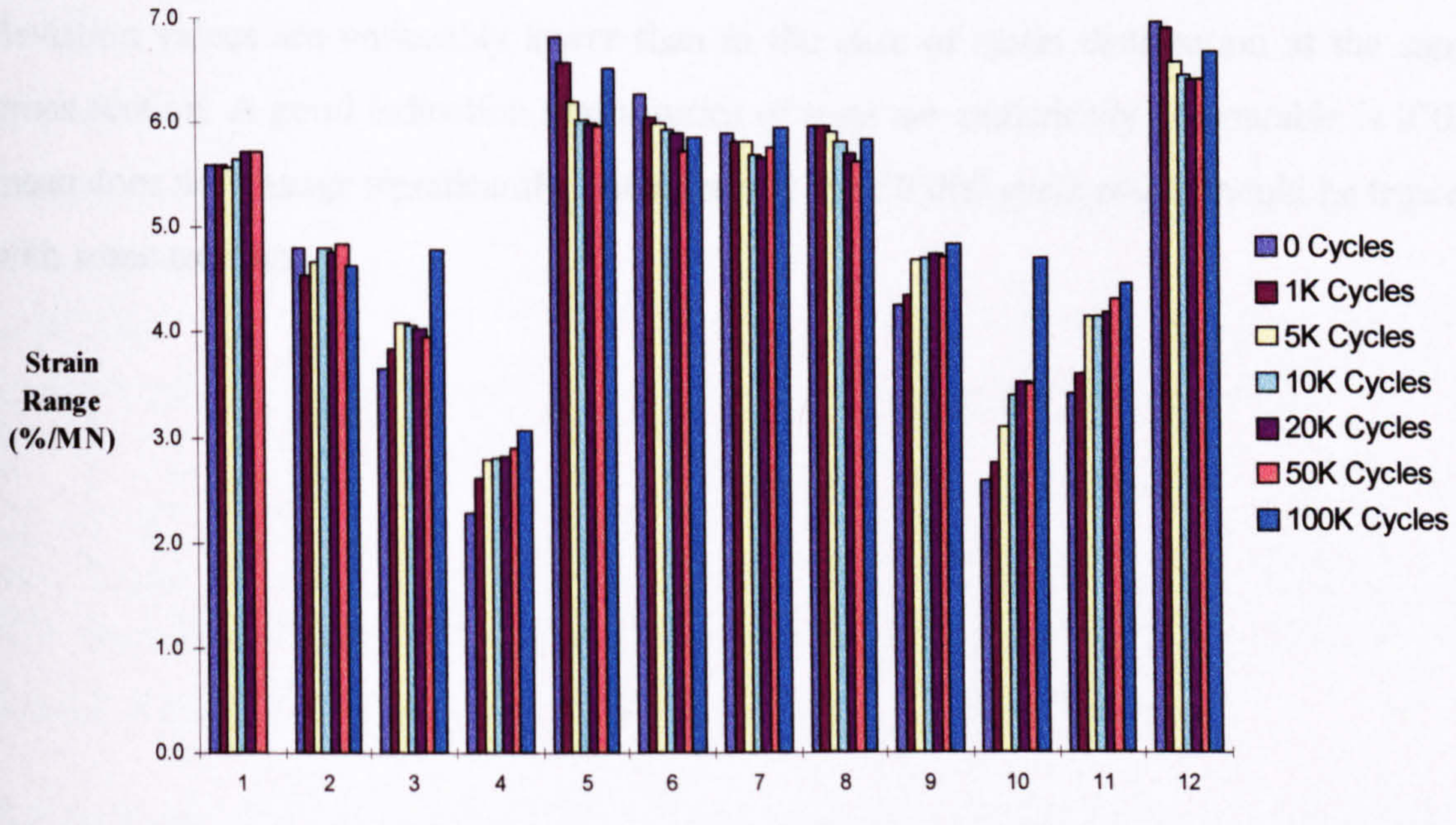

Figure 3.10. Changes in normalised strain ranges of 12 wires at the same cross section due to fatigue cycling.

Table 3.1. Normalised strain range (as %/MN) on 12 wires for the first 100,000 cycles.

Cycles	Gauge												Mean	Std Deviation
	1	2	3	4	5	6	7	8	9	10	11	12		(% Mean)
0	5.59	4.79	3.66	2.27	6.82	6.27	5.89	5.96	4.26	2.58	3.41	6.95	4.87	33.24
1k	5.59	4.54	3.84	2.61	6.56	6.04	5.82	5.97	4.35	2.76	3.59	6.89	4.88	30.00
5k	5.56	4.67	4.08	2.78	6.20	5.99	5.81	5.92	4.69	3.09	4.13	6.58	4.96	25.13
10k	5.64	4.79	4.07	2.81	6.02	5.92	5.69	5.81	4.71	3.39	4.15	6.43	4.95	23.20
20k	5.72	4.75	4.02	2.82	5.98	5.90	5.67	5.71	4.74	3.52	4.18	6.40	4.95	22.69
50k	5.72	4.83	3.96	2.90	5.97	5.72	5.76	5.62	4.73	3.50	4.31	6.39	4.95	22.11
100k		4.63	4.78	3.07	6.50	5.85	5.94	5 84	4 84	4.70	4.46	6 67	5.21	20.30

3.3.3 Effect of load cycling on strain distribution along the length of a wire

3.3.3.1 Ordinary Lay

Figure 3.11 and Table 3.2 show the effect of load cycling on the strain ranges along the length of two wires of an Ordinary lay rope. Of the original 12 gauges, three failed before the completion of the test. There is a reduction in the percentage standard deviation, the majority of which seems to be taking place in the first 20,000 cycles after which the rope appears to reach a steady state condition. It can be seen that the percentage standard deviation values are noticeably lower than in the case of strain distribution at the same cross section. A good indication that a series of tests are statistically comparable is if the mean does not change significantly, consequently the 50,000 cycle result should be treated with some caution.

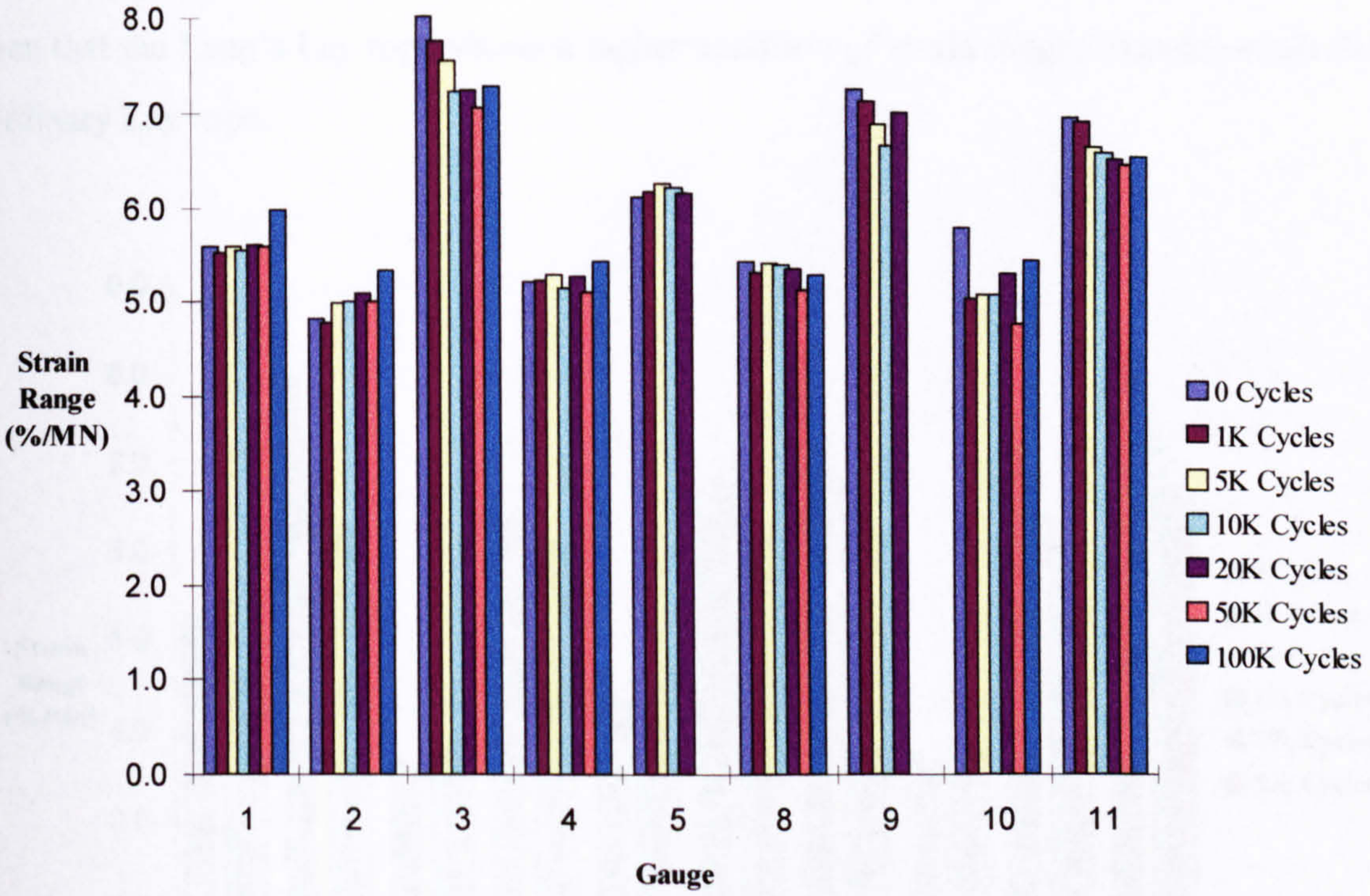

Figure 3.11. Changes in normalised strain range for working gauges on a single wire upto 100,000 fatigue cycles (Ordinary Lay rope).

Table 3.2. Normalised strain range (as %/MN) for working pressures up to 100,000 fatigue load cycles.

Cycles	Gauge									Mean	Std. Deviation
	1	2	3	4	5	8	9	10	11	(%/MN)	(% Mean)
0	5.58	4.81	8.02	5.20	6.11	5.43	7.26	5.81	6.98	6.13	17.39
1k	5.51	4.79	7.75	5.22	6.17	5.30	7.14	5.04	6.93	5.98	17.70
5k	5.58	4.98	7.56	5.29	6.25	5.42	6.89	5.08	6.67	5.97	15.21
10k	5.54	5.01	7.22	5.14	6.21	5.39	6.67	5.09	6.60	5.87	13.89
20k	5.60	5.08	7.25	5.27	6.15	5.35	7.03	5.31	6.55	5.95	13.76
50k	5.57	5.01	7.06	5.10		5.14		4.78	6.49	5.59	15.31
100k	5.96	5.34	7.29	5.43		5.28		5.46	6.56	5.90	12.89

3.3.3.2 Lang's Lay

For the Lang's Lay case the results are shown in Figure 3.12 and Table 3.3. Unfortunately the rope failed prematurely before 100,000 cycles. The results up to 50,000 cycles show a similar trend as in the Ordinary Lay results. The initial range has a standard deviation 27 % of mean, and this has settled to an apparently steady state value of 20 % of mean within

20,000 cycles and there is little change between 20,000 cycles and 50,000 cycles. It can be seen that the Lang's Lay rope shows a higher variation of strain ranges than the equivalent Ordinary Lay rope.

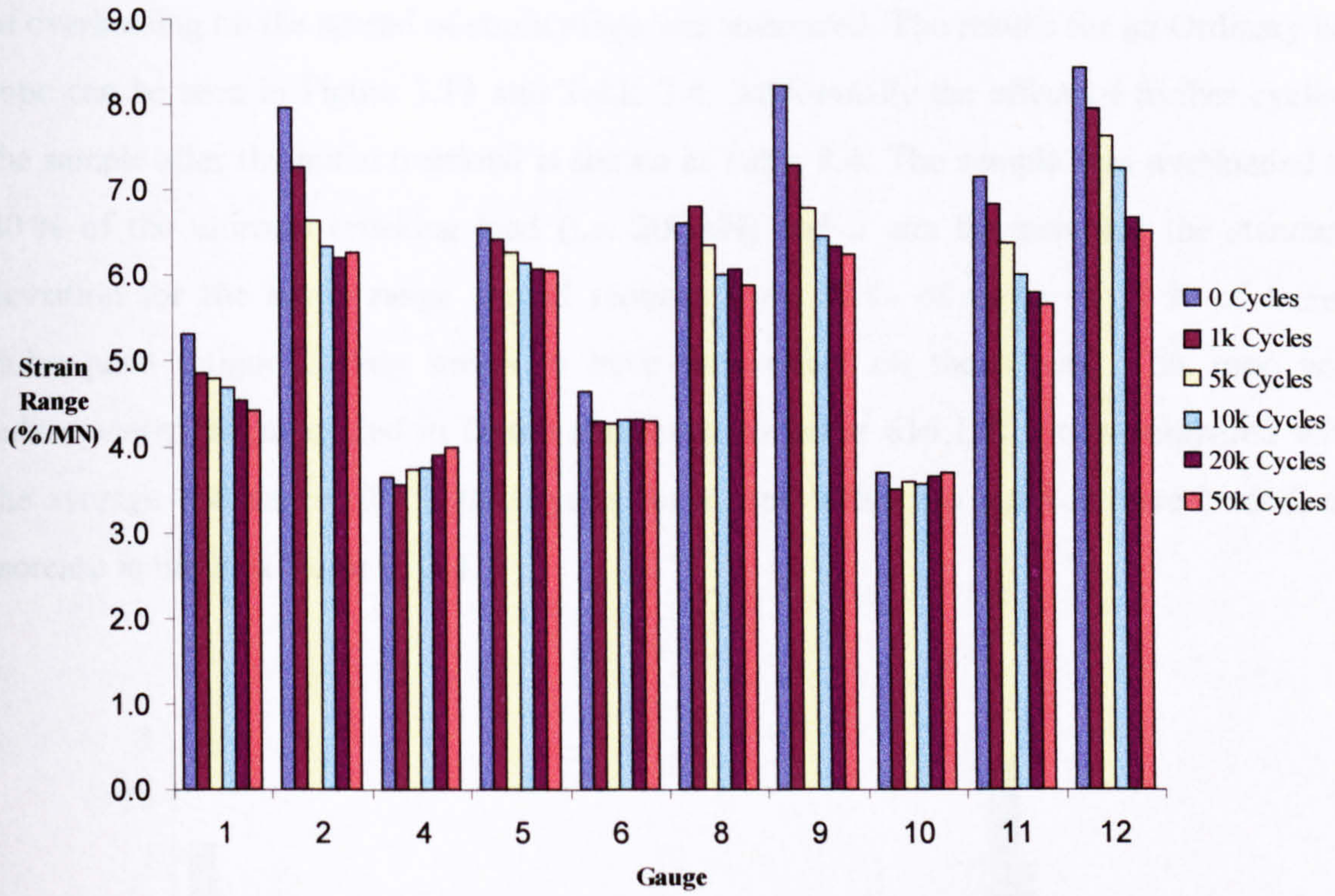

Figure 3.12. Changes in normalised strain range for working gauges on a single wire up to 100,000 fatigue cycles (Lang's Lay rope).

Table 3.3. The effect of fatigue cycling on the normalised strain range (%/MN)

Cycles	Gauge										Mean	Std Deviation
	1	2	4	5	6	8	9	10	11	12		(% Mean)
0	5.31	7.96	3.64	6.56	4.64	6.61	8.22	3.69	7.15	8.44	6.22	27.58
1k	4.86	7.26	3.56	6.42	4.29	6.80	7.28	3.50	6.83	7.97	5.88	26.87
5k	4.79	6.64	3.73	6.26	4.28	6.36	6.80	3.58	6.38	7.63	5.64	23.94
10k	4.68	6.34	3.76	6.14	4.30	6.00	6.46	3.55	6.00	7.26	5.45	22.12
20k	4.54	6.21	3.91	6.07	4.32	6.08	6.33	3.63	5.79	6.68	5.36	19.96
50k	4.42	6.27	3.98	6.05	4.29	5.88	6.24	3.68	5.67	6.53	5.30	19.37

3.3.4 Effect of overload on strain distribution at a single cross section

3.3.4.1 Ordinary lay

Once the rope had reached a 'steady state' condition (i.e. after 100,000 cycles) the effect of overloading on the spread of strain range was measured. The results for an Ordinary lay rope can be seen in Figure 3.13 and Table 3.4. Additionally the effect of further cycling the sample after the initial overload is shown in Table 3.4. The sample was overloaded to 80 % of the ultimate breaking load (i.e. 200 kN) and it can be seen that the standard deviation for the strain range spread reduces from 22 % of mean to 11 % of mean. Subsequent fatigue cycling seems to have little effect on the spread. This rope was subsequently fatigue cycled to failure and found to fail at 616,198 cycles compared with the average endurance of 259,000 cycles for a rope which has not been overloaded, an increase in life by a factor of 2.4.

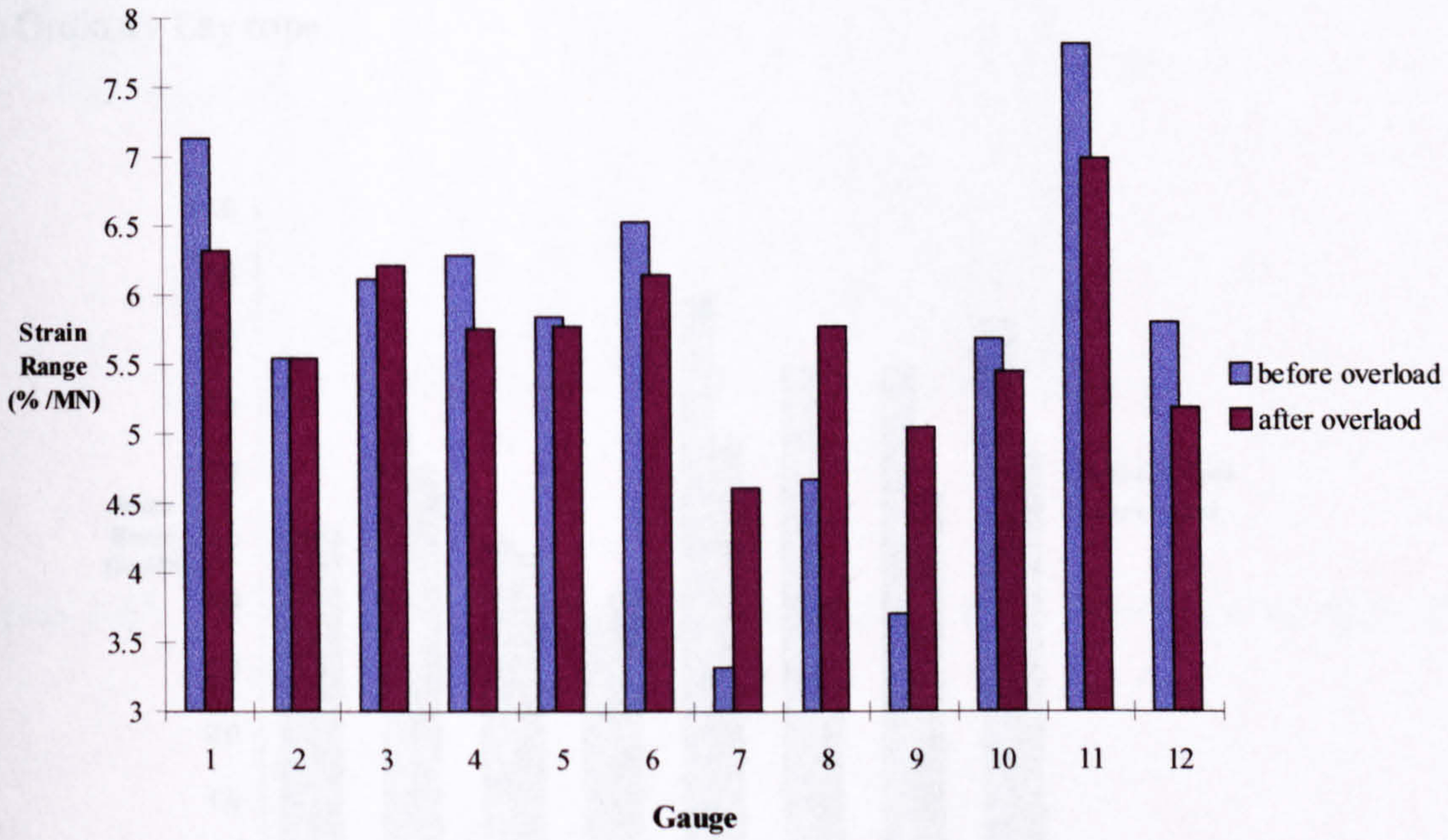

Figure 3.13. The effect of overload on normalised the strain range.

Table 3.4. Wire normalised strain range (as %/MN) during overload and subsequent fatigue cycling.

Loading/ Cycles	Gauge 1	2	3	4	5	6	7	8	9	10	11	12	Mean	Std Deviation (% of Mean)
Bef Overload	7.13	5.54	6.11	6.28	5.84	6.53	3.32	4.68	3.70	5.69	7.81	5.80	5.70	22.72
Aft Overload	6.31	5.55	6.22	5.76	5.78	6.14	4.62	5.77	5.05	5.44	6.98	5.18	5.73	11.08
50K Cycles	5.98	5.22	5.78	5.80		5.66	4.49	5.38	4.64	5.17	6.57	5.10	5.44	11.09
120K Cycles	5.88	5.32	5.79	5.73		5.72	4.51			5.19	6.51	5.09	5.53	10.36
200K Cycles	5.68	5.21	5.86	5.77		5.79				5.26	6.48	5.01	5.63	8.28

3.3.4.2 Lang's Lay

The effect of overload on the spread of strain range for a Lang's lay rope can be seen in Figure 3.14 and Table 3.5. The rope was overloaded to 80 % of breaking load (200 kN) once it had settled in for 20,000 load cycles. Unfortunately a number of gauges failed before the overload was performed and the large change in mean before and after overloading means that these results should be treated with some caution. As in the case of the ordinary lay rope the overload results in a 10 % decrease in the standard deviation as a percentage in mean. The actual spread of the results for the Lang's Lay case seems to be greater, i.e. 27 % before and 17 % after compared with 22 % before and 11 % after for the Ordinary Lay rope.

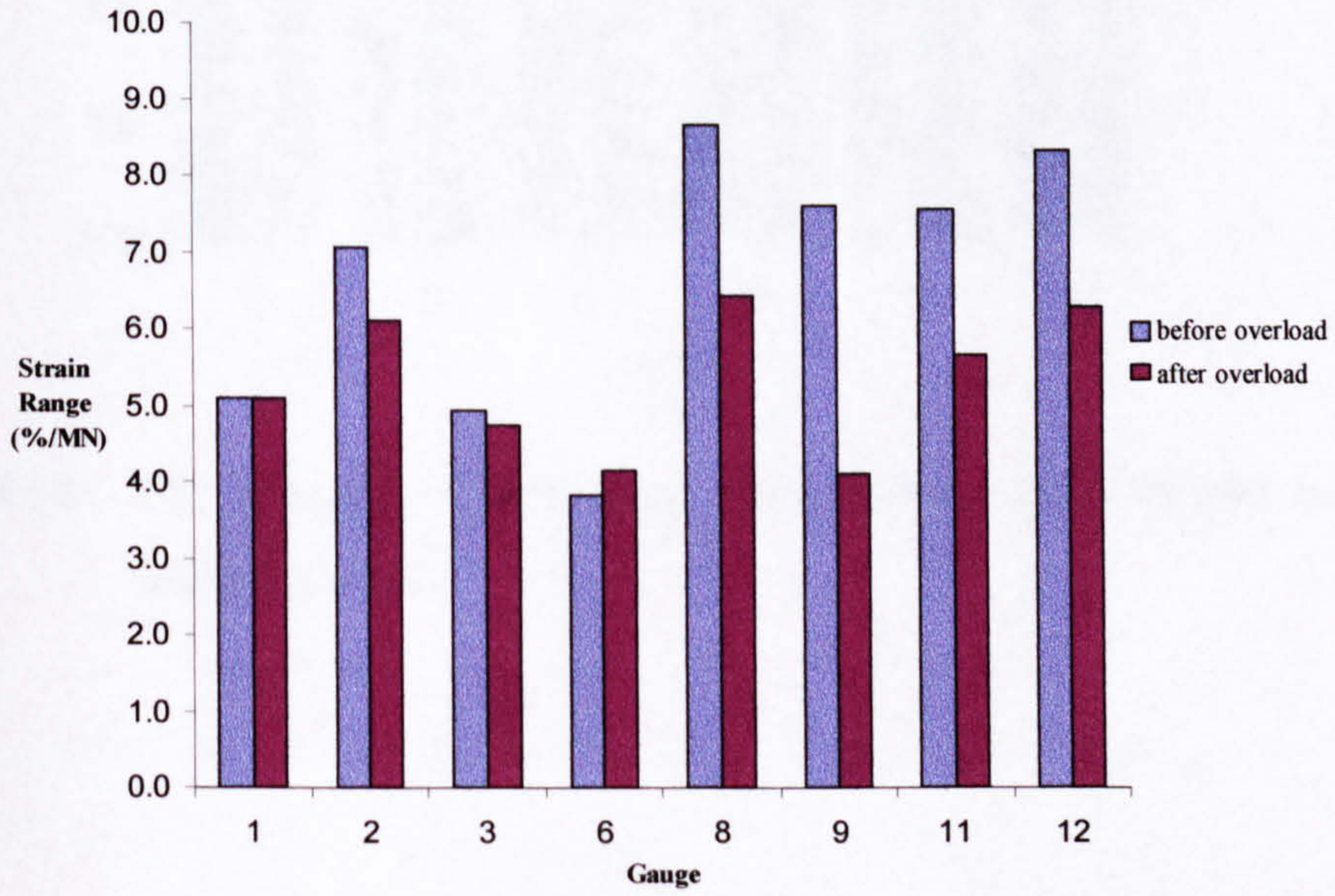

Figure 3.14. The effect of an overload of 200kN on the normalised strain ranges

Table 3.5. The effect of overloading to 200kN on the mean and standard deviation of the normalised strain ranges

Loading	Gauge								Mean	Std Deviation (% Mean)
	1	2	3	6	8	9	11	12		
Bef Overload	5.09	7.06	4.95	3.81	8.65	7.60	7.55	8.29	6.62	26.73
Aft Overload	5.09	6.09	4.73	4.16	6.43	4.09	5.65	6.26	5.31	17.54

The effect of fatigue cycling after the initial overload, was measured and results for this are shown in Figure 3.15 and Table 3.6. It is seen that, as in the Ordinary Lay case, there is relatively little change in the spread of values up to 500,000 cycles (the last sampling point).

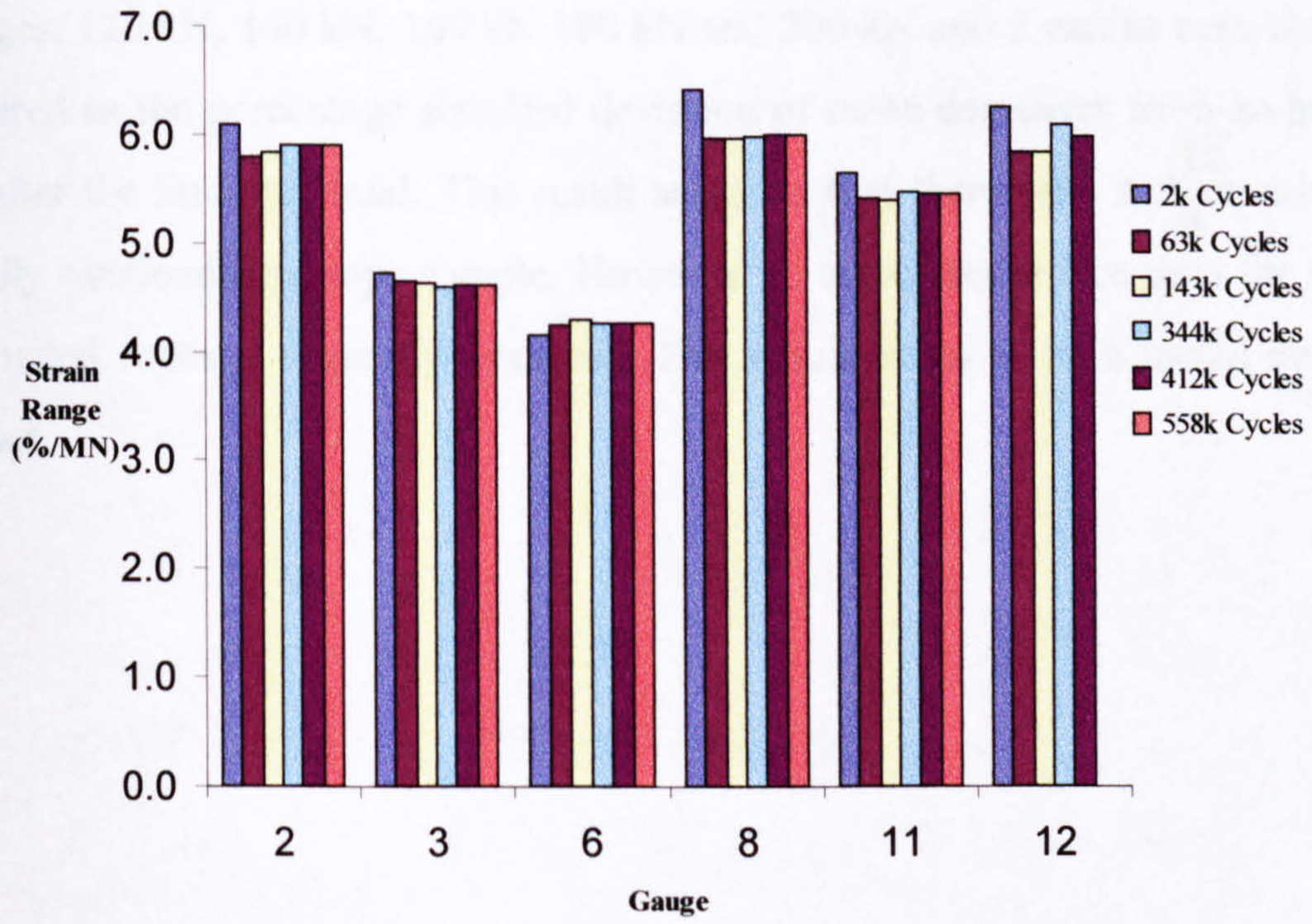

Figure 3.15. The changes in normalised strain ranges after various cycles after the initial overload

Table 3.6. The effect of cycling on the normalised strain ranges (%/MN)

Cycles	Gauge						Mean	Std Deviation
	2	3	6	8	11	12		(% Mean)
2k	6.09	4.73	4.16	6.43	5.65	6.26	5.55	16.47
63k	5.80	4.65	4.24	5.95	5.41	5.83	5.31	13.34
143k	5.84	4.63	4.30	5.95	5.40	5.84	5.33	13.19
344k	5.90	4.60	4.26	5.97	5.47	6.08	5.38	14.36
412k	5.91	4.60	4.27	5.99	5.45	5.98	5.37	14.09
558k	5.91	4.60	4.27	5.99	5.45	0.00	5.25	14.80

3.3.5 Effect of overload on strain along the length of a wire

The effect of overloading on the spread of strains along the length of a wire of a Lang's Lay rope can be seen in Figure 3.16 and Table 3.7. As in previous tests the overload was performed after the rope had settled in for 20,000 cycles. The overloading was performed in stages: 120 kN, 140 kN, 160 kN,180 kN and 200 kN and it can be seen that the spread, measured as the percentage standard deviation of mean decreases from an initial 20 % to 8 % after the final overload. This result suggests that there may well be an advantage from partially overloading a rope sample. However no actual endurance data for such partially overloaded ropes is currently available. This would seem to be a useful investigation to conduct.

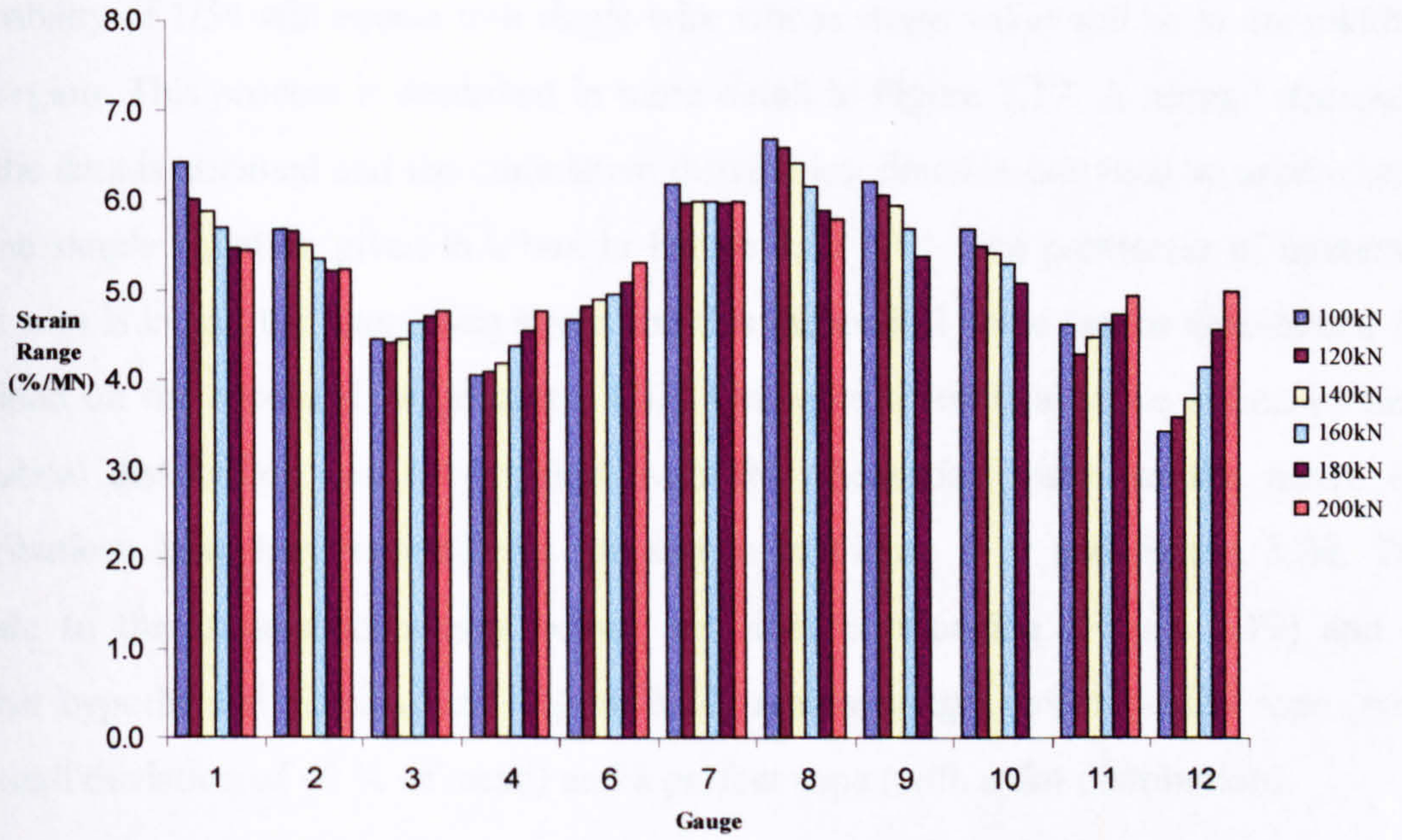

Figure 3.16. Changes in normalised strain range from a series of gradual overloads.

Table 3.7. Changes in normalised strain range from a series of gradual overloads.

Overl. value	Gauge											Mean	Std Deviation
	1	2	3	4	6	7	8	9	10	11	12		(% Mean)
100kN	6.41	5.68	4.44	4.04	4.67	6.18	6.67	6.21	5.70	4.62	3.45	5.28	20.45
120kN	6.00	5.66	4.40	4.08	4.81	5.96	6.58	6.06	5.50	4.30	3.58	5.18	18.97
140kN	5.87	5.49	4.45	4.17	4.89	5.97	6.41	5.94	5.42	4.49	3.81	5.17	16.56
160kN	5.68	5.33	4.63	4.38	4.94	5.98	6.15	5.68	5.30	4.62	4.16	5.17	12.92
180kN	5.46	5.20	4.70	4.54	5.08	5.97	5.89	5.39	5.08	4.74	4.58	5.15	9.61
200kN	5.43	5.22	4.76	4.75	5.29	5.99	5.78			4.95	5.01	5.24	8.26

3.4 Modelling of wire strain distribution

3.4.1 Modelling technique

The effect of the wire strain variation on the fatigue life of a rope has been modelled based broadly on the principles of a technique proposed by Tytko [18]. As the strain range distribution is not known for all the wires a technique must be used to extrapolate the measured data of the 12 wires to the full distribution of the 54 wires. This has been done in the following way: using the mean and standard deviation of the data, the cumulative distribution function $\Phi(x)$ can be used to predict the probability within a region of the distribution. As the distribution is divided into 54 discrete wires then a region with a

probability of 1/54 will equate to a single wire whose stress value will be in the middle of the region. This process is described in more detail in Figure 3.17. A normal distribution for the data is assumed and the cumulative distribution function can thus be approximated by the simple equation given in a box in Figure 3.17 [19]. The parameter of interest for each wire is in fact the alternating stress and this theoretical value can be determined from the load on the rope and its geometry [10]. Once the theoretical value is known then a statistical distribution can be imposed with this theoretical value as the mean. Four distributions have been created and are shown in Figure 3.19 and Figure 3.20. These equate to the strain distributions before and after overloading (Figure 3.19) and two further hypothetical distributions (Figure 3.20) representing a lower quality rope (with a standard deviation of 40 % of mean) and a perfect rope (with a flat distribution).

Once the full alternating stress distribution in the wires has been assumed then it can be used to predict the fatigue life using the following simple technique: given the fatigue data (S-N curve) for the wires the highest stressed wire in the distribution is considered and the number of cycles for it to fail is then calculated. All the other wires are assumed to have deteriorated by the proportion of the number of cycles to failure (for their particular stress) they have received using the principle of cumulative damage from Palmgren/Miner [20, 21]. At this point the most highly stressed wire is assumed to fail and the other wires then see an increase in stress to take up the load of the broken wire (divided equally). For the next iteration consideration is directed to the new most highly stressed wire and the number of cycles to failure is calculated taking into account the previous damage it has seen using the Miner's summation. The most appropriate S-N data available is that of Waterhouse [22] as shown in Figure 3.21, but this was based on a cross wire fretting configuration and is therefore too harsh for an equal lay Seale rope. An S-N curve is proposed which gives the closest correlation between predictions and experimental data, this is also given in Figure 3.21 and equates to a ten times higher life prediction for a given alternating stress.

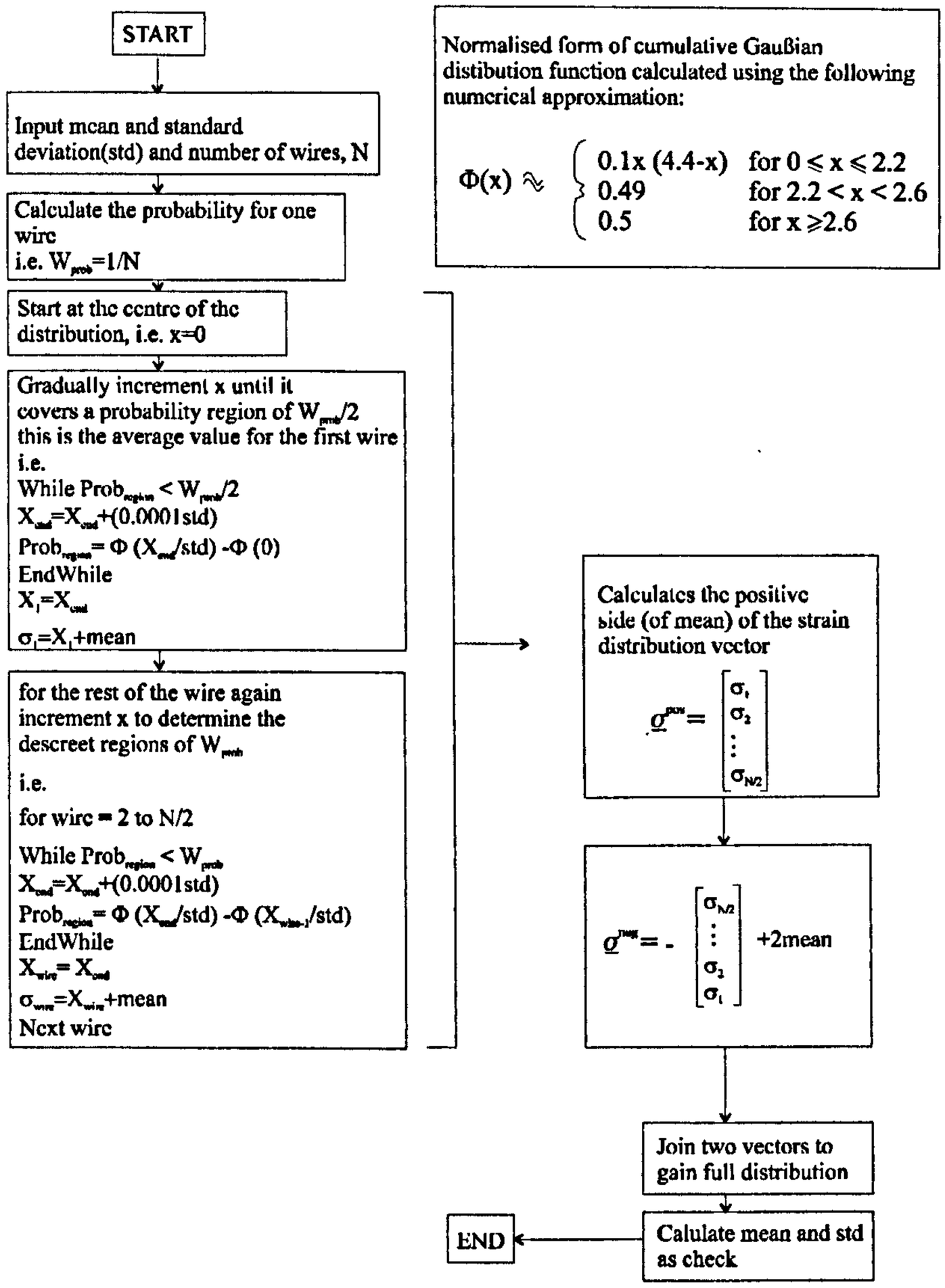

Figure 3.17. Method of attaining a complete wire strain distribution based on the number of wires and the mean and standard deviation of the strain variation of the experimental data.

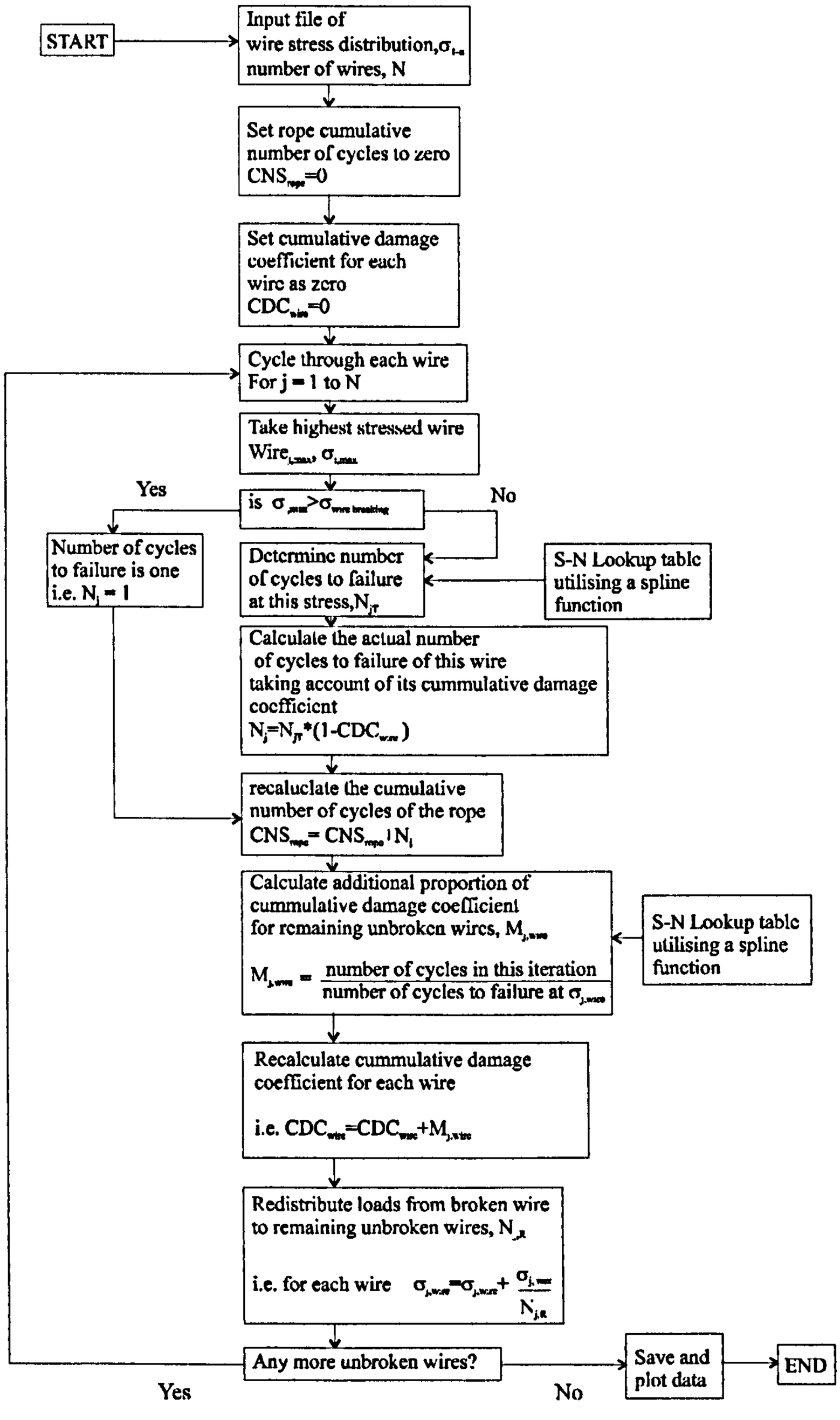

Figure 3.18. The technique for predicting fatigue life based on wire strain variation.

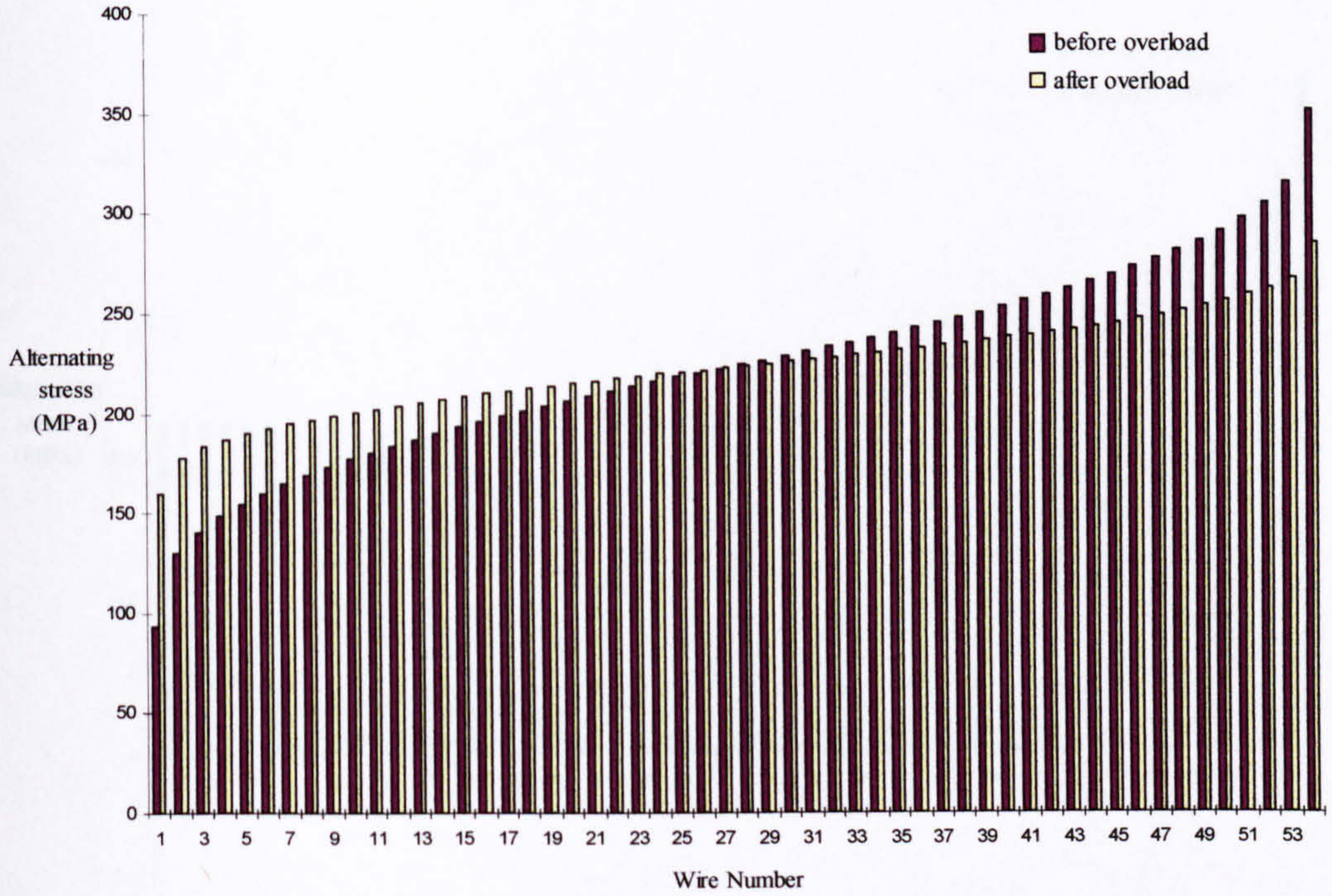

Figure 3.19. Extrapolated wire stress distribution before and after overload.

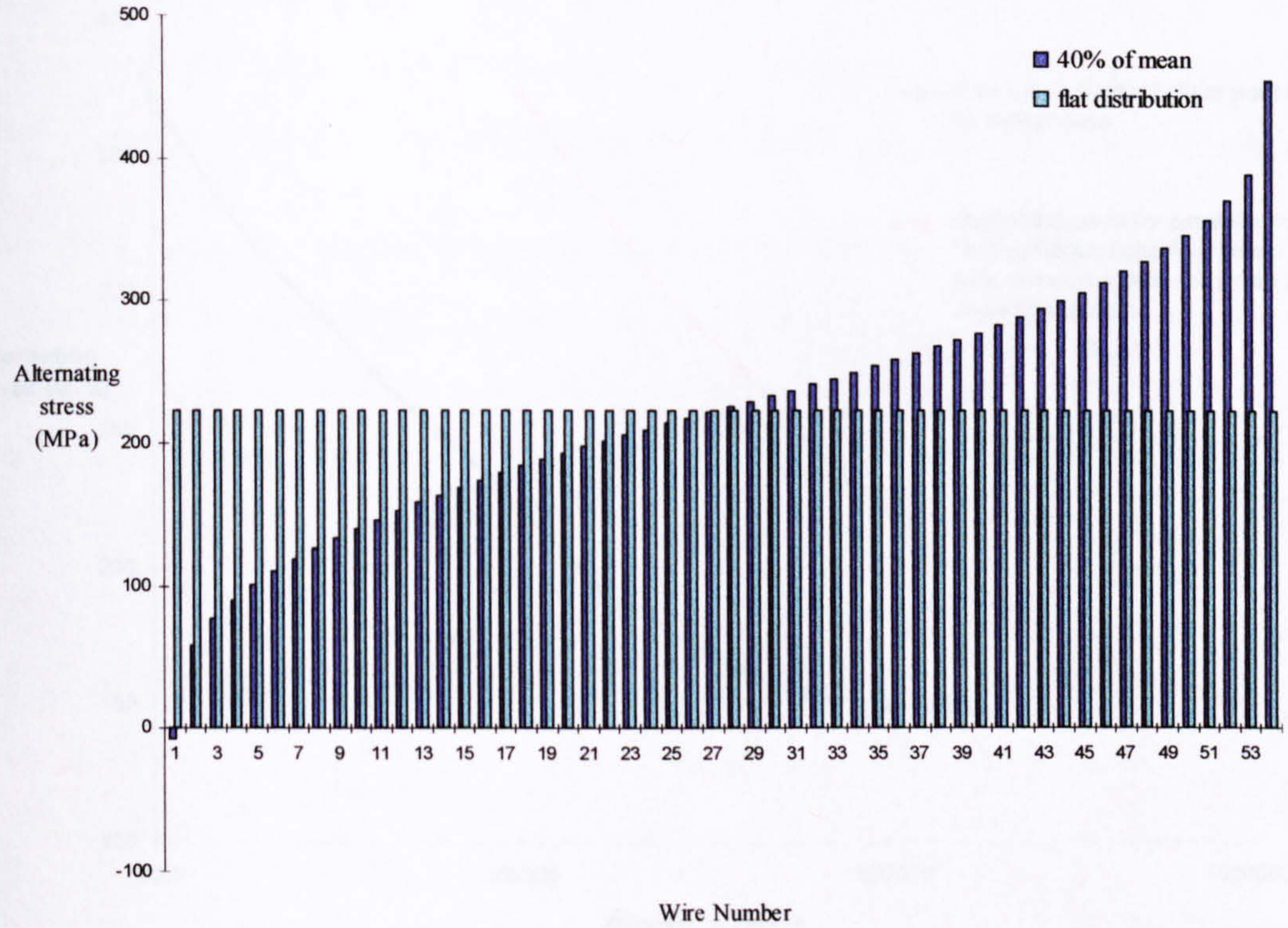

Figure 3.20. Two hypothetical wire stress distributions- no variation and standard deviation 40% of mean.

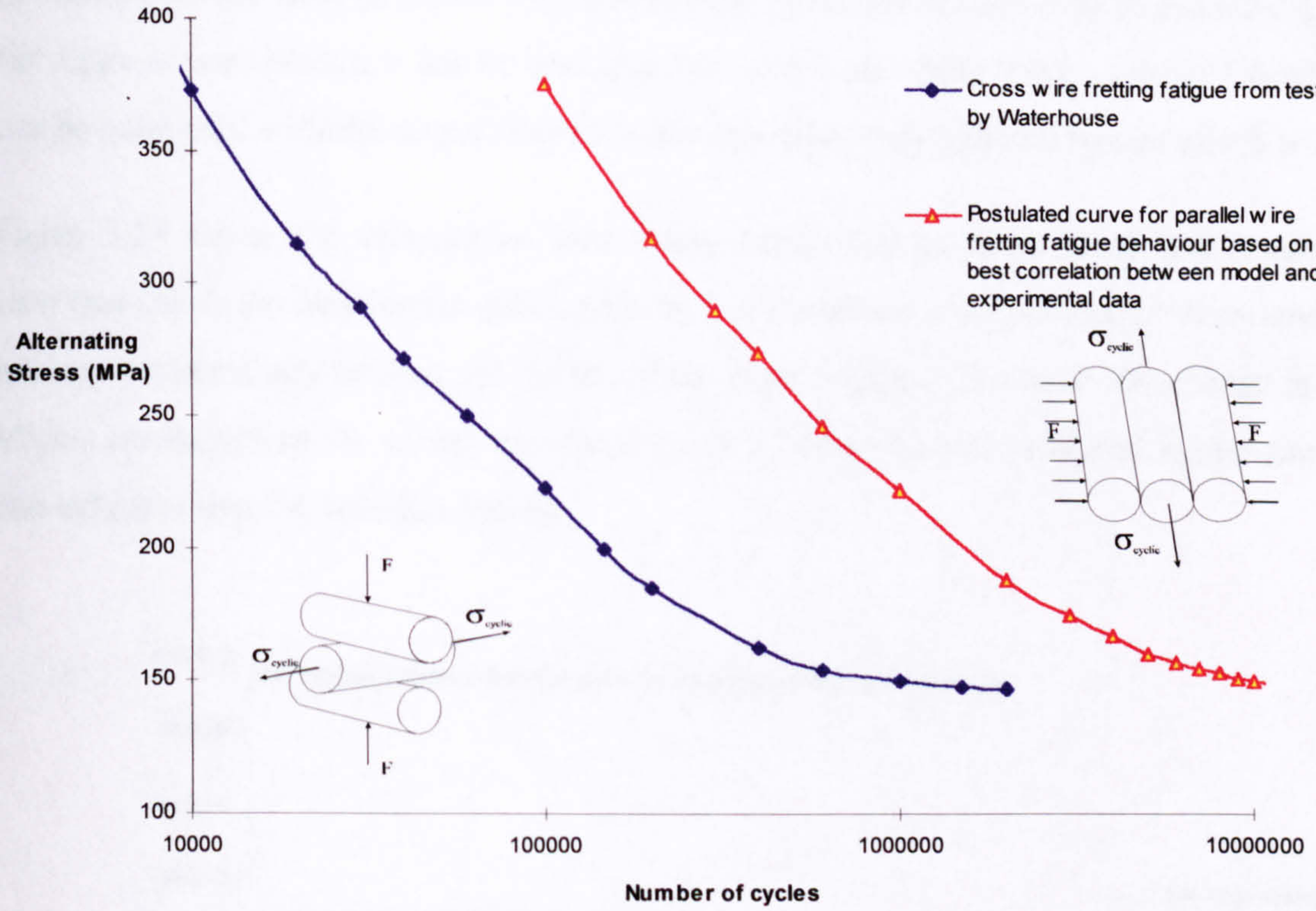

Figure 3.21. Data from Waterhouse for cross wire fretting fatigue of an ungalvanised wire in air and a proposed S-N curve for the parallel wire fretting case which seems to fits the experimental data closest when used as an input to the model.

3.4.2 Results

The model predictions of the Ordinary Lay wire strain distribution have been plotted as the most complete data is available on this rope and also values for fatigue life with and without overloading are known. The plot of wire breaks against fatigue life is shown in Figure 3.22. The model predicts a gradually increasing rate of wire breaks with life until the remaining wires reach their static breaking load at which point the curve flattens off and the rope breaks. The actual endurance values are also shown on the figure.

In Figure 3.23 the ratio of life for overloaded rope to un-overloaded rope is given for the full range of wire breaks, it can be seen that the ratio varies from 2.4 to around 1.6 which can be compared with the actual ratio of endurance from experimental results which is 2.4.

Figure 3.24 shows the variation of wire strain distribution as wires break and it can be seen that the stress distribution gets narrower and the actual stresses on the wires tend to increase exponentially throughout the life of the rope. Figure 3.25 shows the change in the Miners summation of the wires throughout the first half of the test (a Miners summation of one indicates that the wire has failed).

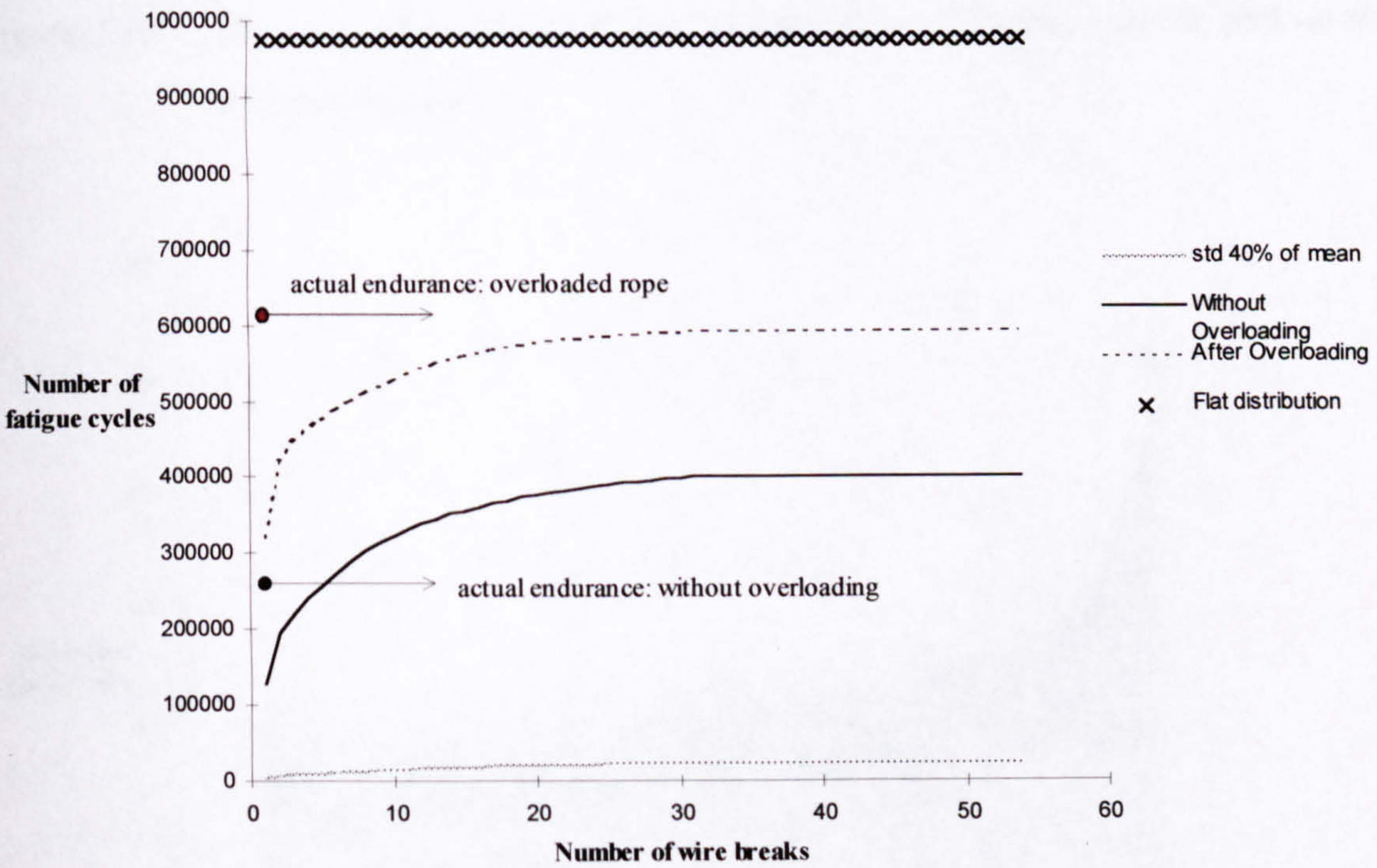

Figure 3.22. The predicted break-up of wires for the four calculated strain distributions.

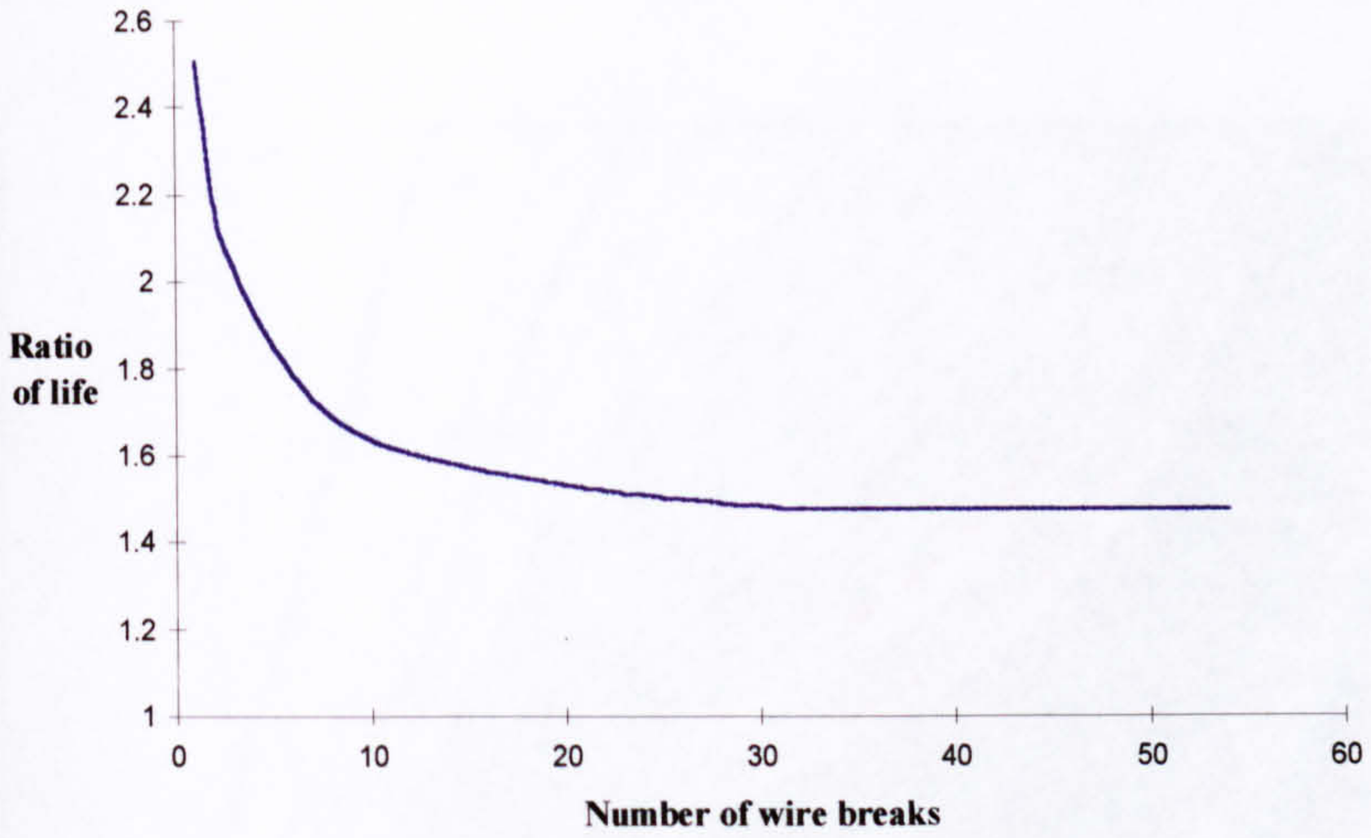

Figure 3.23. The ratio of predicted fatigue life for the overloaded rope to that of the non-overloaded rope.

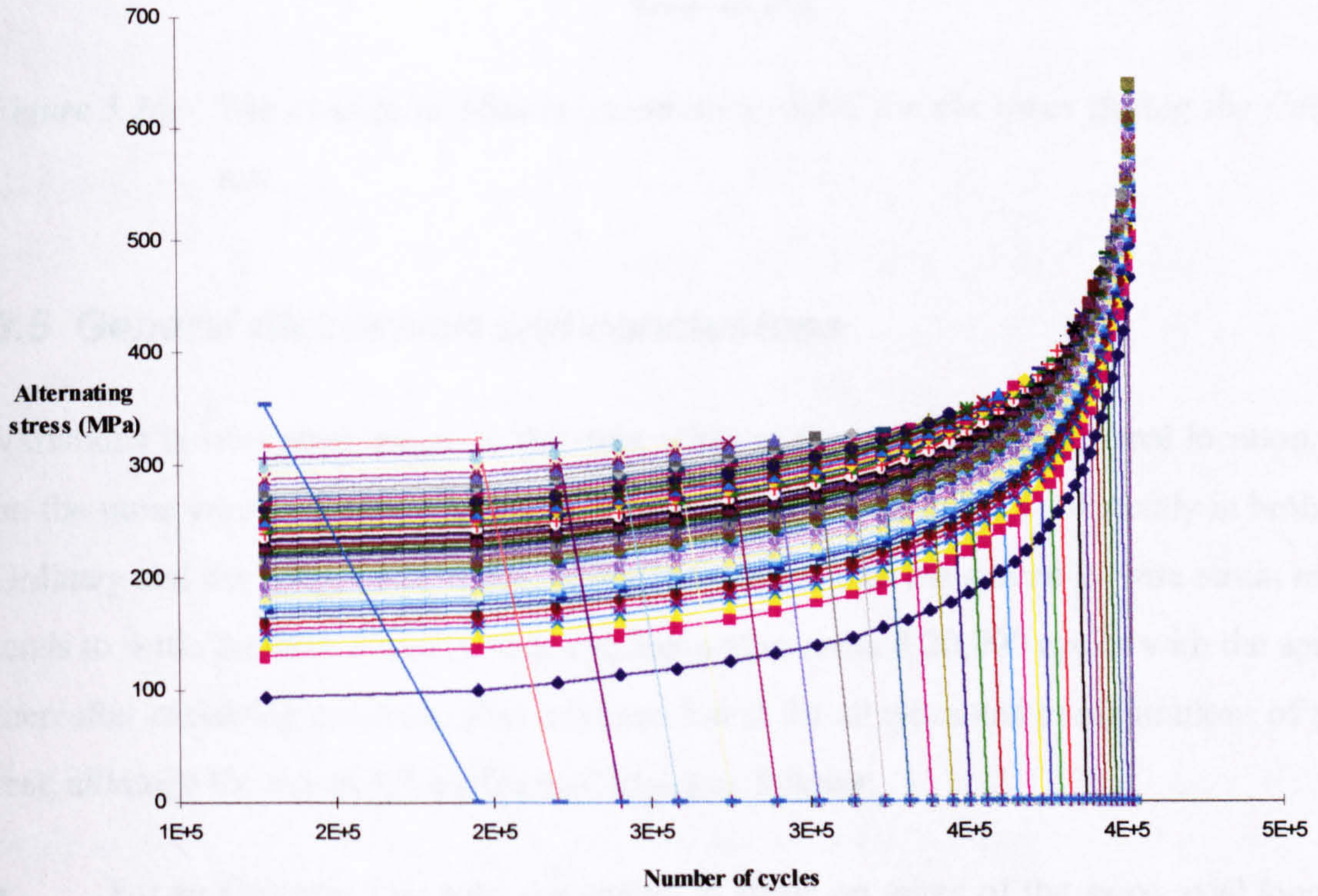

Figure 3.24. Showing the change in strain distribution predicted by the model due to the progressive breaking of wires.

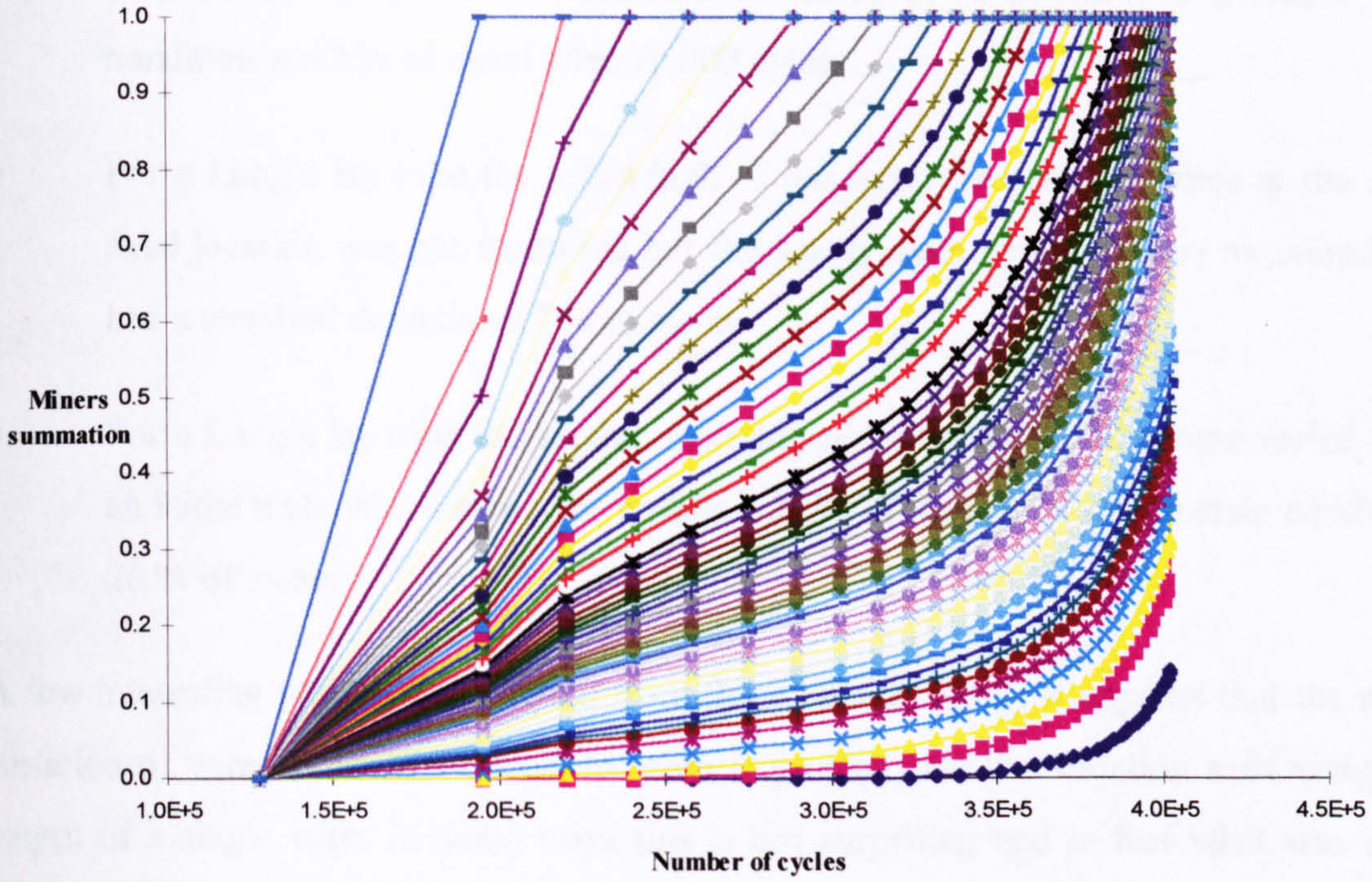

Figure 3.25. The change in Miners' summation value for the wires during the fatigue test.

3.5 General discussion and conclusions

Variations in wire strain range in different wires at the same cross-sectional location and on the same wire at different locations axially have been observed consistently in both the Ordinary and the Lang's Lay ropes. It has been found that the spread in wire strain range tends to settle down to a steady state condition after around 20,000 cycles with the spread thereafter remaining constant. This has been found for all types and configurations of rope test, although the actual value of spread varies as follows:

- For an Ordinary Lay rope the spread in strain on wires of the same axial location decreased from an initial high, with a standard deviation 33 % of mean, to a steady state condition after 20,000 cycles with a standard deviation 20 % of mean.

- For an Ordinary Lay rope the spread in strains along the length of a wire varied from an initial high with a standard deviation 17 % of mean to a steady state condition at 12 % of mean after 20,000 cycles.

- For a Lang's lay rope the initial high of the strain variation of wires at the same axial location was not measured but the steady state condition was measured and had a standard deviation 27 % of mean.

- For a Lang's lay rope the spread in strains along the length of a wire varied from an initial high, with a standard deviation 28 % of mean to a steady state condition, 20 % of mean.

A few interesting points can be noted from these results. Firstly it appears that the strain variation of wires at the same axial location is greater than the variation seen along the length of a single wire. In some ways this is not surprising and in fact what was more surprising was finding any significant variation in strains along the length of a wire. It may be that the variation along the length of a wire is caused by a different aspect of manufacturing than the variation among wires at the same cross section and each could constitute a different aspect of 'rope quality'. Another consistent observation from the strain variations is that the Lang's Lay rope exhibit a higher strain variation than the Ordinary both along the length of a wire and on different wires at the same cross section. This observation seems to be consistent with [8] results of Wiek and, as has been discussed may be connected to the strand winding process which emphases variations in the case of Lang's Lay rope while correcting variations in the case of an Ordinary Lay rope.

It is interesting to make some comparisons with the data of Wiek. He also found that the strain variation along the length of a wire was less than that on different wires at the same locations (standard deviation 60 % of mean around the sample and 50 % of mean along the length of a wire). He found that the variation was greater in Lang's lay than Ordinary Lay rope. These general trends are the same as have been observed in this present work but the actual levels of variation are seen to be much greater in the results of Wiek. This

may be an indication that the rope specimens used by Wiek were representative of a lower 'quality' than the samples used in this thesis. Wiek found a large number of wires going into compression at low loads, whereas this phenomenon was much less evident in the present work (although it was occasionally noted)- again this could be an indication of a lower quality rope. Additionally Wiek noted that there tended to be two groups of wire strains which seem to be clearly separated, but this phenomenon was not observed in the present rope specimens. Finally Wiek noted a settling down in the wire strain distribution to a steady state after approximately 3,000 cycles (which can be compared with the 20,000 cycles found in the present work). With such a large variation in actual distribution values between this work and Wiek's there seems to be scope for a much larger scale investigation into the strain distribution seen in ropes of varying construction and origin.

The difference in strain range between wires is significantly decreased with overloading. Apparent plastic deformations in the wires cause a balancing out of the rope. This has been found for all scenarios observed, although the exact values for the strain deviation varied from case to case as follows:

- For an Ordinary Lay rope overloaded to 80 % breaking load (200 kN) with strain gauges located at wires at the same cross section, the strain ranges decrease from a standard deviation 22 % of mean to 11 % of mean.

- For a Lang's Lay rope overloaded to 80 % breaking load (200 kN) with strain gauges at the same axial location, the strain ranges decrease from a standard deviation 27 % of mean to one 17 % of mean.

- For a Lang's Lay rope overloaded to 80 % breaking load (200 kN) where the gauges were placed along the length of two wires there is a reduction in the standard deviation of the strain ranges from 20 % to 10 % of mean.

Again it seems that the spread of strain range is greater in the Lang's Lay than Ordinary Lay for a given situation. Also it can be seen that the strain distribution along the length of

a rope after overload is less than the equivalent distribution among wires at the same cross section.

It has been seen that an overloaded rope seems to last significantly longer than a rope which has not been overloaded. For example the Ordinary Lay rope loaded to 80 % breaking load lasted 2.4 times as long as its non-overloaded counterpart under fatigue loading.

The standard deviation seems to decrease gradually with each increment of overload suggesting that there should be a benefit in the fatigue life from a partial overload. It can also be seen that, for both Ordinary and Lang's lay ropes, fatigue cycling after the initial overload does not greatly effect the statistical distribution of the strain range.

The statistical theory and experiment do not match exactly but this is not surprising considering the relative simplicity of the model. The comparison is thought sufficiently close, however, to conclude that strain distribution is likely to affect the fatigue life with broadly the same mechanism of degradation as is assumed in the model. One thing that is not clear from this model is how many wire breaks can be taken as representing a total failure of the rope. It is quite likely that, as the model considers a single cross section of rope, that the assumption that the rope will fail when the wires fail statically (i.e. when the curves flatten off) is over optimistic. Wires breaking at other axial locations close to the cross section of interest are likely to make a contribution to the failure of the rope. A more realistic model may try to sum wire breaks for a region (possibly the effective length) of rope and then utilise 'take up' theories to summate the cumulative effect. One possible method of extending the model in this way would be to incorporate the strain distribution along the lengths of the wire (as measured experimentally) at a number of discrete locations. A similar analysis at all these points would then be carried out, but additionally some kind of summation based on the wire 'effective length' could be used to calculate the interference that a broken wire in one region would have on the strain distribution in another.

3.6 References

1. Chaplin, C.R., Prediction of the Fatigue Endurance of Ropes Subject to Fluctuating Tension. OIPEEC Bulletin, 1995. **70**: p. 31-39.

2. Kies, J.A., Overload Effects on Fatigue Damage of Wire Rope Pendants. Journal of Engineering Materials Technology, 1977. **July**: p. 277-278.

3. Stonesifer, F.R. and H.L. Smith. Tensile Fatigue in Wire Ropes. in Offshore Technology Conference. 1979. Housten, Texas.

4. Smith, H.L., F.R. Stonesifer, and E.R. Seibert. Increased Fatigue Life of Wire Rope through Periodic Overloads. in Offshore Technology Conference. 1978. Housten.

5. Matanzo, F. and J.T. Metcalf. Efficiency of Wire Rope Terminations Used in the Mining Industry. in OIPEEC Round Table Conference. 1977. Luxenburg: OIPEEC.

6. Wiek, L., Facts and Figures of Stresses in Ropes, Part 2. Wire, 1975. **26**(5): p. 214-216.

7. Wiek, L., Facts and Figures of Stresses in Ropes, Part 1. Wire, 1975. **26**(4): p. 173-178.

8. Wiek, L., Measured differences in stress between steel wire ropes in normal lay and lang lay. OIPEEC Bulletin, 1976. **28**: p. 47-59.

9. Wiek, L., Strain gauge measurements at multi-strand nonspinning ropes. OIPEEC Bulletin, 1980. **37**: p. 30-53.

10. Hruska, F.H., Calculation of Stresses in Wire Ropes. Wire, 1951(September): p. 766-801.

11. Wiek, L. Stress Deviations in Steel Wire Rope. in OIPEEC Round Table Conference. 1981. Krakov: OIPEEC.

12. Durelli, A.J., S. Machida, and V.J. Parks, Strains and Displacements on a Steel Wire Strand. Navel Engineers Journal, 1972. **84**(6): p. 85-93.

13. Durelli, A.J. and S. Machida, Responce of Epoxy Oversized Models of Strands to Axial and Torsional Loads. Experimental Mechanics, 1973. **13**: p. 313-321.

14. Paolini, G. and E. Bazzaro. Study of the State of Stress in the Wires of Steel Ropes Under Tensile Loads. in OIPEEC Round Table Conference. 1973. Milan.

15. Utting, W.S. and N. Jones, Tensile Testing of a Wire Rope Strand. Journal of Strain Analysis, 1985. **20**(3): p. 151-163.

16. Utting, W.S. and N. Jones, The Responce of Wire Rope Strands to Axial Tensile Loads,. 1985, Department of Mechanical Engineering, University of Liverpool: Liverpool.

17. Raoof, M., Interwire Contact Forces and the Static, Hysteretic and Fatigue Properties of Multi-Layer Structural Strands (PhD Thesis), in Department of Civil Engineering. 1983, Imperial College: London. p. 500.

18. Tytko, A. Numerical Model for Prediction of Endurance of Wire Ropes. in OIPEEC Round Table Conference. 1997. Reading, UK.: OIPEEC.

19. Weisstein, E., W., CRC Concise Encyclopaedia of Mathematics. 1998: CRC online (http://www.astro.virginia.edu/~eww6n/math/).

20. Palmgren, A., Die Lebensdauer von Kugellagern. Zeitshrift Vereines Deutscher Ingenieure, 1924. **68**: p. 339-341.

21. Miner, M.A., Cumulative Damage in Fatigue. Journal of Applied Mechanics, 1945. **September**: p. 159-164.

22. Waterhouse, R.B., Fretting and Fretting Fatigue of High Tensile Steels in Marine Environments,. 1987, University of Nottingham, Department of Metallurgy and Materials Science.

4. Development and verification of a structural model for high pressure helical wound thermoplastic-wire hose

4.1 Summary

This chapter develops a new structural model for thermoplastic-wire hose and then compares it with experimental results obtained for pressure deformation response in terms of hose axial strain and reinforcement wire strain.

The model is based on a model previously developed by Entwistle and incorporates several new modifications. Firstly the inner core is introduced into the equations and assumed to be compressible. Expressions for its behaviour are derived from Lamé's thick walled cylinder theory. The other main modification to the model is the introduction of a theory to allow for the squeezing effect on wires when a hose gets shorter. Expressions for this behaviour are derived based on a linearised numerical solution to Hertzian contact theory. The governing equations to the theory were solved using a minimising Newton Raphson technique and solutions were calculated for all the hose models which were investigated experimentally.

The theoretical and experimental results show encouraging agreement. For the only hose that increased in length on pressurisation the sensitivity of the model to the Poisson's ratio of the inner core is seen and although the exact Poisson's ratio of the core is not known a value of 0.47 seems to be the closest fit to the experimental results.

Some scatter is noted in the experimental results and it is speculated that this may be an indication of the similar types of variations seen from a more comprehensive series of tests on rope in the experiments described Chapter 3. Considerable hysteretical behaviour is seen in the hose axial strain and it is suggested that this may be due to the twisting

contact movements between different layers caused by the fact that the hose is wound in alternate directions.

4.2 Review: models of hose and strands

4.2.1 Introduction

This section is concerned with reviewing all the theory which is directly relevant to the new hose theory developed later in this thesis. Broadly speaking there have been two separate types of hose theory developed: theory based on a hose where the rubber/interlayer plays a dominant role in the hose behaviour (rubber dominated hose) and hose where the wire reinforcement plays a dominant role in the hose behaviour (wire dominated hose).

The theory for rubber dominated hose has been developed predominantly by Kuipers and co-workers [1-3] and is beyond the scope of this current review. The wire dominated hose theory has been developed predominantly from wire strand theory, consequently a review of strand theory is also included, restricted only to the theories which have been utilised in hose theory. For a more complete discussion and review of strand theories the reader is directed to a number of well written articles by Jolicoeur and Cardou [4-6].

4.2.2 Model of strands assuming no twist or radius change

The work of Hruska is widely cited as the first attempt to analyse the stress within a rope. In three articles [7-9] he analysed the axial, tangential and radial stresses within a strand. His assumption for the deformed helical wire geometry was simple (see Figure 4.1), he assumed that the was no change in the reinforcement winding radius, no twist and that the change in lay angle, α, could be ignored. He also assumed that the wires only take tension and ignored the effects of bending and twisting.

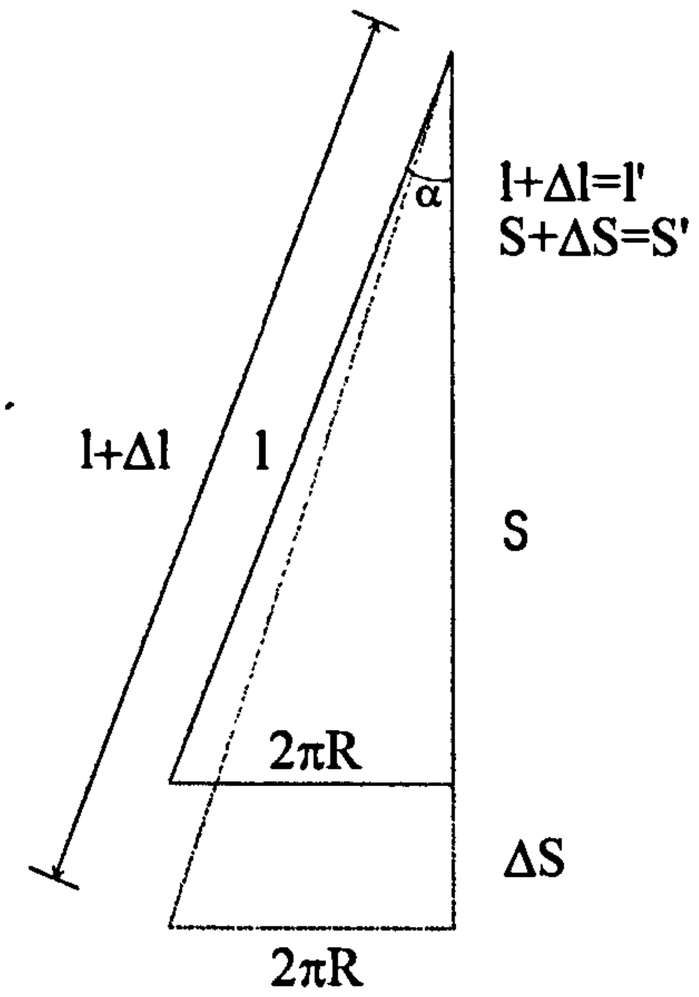

Figure 4.1. Assumption for the deformed helical wire geometry, from Hruska [7].

The expressions for axial and tangential force as a function of tension in the wire, T_i (where i is taken to be the specific layer the wire is in) are given in the following relationships:

$$T_A = T_i \cos\alpha_i \qquad \ldots(4.1)$$

$$T_T = T_i \sin\alpha_i \qquad \ldots(4.2)$$

Although Hruska does not give a derivation for the radial forces (and just gives the final equation) a full derivation appears in Machida and Durelli's paper [10] and is given here. The equilibrium of forces in the radial direction in an element of helical wire is shown in Figure 4.2, where ρ is the radius of curvature of the helix.

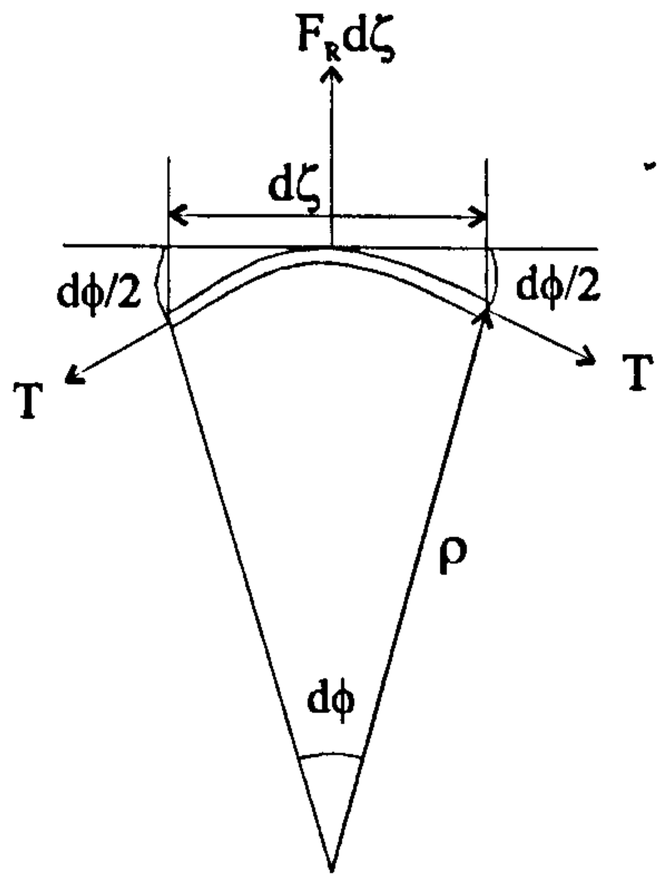

Figure 4.2. Equilibrium of radial force in an element of helical wire, from Machida and Durelli [10].

This results in the following equilibrium:

$$F_R d\zeta = 2T \sin\frac{d\phi}{2} \qquad \ldots(4.3)$$

assuming the angle is small we can make the simplifications as follows:

$$d\zeta = \rho d\phi \qquad \ldots(4.4)$$

$$\sin\frac{d\phi}{2} = \frac{d\phi}{2} \qquad \ldots(4.5)$$

This results in the expression for force per unit length of a wire as a relationship between the wire tension and radius of curvature given as:

$$F_R = \frac{T}{\rho} \qquad \ldots(4.6)$$

The radius of curvature has already been derived in chapter 1 and for a specific layer, *i*, it is given is:

$$\rho = \frac{R_i}{\sin^2 \alpha_i} \qquad \ldots(4.7)$$

This results in an expression for radial force per unit length of hose, R_{RH}, as:

$$R_{RH} = \frac{T_i \sin^2 \alpha_i}{R_i \cos \alpha_i} = \frac{T_i \sin \alpha_i \tan \alpha_i}{R_i} \qquad \ldots(4.8)$$

4.2.3 Model of a strand with twist but no radius change

Machida and Durelli [10] developed a structural model for a seven wire strand (6/1) in tension and torsion. The assumption for the deformed helical wire geometry is shown in Figure 4.3. As the six helical wires are wrapped around a central wire it was assumed that winding radius changes could be neglected. Twist was taken into account in the model however, in terms of a factor γ, which is the rotation coefficient in one pitch, S, of the strand, (i.e. it will twist $2\pi\gamma$ radians in one pitch).

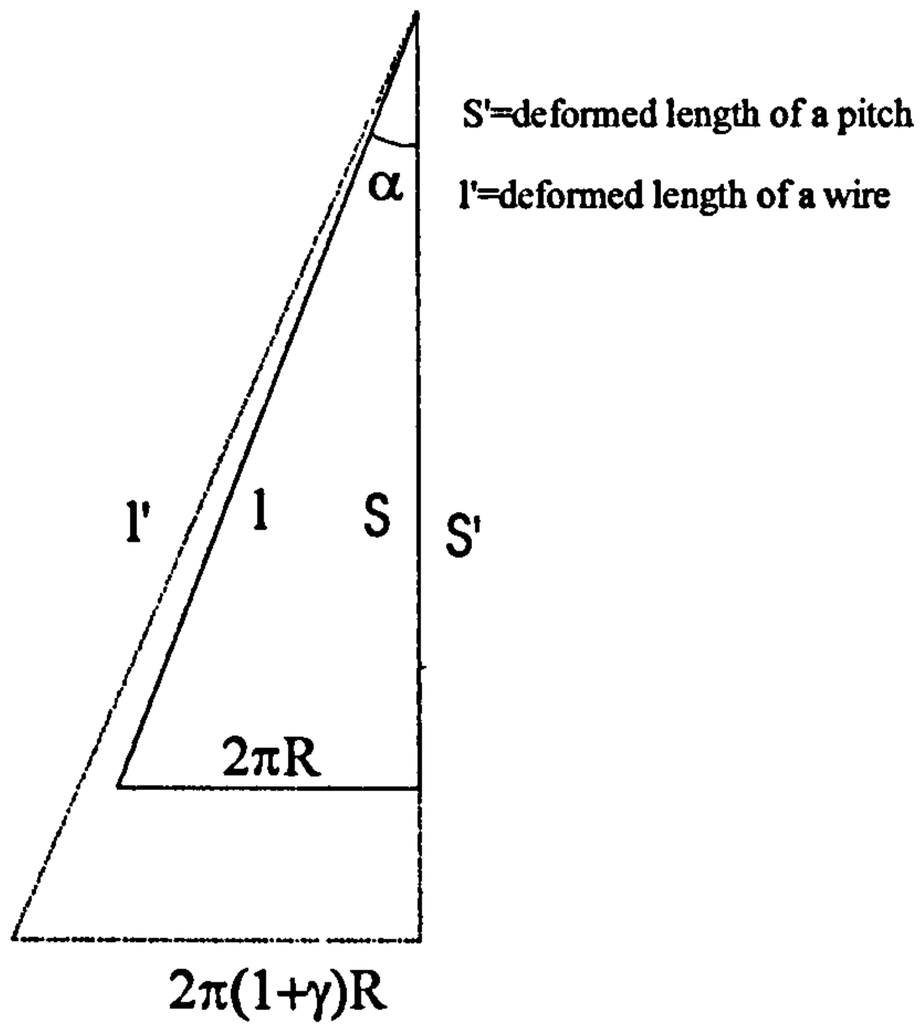

Figure 4.3. Deformed helical wire geometry from Machida and Durelli [10], neglects winding radius changes but includes the effect of twist.

A relationship between the strand axial strain, ε_z, and an individual helical wire strain, ε_i, can be obtained by combining Equations 4.9 and 4.10, which results in the relationship in the form shown in Equation 4.12.

$$S_i(1+\varepsilon_z) = S_i' \text{ and } l_i(1+\varepsilon_i) = l_i' \quad \ldots(4.9)$$

$$\frac{S_i}{l_i} = \cos\alpha_i \text{ and } \frac{S_i'}{l_i'} = \cos\alpha_i' \quad \ldots(4.10)$$

$$\frac{S_i(1+\varepsilon_z)}{l(1+\varepsilon_i)} = \cos\alpha_i' \quad \ldots(4.11)$$

$$(1+\varepsilon_z') = \frac{\cos\alpha_i'}{\cos\alpha_i}(1+\varepsilon_i) \quad \ldots(4.12)$$

Expressions for bending and twisting strains in a wire ($\varepsilon_i^b, \varepsilon_i^t$) were also derived by use of expressions originally proposed by Love [11] which utilise the change in the curvature and torsion of the wire helix and are:

$$\varepsilon_i^{\,b} = (1+\varepsilon_i)y_i(\kappa_i'-\kappa_i) \quad \ldots(4.13)$$

$$\varepsilon_i^{\,t} = (1+\varepsilon_i)r_i(\tau_i'-\tau_i) \quad \ldots(4.14)$$

the curvature and torsion have already been derived in Chapter 1 and are:

$$\kappa_i = \frac{\sin^2\alpha_i}{R_i} \quad \ldots(4.15)$$

$$\tau_i = \frac{\sin\alpha_i\cos\alpha_i}{R_i} \quad \ldots(4.16)$$

The expressions for bending moment, torsion and tension in wires can be summated into their components in the hose axis as shown in Figure 4.4. Where y_i and r_i in Equations 4.13 and 4.14 are the distances from the neutral bending and torsional axes respectively.

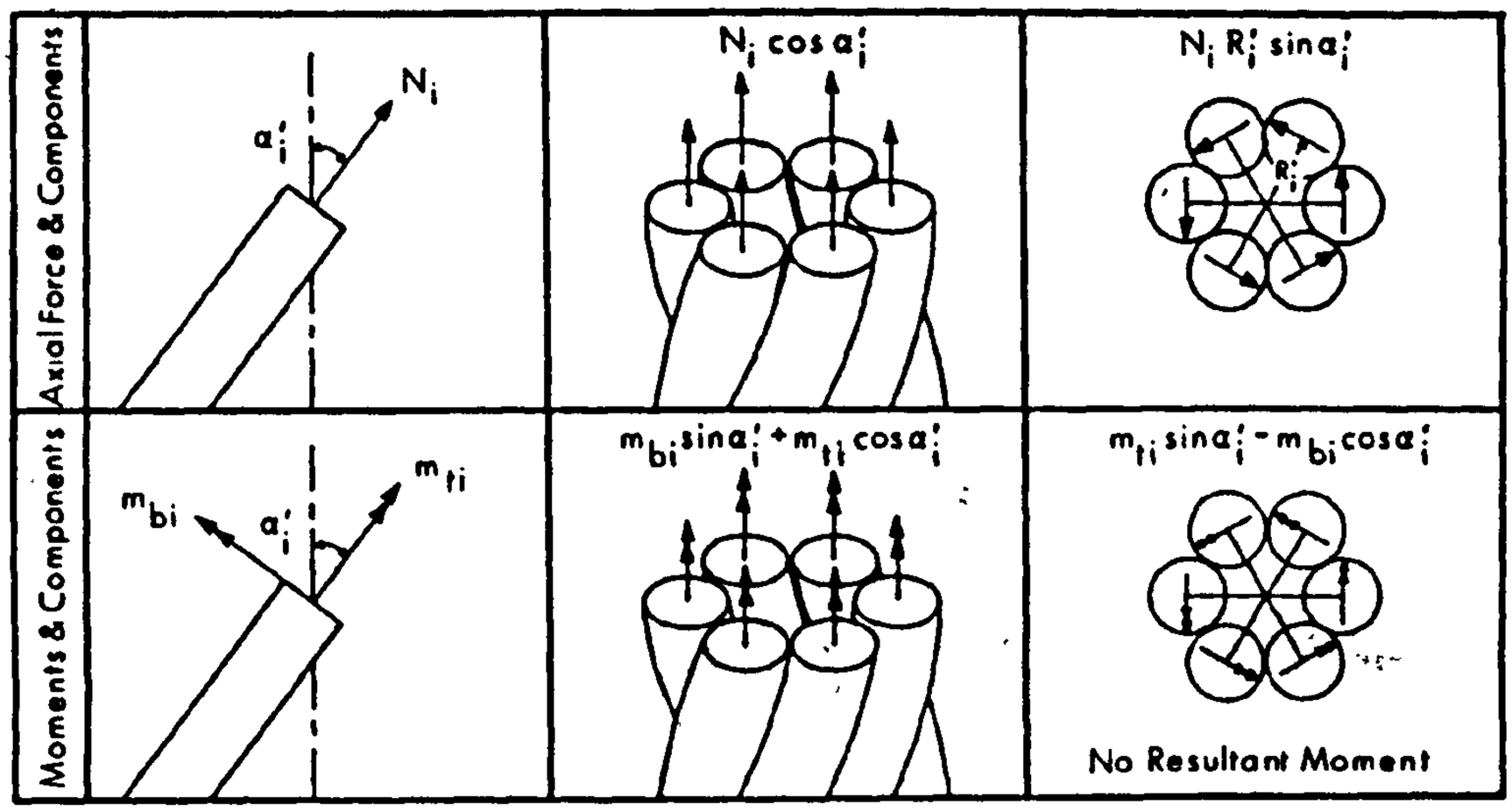

Figure 4.4. Forces and moments on individual wires in a 6 wire strand layer (Where N_i is the tension in a wire, m_{bi} is the bending moment in a wire and m_{ti} is the twisting moment in a wire) figure from Knapp[12] ,modified from Machida and Durelli[10].

Using these relationships they were able to derive a closed form stiffness matrix relating the strand force and torque to the strand axial strain, ε_a and the strand twist coefficient γ as shown in equation (4.17) with the expressions for A, B, C and D as given in equations (4.18-4.21). It should be noted that the expression for B differs from that which appears in the original paper and there is assumed to be a typing error in the original work.

$$\begin{bmatrix} F_{strand} \\ T_{strand} \end{bmatrix} = \begin{bmatrix} A & B \\ C & D \end{bmatrix} \begin{bmatrix} \varepsilon_a \\ \gamma \end{bmatrix} \quad \ldots(4.17)$$

$$A = A_c E + 6A_h E\cos^3\alpha \quad \ldots(4.18)$$

$$B = 6A_h E\sin^2\alpha\cos\alpha \quad \ldots(4.19)$$

$$C = 6A_h RE\sin\alpha\cos^2\alpha - \frac{3GJ\sin 4\alpha\cos\alpha}{2R} - \frac{12EI\cos^2\alpha\sin^3\alpha}{R} \quad \ldots(4.20)$$

$$D = 6A_h RE\sin^3\alpha + \frac{3GJ\sin 4\alpha\cos\alpha}{2R} + \frac{12EI\cos^2\alpha\sin^3\alpha}{R} + \frac{2\pi GJ}{S} \quad \ldots(4.21)$$

4.2.4 Model of a hose allowing for radius change but not for twist

A more appropriate assumption for a hose reinforcement geometry is one which allows a radius change of the inner core as it is pressurised. The first structural model along these lines was proposed by Entwistle [13] for a rubber braided hose. The geometry of the deformed reinforcement is shown in Figure 4.5. The model neglects any twisting in the hose which in practice will be zero for a braided hose and very small for a well designed 'spiralised' hose.

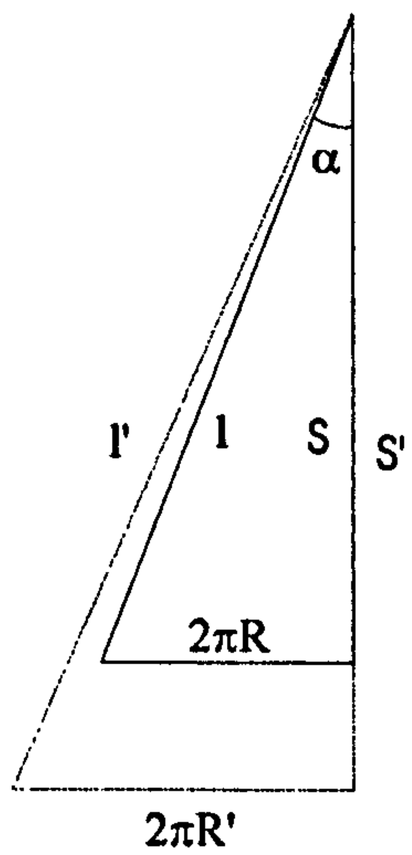

Figure 4.5. Assumption for the deformed reinforcement geometry, from Entwistle[13].

The relationship between the hose axial strain and reinforcement wire strain is unchanged from the Machida and Durelli model as given in Equation 4.12. The relationships between the wire winding radius in undeformed and deformed conditions can be derived by the trigonometric relations for the two cases and are shown in the following two equations:

$$l_i = \frac{2\pi R_i}{\sin\alpha_i} \quad \ldots(4.22)$$

$$l_i' = l_i(1+\varepsilon_i) = \frac{2\pi R_i'}{\sin\alpha_i'} \qquad \ldots(4.23)$$

This results in the following expression:

$$\frac{R_i'}{R_i} = (1+\varepsilon_i)\frac{\sin\alpha_i'}{\sin\alpha_i} \qquad \ldots(4.24)$$

The pressure which one layer applies on another can be derived from the radial force per unit length of hose (i.e. Equation 4.8), if this is divided by the circumference of the layer it gives a pressure in the form:

$$P_i = \frac{N_i T_i \sin\alpha_i' \tan\alpha_i'}{2\pi R_i'^2} \qquad \ldots(4.25)$$

Although Entwistle only gives the case for a two layer hose (the relationship between inner pressure and wire strains), this can easily be extended to a multiple layers hose with n layers in the form of the summation:

$$P_1 = \sum_{i=1}^{n} \frac{N_i T_i \sin\alpha_i' \tan\alpha_i'}{2\pi R_i'^2} = \sum_{i=1}^{n} \frac{N_i A_i E_i \varepsilon_i \sin\alpha_i' \tan\alpha_i'}{2\pi R_i'^2} \qquad \ldots(4.26)$$

The axial equilibrium equation is shown (extended to multiple layers). in the following summation:

$$\pi R_1'^2 P_1 + \pi \sum_{i=1}^{n-1} (R_{i+1}'^2 - R_i'^2) P_{i+1} = \sum_{i=1}^{n} N_i A_i E_i \varepsilon_i \cos\alpha_i' \qquad \ldots(4.27)$$

The right hand side of the equation represents the axial force of the helical wires as proposed by Hruska. The left hand side represents the pressure of the fluid medium acting against the end of the hose, the outer diameter of the inner core is used because the inner core is assumed to have no shear stiffness .This expression is added to a summation which represents the pressure effect of rubber between each pair of reinforcement layers, this

was also assumed to be incompressible and therefore to act hydrostatically exactly like a fluid.

Finally the relationship between the winding radius of one layer and the next was determined by the incompressible rubber between them and this was enforced by the constant volume equation derived in the following two expressions:

$$(\pi {R_{i+1}}^2 - \pi {R_i}^2) S_i = (\pi {R_{i+1}}'^2 - \pi {R_i}'^2) S_i (1+\varepsilon_z) \qquad \ldots(4.28)$$

$${R_{i+1}}^2((1+\varepsilon_{i+1})^3 \frac{\sin^2\alpha_{i+1}'\cos\alpha_{i+1}'}{\sin^2\alpha_{i+1}\cos\alpha_{i+1}} - 1 = {R_i}^2((1+\varepsilon_i)^3 \frac{\sin^2\alpha_i'\cos\alpha_i'}{\sin^2\alpha_i\cos\alpha_i} - 1 \qquad \ldots(4.29)$$

This led to a series of n+1 equations with n+1 unknowns (assuming the pressure is prescribed) and was solved using an iterative Newton Raphson numerical solution.

4.2.5 Models of strand and hose allowing both twist and radius change

4.2.5.1 Soft core strand theory

Knapp [12] developed a new stiffness matrix along the same lines as Machida and Durelli, but allowing for radius changes in the helical wires caused by the compression of the core. The reason for the development of this theory was because some electrical conductor cables have a plastic insulating core. The deformed helical wire geometry is shown in Figure 4.6.

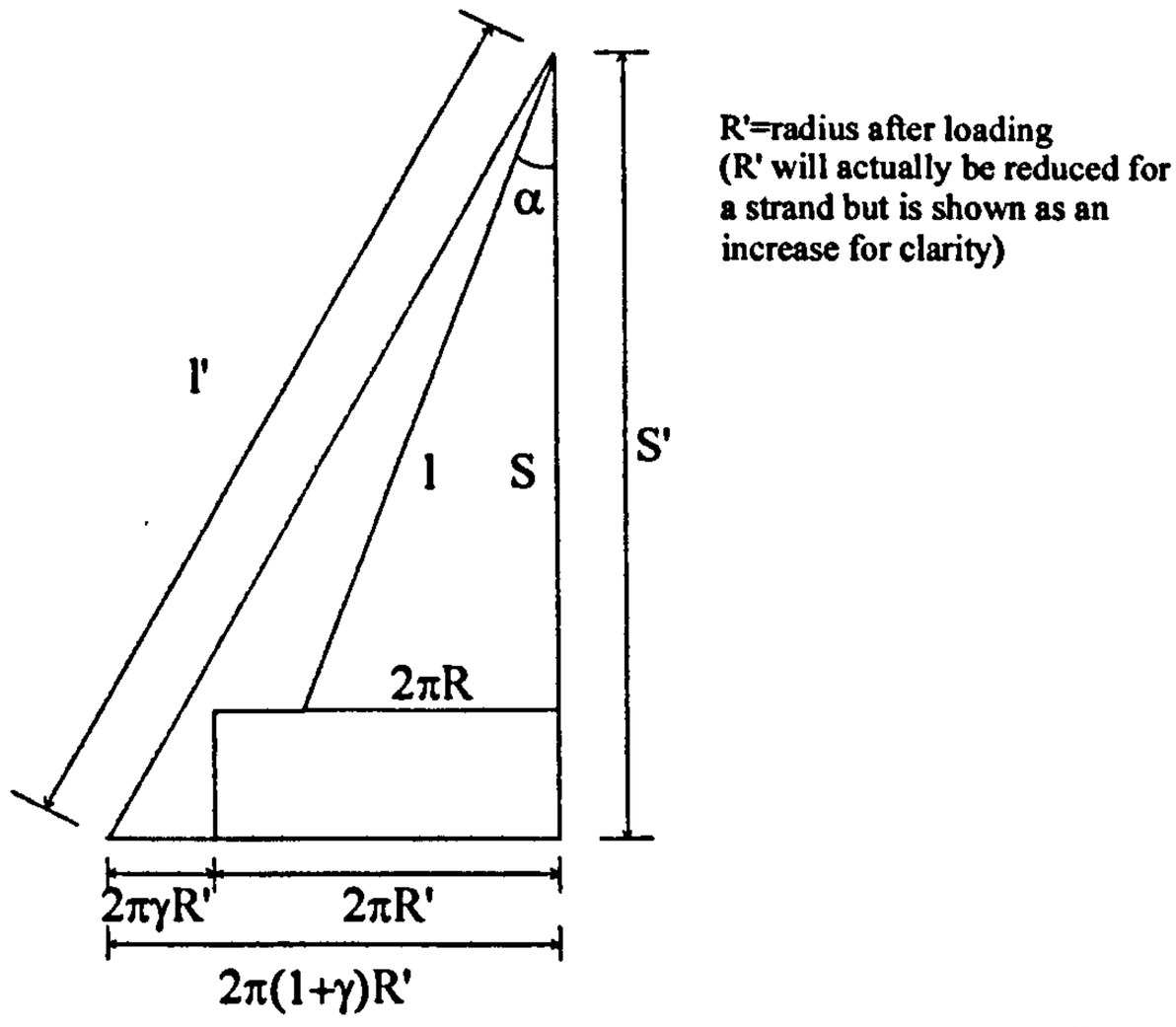

Figure 4.6. Deformed helical wire geometry according to Knapp[12].

The relationship between axial and strand strain is unchanged (i.e. Equation 4.12) but the relationship between the winding radius before and after loading can be derived from the following three expressions:

$$l_i = \frac{2\pi R_i}{\sin \alpha_i} \qquad \ldots(4.30)$$

$$l_i' = \frac{2\pi(1+\gamma_i)R_i'}{\sin \alpha_i'} \qquad \ldots(4.31)$$

$$l_i' = l_i(1+\varepsilon_i) \qquad \ldots(4.32)$$

Combining these results in the following relationship:

$$R_i' = R_i \frac{(1+\varepsilon_i)\sin \alpha_i'}{(1+\gamma_i)\sin \alpha_i} \qquad \ldots(4.33)$$

Bending and twisting forces are taken into account in the same way as Macheda and Durelli's theory and the change in the radius is calculated by the pressure acting on the core and a relationship derived from Lamé's thick walled cylinder solution for the case

with a rigid core inside a compressible tube externally pressurised. After a number of linearising assumptions a closed form stiffness matrix is presented in a similar form to that of Macheda and Durelli.

4.2.5.2 Hose theory

Breig [14] develops a theory which attempts to take into account the twisting effect that a 'spiralised' reinforcement will have on a hose. Using the same deformed helical wire geometry as Knapp (see Figure 4.6) the geometrical relationships given in Equations 4.12 and 4.33 were derived. Unlike Knapp only the axial strains in the wires are taken into consideration and the torsional effect of the helical wires is derived from the tangential force (as derived by Hruska) multiplied by its effective lever arm giving the expression:

$$q_i = T_i \sin\alpha_i'(R_i' + {}^{d_i}/_{2}) \qquad \ldots(4.34)$$

Eliminating T in terms of wire strains, the total torque for a layer will then be:

$$Q_i = N_i A_i E_i \varepsilon_i \sin\alpha_i'(R_i' + {}^{d_i}/_{2}) \qquad \ldots(4.35)$$

The twist is then calculated by the standard strength of materials equation given as:

$$\frac{\Delta\Phi}{l_i} = \frac{2\pi l_i \gamma_i}{S_i} = \frac{Q_i}{J_i G_i} \qquad \ldots(4.36)$$

The polar second moment of area of a single layer is approximated by a tube with thickness *t*, i.e. using the relationship:

$$J_i = \frac{\pi d^3 t}{4} \qquad \ldots(4.37)$$

If the tube has the same thickness as a wire diameter the value for *J* will be given by the expression:

$$J_i = 2\pi(R_i' + {}^{d_i}/_{2})^3 d_i \qquad \ldots(4.38)$$

Combining these relationships gives an expression for γ_i as follows:

$$\gamma_i = \frac{R_i N_i A_i E_i \varepsilon_i \sin\alpha_i'}{2\pi(R_i' + {}^{d_i}/_{2})^2 d_i G_i \tan\alpha_i} \qquad \ldots(4.39)$$

All the other relationships in his theory are taken directly from Entwistle (i.e. Equations 4.26,4.27 and 4.29). After some algebraic manipulations he ends up with a system of $2n$ equations with $2n$ unknowns being $\alpha'_{1\text{-}n}$ $\gamma_{1\text{-}n}$ with the internal pressure and the axial strain, ε_a, as input parameters. He also presents expressions for the inner core assuming relationships given in the following two expressions:

$$R_0' = \left[R_1'^2 - \frac{(R_1^2 - R_0^2)}{(1+\varepsilon_a)} \right]^{1/2} \qquad \ldots(4.40)$$

$$P_0 = P_1 + \frac{2E_{IC}}{3}\left[R_1' - R_1 + \frac{R_1\varepsilon_a}{2} \right]\frac{(R_1^2 - R_0^2)}{R_1 R_0^2} \qquad \ldots(4.41)$$

It is not clear from his paper, however, whether these were added into the structural model or not.

Jakeman and Knight [15] used Breig's theory for a thermoplastic hose, but they changed the interlayer compatibility condition to the following:

$$R_{i+1}' = R_i' + 2d_i \qquad \ldots(4.42)$$

This is because there were no inter layer of rubber in the hose construction. The expression is $2d$ because the layers are braided and so each layer is $2d$ thick (as it is two sets of wires counter wound).

Additionally they added a number of other factors to account for the fact that it is a polymer fibre reinforced hose rather than a wire reinforced hose. These included

accounting for the radius of curvature effect on the yarn strength and including the friction at the braid crimp locations in an attempt to account for hysteresis.

4.2.6 Discussion

It can be seen that no hose theory attempts to model the individual wire bending and twisting effects,. There is however some justification for this as the relative diameter of the wires in the hose is generally considerably smaller, as a proportion to the overall structure, compared with that of a 7 wire strand. However it would seem that a model incorporating bending and twisting strains may be useful simply as a comparison to the existing models in order to gauge the errors incurred in utilising the current simplifying assumptions.

There are a number of specific criticisms of the Breig model. Firstly, the assumption that the polar second moment of area is equivalent to a solid tube seems over simplistic and will result in much stiffer behaviour than actually exists. It seems that it is roughly equivalent to assuming the bending stiffness of the hose is equivalent to that of a solid pipe. Perhaps a more realistic (approximate) assumption for the polar moment of inertia would be the sum of the individual polar moment of inertia of each wire about its own axis. Another criticism of Breig's model is that he uses the axial strain as an input, yet it would not be difficult to rearrange the equations of the model to allow prediction of the axial strain. Since this is one of the few easily measured characteristics of a hose it seems sensible to predict values that can be compared with the experimental results and thus give an indication of the accuracy of the model. Finally Breig's numerical solution involves $2n$ unknowns $\alpha'_{1\text{-}n}$ $\gamma_{1\text{-}n}$ with $2n$ equations. This solution has a parameter for twist, γ, for every layer and yet all the layers in the hose must twist together. It would be trivial to eliminate this parameter in favour of an overall twist parameter and reduce the $2n$ equations down to $n+1$. It would be possible to compare deformation response predictions from the Entwistle and Brieg models, although it is not thought that there would be much noticeable difference between the two.

4.3 Development of a structural model

4.3.1 Basic assumptions

The geometrical relationships developed by Entwistle [13] for the behaviour of the reinforcement before and after pressurisation have been taken as the basis for this current model. The geometry is shown graphically in Figure 4.7 and the fundamental relationships given in Equations 4.12 and 4.24 can be rearranged into the following expressions:

$$\varepsilon_i = (1+\varepsilon_z)\frac{\cos\alpha_i}{\cos\alpha_i'} - 1 \qquad \ldots(4.43)$$

$$R_i' = R_i(1+\varepsilon_z)\frac{\tan\alpha_i'}{\tan\alpha_i} \qquad \ldots(4.44)$$

Like Entwistle [13] this model assumes no twist of the hose on pressurisation. This is thought a reasonable assumption, since there is no noticeable twist of these hoses in experience (they are designed with layers of alternate direction). As is already discussed the torsional assumptions in the form proposed by Brieg [14] are not thought to be a realistic addition to the model and are therefore not included.

The definition of the winding radius of the various reinforcement layers and the inner core is taken to be the inner dimension as shown in Figure 4.7. As there are no layers of rubber or plastic between reinforcement layers in the hose being modelled the expression within the axial equilibrium equation relating to this in the expression of Entwistle[13] has been dropped. Additionally the interlayer compatibility has been replaced by a new simple expression similar to that used by Jakeman and Knight [15].

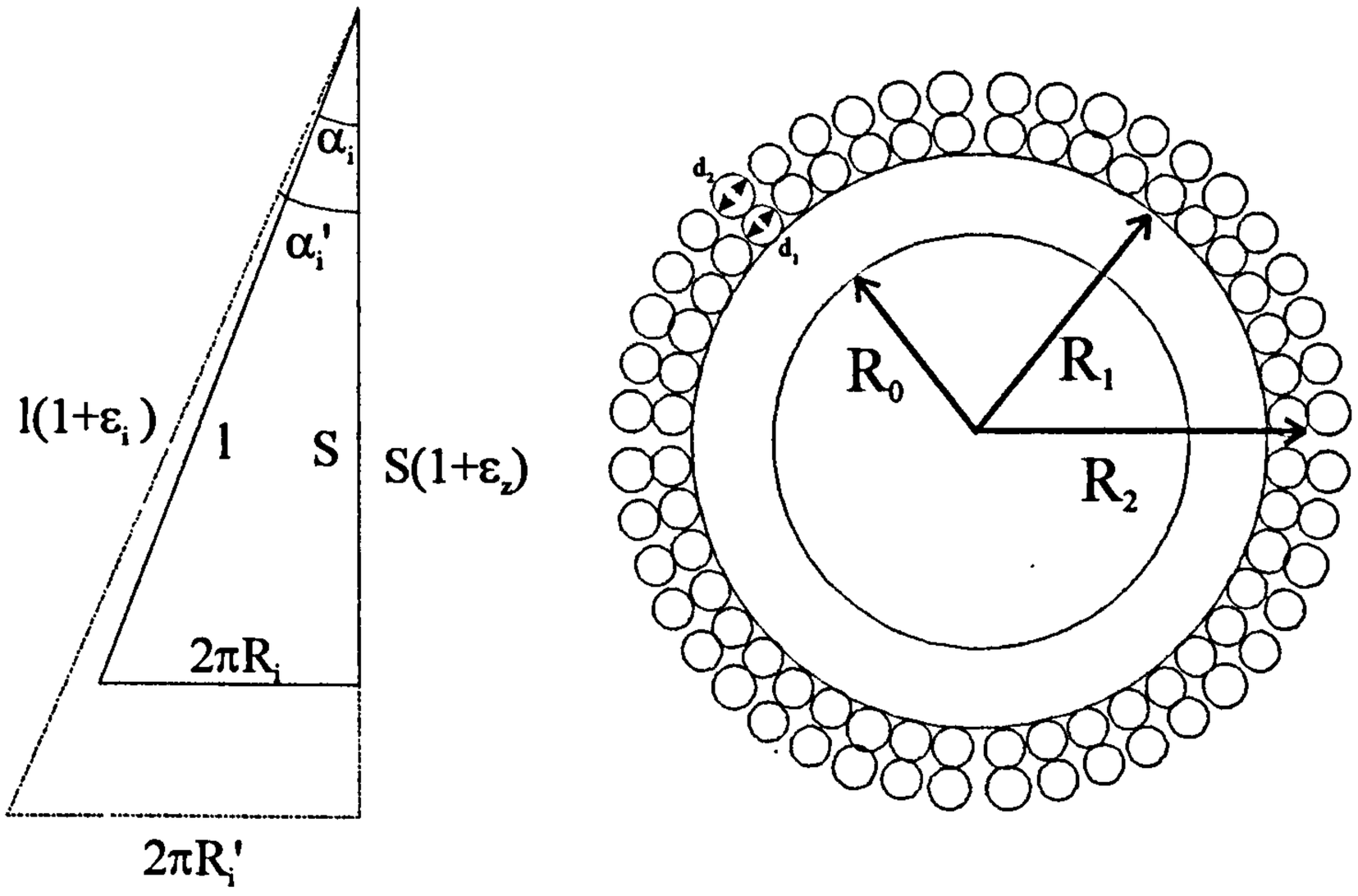

Figure 4.7. (a)Definition of geometry before and after pressurisation (b) Definition of various radial locations in the hose.

The new model incorporates a plastic inner core into the equilibrium equations. As the inner core is plastic rather than rubber the incompressibility assumptions of Brieg [14] is no longer valid. More precise compatibility and equilibrium relationships based on Lamé's thick walled cylinder solution, have been developed to include the Poisson's ratio of the inner core, ν_{ic}, as a variable.

This type of hose is usually designed so that the hose will get shorter on pressurisation. As the hose is also designed so that the wires within each reinforcement layer are touching when they are manufactured (to maximise packing density) there will clearly be an additional axial load bearing caused by the wires being squeezed together. An explicit expression has been developed for this behaviour based on a numerical solution to Hertzian contact theory,Expressions have been derived to enable this effect to be incorporated into the axial and radial equilibrium equations.

4.3.2 Inner core relationships

4.3.2.1 Pressure strain relationships

The theory originally developed by Lamé and Clapeyron [16] can be used to develop expressions relating the internal and external pressures with the internal and external radius of the cylinder before and after pressurisation, in this form they can be incorporated into the governing equations of the model.

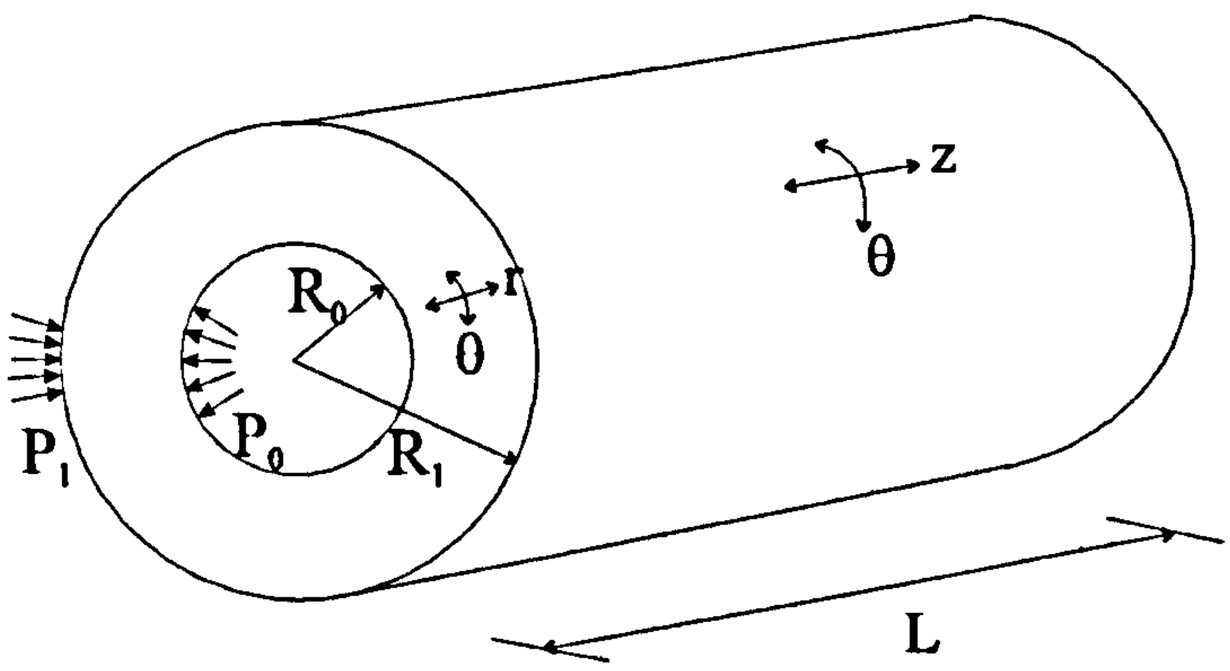

Figure 4.8. Definition of geometry, loading conditions and cylindrical co-ordinate system for the inner core .

For the particular case of a cylinder loaded with internal and external pressure, expressions can be derived for the radial and hoop stresses (see for example [17]). Both expressions are a function of the radius *r* and are as follows:

$$\sigma_r = \frac{P_0 R_0^2\left[1-\frac{R_1^2}{r^2}\right]-P_1 R_1^2\left[1-\frac{R_0^2}{r^2}\right]}{\left[R_1^2-R_0^2\right]} \qquad \ldots(4.45a)$$

$$\sigma_\vartheta = -\frac{P_0 R_0^2\left[1+\frac{R_1^2}{r^2}\right]-P_1 R_1^2\left[1+\frac{R_0^2}{r^2}\right]}{\left[R_1^2-R_0^2\right]} \qquad \ldots(4.45b)$$

Using Hooke's law in three dimensions, an expression can also be derived for the axial stress and reduces to:

$$\sigma_z = E\varepsilon_z + \nu(\sigma_r + \sigma_\vartheta) = E\varepsilon_z + \frac{2\nu(P_0 R_0^{\,2} - P_1 R_1^{\,2})}{(R_1^{\,2} - R_0^{\,2})} \qquad \ldots(4.46)$$

It can be seen that this expression is not a function of radius and is in fact constant across the cross section of the cylinder. The axial force contribution of the inner core $F_{zic,}$ is simply the axial stress multiplied by the deformed cross sectional area of the cylinder i.e:

$$F_{zic} = \sigma_z \pi (R_1'^2 - R_0'^2) \qquad \ldots(4.47)$$

The hoop strain can be derived in terms of the stresses in the three cylindrical components and the elastic constants of the tube as:

$$\varepsilon_\vartheta = \frac{\sigma_\vartheta}{E} - \frac{\nu}{E}(\sigma_r + \sigma_z) \qquad \ldots(4.48)$$

As can be proved (see for example [17]) the hoop strain is equal to the radial displacement, u, divided by the radius (i.e. u/r). Substituting the hoop axial and radial stresses into Equation 4.48 we gain an expression for u/r as follows:

$$\varepsilon_\vartheta = \frac{u}{r} = \frac{1}{E}\left[\frac{(R_0^{\,2}P_0 - R_1^{\,2}P_1)(1-\nu) + (P_0 - P_1)\frac{R_0^{\,2}R_1^{\,2}}{r^2}(1+\nu) - 2\nu^2(P_0 R_0^{\,2} - P_1 R_1^{\,2})}{R_1^{\,2} - R_0^{\,2}} - \nu E\varepsilon_z\right] \qquad \ldots(4.49)$$

For the specific case of $r = R_1$ then $u = R_1' - R_1$, substituting in these values and solving for P_0 we get the following expression:

$$P_0 = \frac{P_1}{2(1-\nu)}\left[1 + \frac{R_1^{\,2}(1-2\nu)}{R_0^{\,2}}\right] + \frac{E(R_1^{\,2} - R_0^{\,2})}{2R_1 R_0^{\,2}(1-\nu^2)}\left[R_1' - R_1 + R_1\nu\varepsilon_z\right] \qquad \ldots(4.50)$$

and rearranging the expression we can also solve for P_1 as follows:

$$P_1 = \frac{2(1-\nu)}{\left[1+\frac{R_1^{\,2}(1-2\nu)}{R_0^{\,2}}\right]}\left[P_0 - \frac{E(R_1^{\,2}-R_0^{\,2})}{2R_1R_0^{\,2}(1-\nu^2)}(R_1'-R_1+R_1\nu\varepsilon_z)\right] \quad \ldots(4.51)$$

The expressions for F_{zic}, P_0 and P_1 are used later in the general model for the hose. It can be seen that if a Poisson's ratio, ν, of 0.5 is substituted in Equation 4.51 it reduces to Brieg's [14] expression for P_0, i.e. Equation 4.41. A further expression is required in order to relate the deformed internal radius of the core to the pressures, geometry and material properties. This is achieved by solving Equation 4.49 at the internal boundary condition, where r= R_0 and u = R_0'-R_0, after some algebraic manipulation the internal deformed radius R_0' is given by the following:

$$R_0' = \frac{R_0(1+\nu)}{E(R_1^2-R_0^2)}\left[P_0(R_0^2(1-2\nu)+R_1^2)-2P_1R_1^2(1-\nu)\right]+R_0(1-\nu\varepsilon_z) \ldots(4.53)$$

4.3.3.1 Development of an explicit force-strain relationship

Hertz [18] was the first person to tackle the problem of two curved bodies in contact, and gained his insights from the defraction patterns generated by lenses pressed together. Motivated by a roller bearing problem Radzimovsky [19] developed expressions for stress, strain and change in distance between centres for the case of two cylinders pressed together with a line force as shown in Figure 4.10

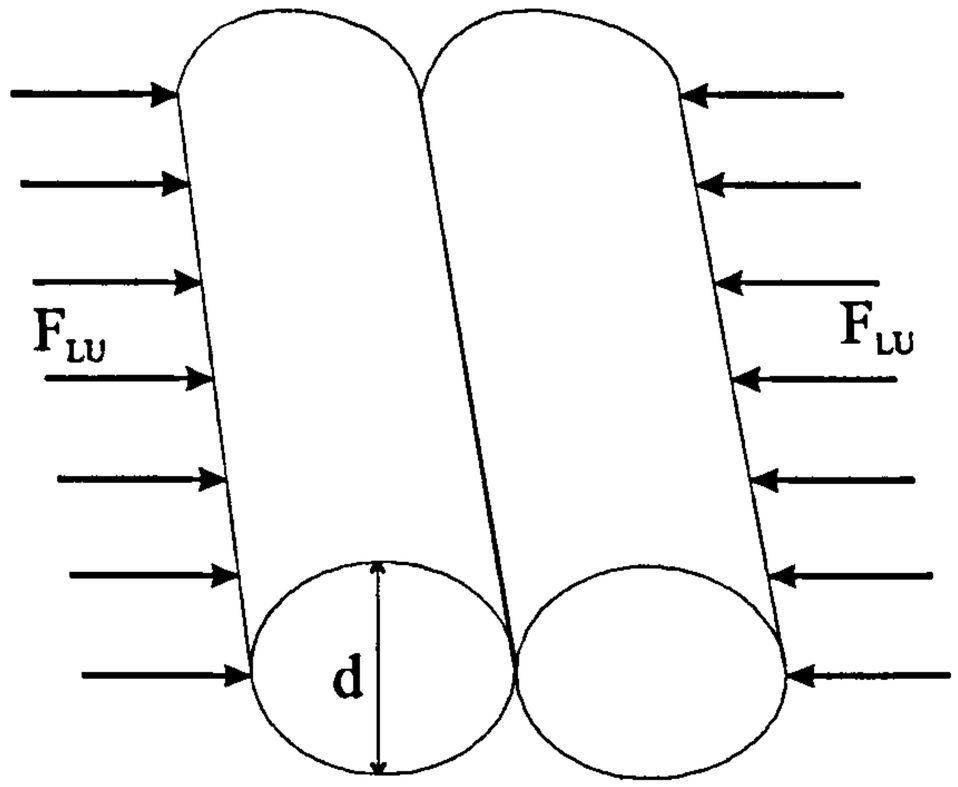

Figure 4.10. Two cylinders with a distributed line force pressing them together.

The expression has been conveniently tabulated by Young [20] and can be expressed in terms of a lateral strain ε_L, and once the appropriate substitutions are made it can be reduced into the following form

$$\varepsilon_L = \frac{\delta d}{d} = \frac{2F_{LU}(1-\nu^2)}{d\pi E}\left[\frac{2}{3} + 2\ln\left[\frac{2d}{2.15\sqrt{\frac{F_{LU}d}{2E}}}\right]\right] \qquad \ldots(4.58)$$

The expression in this form cannot be utilised in the structural theory because an expression for the force per unit length, F_{LU}, is needed and this parameter is embedded implicitly in the equation which cannot be solved using standard manipulation techniques.

A numerical technique must therefore be used to gain an expression for the force per unit length and this has been done in the following way: First of all the relationship in Equation 4.58 has been evaluated for the relevant range of strain for a number of wire diameters; these relationships are shown in Figure 4.11.

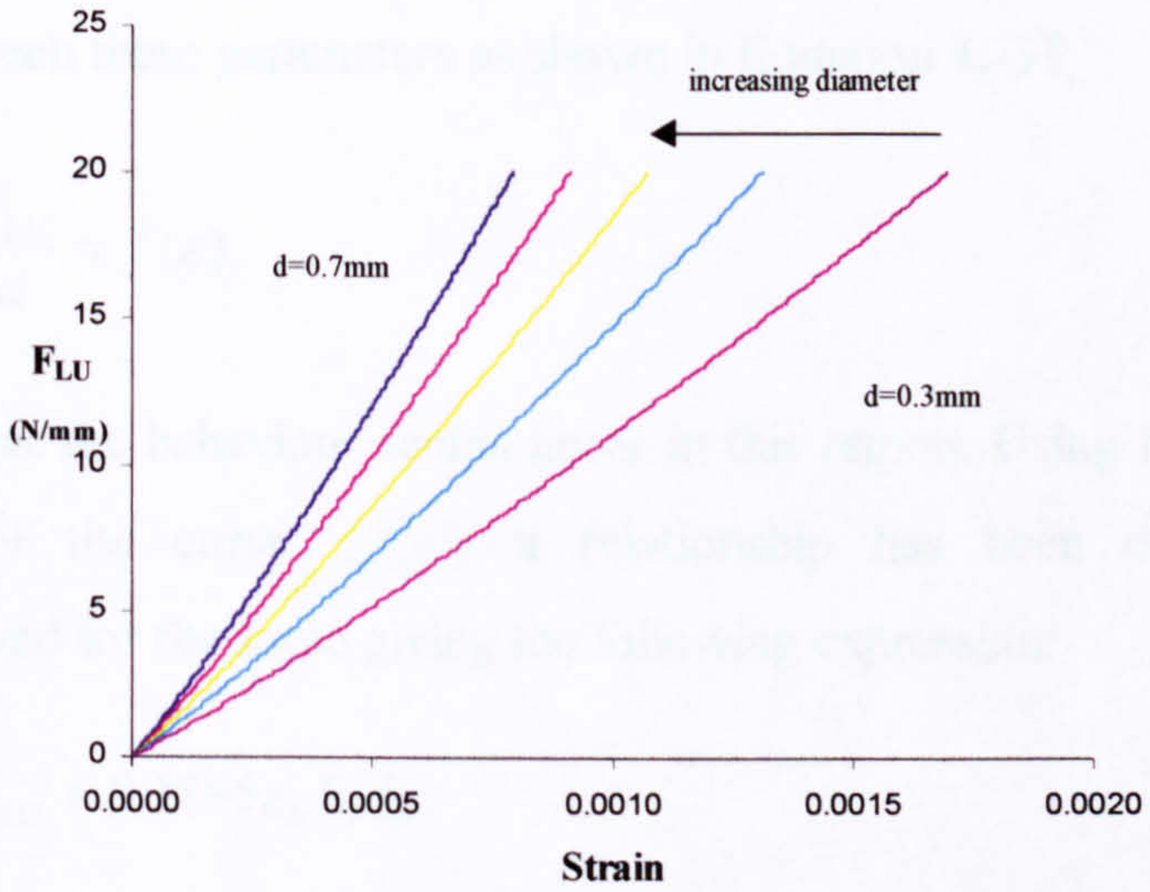

Figure 4.11. The relationship between force per unit length and strain using the contact theory for various wire diameters.

As would be expected, the relationship does not remain constant for different wire diameters but gets steeper for larger wire diameters. A second plot has been made which compares the force per unit length divided by the diameter versus the strain and this is shown in Figure 4.12.

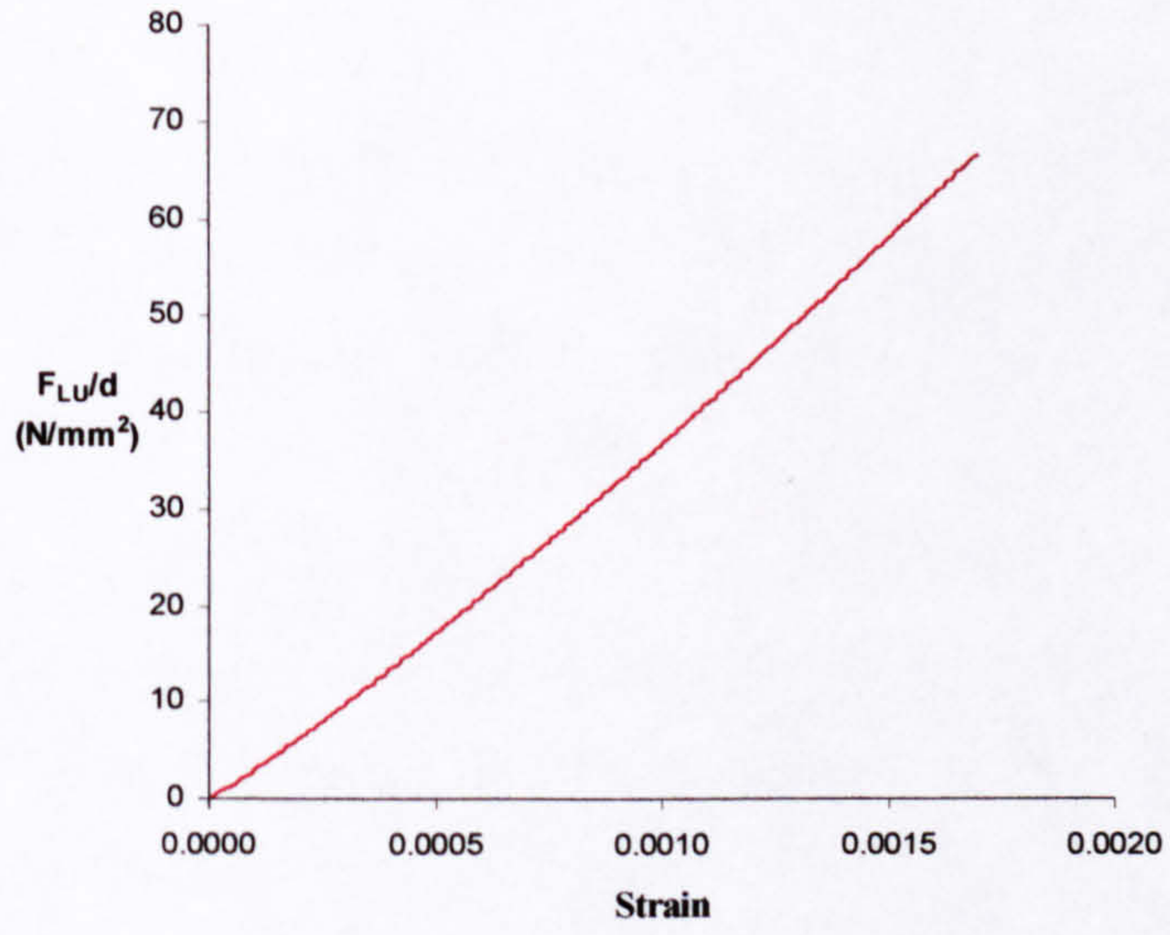

Figure 4.12. $F_{LU}./d$ vs. strain showing a constant relationship for all wire diameters.

Figure 4.12 shows a constant relationship for all wire diameters and so there is a relationship between these parameters as shown in Equation 4.59.

$$\frac{F_{LU}}{d} = f(\varepsilon) \qquad \ldots(4.59)$$

It can be seen that the behaviour seems linear in this region. Using a linear least squares approximation of the curve, a relationship has been obtained which was subsequently solved for the force giving the following expression:

$$F_{LU} = 0.1895\varepsilon_{li}E_i d_i \qquad \ldots(4.60)$$

4.3.3.2 Component in hose axial equilibrium equation

The force, F_l for a given length l can easily be extracted from Equation 4.60 as:

$$\frac{F_L}{l} = 0.1895\varepsilon_{li}E_i d_i \qquad \ldots(4.61)$$

This relationship must now be converted into the relevant hose co-ordinate system in order that it can be incorporated into equilibrium equations. The geometrical configuration of the squeezing effect is shown graphically in Figure 4.13

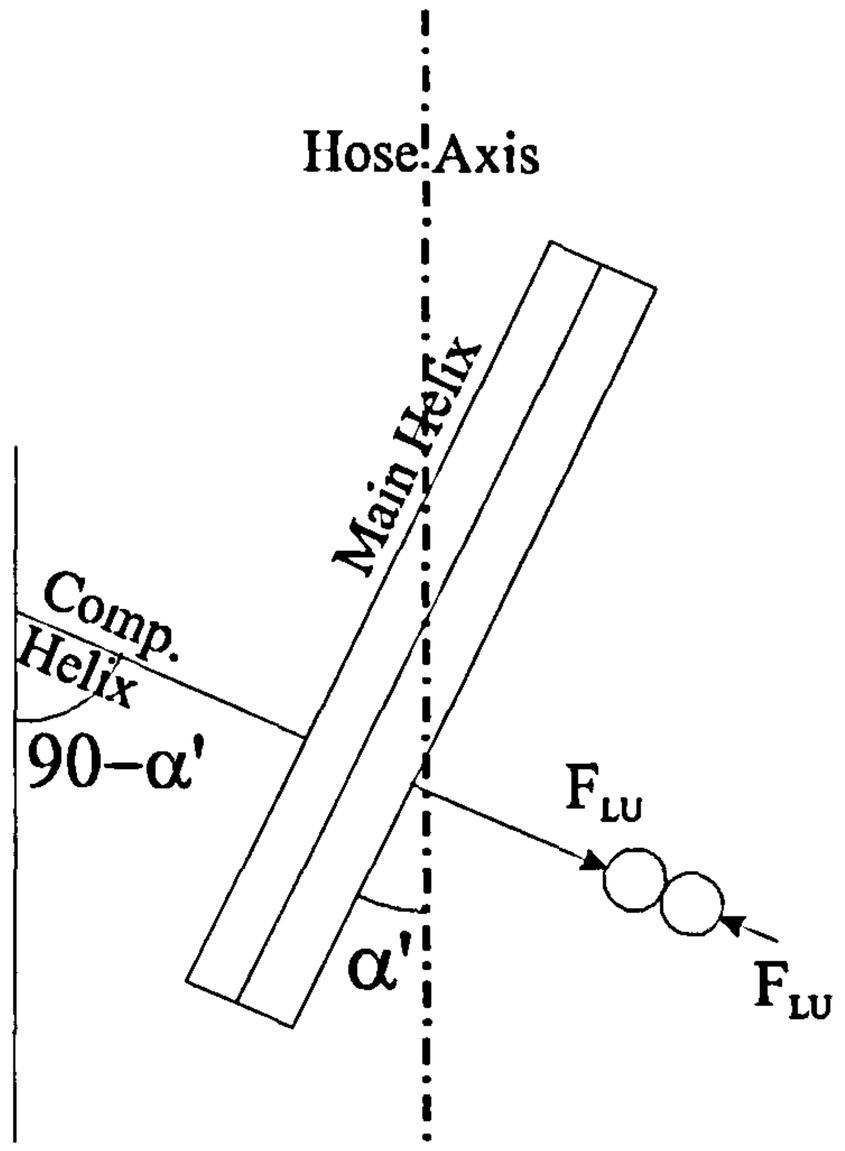

Figure 4.13. The configuration of the wires pressed together with respect to the hose axis, and also the complementary helix angle.

Converting the force per unit length is a simple matter of converting the force and the length parameters using the reinforcement triangle, and the relationship is:

$$\frac{F_L}{l} = \frac{F_a}{2\pi R_i'} \qquad \ldots(4.62)$$

The length of wire which will contribute to this aspect of the axial force equation will be one pitch, as the wire within a pitch occupies different locations laterally and therefore will have a cumulative effect. After one pitch the wire will wrap back on itself and will not change the axial stiffness.

The calculation of the lateral strain acting on a wire in the i^{th} layer is based on the following logic: The available space for a wire d_{sp} (see Figure 4.13b) can be calculated from the deformed hose geometry and the number of wires in a layer and can easily shown to be the following relationship (Equation 4.63):

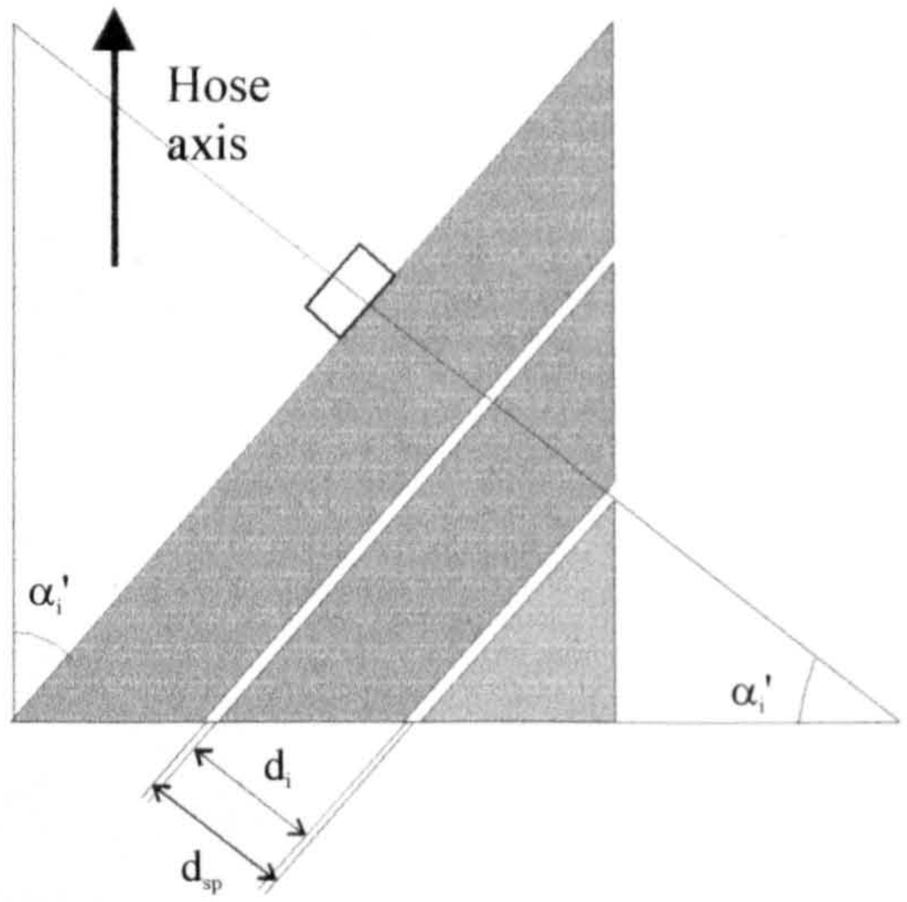

Figure 4.13b The available space for a wire, d_{sp} compared with a wire diameter, d_i, for the case where $d_{sp} > d_i$, i.e $\varepsilon_{li} = 0$ and there will be no squeezing of wire.

$$d_{sp} = \frac{\cos\alpha_i' 2\pi\left[R_i' + \frac{d_i}{2}\right]}{N_i} \qquad \ldots(4.63)$$

Clearly the lateral strain will only be non zero if it is negative, it can be easily calculated from the following relationship:

$$\varepsilon_{li} = \frac{d_{sp} - d_i}{d_i} \qquad \ldots(4.64)$$

Combining the above relationships we gain an expression for the axial force caused by the crushing effect on one layer of reinforcement as

$$F_a = (0.1895)2\pi R_i' \varepsilon_{li} E_i d_i \qquad \ldots(4.65)$$

It should be noted that the term does not have to be multiplied by the number of wires in a layer, because as the wires are in effect in series in an axial sense, the total stiffness will come from the force per unit length of a single wire taken over one pitch.

In considering all layers the relationship must be made into a summation as follows:

$$F_a = \sum_{i=1}^{n} \xi_i (0.1895)2\pi R_i' \varepsilon_{li} E_i d_i \qquad \ldots(4.66)$$

where for i is 1 to n and if $\varepsilon_{li} \geq 0; \xi_i = 0$ else $\xi_i = 1$.

A new series of factors are introduced at this point, ξ_i, these are switch variables, one for each layer. If the available space for the wire is less than the wire diameter, a crushing force will exist and the switch variable will be turned on (i.e. ξ_i,=1), if not there will be no crushing effect and the switch variable will be turned off (i.e. ξ_i,=0).

4.3.3.3 Component in hose lateral equilibrium equation

The lateral squeezing effect on the wires will enable the wires to bear some of the pressure as a result of equilibrium considerations as shown in Figure 4.14.

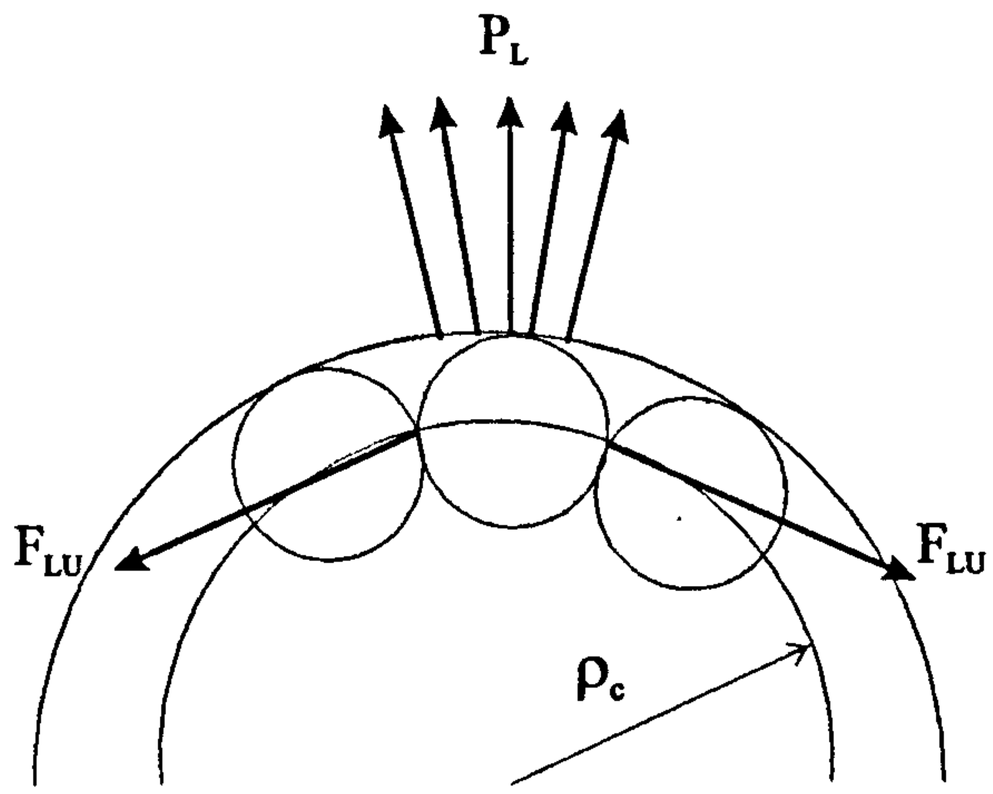

Figure 4.14. The pressure caused by the compression of the wires together (note this is looking along the length of the wires and not the hose).

This effect can be incorporated into the lateral equilibrium equation. The pressure component of the squeezing effect can be calculated by means of the radius of curvature of its helix, however this effect runs perpendicular to the wire axis and therefore the radius of curvature will be the complimentary helix as shown in Figure 4.13. The radius of curvature of the complimentary helix, ρ_c is given as:

$$\rho_c = \frac{R_i'}{\sin^2(90-\alpha_i')} = \frac{R_i'}{\cos^2\alpha_i'} \qquad \ldots(4.66)$$

The lateral pressure effect is then simply the force per unit length divided by the complimentary helix as shown in Equation 4.67, a proof for a related problem has already been given in Section 4.2.2.

$$P_L = \frac{F_{LU}}{\rho_c} \qquad \ldots(4.67)$$

It can be shown that there is no need to obtain this expression in the hose axis as it is a pressure and would therefore be unchanged. Substituting Equations 4.60 and 4.66 into the previous expression we gain the following relationship:

$$P_L = \frac{0.1895\varepsilon_{li} E_i d_i \cos^2 \alpha_i'}{R_i'} \qquad \ldots(4.68)$$

Substituting the expressions for R_i' (Equation 4.44) and ε_{li} (Equation 4.63) into the previous expression and adding the switch variable ,ξ , we gain an expression for the pressure caused by the crushing effect on one layer as follows:

$$P_L = \xi_i \left[\frac{(0.1895)\varepsilon_{li} E_i d_i \cos^2 \alpha_i'}{R_i'} \right] \qquad \ldots(4.69)$$

The pressure acting on any particular layer will be a summation of the pressure caused by itself added to the pressure caused by all the layers which are further out radially than itself.

4.3.4 Equations for the structural model

4.3.4.1 The General form of the equations

Having derived expressions for the aspects of the behaviour peculiar to the hose of current interest, it is now possible to derive a new set of governing equations for a structural model. Firstly the axial equilibrium equation takes the form:

$$\pi R_0'^2 P_0 + F_{zic} = \sum_{i=1}^{n} N_i A_i E_i \varepsilon_i \cos\alpha_i' + \sum_{i=1}^{n} \xi_i (0.1895) 2\pi \dot{R}_i' v_i \varepsilon_{li} E_i d_i \qquad \ldots(4.70)$$

It is seen that it is the internal pressure multiplied by the end area of the hose plus an axial force component caused by the inner core, F_{zic} which has been derived and is given in Equation 4.47. These are equated to the load bearing of the wires in the tension component, unchanged from the original Entwistle model (i.e. in Equation 4.27) added to the axial component of the squeezing effect as derived in the previous section. The units for this equation are force. The lateral equilibrium equation is in the form:

$$P_1 = \sum_{i=1}^{n} \frac{N_i A_i E_i \varepsilon_i \sin\alpha_i' \tan\alpha_i'}{2\pi R_i'^2} + \sum_{i=1}^{n} \xi_i \frac{(0.1895)\varepsilon_{li} E_i d_i \cos^2\alpha_i'}{R_i'} \quad \ldots(4.71)$$

It equates the interfacial pressure between the outside of the inner core and the first layer of reinforcement, i.e. P_1 (this has been derived in terms of the internal pressure P_0 in Equation 4.51). This is equated to the pressure bearing of the wires acting in tension as proposed by Entwistle (as shown in Equation 4.26) added to the pressure bearing component born by the wires when they are put under lateral compression as derived in the previous section. The units of this equation are pressure (i.e. N/mm^2)

The inter layer compatibility of the wires has been approximated by a similar assumption to that used by Jakemen and Knight [15] and is as follows:

$$R_i' + d_i = R_{i+1}' \quad \ldots(4.72)$$

for $i = 1$ to n-1

The changes from $2d_i$ to d_i is because this is a helical wound hose which has a layer thickness of d_i compared to a braided hose modelled by Jakeman and Knight, which has a layer thickness of $2d_i$. The implementation of a more exact theory for the inter layer compatibility will be discussed later in this chapter. The units of the equation are length (mm) and there will be one equation for every inter layer existing, i.e. n-1 in a hose with n layers.

4.3.4.2 Numerically solvable format to equations

The expressions as shown in the previous section have been manipulated into a numerically solvable form, eliminating ε_i and R_i' using Equations 4.43 and 4.44. P_1 and R_0' can also be removed but since they equate to lengthy algebraic terms and occur a number of times they have been left as substations. Each equation has been equated to a new variable, Y_i. This new series of variables allows a minimising technique to be used in a

numerical solution. The general expressions for an n layer hose are given in the following series of equations:

$$Y_1 = \pi R_0{}'^2 P_0 + \pi\left[\left(R_1(1+\varepsilon_z)\frac{\tan\alpha_1'}{\tan\alpha_1}\right)^2 - R_0'^2\right]\left[E_{ic}\varepsilon_z + \frac{2\nu_{ic}(P_0R_0^2 - P_1R_1^2)}{R_1^2 - R_0^2}\right]$$
$$-\sum_{i=1}^{n} N_iA_iE_i\left[(1+\varepsilon_z)\frac{\cos\alpha_i}{\cos\alpha_i'} - 1\right]\cos\alpha_i'$$
$$-\sum_{i=1}^{n}\xi_i(0.1895)2\pi\left(R_i(1+\varepsilon_z)\frac{\tan\alpha_i'}{\tan\alpha_i}\right)\left|\frac{\cos\alpha_i' 2\pi\left(R_i(1+\varepsilon_z)\frac{\tan\alpha_i'}{\tan\alpha_i}\right) + 0.5d_i}{N_id_i} - 1\right|E_id_i \quad \ldots(4.73)$$

$$Y_2 = P_1 - \sum_{i=1}^{n}\frac{N_iA_iE_i\left[(1+\varepsilon_z)\frac{\cos\alpha_i}{\cos\alpha_i'} - 1\right]\cos\alpha_i'\tan^2\alpha_i}{2\pi R_i{}^2(1+\varepsilon_z)^2}$$
$$(0.1895)\left|\frac{\left(\cos\alpha_i' 2\pi\left(R_i(1+\varepsilon_z)\frac{\tan\alpha_i'}{\tan\alpha_i}\right) + 0.5d_i\right)}{N_id_i} - 1\right|E_id_i\cos^2\alpha_i' \quad \ldots(4.74)$$
$$-\sum_{i=1}^{n}\xi_i\frac{\left(R_i(1+\varepsilon_z)\frac{\tan\alpha_i'}{\tan\alpha_i}\right)}{\left(R_i(1+\varepsilon_z)\frac{\tan\alpha_i'}{\tan\alpha_i}\right)}$$

$$Y_{2+i} = R_i(1+\varepsilon_z)\frac{\tan\alpha_i'}{\tan\alpha_i} + d_i - R_{i+1}(1+\varepsilon_z)\frac{\tan\alpha_{i+1}'}{\tan\alpha_{i+1}} \quad \ldots(4.75)$$

where i=1 to n-1 and if $\varepsilon_z \geq 0; \xi = 0$ or if $\varepsilon_z < 0; \xi = 1$ with the following substitutions for P_1 and $R_o{}'^2$

$$P_1 = \frac{2(1-\nu_{ic})}{\left[1 + \frac{R_1{}^2(1-2\nu_{ic})}{R_0{}^2}\right]}\left[P_0 - \frac{E_{ic}(R_1{}^2 - R_0{}^2)}{2R_1R_0{}^2(1-\nu_{ic}{}^2)}\left(R_1(1+\varepsilon_z)\frac{\tan\alpha_1'}{\tan\alpha_1} - R_1 + R_1\nu_{ic}\varepsilon_z\right)\right] \quad \ldots(4.76)$$

$$R_0{}' = \frac{R_0(1+\nu)}{E(R_1^2 - R_0^2)}\left[P_0(R_0^2(1-2\nu) + R_1^2) - 2P_1R_1^2(1-\nu)\right] + R_0(1-\nu\varepsilon_z) \quad \ldots(4.77)$$

There are n+1 equations and n+2 unknowns which are the n winding angles, α_i', the axial hose strain, ε_z, and the internal pressure P_0. Since the solution is generally sought for a

given pressure this leaves n+1 unknowns and the solution is therefore feasible. It is not possible to manipulate these equation into an explicit closed form solution and a numerical technique must be used to reach a solution: the details of this solution are discussed in the next section.

4.4 Numerical solution

4.4.1 General technique

In his 'Apologia pro opus nostro' Forman Acton [21] discusses the problem of finding roots of transcendental functions and makes the observation 'if there exists one reliable algorithm for finding the roots of transcendental functions it is not yet found' and later that 'finding roots to systems of equations almost always requires special methods specially tailored to the system at hand'. Consequently it is thought useful to go into some detail about the numerical technique which has been employed (and found to work) in this particular circumstance.

The solution to the equations is found using a Minimising Newton Raphson technique [22]. This involves shifting all parts of the equation to one side and equating this to a new variable Y_i which is then solved by minimising Y_i. The technique requires an initial estimate for all the variables being solved (in this case $\alpha_{1\text{-}n}$' and ε_z). The vector of function of $Y_{1\text{-}n+1}$ is then evaluated by putting the variables and constants into equations as derived in the previous section. The matrix of partial derivatives is then calculated (see the next section for details) and used to calculate the change in variables by multiplying it by the vector of functions (see Figure 4.15 for details). This iteration is repeated until the desired precision is reached. This technique sounds simple enough in principle but there are some problems- the solution is not guaranteed to converge or may converge to a local inflexion or may diverge. One advantage in this particular problem is that fairly good guesses for variables can be made. Generally it was found that a solution did converge within 10 cycles and if it took longer than this it was probably drifting off to some irrelevant root with no physical meaning. It was found in some cases that the initial guess was critical as to whether the

solution was going to converge or not, hence if it had not converged within 10 cycles the initial guesses were changed and the iteration repeated. In this way the full range and combination of likely roots could be tried and this technique worked well for a few situations which were very sensitive to the initial estimated values. For the majority of cases however the iteration was relatively robust and not that sensitive to the initial values input. The most difficult cases to solve tended to be the problems around an axial strain of zero and this may have something to do with the fact that, because of the switching variable ξ, some of the functions were not continuous in this transition region of positive to negative axial strain. Once the first pressure case had been solved the solution to the variables was then used as the estimate for the next pressure case and often this resulted in a convergence within three cycles. The solution to a complete hose pressure region, even for most complex hose, solving for fifty pressure points, would not take more than a few minutes A more detailed description of the numerical method can be found by examining the flow chart given in Figure 4.15.

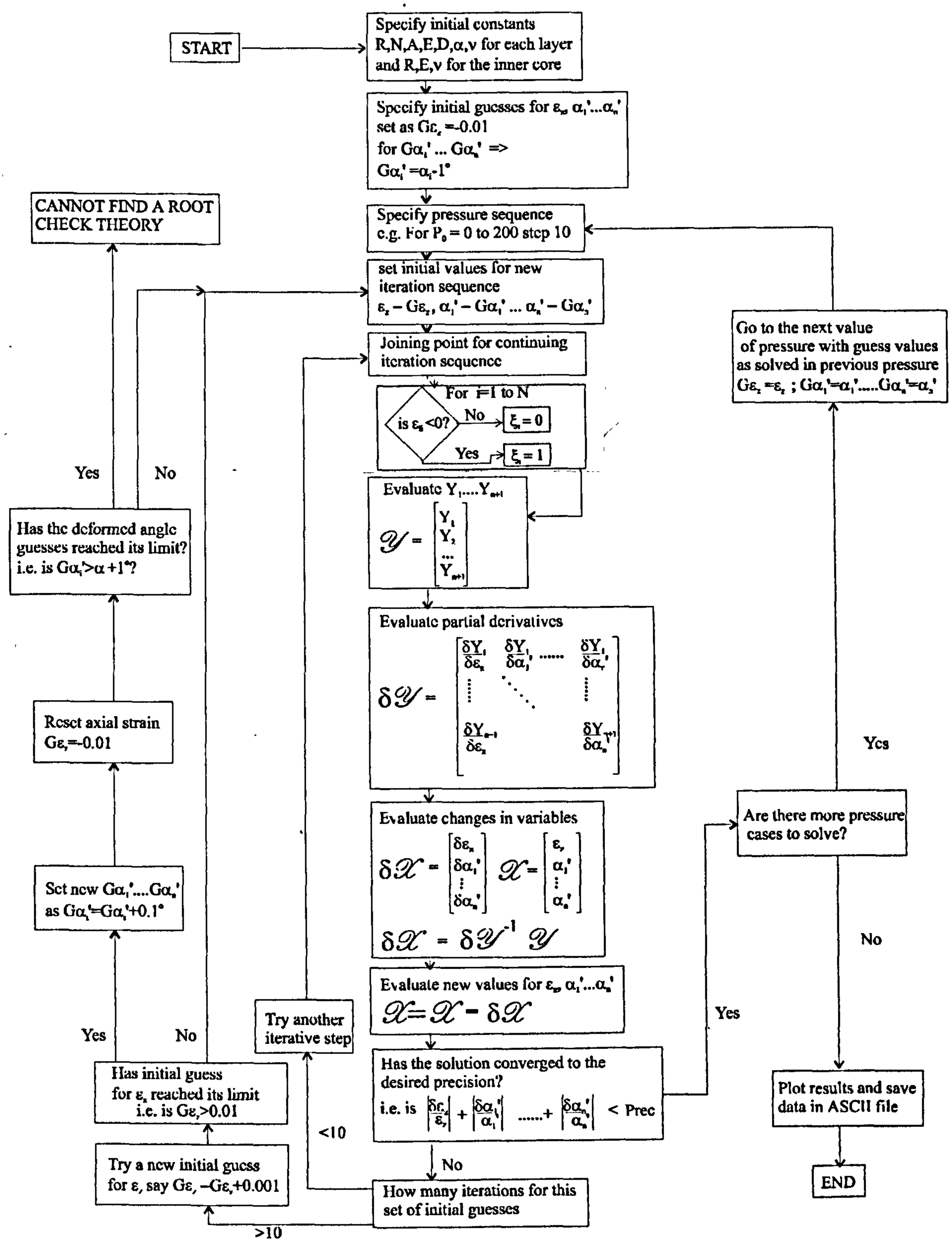

Figure 4.15. Flow chart for numerical method.

4.4.2 Partial differentials

The partial derivatives have been calculated in two ways: using a simple numerical technique and using the exact symbolic equations. The advantage of using two techniques to calculate the partial derivatives was that it provided a useful method of error checking. Each expression within a function could be differentiated separately and algebraic mistakes could be quickly localised and corrected before they were put into the iterative sequence.

4.4.2.1 Exact symbolic derivatives

The exact partial derivatives were found by differentiating general Equations (i.e. 4.69,4.70 and 4.71) with respect to all the variables separately. This involved using standard calculus techniques such as the Chain Rule, the Product Rule, techniques for partial differentiation and the Quotient Rule (for example see [23]). This technique provided a useful method of error checking of equations since the results partial derivatives could be compared with numerical derivatives (see next section for details) in sections.

4.4.2.2 Numerical derivatives

This technique for obtaining the values of the derivatives of the general equations comes from the standard limit definition of a derivative as:

$$f'(x_0) = \lim_{h \to 0} \frac{f(x_0 + h) - f(x_0)}{h} \qquad \ldots(4.90)$$

an approximation to the derivative can therefore be made using [24]:

$$f'(x_0) \approx \frac{f(x_0+h)-f(x_0)}{h} \text{ (where h is a small number)} \qquad \ldots(4.91)$$

In practice it was found that a value of 10^{-8} for h usually agreed with the exact derivative to 8 significant figures.

4.5 Experimental technique

4.5.1 General set up

There are no standard methods for this kind of test, the only kind of length change test carried out by hose manufactures is the measurement of the length change (with a ruler) at the test pressure only, the hose being simply held straight by hand.

The basic experimental set-up is shown in Figure 4.16, the hose was pressurised using a hydraulic pump driven pneumatically by line pressure. The pump was capable of delivering very high pressures up to 2,759 bar (40,000 PSI) by nature of being an intensifier, i.e. with a step down large to small diameter on the main piston. The hose was connected to the pump by means of a custom made manifold, which allowed the connection of a pressure transducer, Bourdon pressure gauge and a pressure release valve.

The actual connection between the hose and test rig was custom made with an autoclave fitting utilising 60° cone to cone sealing line contact. The other end of the hose was plugged with a blank version of the same fitting.

On the plugged end of the hose a Linear Variable Displacement Transformer (LVDT) was attached to the angle by means of a clamp. The LVDT was excited by a 10 v DC power source .and gave an output which was amplified to a signal between 0 and 6 v and channelled into the computer via an A/D card. In the centre of the hose a section of the outer cover was stripped off to expose the outer reinforcement wires. These were then cleaned and treated to allow small strain gauges to be attached along the axis of the wires. Single strain gauges were used in a quarter bridge configuration (see Figure 4.17) and amplified (Micro Measurements 2120) before the signals were fed into the data acquisition computer via the A/D card.

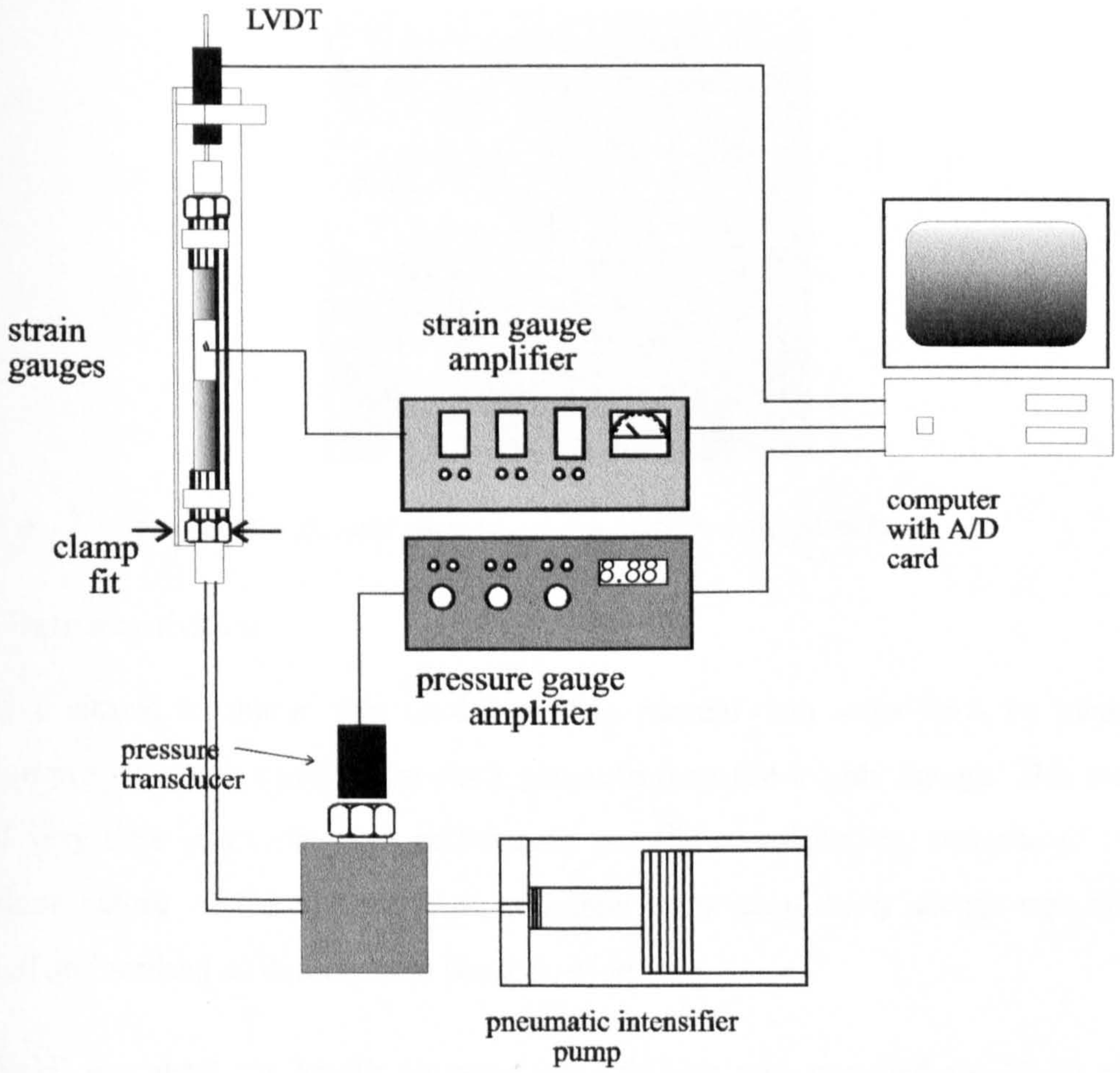

Figure 4.16. Schematic view of the experimental test set-up for hose assembly tests.

Keeping the hose straight under pressurisation was difficult because of the slightly curved nature of the hose caused by being stored on a reel. For this reason it was found that the hose had to be kept straight by strapping it directly to a steel angle iron by means of a number of lubricated cut car inner tube rings. The details of the data acquisition are given in the next section.

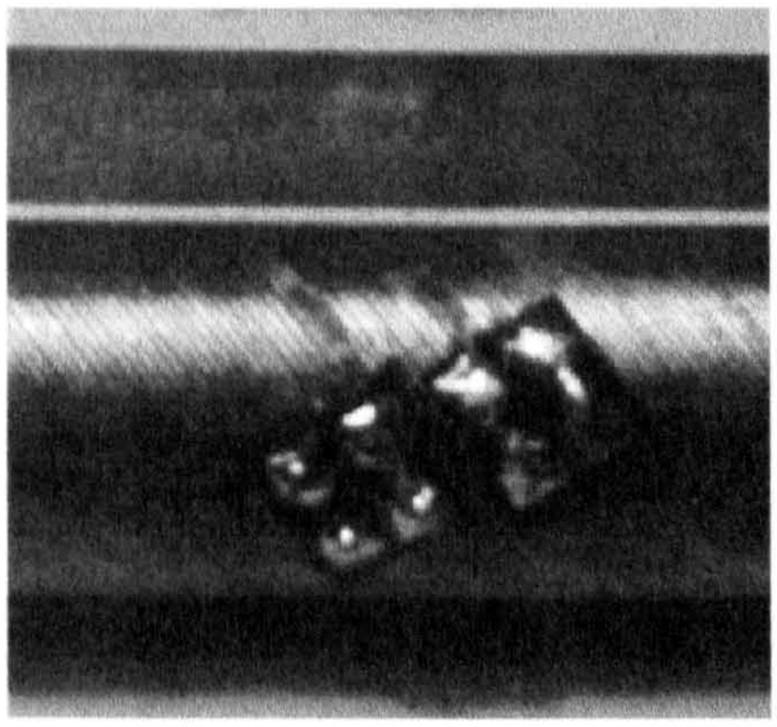

Figure 4.17. Two strain gauges placed on the hose reinforcement.

4.5.2 Data acquisition

Initially a simple technique was used involving manual data acquisition by means of a Bourdon pressure gauge and a dial clock gauge to measure length change. This technique proved very time consuming but additionally proved unsatisfactory because of the time dependant nature of the results. An automatic data acquisition set-up was therefore designed and utilised as described in the following.

An LVDT was used for length measurements (which was attached rigidly to the steel angle that the hose was connected to) and a pressure transducer was connected by means of a manifold. These two devices were then interfaced with a 386 PC via an A/D Card and a custom written C program. The program produced pressure, length change and strain in ASCII Column data files which were subsequently analysed and plotted using Matlab subroutines and Excel macro programs. Because of significant amounts of noise in the signal all cables were shielded and a simple electronic low pass filter was built. Additionally a simple software filter was written into the data acquisition program, this gave a reading as an average of a number of samples, the number being set by the user.

4.5.3 Calibration of the test rig

The strain gauges chosen were the smallest available from the manufacturer, (TML) and were 0.7 mm wide and 1 mm long (manufacturers part number Q-FLK-1 [25]). In order to calibrate the strain gauge set-up a small rig was constructed as shown in Figure 4.18. The

strain gauge was stuck close to the base end of a cantilever beam which was deflected at the free end as also shown in Figure 4.18.

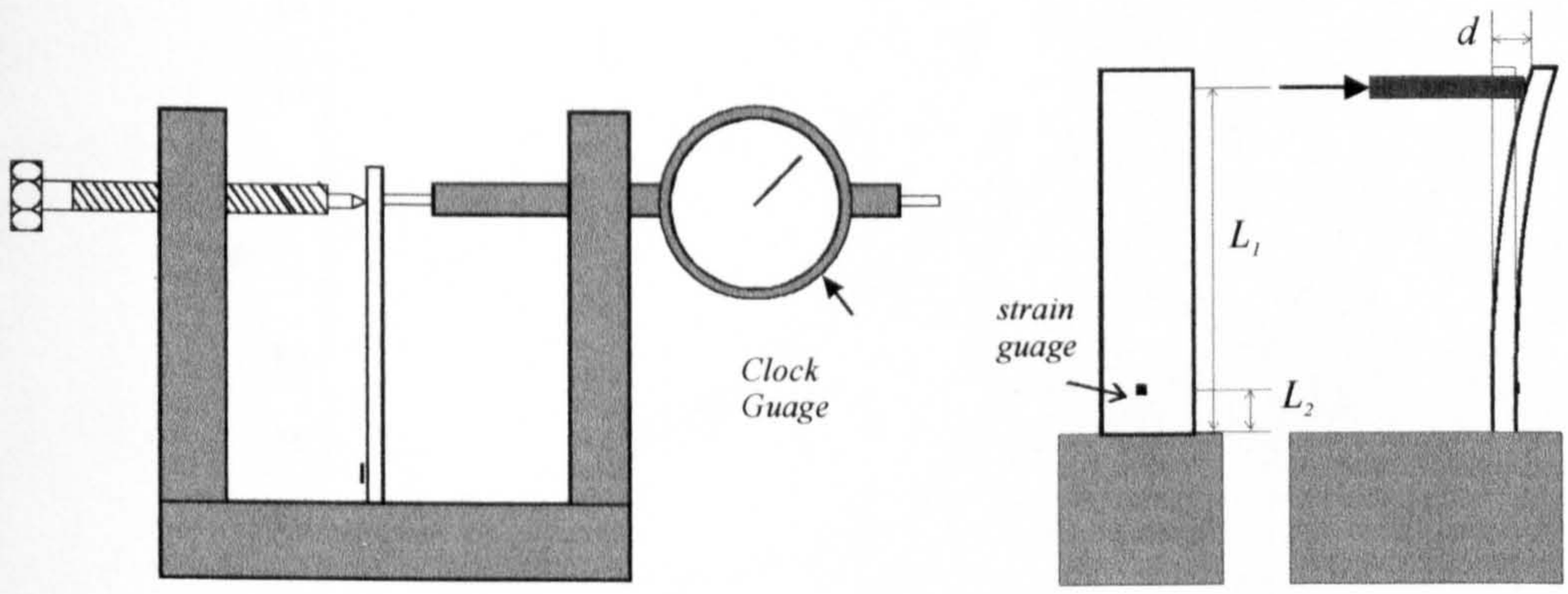

Figure 4.18. Details of Strain gauge calibration device.

The deflection of the cantilever beam was measured with a clock gauge and can be directly related to the strain gauge reading using simple beam theory (for example see [26]). The nomenclature is shown in Figure 4.18 and the relationship can be shown to be the following:

$$\varepsilon = \frac{3(L_1 - L_2)d_1}{L_1^{\,3}} \qquad \ldots(4.92)$$

Using this device it was possible to get a calibration curve of strain against voltage (see Figure 4.19). It can be seen that the curve is linear, with some slight non-linearities beyond 0.4 % strain.

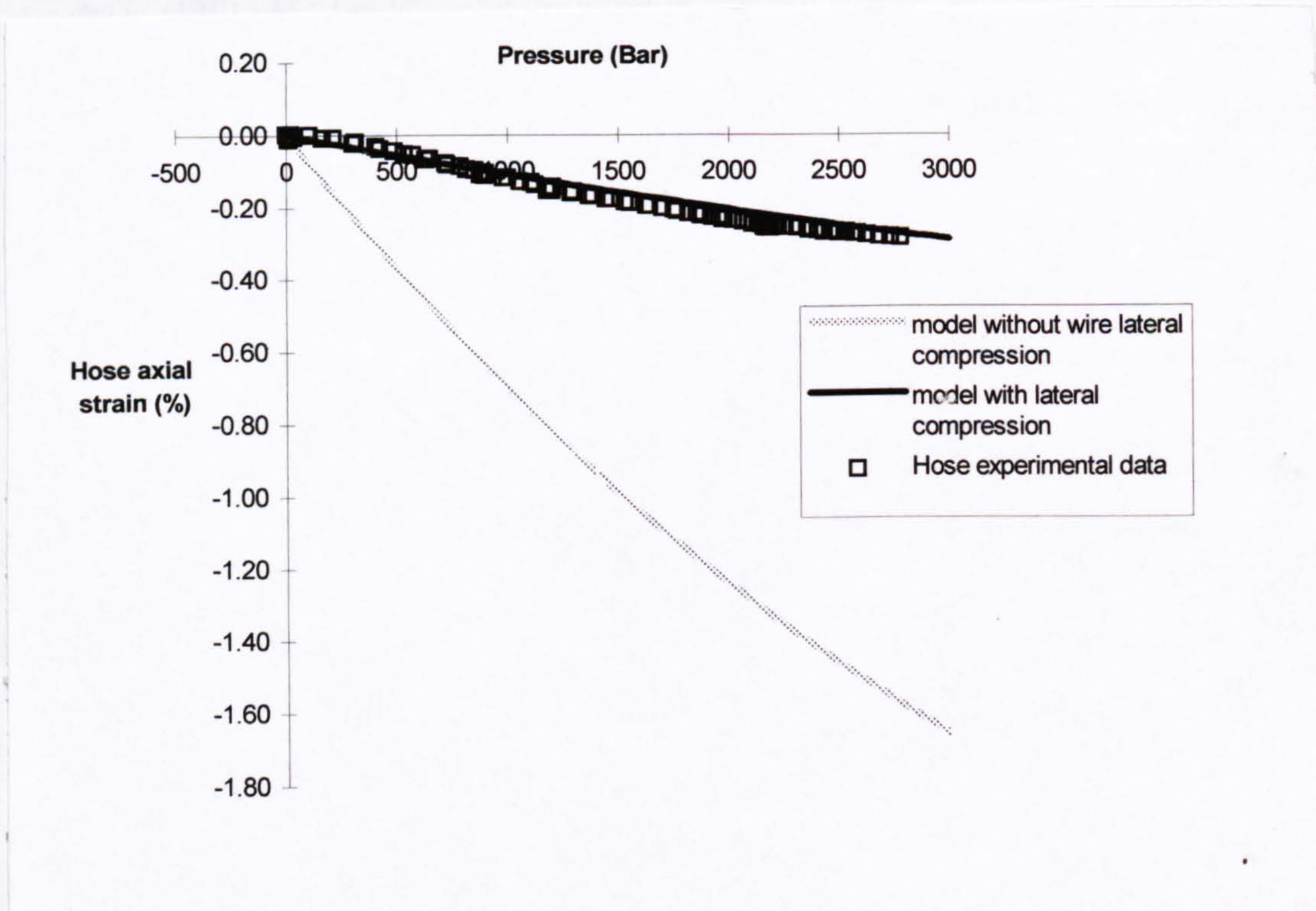

Figure 4.18b A typical example of a hose getting shorter compared with model predictions from the model which incorporates wire squeezing to the model that ignores it- justifying the inclusion of the theory.

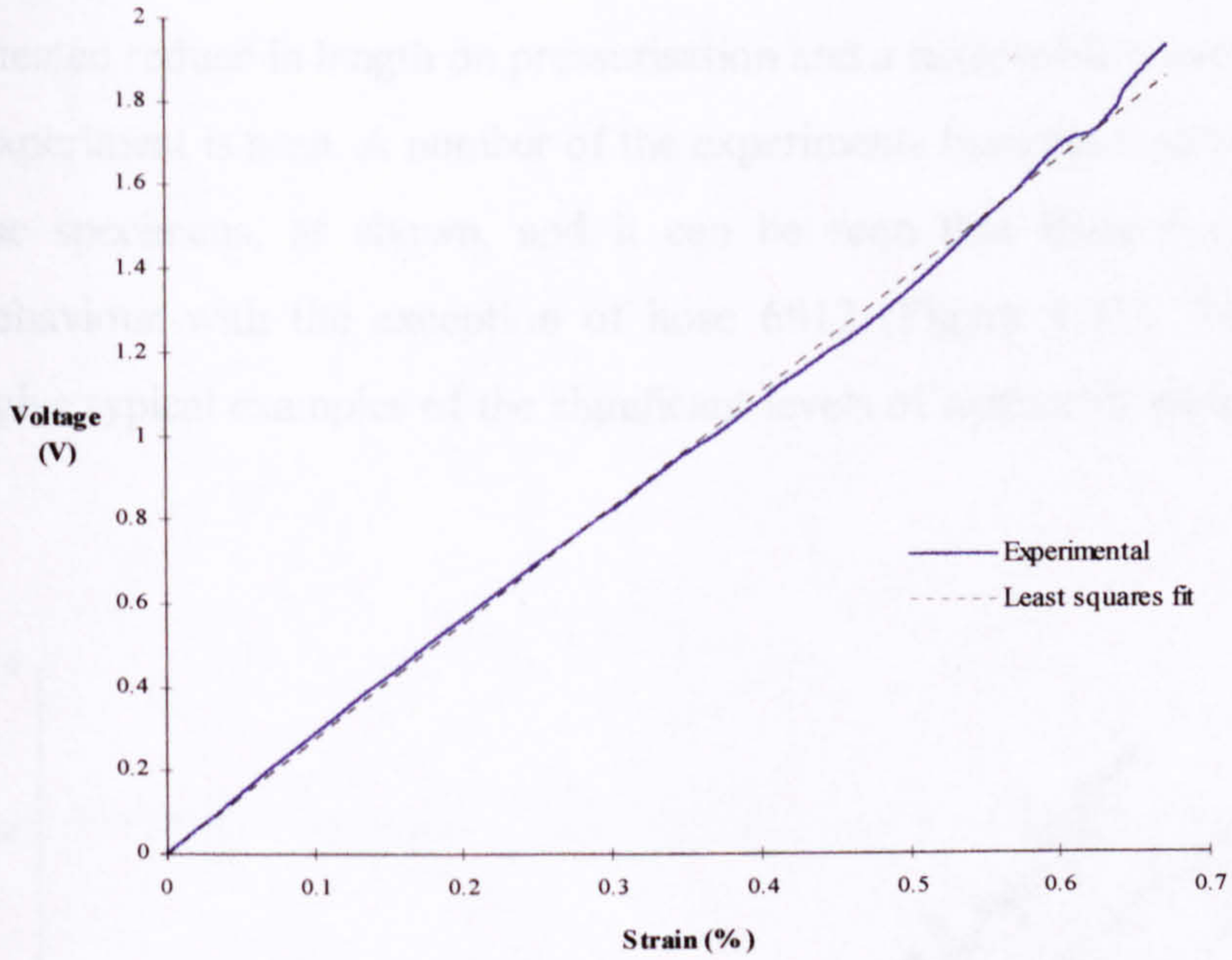

Figure 4.19. Calibration curve for the strain voltage relationship.

Calibration of the LVDT was achieved by means of a device which held it in line with a barrel micrometer. This could then be used to displace the micrometer accurately at specific intervals. The LVDT gave a very linear response. The pressure gauge was calibrated using a dead weight calibrator, and also gave a very linear response.

4.6 Theoretical and experimental results

4.6.1 Length change

This section compares the theoretical predictions and the experimental results for length change as well as showing some interesting features of the results. Figure 4.20 shows the length change of hose 2012, which is the only hose that gets longer, from the tests carried out. It has been found that when the length change is in the transition between getting shorter and getting longer then the results are very sensitive to the Poisson's ratio of the inner core, this effect is shown in Figure 4.21. The exact Poisson's ratio of the inner core material is not known but book values for this type of plastic suggest a value between 0.45

and 0.5. As is seen a value of around 0.47 seems to fit the experimental data well. The rest of the hoses tested reduce in length on pressurisation and a reasonable correlation between theory and experiment is seen. A number of the experiments have been carried out on two separate hose specimens, as shown, and it can be seen that these hoses show very consistent behaviour with the exception of hose 6012 (Figure 4.25). Figure 4.27 and Figure 4.28 give typical examples of the significant levels of hysteresis which is seen in all these hoses.

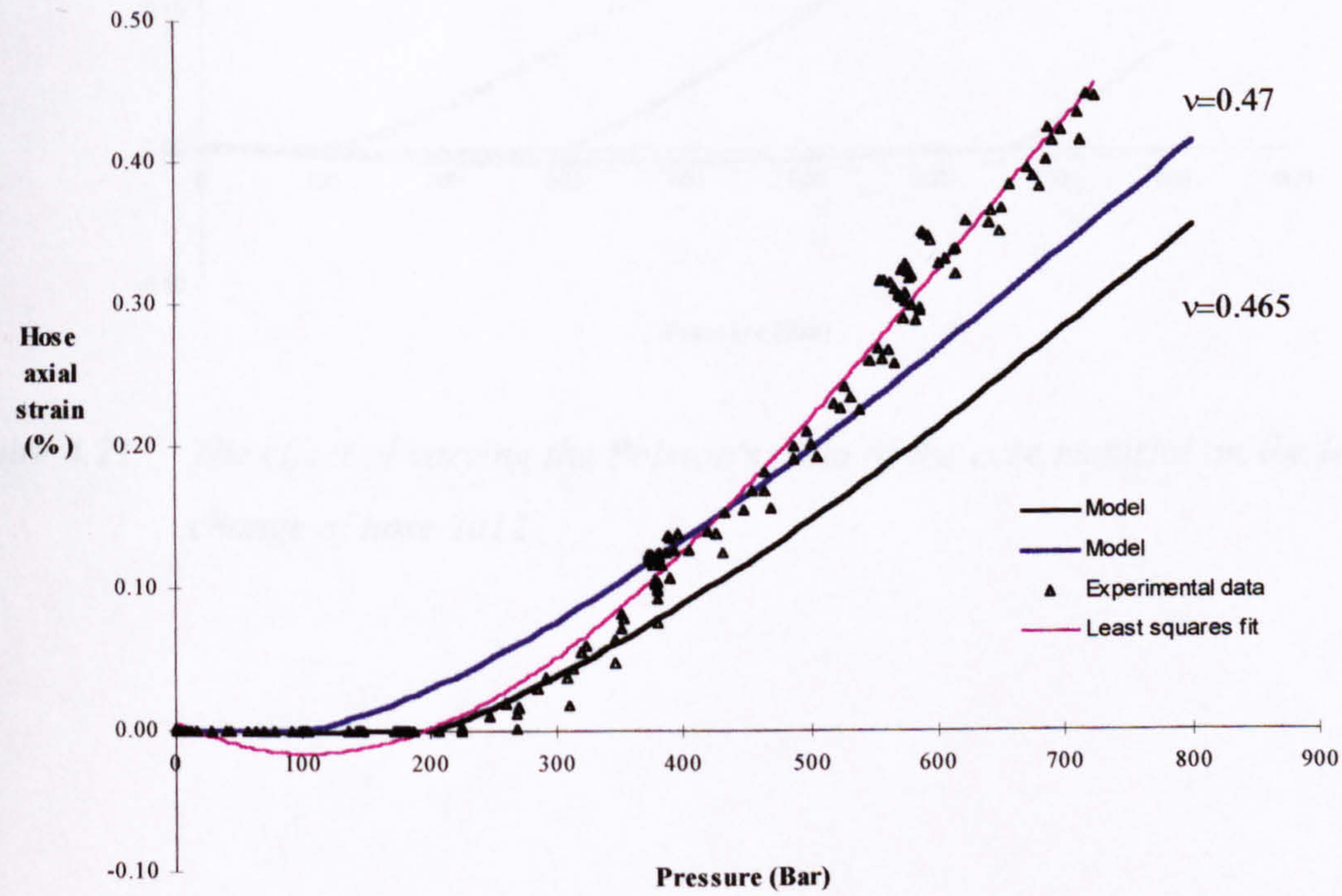

Figure 4.20. Hose 2012 Axial strain- experimental data compared with the model predictions for values of Poisson's ratio of the core material.

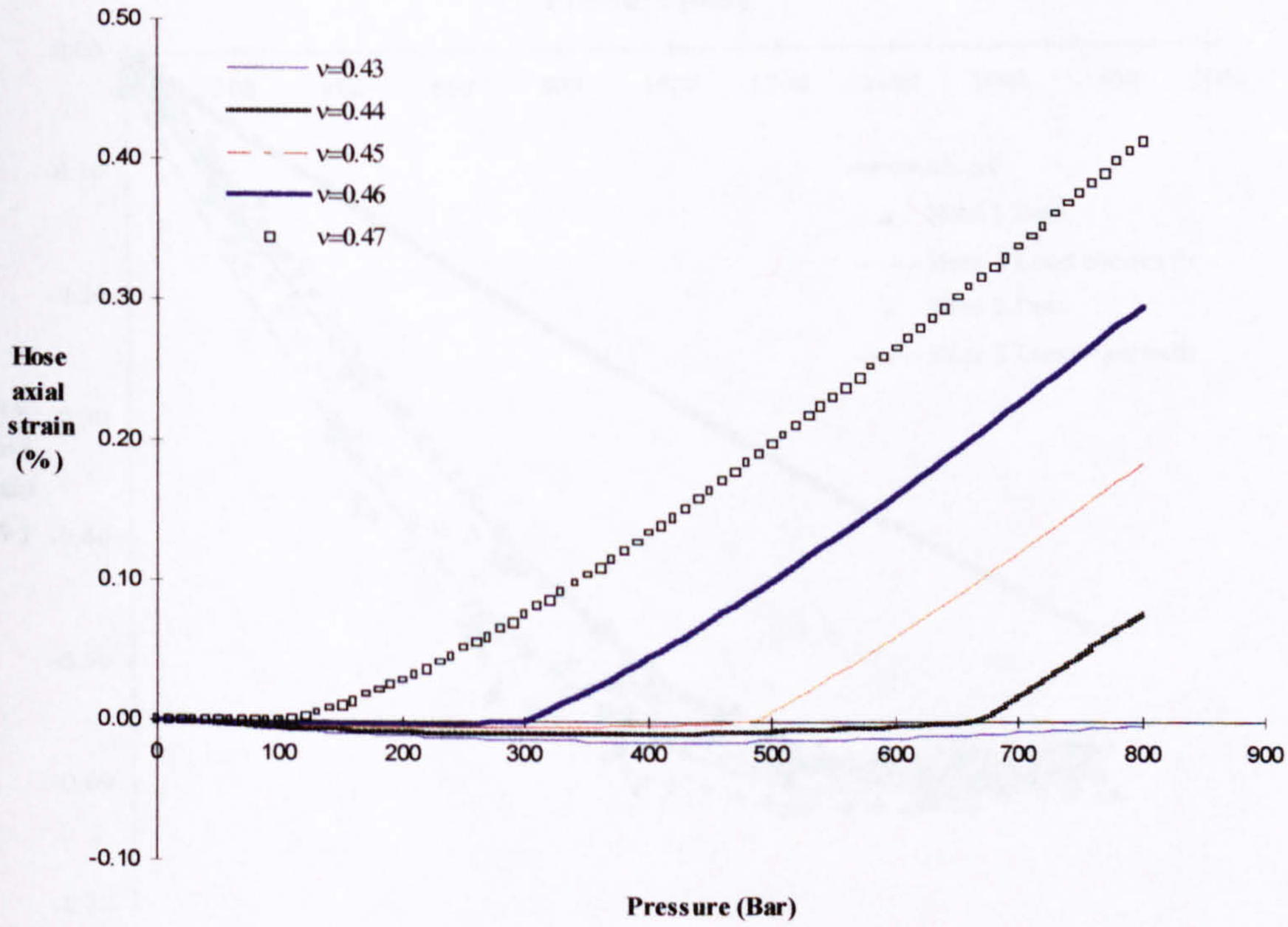

Figure 4.21. The effect of varying the Poisson's ratio of the core material on the length change of hose 2012.

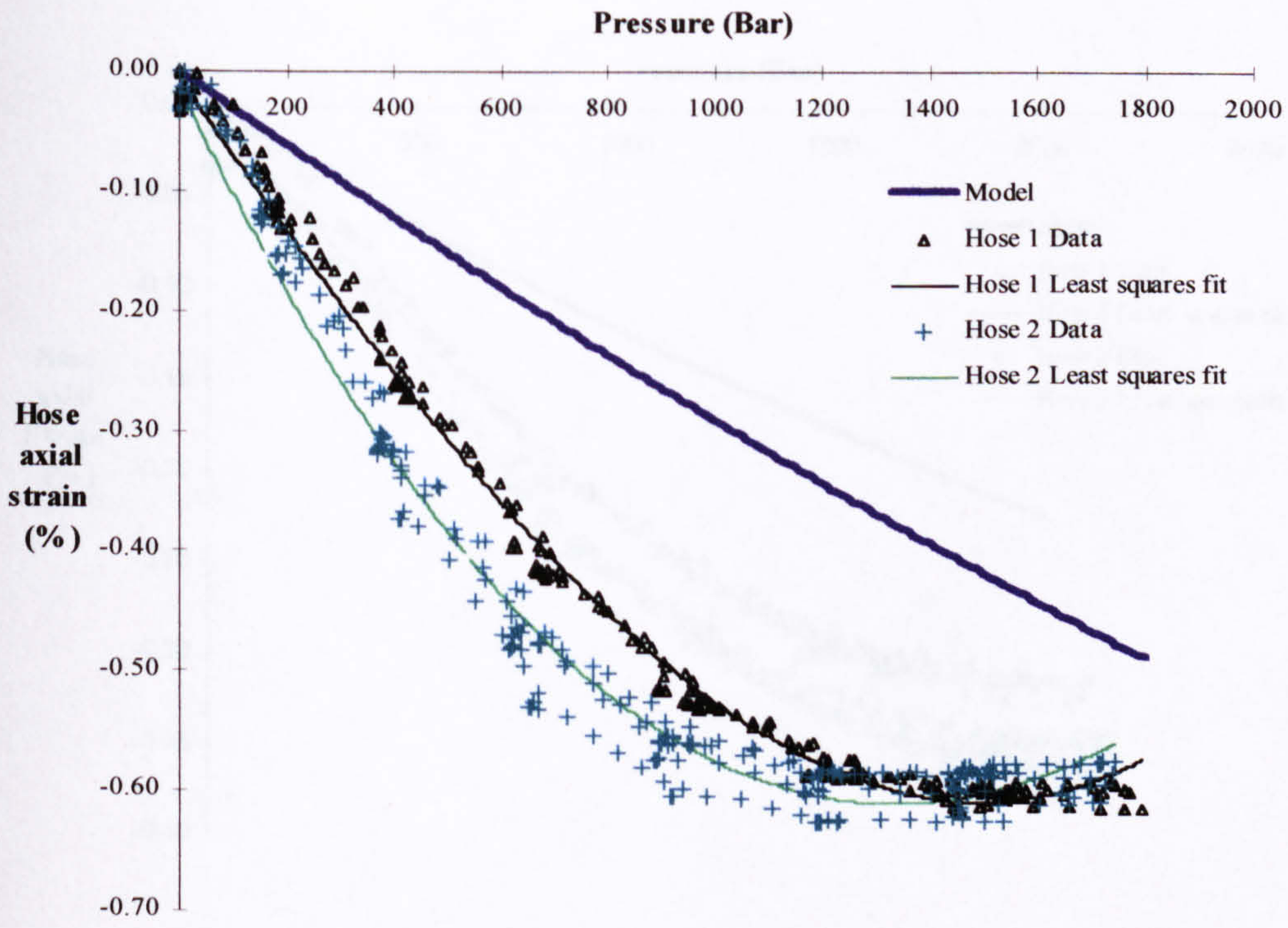

Figure 4.22. Experimental data of two samples of hose 4012 compared with model prediction.

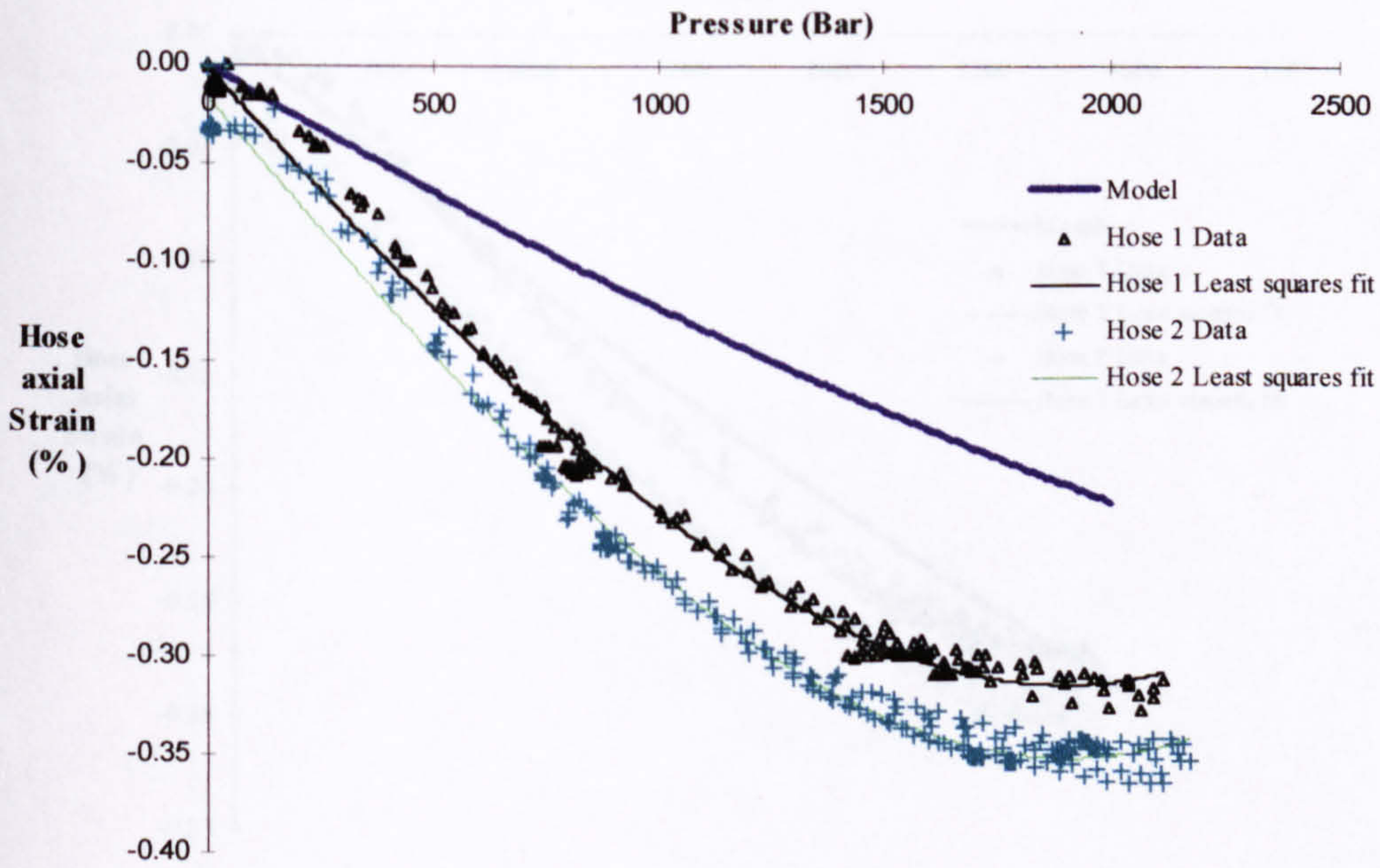

Figure 4.23. Experimental data of two samples of hose 4006 compared with model prediction.

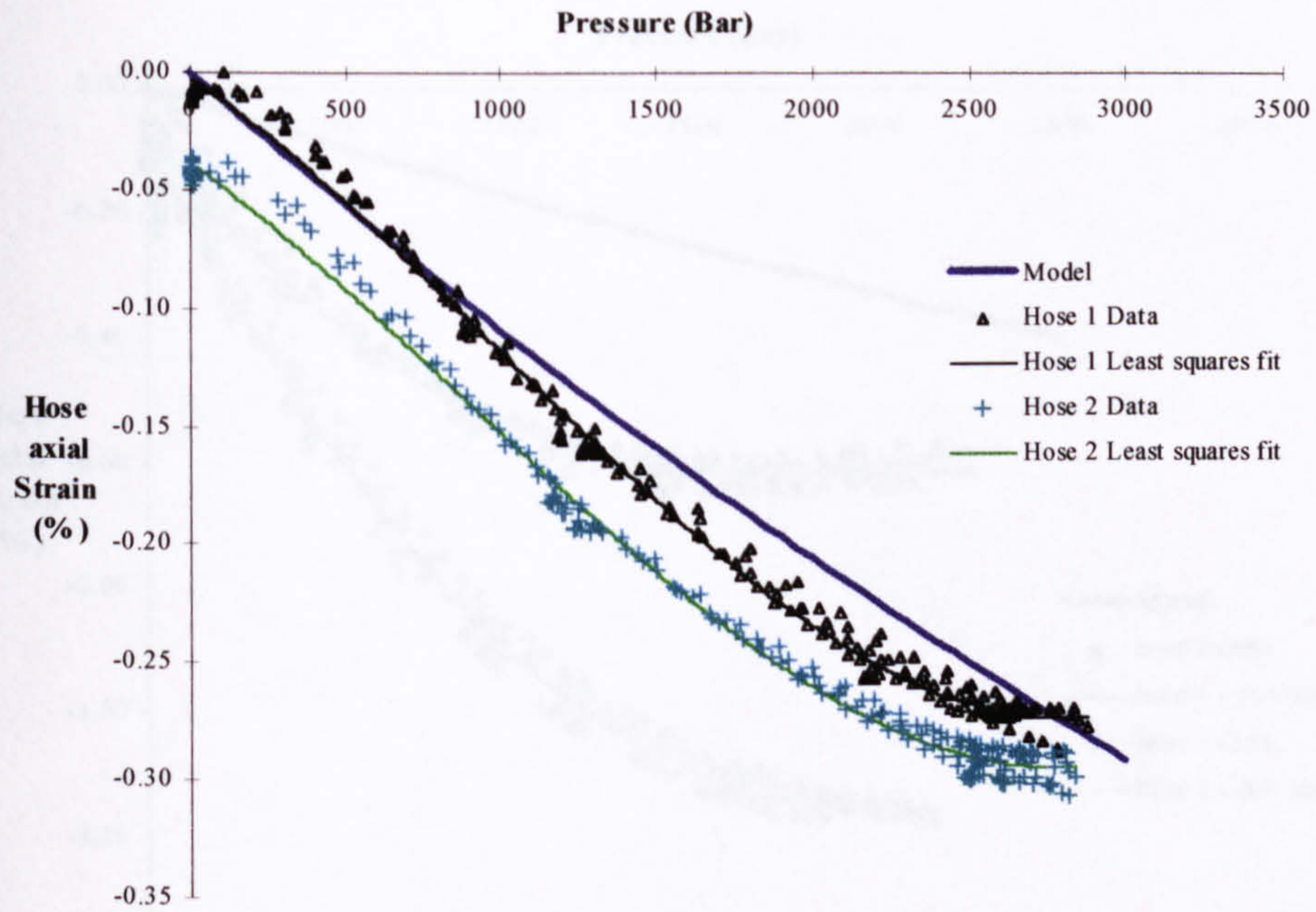

Figure 4.24. Experimental data of two samples of hose 6005 compared with model prediction.

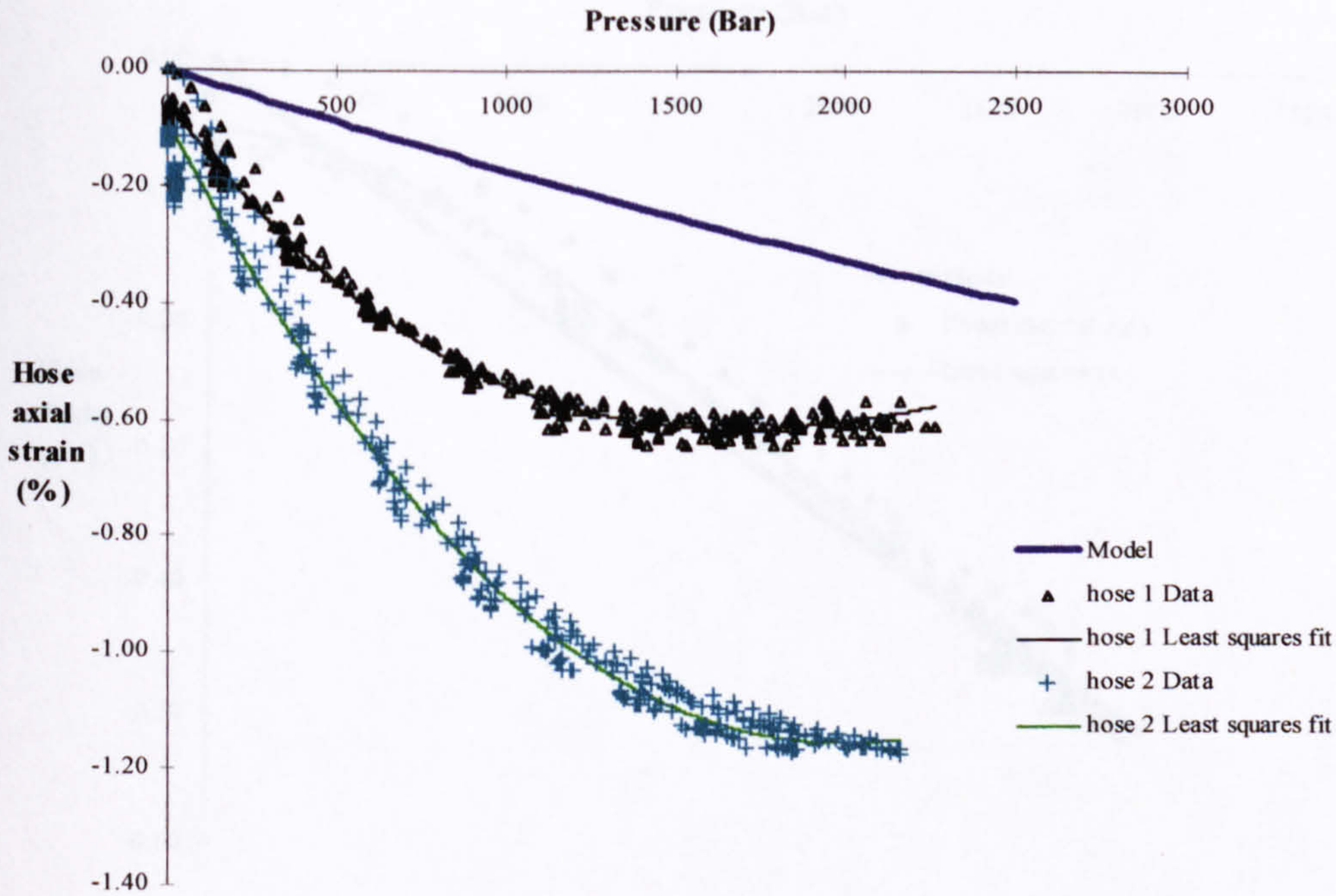

Figure 4.25. Experimental data of two samples of hose 6012 compared with model prediction.

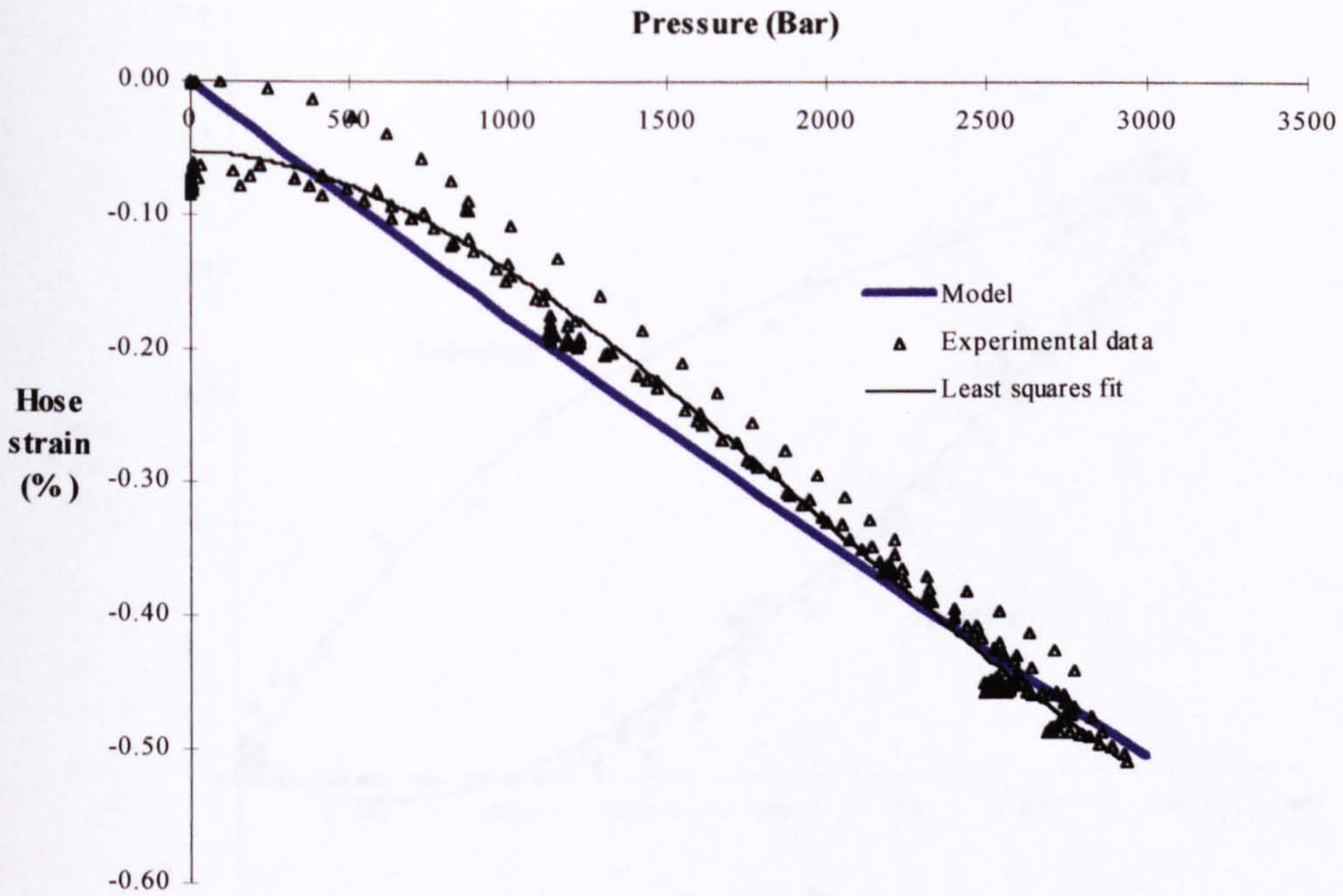

Figure 4.26. Experimental data of one sample of hose 8005 compared with model prediction.

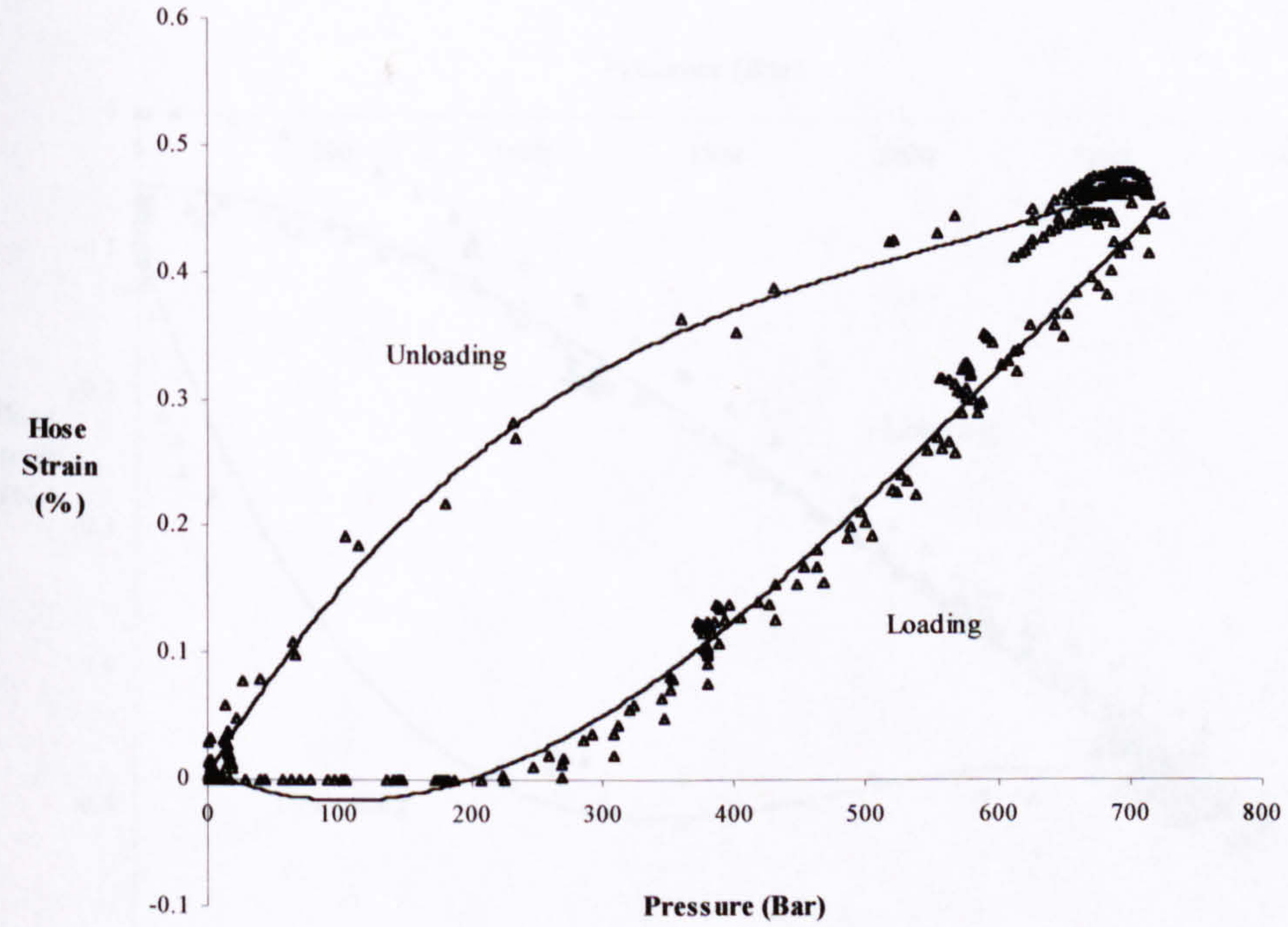

Figure 4.27. Hysteresis seen in length change during pressure cycling, (hose 2012).

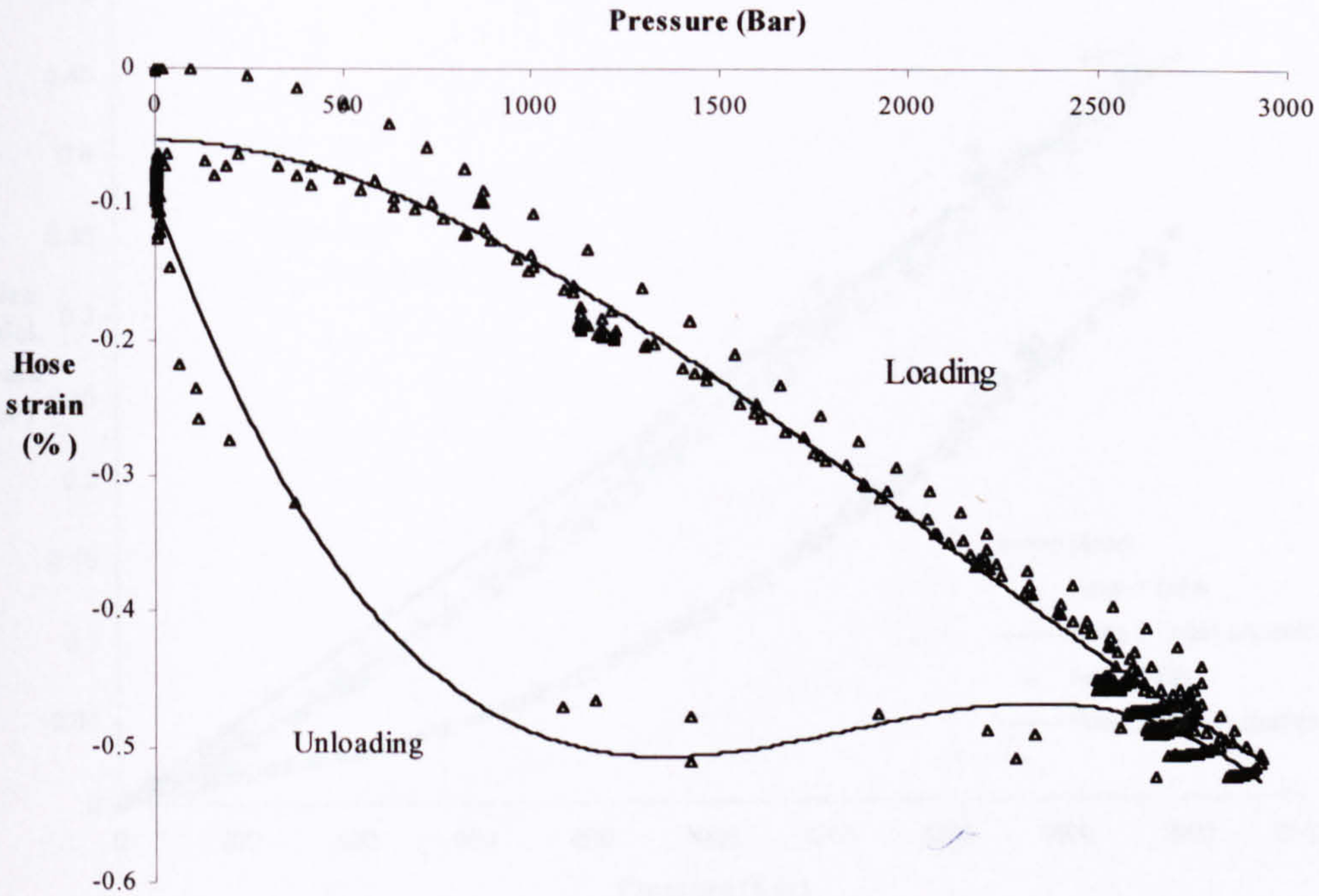

Figure 4.28. Hysteresis seen in length change during pressure cycling (hose 8005).

4.6.2 Outer wire strain

This section compares the experimental values of outer reinforcement wire strain with the theory. The majority the experimental work was carried out on two samples of each hose and in a number of cases there is a considerable variation between the results from the two samples. The theory shows good agreement with the experimental data and in two cases, Hose 4012 and 4005 (Figure 4.29 and Figure 4.30) there is an extremely close agreement to one of the experimental results.

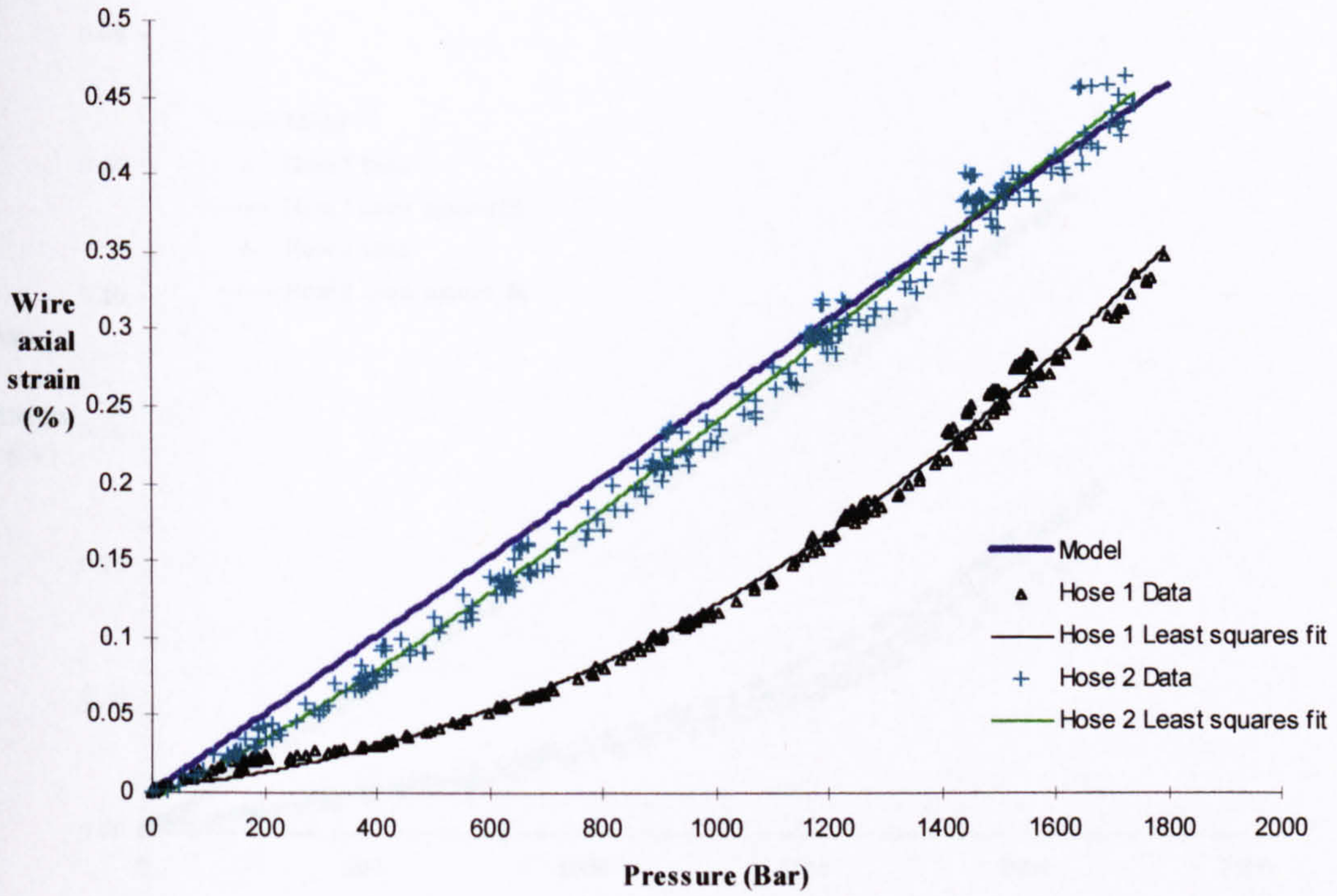

Figure 4.29. Comparison of experimental results from two samples of hose 4012 with theoretical prediction.

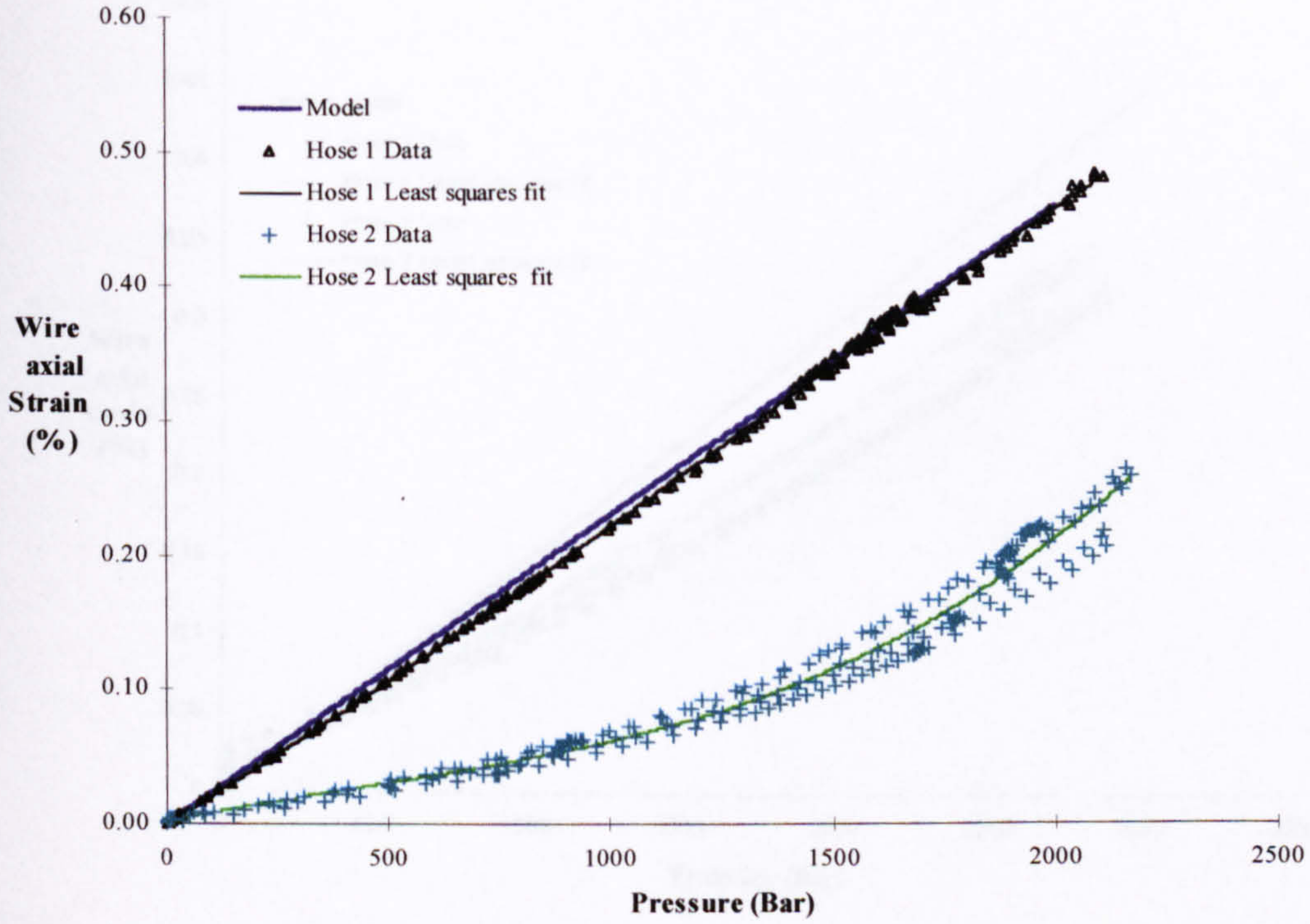

Figure 4.30. Comparison of experimental results from two samples of hose 4006 with theoretical prediction.

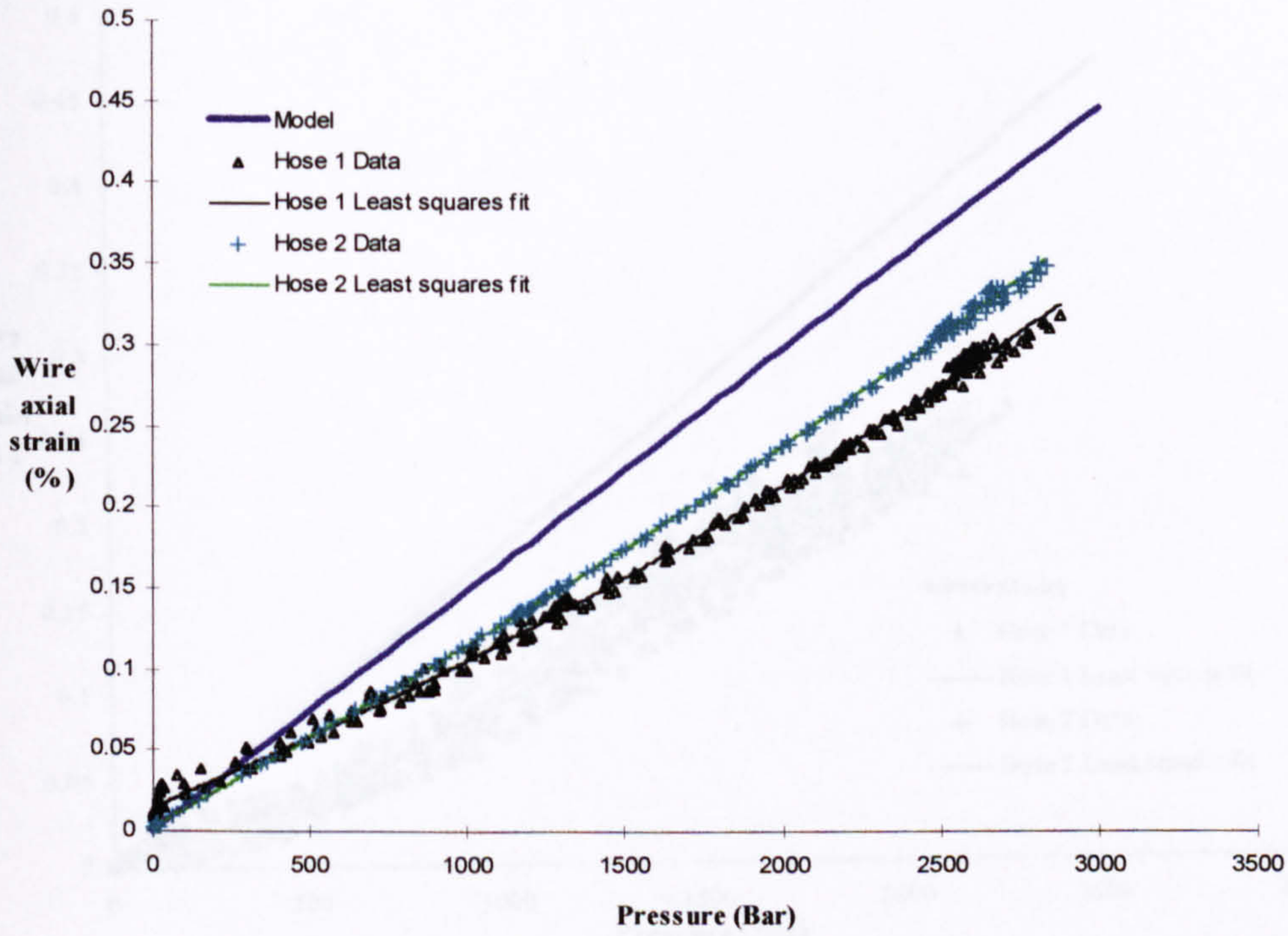

Figure 4.31. Comparison of experimental results from two samples of hose 6005 with theoretical predictions.

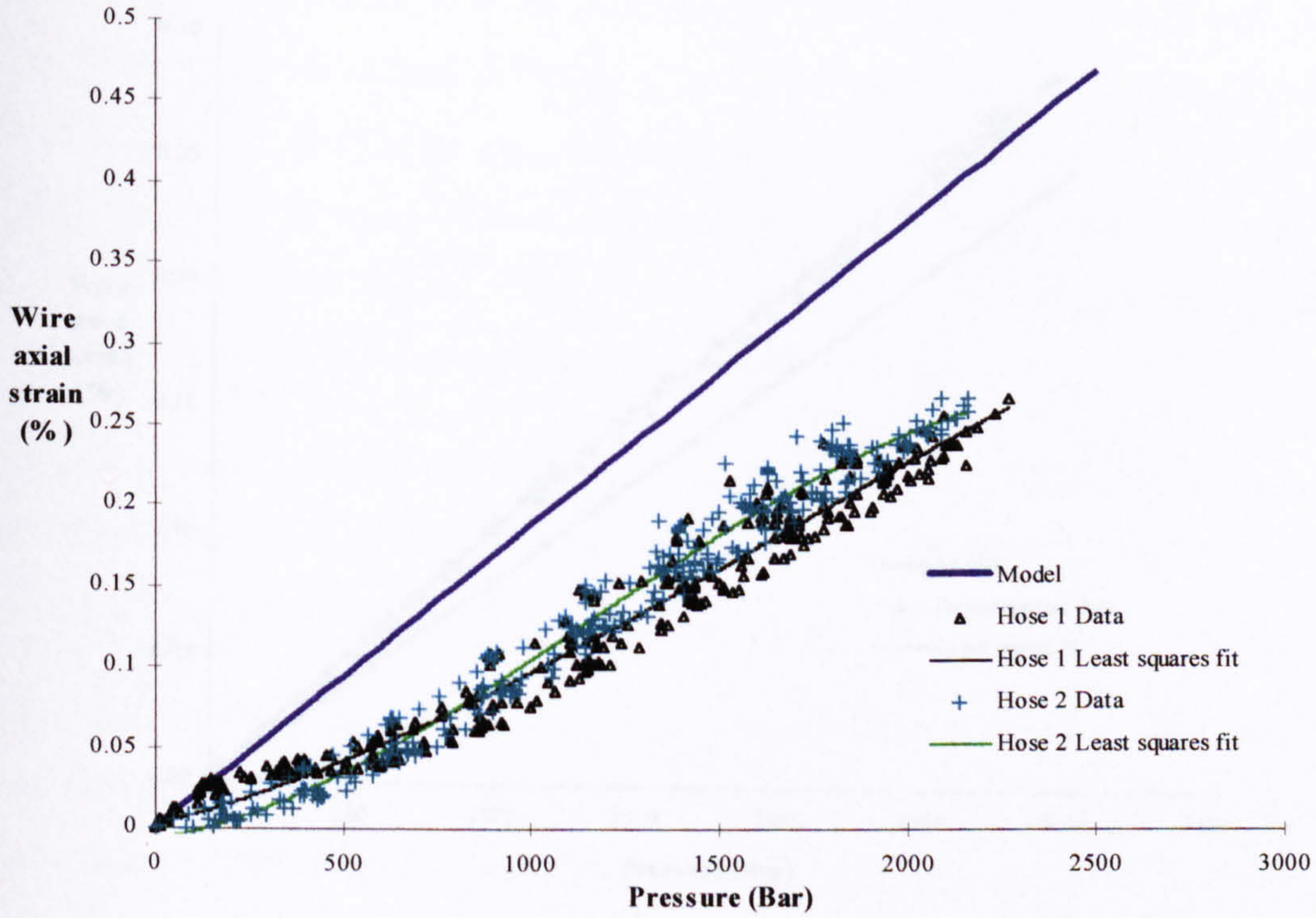

Figure 4.32. Comparison of experimental results from two samples of hose 6012 with theoretical predictions.

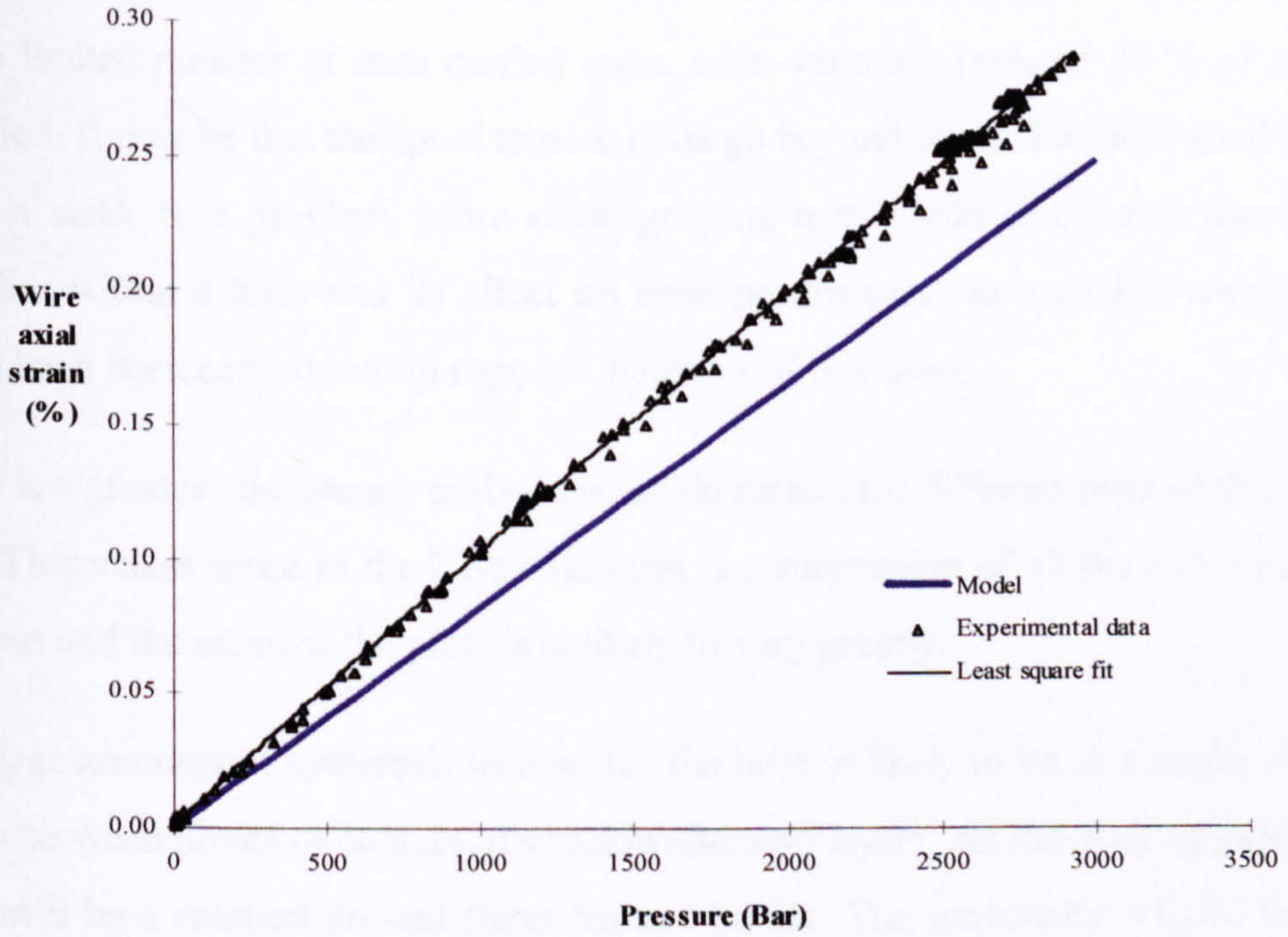

Figure 4.33. Comparison of experimental results from one sample of hose 4006 with theoretical predictions.

4.7 Discussion and conclusions

4.7.1 Experimental results

There is a number of hose types for which two tests carried out on two separate samples resulted in considerable variation in wire strain. It is not known whether this is a reflection of the variation in construction between hoses or reflects a scatter among wires in the same hose. Judging by the consistency of the hose strain results, however, it is thought likely that it is caused by the latter. In the case of hoses 4005 and 4012 one result is very nearly linear and corresponds exactly with the prediction of the model, whereas the other is non-linear, getting steeper with increasing pressure and is always lower than the model prediction. One possible explanation of this is that the non-linear behaviour is that of a slacker wire. When wires are wound onto the hose the winding drums are controlled with a friction brake. During a down period of a particular machine of Polyflex a spring balance

was used to gain an indication of the variation in braking force between different spools. In the limited number of tests carried out a wide variation (around 75 % of mean) was recorded. It may be that the spool tension must go beyond some threshold level in order to avoid a slack wire problem. More strain gauging tests could investigate the wire strain variation within a hose and its effect on hose performance in a similar way to the test which have been carried out on rope in Chapter 3 of this thesis.

There is a greater consistency in the hose strain results for different tests of the same hose type. This makes sense as the hose strain test is a summation of all the individual parts of the hose and the mean of the parts is unlikely to vary greatly.

The large amounts of hysteresis seen within the hose is likely to be as a result of frictional forces between points of contact of wires in alternate layers. As the hose changes in length there will be a rotation around these contact points. The movement will be inhibited by frictional effects and this would also account for the heating up of the hose during fatigue testing. No attempt has been made to model the hysteresis in this current work although others have introduced empirical factors to account for it [15]. The level of hysteresis may be a good method of gaining an insight into the relative motion between layers of reinforcement caused by pressure cycling. Clearly hysteretic loss will be a function of both interlayer pressure and motion and given that fretting of wires is dependant among other things on stress and motion between contacting wires, then hysteresis might correlate with the likely degree of fretting.

The contribution of the polymeric components of the hose to the hysteretic behaviour will be relatively small as these are highly deformable elastic materials.

One simple method of gaining a rough indication of the level of hysteresis (without actually measuring the load strain behaviour) would be by measuring the temperature of a hose undergoing cyclic loading, since much of the energy caused by the hysteresis is dissipated in the form of heat. It has been found on these hoses that cyclic loading must be conducted at a very low frequencies (around 0.1-0.05 Hz) in order to prevent the hose overheating and melting the plastic components within it.

4.7.2 Model predictions and possible improvements to model

One interesting aspect of the model predictions is the importance of the Poisson's ratio of the inner core for hose that gets slightly longer on pressurisation. For hoses that get substantially longer, or get shorter no such dependence has been found. When the hose strain is very small (but positive), the positive and negative terms within the axial equilibrium equation are balanced, but the hose has a relatively low axial stiffness in tension and so any slight change in the force balance will greatly effect the hose axial strain.

A number of other aspects could be incorporated into the hose model, it is clear from looking at inner core samples that the core tends to extrude into the wire spaces during hose pressurisation, this is likely to have an influence on the deformed winding radius of the reinforcement layers and may also be an important factor in the hose hysteresis. Another improvement to the compatibility equations which could be made would be to include the contraction of layers caused by point contact stresses between wires in adjacent layers, this could be done using a simple Hertzian theory.

4.8 References

1. Kuipers, M. and M. Van der Veen, *On Stresses in Reinforced High Pressure Hoses.* Acta Mechanica, 1989. **80**: p. 313-322.

2. Teerling, H.L.J., *Strength and Stiffness of High Pressure Hoses (PhD Thesis in English)*, in *Wiskunde en Natuurwetenschappen.* 1994, Rijksuniversiteit Groningen: Groningen. p. 150.

3. Van Den Horn, B.A. and M. Kuipers, *Strength and stiffness of a reinforced flexible hose.* Applied Scientific Research, 1988. **45**: p. 251-281.

4. Cardou, A. and C. Jolicoeur, *Mechanical Models of Helical Strands.* Applied Mechanics Reviews, 1997. **50**(1): p. 1-14.

5. Jolicoeur, C. and A. Cardou, *Numerical Comparison of Current Mathematical Models of Twisted Wire Cables Under Axisymetric Loads.* Journal of Energy Resources Technology, 1991. **113**(4): p. 241-249.

6. Jolicoeur, C., *Comparative study of two semicontinuos models for wire strand analysis.* ACSE Journal of Engineering Mechanics, 1997. **123**(8): p. 792-799.

7. Hruska, F.H., *Calculation of Stresses in Wire Ropes.* Wire, 1951(September): p. 766-801.

8. Hruska, F., *Radial Forces in Wire Ropes.* Wire and Wire Products, 1952. **27**(5): p. 459-463.

9. Hruska, F., *Tangential Forces in Wire Ropes.* Wire and Wire Products, 1953. **28**(5): p. 455-460.

10. Machida, S. and A.J. Durelli, *Responce of a Strand to Axial and Torsional Displacements.* Journal of Mechanical Engineering Science, 1973. **15**(4): p. 241-251.

11. Love, A.E.H., *A Treatise on the Mathematical Theory of Elasticity*. 1944: Dover.

12. Knapp, *Derivation of a New Stiffness Matrixc For Helically Armoured Cables Considering Tension and Torsion.* International Journal for Numerical Methods in Engineering, 1979. **14**: p. 515-529.

13. Entwistle, K.M. and G.W. White, *A method for achieving effective load transfer between the inner and outer layers of a two- layer braided high pressure hydraulic hose.* Int. Journal of Mech Science, 1977. **19**: p. 193-201.

14. Breig, W.F., *Mathematical and experimental pressure- deformation response of helically wound wire reinforced elastomeric hose.* SAE Technical Paper Series, 1988(881301.): p. 6.1593-6.1607.

15. Jakeman, R.R. and P.H. Knight. *Development of a High Pressure Thermoplastic Hose*. in *Umbilicals: The Future*. 1995: Society for Underwater Technology.

16. Lamé, G. and B.P.E. Clapeyron, *Mémoire présentés par Divers Savants*. 1833, Paris.

17. Housner, G.W. and T. Vreeland, *The Analysis of Stress and Deformation*. 1966, London: Collier-Macmillan Ltd.

18. Hertz, H., *Gesammelte Werke*. Vol. 1. 1895, Leipzig.

19. Radzimovsky, E.I., *Stress distribution and strength conditions of two rolling cylinders pressed together.* Engineering Experiment Station (University of Illinois), 1953. **408.**

20. Young, W.C., *Roark's Formulas for Stress and Strain.* 1989: McGraw-Hill.

21. Acton, F.S., *Numerical Methods that Work.* 1970, New York: Harper International.

22. Ortega, J.M. and W.C. Rheinboldt, *Iterative Solution to Nonlinear Equations in Several Variables.* 1970, New York: Academic Press.

23. Jeffrey, *Mathematics for Engineers and Scientists.* 1996, London: Chapman and Hall.

24. Press, W.H., *et al.*, *Numerical Recipes in Fortran.* 1992, Cambridge: Cambridge University Press.

25. TML, *TML Strain Gauge Catalogue.* 1990.

26. Benham, P.P., R.J. Crawford, and C.G. Armstrong, *Mechanics of Engineering Materials.* 2nd ed. 1996, Essex: Longman.

5. The fatigue behaviour of high pressure thermoplastic-wire hose: implications for design

5.1 Summary

This chapter examines certain aspects of the fatigue behaviour of thermoplastic wire hose, particularly relating to contact stresses and fretting fatigue. The lack of literature on hose fatigue indicates that this is not a major consideration of most hose constructions and applications. The most relevant work that is published comes from the field of rope and strand fatigue and a concise review of this work has been conducted.

The general failure mechanism of the hose is seen to be break-up of the inner wires until one of the broken wires causes a puncture of the core. The stochastic nature of this type of failure means that there is a very wide scatter in hoses' fatigue performance, ranging from when the first wire failure causes leakage, to when many wire failures occur before the core is punctured.

The stress caused by the cross wire contact points between layers of the hose is calculated and this value is compared with two further hypothetical contact conditions: both line contacts resulting from reinforcement layers wound in the same direction. It is seen that the line contact condition results in a reduction in the contact stresses by a factor of 5 and the feasibility of introducing this type of construction into a hose is discussed. The ultimate failure of the hose is through one of the inner wires puncturing the core, the most important consideration is to prevent wires in this inner layer from breaking. The chapter concludes with a discussion of a number of other possible ways the hose fatigue characteristics could be improved, including the possible introduction of a lubricant.

5.2 Review : hose fatigue and related research

5.2.1 Mechanisms of fatigue in hose

There has been very little research aimed at identifying the types of degradation that occur in hose under fatigue conditions. Some authors have mentioned mechanisms of failure as an aside when discussing testing methods and design techniques. Buzzelli [1] states that a hose may fail in fatigue, but gives no discussion of the mechanism. Briggs [2] attributes fatigue failure to the random break up of wires along the entire length of the hose, but also discusses the possibility of pin hole cracks in the inner core. Reichel [3], also relates observations of random wire breaks which he attributes to the degradation seen in fatigue. An anonymous work [4], discusses the neutral angle theory and whether two layer hoses which are wound at other angles than this will see more fretting fatigue because of relative movements between the wires. It concludes that there will not be relative slip between wires and therefore hoses of non-neutral angle construction will be no more susceptible to fretting fatigue than neutral angle wound hoses. It also states that many hoses will not experience fretting fatigue because of the intermediate layers of rubber in the hose preventing contact between the wires. The paper does not suggest any possible other mechanisms of failure in fatigue except for that caused by misuse of the hose. However this paper should be treated with some caution since there is very little justification for any of the claims it makes.

All the hoses discussed in this section were related to braided hose designs, no published observations have been made on the mechanisms of fatigue degradation seen with helical wire hose constructions.

5.2.2 Hose testing relating to endurance

Standard procedures involve the testing of a hose assembly, (i.e. a length of hose with end fittings). As there is no standard that relates to ultra high pressure hose, working pressures above 1,000 bar, the most relevant standard will be discussed, this is SAE J343 [5]. This

standard is for the testing the SAE 100R series hoses [6]. Both the burst and 'impulse' test are used to characterise the fatigue behaviour of the hose.

5.2.2.1 Burst test

In the burst test a hose assembly of a specified length (related to the hose internal diameter) is subjected to a constantly increasing pressure until failure. The rate of pressure increase is not critical but should not be too fast, a test time of one minute is common. Once the minimum burst pressure of a particular hose has been determined, the maximum safe working pressure is calculated using the safety factor. This number may be anywhere between 2.5 and 4 depending on the hose and manufacturer. The SAE[5] recommended safety factor is 4.

5.2.2.2 Impulse test (fatigue test)

The SAE standard [5] specifies that the hose assembly should be subjected to a specific cyclic pressure with a pressure magnitude of 133 % of the working pressure. The bounds for the pressure response curve is stipulated (see Figure 5.1 (a)) and the test frequency is specified at around 0.5 to 1 Hz. The standard advises a fixed bend of 90° or 180° during testing (Figure 5.1 (b)) but also states that in certain instances it may be appropriate to test the hose straight. The test should continue until failure or until a set number of cycles have been completed, 200,000 for a two layer hose and 400,000 for a 4 layer hose.

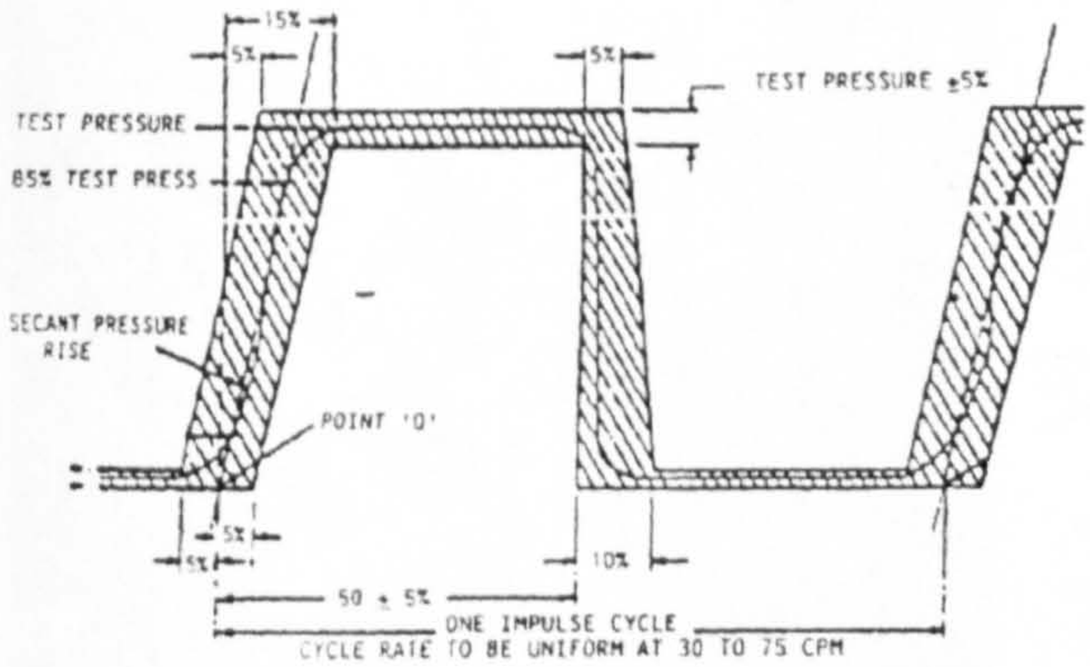

(a)

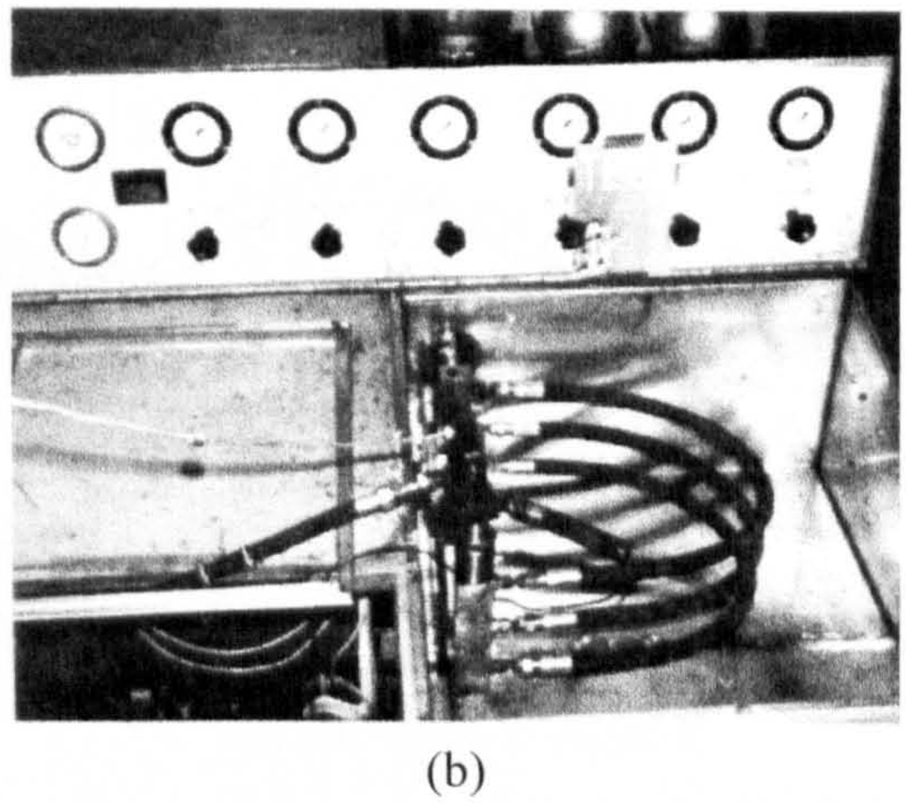

(b)

Figure 5.1. (a)The Stipulated fatigue pressure curve according to SAE J343[5] (b) The constant bend configuration of hoses during an impulse test, from Reichel [3].

It has been found from experience [7] that the SAE standard with a constant bend radius during testing is not a good representation of hose loading conditions in applications which see significant levels of bending during every pressure cycle. Because of a significant number of failures in the hydraulic actuator hoses of JCB diggers, a new test was introduced by JCB. This test has become known as the omega flex impulse test: during every pressure cycle the hose is bent into an omega shape (see Figure 5.2, (a)) and then straightened. This demonstrated that braided hoses were far superior to spiral hoses in this harsh bending environment. Spiral hoses tended to develop bird caging and other distortional problems leading to premature failure. This test was eventually introduced into the standard as an optional recommendation for applications which see a high level of bending during operation [8]. It was decided, however, that a half omega test was more generally appropriate (see Figure 5.2, (b)).

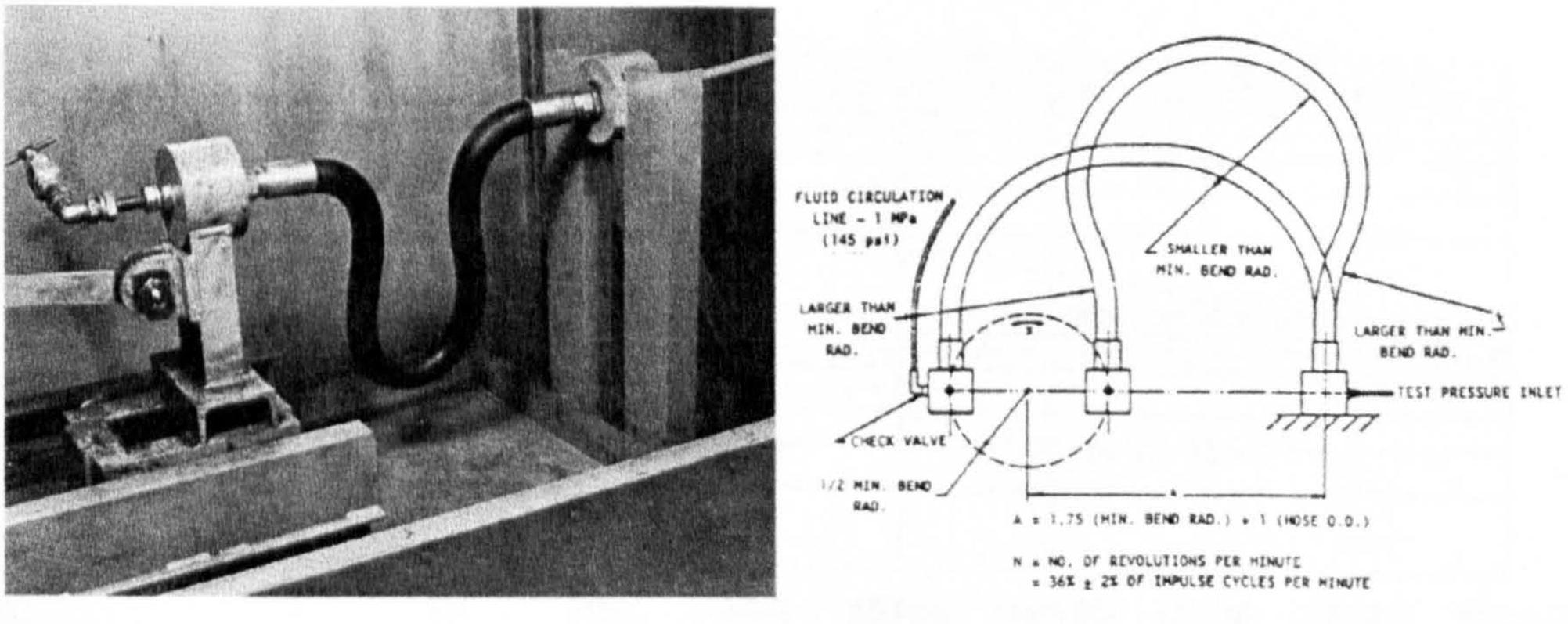

(a) (b)

Figure 5.2. (a)A hose in flex impulse test with full omega bend configuration from Evans[9] (b) Half omega configuration according to the SAE_J1405 optional recommendations for additional impulse tests [8]]

5.2.3 Fatigue life prediction in hose

For certain applications it may be necessary to have a method for estimating the life of the hose to avoid in service failure or possibly to assess the suitability of the product given the loading regime. Berns and associates [10, 11] have conducted tests to verify a technique for doing this. It was proposed to use the burst and impulse tests as two points to produce a P-N curve, which was assumed to be linear on a log-log scale as shown in Figure 5.3. Berns conducted a series of tests at other load levels to better characterise the hose pressure versus cycles to failure behaviour and to see whether this technique was valid. He produce standard reference curves for SAE 100R series hoses [6] based on statistical analysis. If a hose pressure history comprises a constant pressure range then the P-N curves can be used directly to predict the fatigue life of the hose.

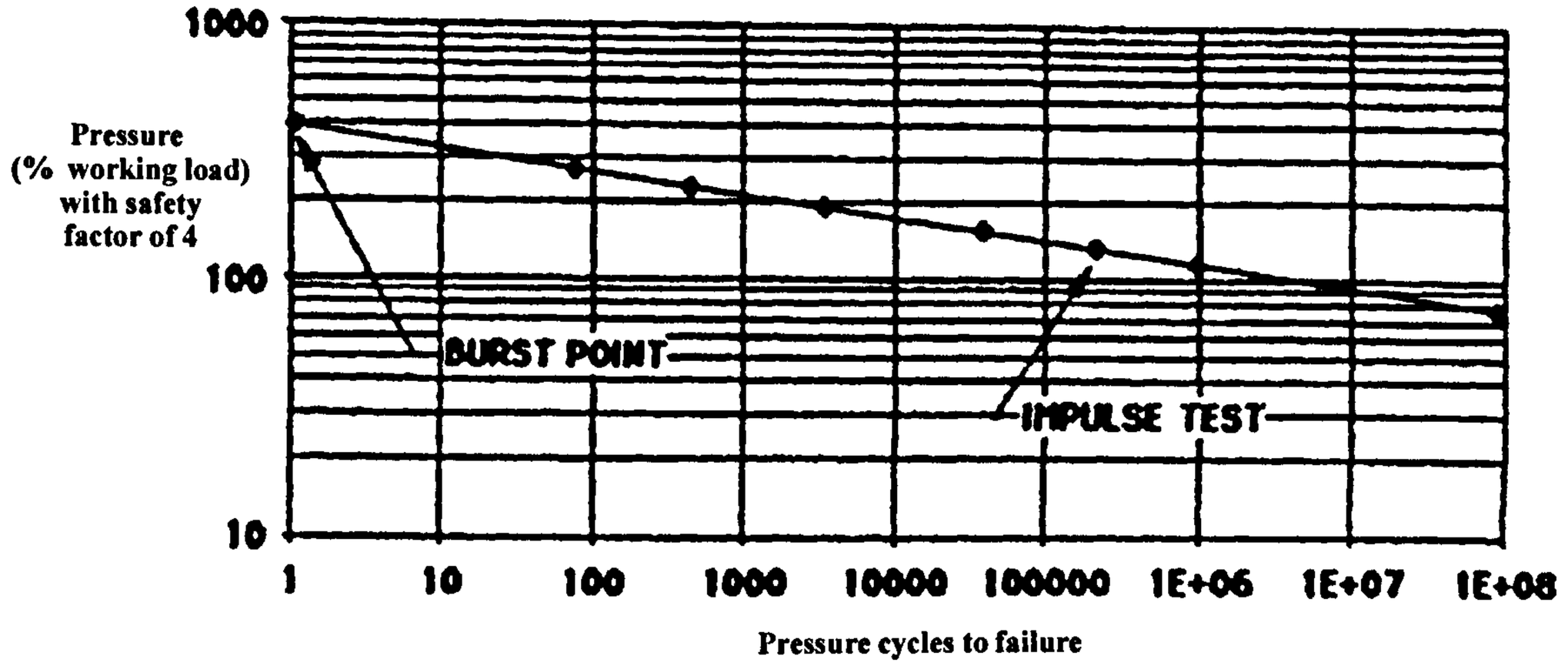

Figure 5.3. P-N Curve for hoses as proposed by Berns et. al [11].

Berns also proposed a method for summating the effects of variable amplitude pressure loading using the standard cumulative damage summation techniques developed by Palmgren and Miner [12, 13]. Methods are given for counting the various values of pressure amplitude seen in a representative sample of an in service pressure history. Variable amplitude block loading fatigue tests were carried out to verify this method and the results showed that the method would generally give a conservative prediction of hose life. In comparison Potts and Chaplin. [14] have performed a verification of the cumulative damage analysis for six strand wire rope and found a Miner's summation going from 0.9 to 2, and they suggested that the larger value may be a result of shifting fretting fatigue.

5.2.4 Stress environment in strands

The most highly stressed regions within a strand in tension are at the locations where adjacent wires are in contact. This equally applies to a construction of hose with no interlayers between the reinforcement.

There are two general kinds of contact: the cross wire configuration resulting in discreet contact points between wires and the parallel wire configuration resulting in a continuos line contact along the length of wires. The basic solution to the problem of contacting

cylinders was found by Hertz [15]. This was extended for the full tri-axial stress state and expressed in more useable elliptic integrals by Thomas and Hoersh [16].

Based on these expressions Liessa [17] derived the first solution to the contact stresses in a wire rope. Assuming parallel contact he solved for the simplest case of a 6x7 stranded rope. The solution was extended for the same type of rope, but for cross wire contact, by Starkey and Cress [18]. Both solutions require a value for the bulk radial forces acting between wires and these were derived from the theory of Hruska [19]. Stresses due to contact were superimposed on to the bulk tensile stresses in the wires, calculated from Hruska's [20] theory for stresses in wires.

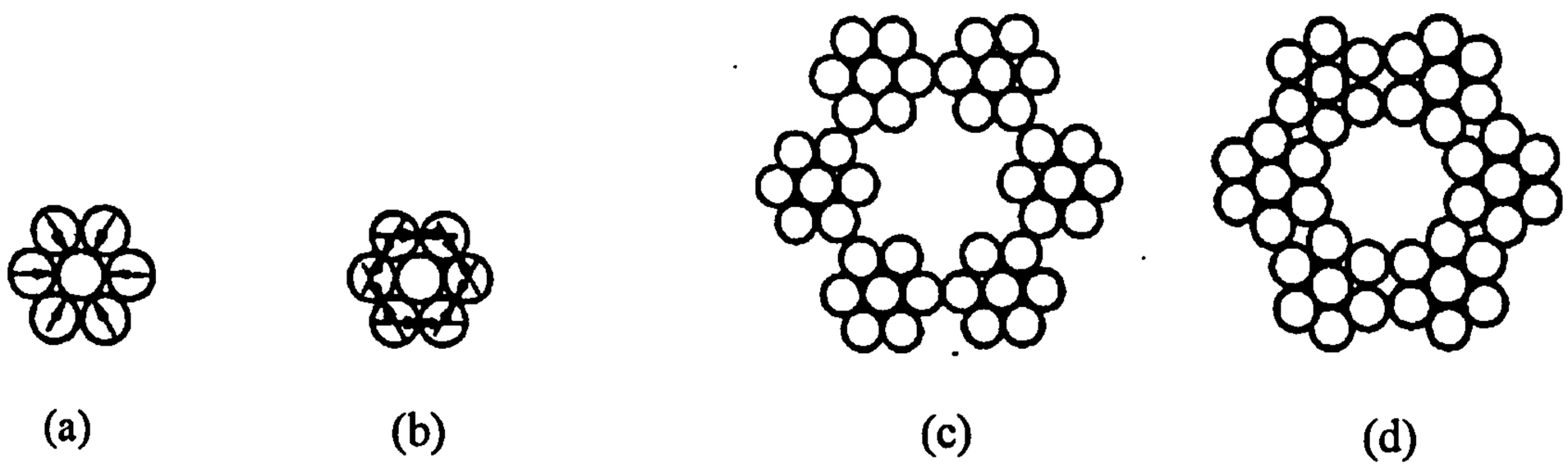

Figure 5.4. (a) and (b) show the two possible conditions of contact within a strand, (c) and (d) show two possible conditions of contact between adjacent strands of a wire rope with a soft core from Starky and Cress [18].

An assumption which had to be made in the analysis was the location of the critical regions of contact. Take for example a seven wire strand (see Figure 5.4 (a) and (b)). where there are two extreme possibilities for the configuration relevant to the contact: when the central wire is slightly smaller than the outside ones then the external wires will be in contact and there will not be contact with the core and on the other hand, if the king wire is slightly larger than the external wires there will be contact between the outside wires and the core wire, but no circumferential contact between the wires in the same layer. The level of cyclic stress induced by contact loading alone will induce crack nucleation and accelerated fatigue failure of wires within the rope, as for example might be

seen in a ball bearing [21]. There is however an additional factor in a wire rope which will compound the likelihood of crack growth. This contact condition is further aggravated by the slight fretting movements between the contacting surfaces as discussed in the next section.

5.2.5 Wire fretting fatigue

Two archetypal fretting modes have been classified by Blakeborough and Cullimore [22] for a strand under tensile load with no relative twist at the ends. These could equally apply to spiral hose and are as follows:

- Longitudinal fretting occurs between two adjacent wires in the same layer of a strand, or between two wires in neighbouring strands which are laid at the same lay length. It is caused by relative longitudinal displacements of a line in contact as the lay angle changes during axial extension.

- Rotational fretting occurs at wire cross contacts, especially when layers are wound in opposite directions. The fretting is caused by one wire rotating relative to another during axial extension and will occur at a point.

Methods of simulating this type of fatigue were developed (see [22] for details) and then fretting fatigue life was compared with unfretted wires for a range of contact forces and alternating axial stress. For longitudinal fretting it was found that increasing the contact forces decreased the fatigue life and a not unreasonable line contact force of 170 kNm^{-1} roughly halved the life from the un-fretted wire. The rotational fretting situation seemed to be much less clear however. The results were scattered and no obvious trend presented itself. It was also found that a lower clamping force seemed to reduce the fatigue life, which was not expected but may be caused by an increased level of movement between the wires.

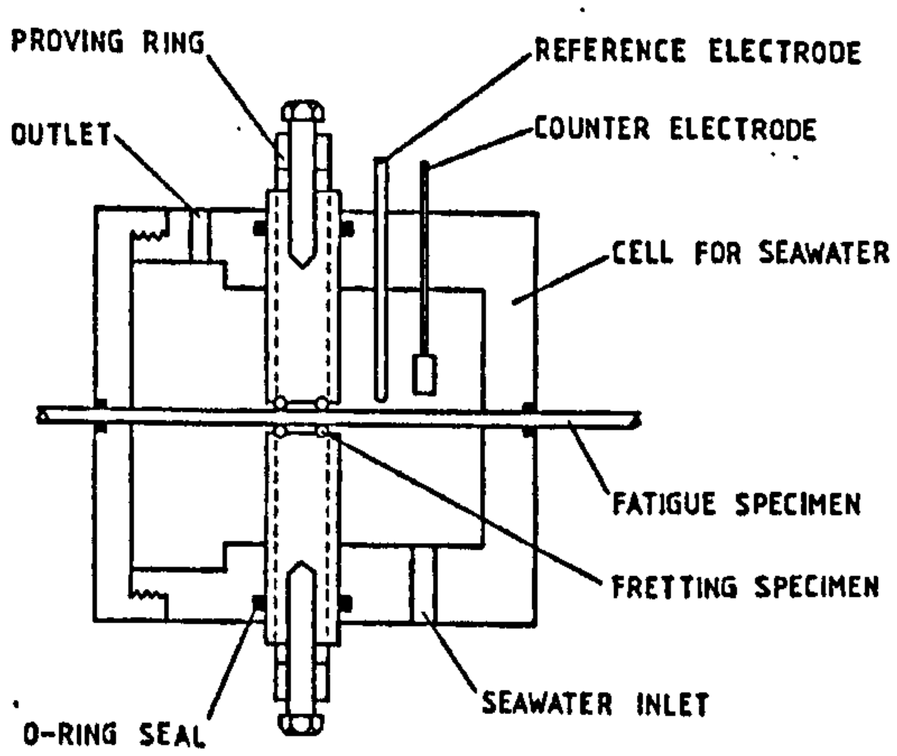

(a)

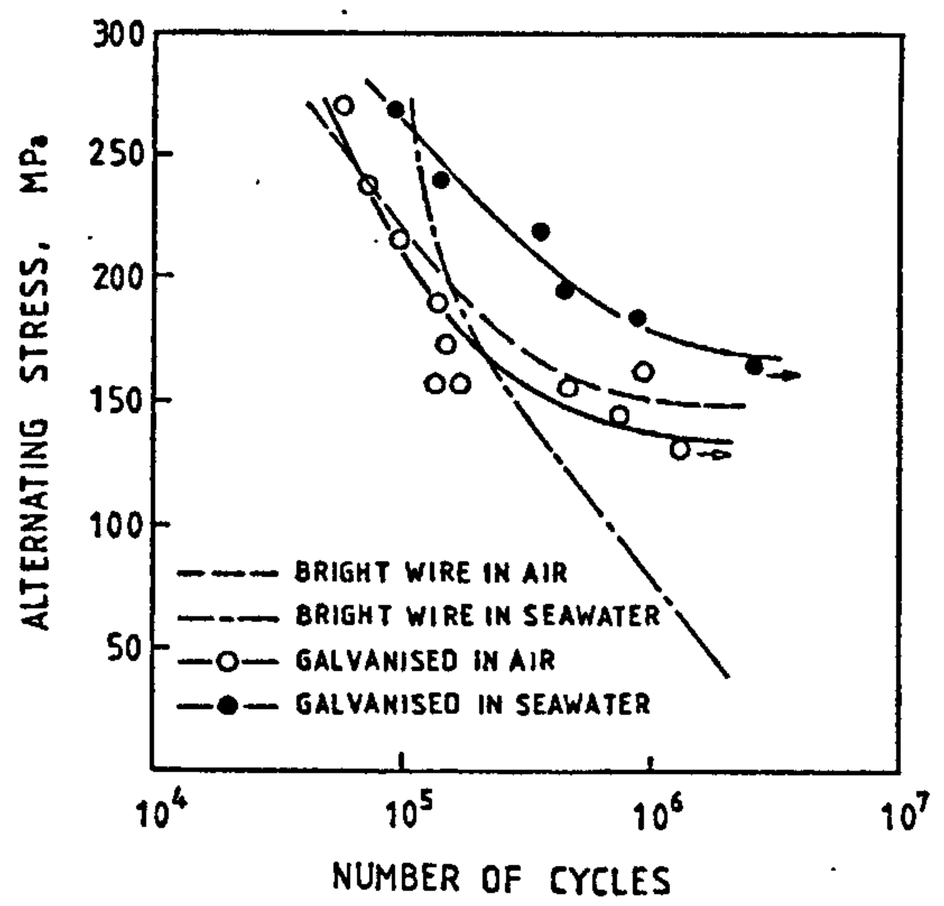

(b)

Figure 5.5. (a) The fretting fatigue cell used for S-N curve experiments on wires (b) some SN curves for wire under different conditions from Waterhouse [23].

An extensive series of experiments on fretting of rope wires has been carried out by Waterhouse and his colleagues [23-28]. Much of this work concentrates on environmental effects on fretting behaviour such as the presence of lubrication or corrosive elements and the mechanical conditions are kept consistent throughout these tests. Briefly the simulated fretting conditions are as follows: two bridges each with sections of the same wire as is being tested are clamped onto the tested wire by means of a proving ring. The whole unit is mounted on the test wire inside a sealed watertight cell which enables the environment to be controlled (see Figure 5.5 (a)). The wires are at 90° to the tested wire but cause a longitudinal fretting condition with a point load. This is likely to be closest to the cross wire fretting fatigue condition and the work was aimed at structural strands for bridges which have this type of contact environment. An example of the findings of this work can be found in Figure 5.5 (b)

In a more recent series of studies Waterhouse and others [24, 27] have concentrated in studying the wear patterns caused by fretting fatigue without concerning themselves with the tensile fatigue properties. A simple experimental rig was used (see Figure 5.6(a)) to simulate rotational fretting between two wires and fretted surfaces were then studied using

a scanning electron microscope and mapped using a profilometer (see Figure 5.6(b) and (c)). Using this technique parameters such as normal force and lubrication have been controlled to assess their effect on the development of a wear scar.

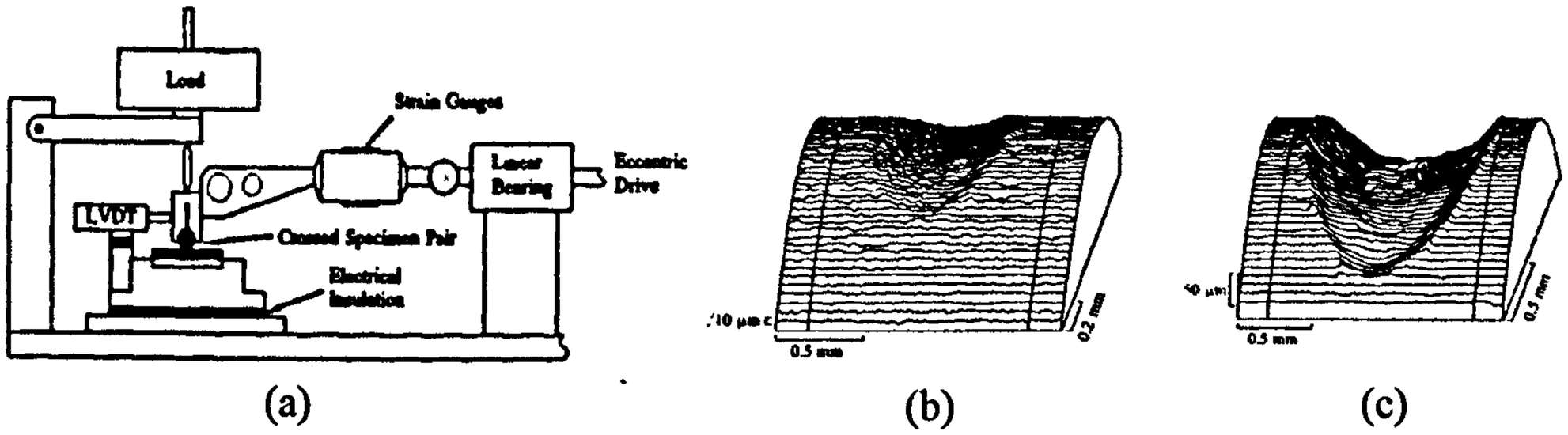

(a) (b) (c)

Figure 5.6. (a) schematic arrangement of the fretting rig, (b),(c) profilometer map of a fretting scar produced by a normal force of 150N after 3000 cycles in (b)grease lubricated and (c) dry conditions from McColl et. al. [27].

5.2.6 Fatigue models in strands

Three broadly similar models have been developed to predict the overall fatigue performance of helical strands. Knapp and Chiu [29] developed a fatigue model for overhead power cable with two layers of helical wires. They use the static model previously developed by Knapp [30] to calculate the radial forces acting between the layers. This was then used to calculate the triaxial stress state caused by the contacts using a similar technique to Leissa [17]. Once the stress state had been determined the peak Von Mises stresses were calculated and treated as a stress raiser to calculate the fatigue life (see for example Shigley [31]). The fact that the loading is T-T is accounted for using the Goodman diagram technique (again, see Shigley [31]).

Raoof used a similar technique for his model to predict the fatigue life of large structural strands. The static model used as a basis of his fatigue model was the 'Orthotropic sheet' model developed by Raoof and Hobbs [32]. The results compared favourably with the experimental data for spiral strands in air and sea water from Tilley [33].

The model from Zhang and Costello [34] proceeds along similar lines as both Knapp and Raoof to demonstrate how the fatigue life of a 6/1 strand bent over a sheave can be predicted. The basis of their fatigue model is the curved rod model of rope developed by Costello and co workers [35]. No comparison was made with experimental results.

5.2.7 Discussion

The fact that there has been virtually no research carried out on fatigue in hoses indicates perhaps that for the vast majority of hose applications, fatigue is not a major problem. Often a hose will be discarded for other reasons (which have been discussed in Chapter 1) before it fails from mechanical fatigue.

The most relevant research work in the kind of fatigue seen in the hose of current interest seems to be in the field of wire ropes and strands. The two kinds of contact stress condition defined by Liessa[17] are relevant to hose. Two possible loading conditions between the wires of a strand are identified by as shown in Figure 5.4 (a) and (b) are identified by Starky and Cress [18]. In the case of the thermoplastic hose which is the subject of this work there is no need to assume one condition or the other since the combination of forces between wires of the same layer and between layer forces have been precisely calculated in the structural model of chapter 4.

Equally the two types of fretting condition identified by Blakeborough [22] will also be experienced in a hose. The work of Waterhouse seems to give a clear indication of the benefits of using lubrication to reducing fretting wear. Rope designers have long been aware of this benefit but there is no record in the literature of lubrication ever being introduced into a hose.

It seems that many of the analytical techniques developed in rope research could be used in a modified form for some types of wire hose.

5.3 Experience in polyflex fatigue failures

Polyflex hose, with operating pressures which exceed those dealt with in SAE standard[5] are not covered by any standard test method for fatigue. Additionally no machine is currently capable of delivering the pressure wave form specified in the low pressure standard shown Figure 5.1 (a). Polyflex has a built . . number of in house machines which can subject hose assemblies to a cyclic pressure. Although the exact nature of the pressure curve is not monitored, the shape of the curve tends to resemble a half sine wave. Results from fatigue tests are used to give an indication of the fatigue strength of a particular hose for in house design purposes. A short description of Polyflex hose fatigue behaviour of various hoses taken from the notes of a Polyflex Engineer, William Lees [36] is now given.

The usual manner in which a Polyflex hose will fail in fatigue is from a break up of wires on the first and second layers, this causes 'pits and spirals' in the inner core extruding into the gaps left by the broken wires. Many wire failures can occur before the hose fails, but equally the hose may fail because of the first wire failure 'puncturing' the inner core. One of the biggest problems in characterising the fatigue behaviour is the inconsistency in results; for example one hose may fail at 15,000 cycles with one wire failure (and one pit) while a similar hose may go up to 50,000 cycles with so many pits and spirals in the core that it is 'unbelievable that the hose lasted as long'.

Another cause of hose failure in fatigue is known as a 'slack wire' failure. The symptom of a slack wire failure is a large gash running perpendicular to the wires in the first reinforcement layer and is said to results from a loose wire in the second layer. This causes the wires on the first layer to break, presumably because of high local bending stresses.

Yet another cause of hose failure in fatigue is that of cracks developing in a particular type of Polyoxymethylene (P.O.M.) core. This causes the hose to fail in less than 2,000 cycles and seems to occur in around 20 % of the hoses made with this type of core; of this 20 %, three quarters will fail within 500 cycles!

The hose designers have found from experience that producing a hose which gets slightly shorter on pressurisation gives a better fatigue life. Additionally it has been found that smaller wire diameters on inner layers seems to give a better fatigue life.

5.4 Contact stresses in hose

It is evident from the mode of hose failure in fatigue that the break up of inner wires is the major initiating mechanism. The contact stresses between wires in the hose are likely to have a major influence on this wire break-up behaviour and for this reason the rest of this section is dedicated to calculating the contact stresses between wires for a number of possible hose designs and resulting wire to wire configurations.

5.4.1 Theoretical derivations

Expressions will now be derived for the critical stresses caused by contacting wires between two reinforcement layers. Three cases will be studied: the cross wire contract, which is closest to the actual hose configuration and a two hypothetical line contact cases. The first stage in determining the critical stress is to calculate the forces pushing the wires together. For the line contact case an expression for force per unit length of wire has already been derived as a halfway stage to calculating the interlayer pressure, The equation is

$$F_{L(1-2)} = \frac{P_{1-2} 2\pi R_2' \cos\alpha_2'}{N_2} \qquad \ldots(5.1)$$

R_2' is eliminated to put the equation in a suitable form to be easily calculated in the structural model developed in Chapter 4. giving the final form of the equations for the general case as:

$$F_{L(i-i+1)} = \frac{P_{(i-i+1)} 2\pi R_{i+1} (1+\varepsilon_z) \sin\alpha_{i+1}'}{N_{i+1} \tan\alpha_{i+1}} \qquad \ldots(5.2)$$

For the cross contact force the geometry of the crossing wires has to be taken into account to work out the length of wire between contact point, d_i* (see Figure 5.7) The expression is as follows:

$$d_1^* = \frac{d_1}{\cos \vartheta_{1-2}'} \qquad \ldots(5.3)$$

A new variable, $\theta_{1\text{-}2,}$' is introduced which takes into account the angles of wires in the two contacting layers. This is defined in Figure 5.7.

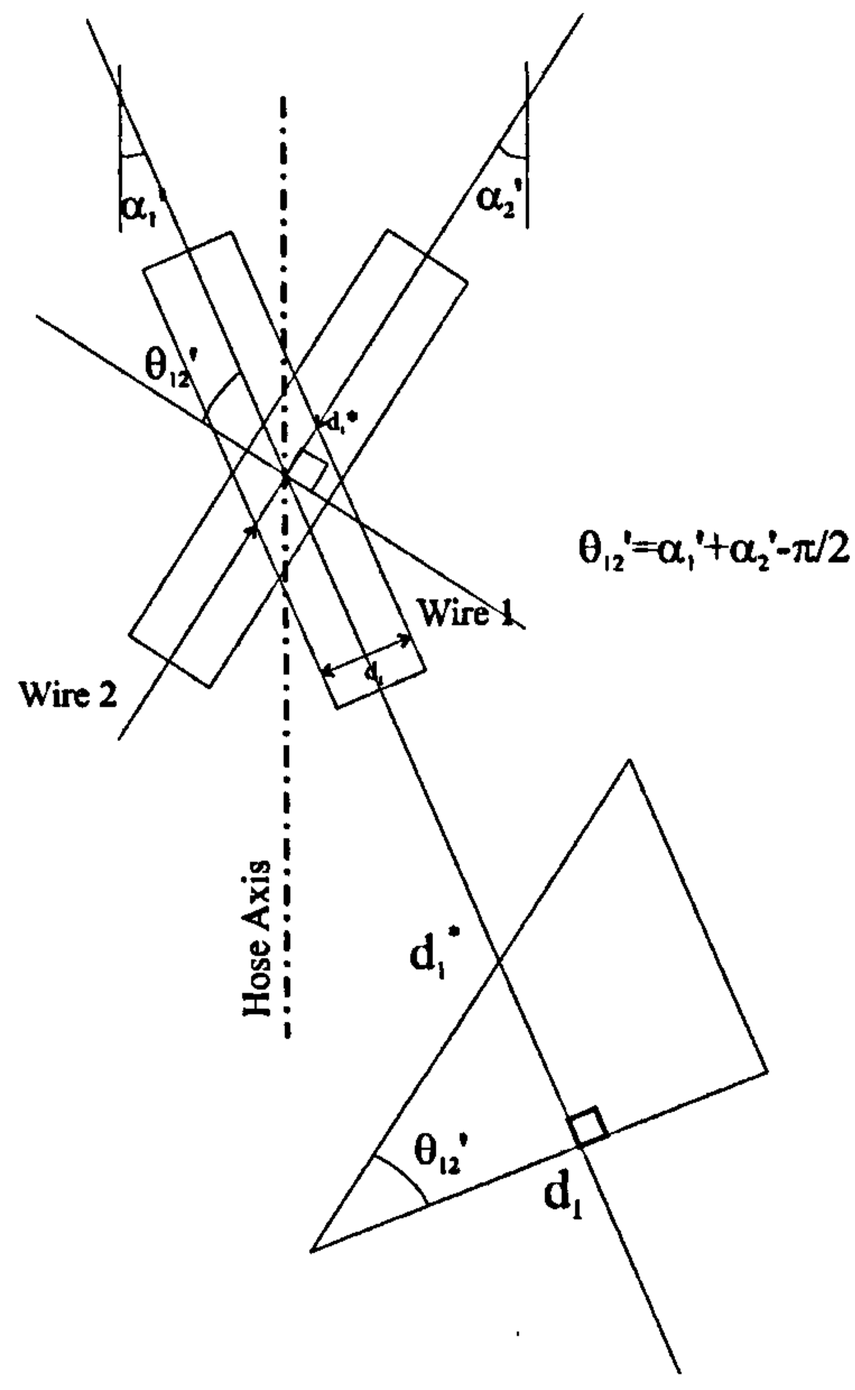

Figure 5.7. Cross contact geometry showing the length of wire d_i^* for one discrete contact point.

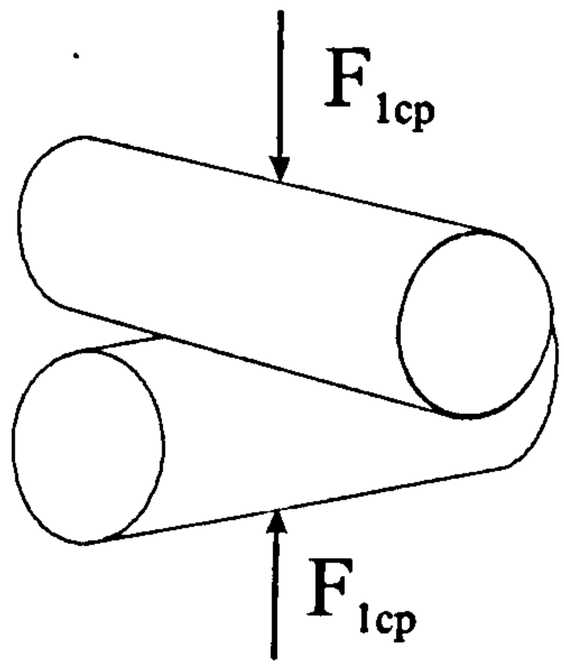

Figure 5.8. The configuration of the cross wire contact.

The force at each contact point is then the force per unit length along the wire multiplied by the length for one contact point, d^* :

$$F_{1CP} = F_L d^* \qquad \ldots(5.4)$$

Replacing the expression for F_L (i.e. Equation 5.2) yields:

$$F_{1CP(1-2)} = \frac{P_{1-2} 2\pi R_2 (1+\varepsilon_z) \sin \alpha_2' d_1}{N_2 \tan \alpha_2 \cos \vartheta_{1-2}'} \qquad \ldots(5.5)$$

The exact solution for stress distributions of various configurations of two cylindrical bodies in contact are given by the theory of Thomas and Hoersch [16]. Young [37] has conveniently tabulated simple expressions for the critical stresses of two conditions and these reduce to the following equation for line contact(where 6_c is the critical stress):

$$\sigma_c = 0.591 \sqrt{\frac{2F_L E}{d}} \qquad \ldots(5.6)$$

and for point contact:

$$\sigma_c = \frac{1.819 F_{1CP}}{\pi} \left[\frac{F_{1CP} d (1-\nu^2)}{E} \right]^{\frac{-2}{3}} \qquad \ldots(5.7)$$

The third contact scenario can be simply analysed as an extension to the hypothetical line contact case. The line contact case assumed that the crown of a wire in one layer would contact directly the crown of a wire in the next, but if the crown of one wire lies in the valley between two wires in the next then the contacting forces will be reduced by a factor of 1.73 as shown Figure 5.9.

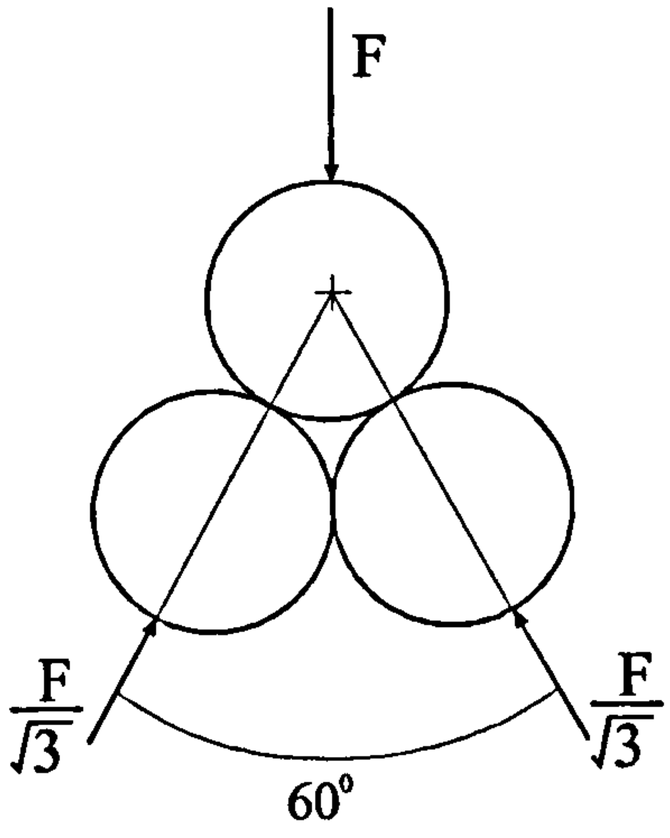

Figure 5.9. Reduced force (and therefore stress) caused by wire seating in an inter wire valley of an adjacent layer.

5.4.2 Contact stress predictions

The expressions for force and stress derived in the previous section can easily be evaluated by incorporating them into the structural model developed in Chapter 4. A few typical predictions of contact stresses are given in this section. Figure 5.10 shows the critical stresses for the three contact conditions: cross contact, crown to crown line contact and crown in valley line contact. It can be seen that the cross contact stresses are roughly three times higher than the crown to crown line contact. The high values of stress suggest that there must be some local yielding in the wires during pressurisation.

Figure 5.11 and Figure 5.12 show the variation in critical stress (as defined by Young [37]) caused by cross wire contact for the different interlayer conditions in a four and a six layer hose. It can be seen that the contact stresses gradually decrease for layers further out

in the hose and the contact stress between the outer two layers of reinforcement are roughly half of that between the inner two layers of reinforcement. Finally Figure 5.13 shows the decrease in interlayer pressure caused by the fact that the wires are squeezed together, i.e. it shows the interlayer pressure with and without the transverse compression expression in the radial equilibrium equation as used in the structural model of Chapter 4. This decrease will result in a proportionally similar decrease in the critical contact stress.

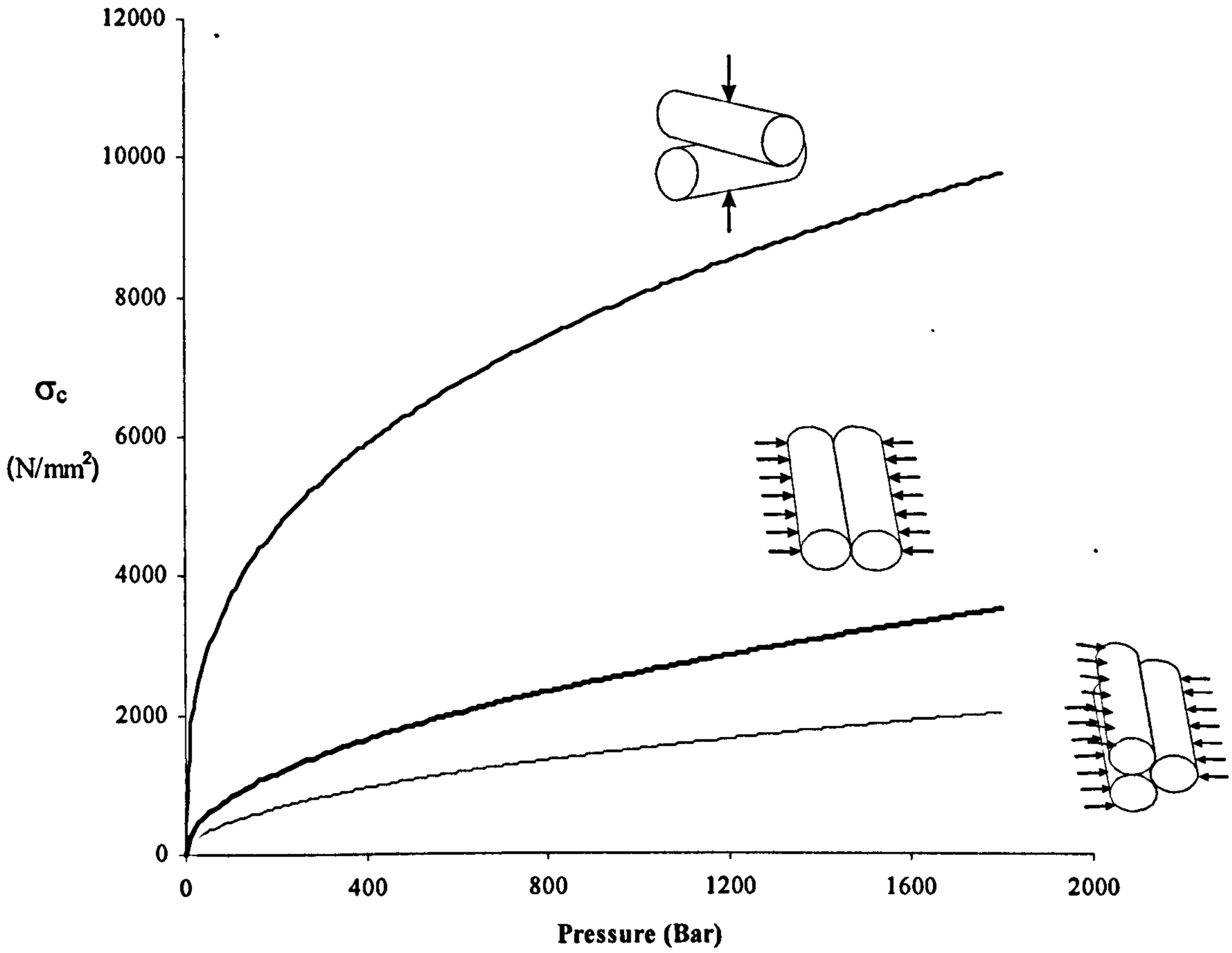

Figure 5.10. The critical stresses between wires of the firsts two layers of a hose for three different contact conditions (hose 2012).

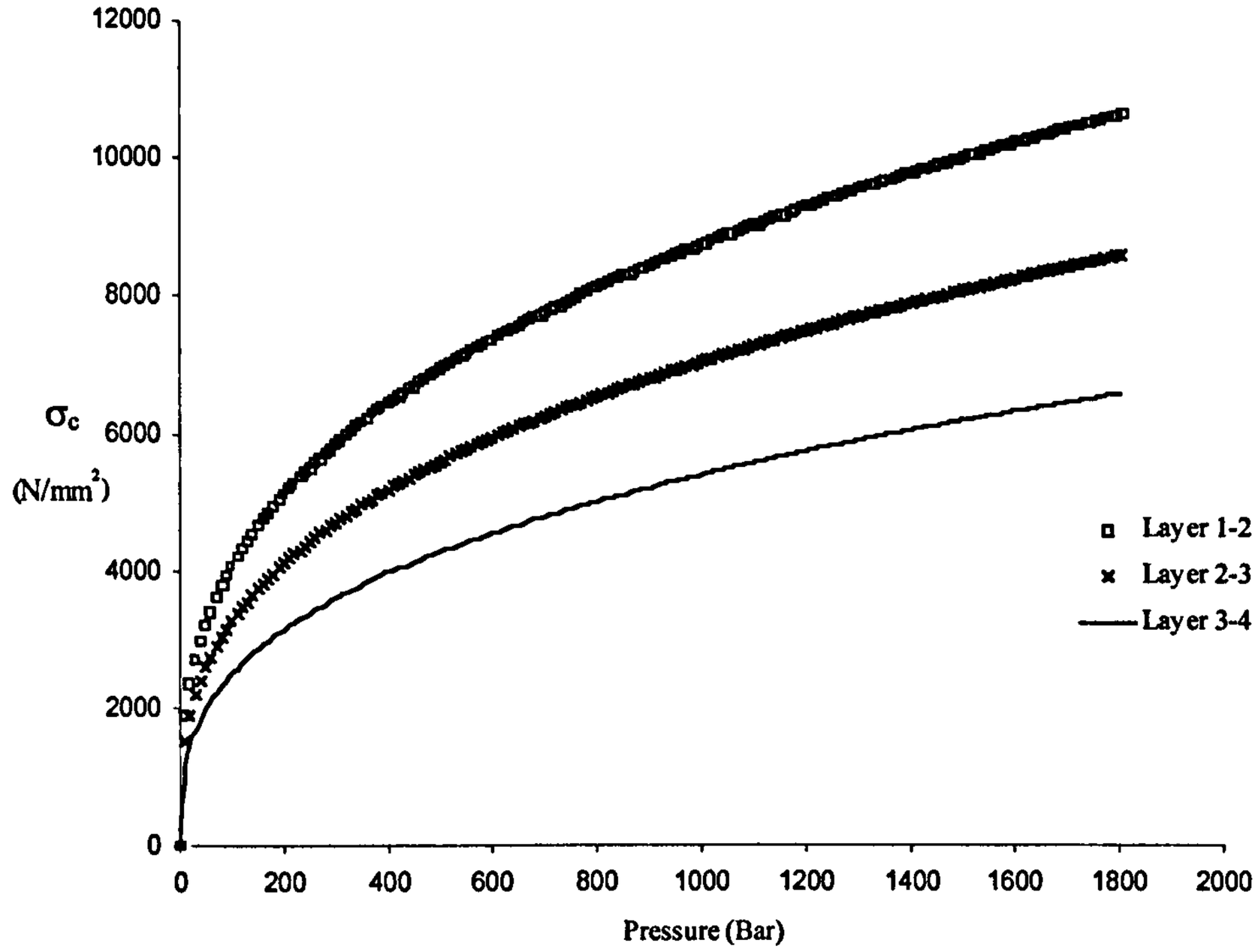

Figure 5.11. Critical interlayer contact stresses (resulting from cross wire contact points) calculated for hose 4012.

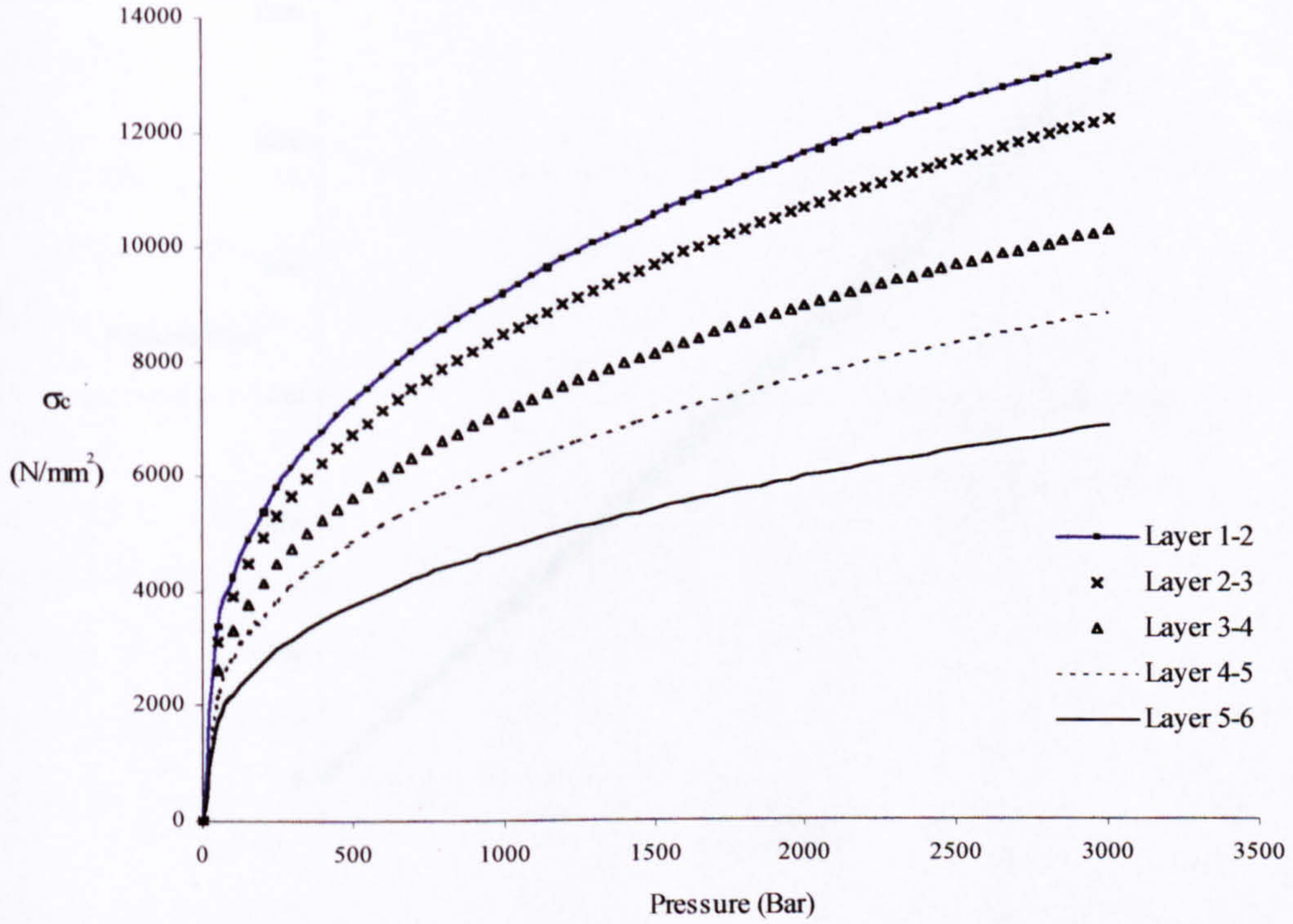

Figure 5.12. Critical inter-layer contact stresses (resulting from cross wire contact points) as calculated for hose 6005.

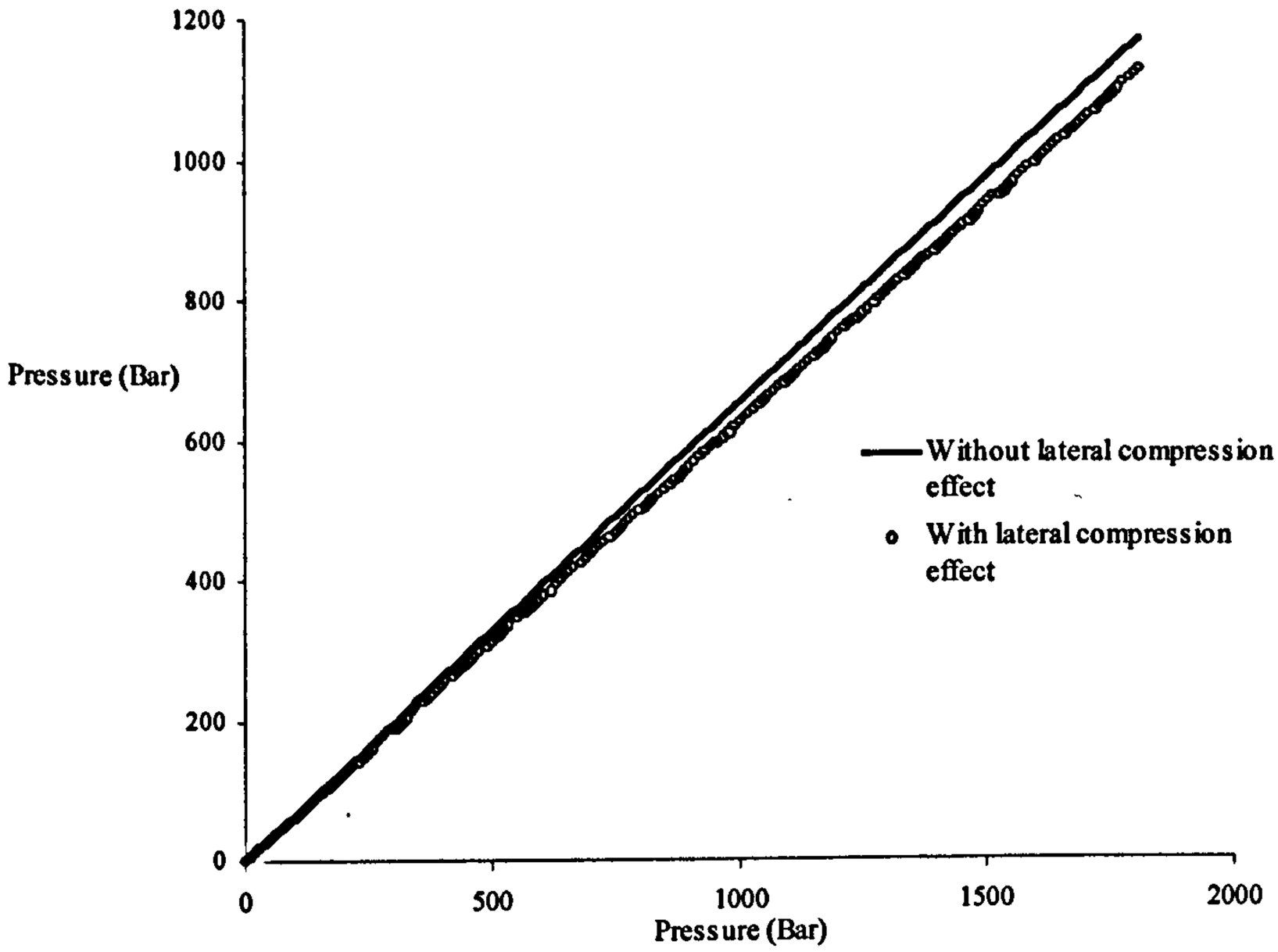

Figure 5.13. The effect of lateral compression on the interlayer pressures, theoretical calculation for hose 4012

5.5 Discussion and conclusions

What evidence there is indicates that the critical determining factor in Polyflex hose life is the break up of wires in the inner two layers. This break up will ultimately cause the inner core to be punctured and leak and this is why the fatigue life is so variable, since rather like a bicycle tyre puncture, it is impossible to predict when a puncture will occur. It is dependant on the stochastic nature of the geometry of an individual wire break.

Practical experience has demonstrated that a hose which gets slightly shorter will perform better in fatigue. With the help of the model developed it is possible to gain an insight into the possible reasons for this. Firstly there is a slight decrease in interlayer pressure as the wires bear a proportion of the pressure by being pressed together laterally. Secondly, there may be a decrease in the length for a wire needed to take up full tension beyond a break

(the effective length) because of the frictional forces between the adjacent wires in the same layer.

The 'slack wire' problem experienced in practice may well be worsened in the case of a hose which gets shorter. Since if layers are pressed together a slack wire is much more likely to get squeezed out of the layer which would then cause a gap on the other side of the layer. This would increase the bending on wires in adjacent layers.

There are a number of reasons why a smaller inner layer wire diameter could result in an increase in fatigue life. For example a smaller wire diameter would result in lower forces pressing each contact point together. Another reason is that a small broken wire is likely to allow less distortion of the inner core and therefore there will be less likelihood of a puncture

The predictions of contact stresses for the cross and line configurations show that a line contact (crown in valley) will generate approximately five times lower critical stresses. The extremely high contact stresses predicted for the cross wire condition is much higher than the yielding stress of the material and therefore there will be some level of local plastic deformation at the contact point resulting in a permanent indentation in the wire. The two indentations from wires in adjacent layers are likely to interlock as shown in Figure 5.14. This condition combined with the rotating movement around a contact point is likely to give an ideal environment for rapid fretting of the wire. This is borne out by the wire break up phenomenon observed in fatigue tests. In contrast, a line contact condition will not only produce a much lower stress resulting in less plastic deformation, but will also experience minimal relative movement between wires. Any movement there is will be longitudinal and therefore have much less local displacement at the point of contact. The difference in the types of relative movements for the two configurations would suggest that a line contact is likely to result in a bigger improvement in fatigue life than the difference in critical contact stresses would initially suggest.

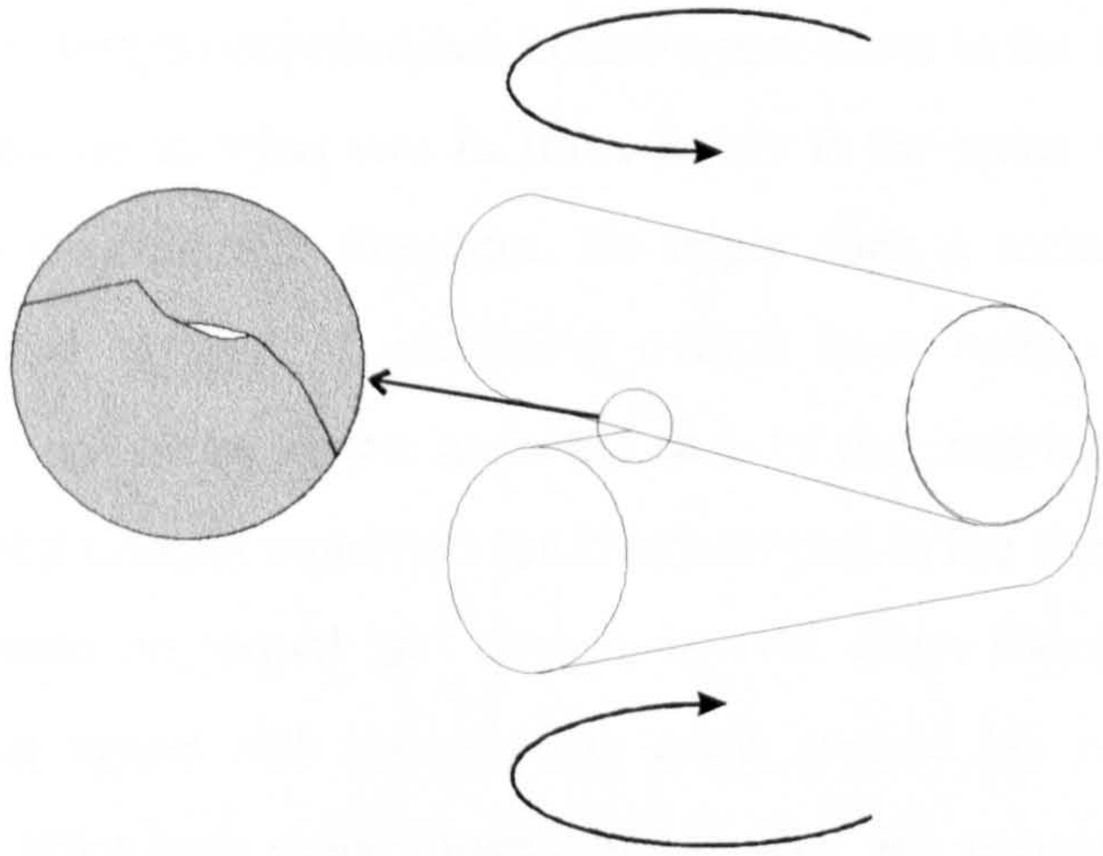

Figure 5.14. The problem of interlocking wire indentations coupled with the rotational rubbing between cross layers contributing to a rapid fretting of the wire as seen in fatigue tests.

Another aspect of the cross wire contact condition which is likely to be detrimental to the inner layer of wires is the fact that the core, in pressing the inner layer wire against the second layer is likely to cause very high local bending stresses at each cross point. This could explain the phenomenon of inner wires breaking into small pieces as sometimes observed in practice. There is likely to be a propagation of breaks along a wire as one break will increase the bending stress at the neighbouring interwire segment.

It would appear that a few simple design changes might greatly improve the fatigue life of the hose. If the first two, or possibly three reinforcement layers were wound in the same direction and with the same pitch then there should be a much lower incidence of wire breaks within these first few critical layers. The next two or three layers could then be wound in the opposite direction to balance the hose torsionally. The net result of this type of design would be that there may be only one or two cross contact inter layers and they would not be adjacent to the inner core. A plastic tube could be put between the critical cross wire contact layers to avoid the high contact stresses in these layers as a further improvement. This may not be necessary, however, as the most important consideration is to reduce the chances of the inner layers breaking and thus effectively puncturing the core. Wire breaks in the outer layers are much less critical.

The fairly radical hose design proposed has in fact a precedent in the field of strand design, where it is not uncommon to wind two or three layers in the same direction followed by the same number in the opposite direction. To apply such a technique in hose design would require a model capable of predicting overall hose twist, as making a torque balanced hose would not be as simple as in the case of the traditional alternate lay hose design. To gain the best contact condition for layers wound in the same direction, the hose design must incorporate an 'equal lay' design, i.e. the pitch should be kept the same between the different layers and the winding angle should be varied accordingly to facilitate this. This effectively cuts down the number of variables of choice when optimising the design of the hose: since once the winding geometry of the first layer is chosen the geometry of all subsequent layers in the same direction will then also be determined.

One very simple way in which the fatigue performance of the hose could be improved without any structural design changes would be to introduce a lubricant between the layers during the winding process (as is done commonly with ropes). The benefit of lubricant in reducing fretting wear has been demonstrated by McColl et al. [27].and can be see in Figure 5.6(b and c). However the compatibility of the lubricant with the thermoplastic elements in the hose would have to be investigated before it could be introduced.

5.6 References

1. Buzzelli, G., *Troubleshooting Hose Failures.* Plant Engineering, 1993. **October:** p. 64-68.

2. Briggs, J., *Causes and Prevention of Hose Failures.* Quality Management and Engineering, 1975. **May:** p. 16-19.

3. Reichel, J., *Im Impulstest Schluchleitungen und Leitungsverbindungen.* Fluid, Zeitshrift für Hydraulik, Pneumatik, Zubehör, 1977. **December.**

4. Anon, *Wire Braid Angle Response Characteristics in Hydraulic Hose.* SAE Technical Paper Series no972706, 1997. **1289:** p. 9-28.

5. SAE_J343, *Test and Procedures for 100R Series Hydraulic Hose and Hose Assemblies.* 1990.

6. SAE_J517, *Hydraulic Hose*,. 1986.

7. Evans, C.W. and T.R. Manley, *Factors Affecting the Impulse Testing of Hydraulic Hose.* Polymer Testing, 1986. **6**: p. 135-149.

8. SAE_J1405, *Optional Impulse Test Procedures for Hydraulic Hose Assemblies.* 1990.

9. Evans, C.W., *Hose Technology.* 1974: Applied Science Publishers.

10. Berns, H.D., *Cumulative Damage Analysis for Hydraulic Hoses.* SAE Technical Paper Series, 1986. **861297**: p. 5.121-5.143.

11. Berns, H.D., O.R. Linger, and R.J. May, *SAE Test Program on Cumulative Damage for Hydraulic Hose Assemblies.* SAE Technical Paper Series, 1988. **880713**: p. 5.136-5.152.

12. Palmgren, A., *Die Lebensdauer von Kugellagern.* Zeitshrift Vereines Deutscher Ingenieure, 1924. **68**: p. 339-341.

13. Miner, M.A., *Cumulative Damage in Fatigue.* Journal of Applied Mechanics, 1945. **September**: p. 159-164.

14. Potts, A.E., C.R. Chaplin, and N.R.H. Tantrum. *Factors influencing the Endurance of Steel Wire Ropes for Mooring Offshore Structures.* in *Proceedings of the 20th annual OTC conference*. 1988. Housten.

15. Jones and Schott, *H Hertz- Micellaneous Papers 1895: English Translation.* 1985, London: Macmillon.

16. Thomas, H.R. and V.A. Hoesch, *Stresses due to the Pressure of one elastic body on another.* Engineering Experiment Station, University of Illinois Bulletin No.22, 1930. **27**(46).

17. Leissa, A.W., *Contact Stresses in Wire Ropes.* Wire and Wire Products, 1959. **34**: p. 307-314 and 372-373.

18. Starkey, W.L. and H.A. Cress, *An Analysis of Critical Stresses and Mode of Failure of Wire Rope.* Journal of Engineering for Industry, 1959. **81**: p. 307-316.

19. Hruska, F., *Radial Forces in Wire Ropes.* Wire and Wire Products, 1952. **27**(5): p. 459-463.

20. Hruska, F.H., *Calculation of Stresses in Wire Ropes.* Wire, 1951(September): p. 766-801.

21. Ligeris, P., *Assessment of the role of Contact Fatigue in the failure of steel Roping Wires.* Wire Journal International, 1994(January): p. 60-67.

22. Blakeborough, A. and M.S.G. Cullimore. *Fretting in the fatigue of wire ropes.* in *Proceedings of the 6th international conference on fracture (Fracture '84).* 1984. New Delhi, India.

23. Waterhouse, R.B., *Fretting and Fretting Fatigue of High Tensile Steels in Marine Environments*,. 1987, University of Nottingham, Department of Metallurgy and Materials Science.

24. Waterhouse, R.B., *et al.*, *Fretting Wear of High Strength Heavily Work Hardened Eutectoid Steel.* Wear, 1994. **175**: p. 51-57.

25. Smallwood, R. and R.B. Waterhouse, *Residual Stress Patterns in Cold Drawn Steel Wires and their effect on Fretting- Corrosion- Fatigue Behaviour in Seawater*, in *Applied Stress Analysis*, T.H. Hyde and E. Olderon, Editors. 1990, Elsevier Applied Science. p. 82-90.

26. Pearson, B.R., P.A. Brook, and R.B. Waterhouse, *Fretting in Aqueous Media, Particlarly of Roping Steels in Seawater.* 106, 1985: p. 225-260.

27. McColl, I.R., *et al.*, *Lubricated Fretting Wear of a High Strength Eutectoid Steel Rope Wire.* Wear, 1995. **185**: p. 203-212.

28. Takeuchi, M. and R.B. Waterhouse. *Fretting- Corrosion-Fatigue of High Strength Steel Roping Wire and Some Protective Measures.* in *EVALMAT 89- International Conference on Evaluation of Materials Performance in Severe Environments.* 1989. Kobe, Japan: The Iron and Steel Institute of Japan.

29. Knapp, R.H. *Axial Fatigue Model for Wire Rope Strand.* in *Proceedings of the ASCE Structures Congress, Materials and Material Behaviour.* 1987. Orlando.

30. Knapp, *Derivation of a New Stiffness Matrixc For Helically Armoured Cables Considering Tension and Torsion.* International Journal for Numerical Methods in Engineering, 1979. **14**: p. 515-529.

31. Shigley, J.E. and C.R. Mischke, *Mechanical Engineering Design.* 5th ed. 1989: McGraw-Hill International. 779.

32. Raoof, M. and R.E. Hobbs, *Analysis of Multilayered Structural Cables.* Journal of Engineering Mechanics, 1988. **114**(7): p. 1166-1182.

33. Tilley, G.P. *Performance of bridge cables.* in *1st Oleg Kerensky Memorial Conference.* 1988. London: ISE.

34. Zhang, Z. and G.A. Costello, *Fatigue Design of Wire Rope.* Wire Journal International, 1996. **February**: p. 106-112.

35. Costello, G.A., *Theory of Wire Rope*. 1st ed. Mechanical Engineering. 1990, New York: Springer-Verlag. 106.

36. Lees, W., *Unpublished notes on the fatigue performance of various Polyflex Hoses.* 1995.

37. Young, W.C., *Roark's Formulas for Stress and Strain.* 1989: McGraw-Hill.

6. Conclusions and future work

6.1 Summary of findings

6.1.1 The effect of wire breaks on local strain variations and effective length

In Chapter 2, the effect of wire breaks on local strain variations revealed a number of interesting points. The transient nature of effective length was demonstrated, for example in one test it was seen to slowly increase up to 20,000 load cycles after the actual wire break had occurred. Some dependence of the effective length on load was found and wire slippage was observed within the fatigue load range. A considerably longer effective length in Ordinary Lay ropes was found, compared to the equivalent Lang's Lay construction. These findings emphasise the limitations of using breaking load as a means to measure the effective length. Such a technique will not account for either the transient effect of load cycling or the dependence of the effective length on load. It is therefore likely to give a much lower effective length than actually exists. This may ultimately result in an over optimistic prediction of residual strength.

6.1.2 Strain distribution and fatigue life

The work described in Chapter 3 investigated wire strain variations in normal and overloaded ropes. It was shown that considerable wire strain variations occur in ropes both on different wires at the same cross section and on the same wire along its length. The variation of strains on different wires at the same cross section was greater than the variation of strain along the length of a wire. Greater strain variation was found for Lang's Lay rope than for the equivalent Ordinary Lay construction. Overloading a rope to 80 % of its breaking load significantly reduced the variation in the strain distributions both around the same circumference and along the length of a wire. Since overloading also significantly increases fatigue life, this suggests a link between wire strain distribution and

fatigue life. This effect is predicted from a fatigue model based on the statistical distribution of wire strains before and after overload.

These findings have some important implications. A measure of the manufacturing 'quality' of a rope can be gauged in terms of the wire strain distribution by a single factor given by the standard deviation as a percentage of mean. The variation in strain distribution will have a negligible effect on the UBL since the strain variations will even out before failure. Hence the T-T fatigue life of a rope cannot be inferred from the rope UBL.

6.1.3 Modelling the static behaviour of high pressure hose

A new structural model of hose, which incorporates Hertzian contact theory between wires and a compressible core based on Lamé.'s thick walled cylinder theory has been developed. The model shows good agreement with experimentally measured axial strain and reinforcement wire strain in a pressurised hose.

Significant hysteresis was observed in the hose axial strain and it has been suggested that this phenomenon may provide an indication of the amount of relative wire movement between layers. It is suggested that the level of hysteresis may be a good indication of the level of fretting taking place.

Significant variations have been seen between the strains measured on individual outer reinforcement wires. It was also suggested that as in the rope, the level of strain distribution may reflect the manufacturing quality of the hose, although this has not yet been experimentally proved.

6.1.4 Fatigue of thermoplastic wire hose

The failure of the hose in fatigue is caused by the break up of wires on the inner layer which will subsequently puncture the core and cause a leakage failure. Large variability is seen in hose fatigue performance and this has been attributed to the random nature of whether an inner wire failure will cause a core puncture or not. Hence, the most important

factor to improve the fatigue performance of this type of hose is to prevent wire failures in the inner layer and thus avoid core puncture failures.

One possible method of improving the fatigue life of this type of hose would be to use a construction where there was line rather than point contact between the wires in the innermost reinforcement layer and those of the next layer. Theoretical calculations for the contact stresses between wires in different layers indicate that this could lead to a decrease in critical stresses by a factor of five.

6.2 General discussion

A number of general comparisons and similarities between rope and hose performance are of interest and these are discussed in this section.

There is an absence of research into the fatigue behaviour of hose, compared to the abundance of work which has been performed on rope and strands. There are a number of reasons for this difference. Firstly it is seen that a large proportion of ropes used are in safety critical applications where failure may result in the loss of life. In contrast, the failure of hose in many applications will only result in a machine being put out of action until the hose is replaced. Another point is that the vast majority of hose designs have intermediate layers of rubber between reinforcement. Such a design will have a relatively low critical stress in fatigue and is likely to be replaced for some other reason, such as outer cover wear, before it fails through fatigue. The Polyflex hose is unusual because of its direct wire to wire contact and the design reflects a relatively recent demand for very high pressure bearing pipe with a limited degree of flexibility.

One common theme throughout this thesis is the inadequacy of using static breaking value as an indication of fatigue performance. Because of the relative ease of gaining a static breaking load value it is easy to see the attraction in trying to use it to infer fatigue properties. The maximum allowable working pressure of a hose is calculated directly from burst pressure and improvements in hose design have focused on improving burst performance with the assumption, presumably, that this improvement will correspond to a

similar improvement in the fatigue performance. As discussed in Chapter 5 the key factors in determining the fatigue performance of the hose are the wire to wire contact and fretting condition and these cannot be determined from the burst pressure. It has been suggested that the level of hysteresis may give an indication of the amount of fretting that will take place. If this is verified, hysteresis could provide a prediction of hose fatigue behaviour and the data could be derived from an easily measurable property of the hose.

In rope, breaking strength is also proposed as a possible test method for assessing the integrity of a rope in service (by testing a sample taken from the end of the rope). But the findings in effective length in this thesis suggest that this may be an inappropriate technique: The take up of load after a wire break has been shown to change considerably with cyclic loading and also to be sensitive, to some extent, to the applied load; neither of these factors will be reflected in a simple rope break test. It has also been shown that a ropes endurance in T-T fatigue is dependant on the wire strain variation within the rope. Clearly a breaking test will not be sensitive to this phenomenon, since a rope must be 'overloaded' for it to fail in tension and any initial differences in wire strain variation among ropes will thus be eliminated.

An interesting comparison can be made between the mechanism of degradation as seen in ropes to that seen in hoses. In the case of a rope, the rope gradually degrades through an increasing number of wire breaks throughout the structure. The ultimate failure of the rope comes when the cumulative effect of the wire breaks leads to the catastrophic breakage of the rope. The degradation of the hose begins in a similar fashion, with wire breaks occurring throughout the hose. However, because the function of a hose is concerned primarily with pressure containment, the ultimate failure occurs through fluid leakage when a broken wire punctures the core. The point at which such a failure occurs is much more random than the failure seen in rope and leads to a large variation in the fatigue life of nominally identical hoses. This failure occurs long before the ultimate catastrophic load bearing failure of the reinforcement would have occurred. Consequently designing for fatigue in hose must concentrate on avoiding punctures of the core rather than optimising the load bearing fatigue of the wire structure as is the case in ropes.

Chapter 3 has demonstrated the importance of wire strain variations in determining the fatigue life of a rope. The limited amount of data in Chapter 4 suggests that there is also some level of wire strain distribution within a hose. From the experience of failures of hose in fatigue however, it seems that failure will not be as closely correlated to the level of wire strain distribution as it is in ropes. Experience with 'slack wire' failures suggests that a hose may be more sensitive to the odd wire with very low strain than to the overall strain distribution. The reason for this is likely to be related to the extremely high contact forces between reinforcement layers. A slack wire in one layer will result in a loss in support of the wires in the next layer (on the inside) over the region of the slack wire and this will lead to high bending stresses in the wire at this location. This effect combined with the increased contact stresses at the two neighbouring wire seating points and additional fretting will to cause the premature failure of the wire at this location. It is suggested that a parallel wire configuration of crucial layers would avoid this problem.

6.3 Future work

6.3.1 Development of a better strain distribution model for fatigue failure in rope

There are a number of ways the simple strain distribution model used in Chapter 3 can be improved. Presently it only considers an element of rope and does not consider the effect of axially spaced wire breaks and their interaction. This effect could be incorporated into the model in the following way: given that the strain distribution both around a rope and along the length of a wire is known then a hypothetical distribution for a given length of rope can be imposed. The model can assume that the strain varies in steps along the length of a wire, with a step occurring at every strand lay length. Once the total distribution has been calculated then the hose is numerically taken to the first breaking point from the most highly stressed wire in a similar way to that used in the original model. However once the wire has broken, the effective length (either assumed or measured) can then be used to calculate the interacting effects of the breaks at the various axial locations. The model can then

continue stepping through the solution until a particular axial location reaches the failure criterion which can be based on the effective length and the number of wire breaks.

6.3.2 More comprehensive wire strain distribution investigation

The wire strain distribution experimental techniques developed in this thesis can be extended to investigate a much wider range of rope designs and manufacture. The relative importance of the two stages of stranded rope manufacture could also be investigated by looking at strain variations in strands before they are closed into a rope and comparing this with strands within a rope. Additionally work could be carried out to try to correlate some easily measurable aspect of rope behaviour with the wire strain variation. Two possible candidates which could be investigated ··· are the rope stiffness and the rope hysteresis.

6.3.3 Improvements to the hose model

There are a number of improvements and additions which could be made to the hose structural model, notably the following:

- Improvement of the radial compatibility relationships to include the contraction of the wires because of their axial strain. Improved modelling of the radial movements between layers caused by interlayer contact forces- this could also include the permanent indentation in the wire caused by the high contact stresses (see [1] for a related phenomenon).

- The bending and torsional stresses in the wires could also be included into the axial and radial equilibrium equations using the expression derived by Love[2] for the torsional and bending strains based on the changes in helix geometry.

- A torsional equilibrium equation could be incorporated into the model to enable the prediction of hose twist; this could use a similar theory to that developed by Machida. and Durelli [3] for strands. The effect of the outer cover could be introduced into the model, Although this is likely to have a small effect.

6.3.4 Experimentation with new hose designs

There are a number of design modifications which the hose manufacturer could investigate to try and improve the fatigue performance of the hose. As has already been suggested in Chapter 5 a hose which winds two or more adjacent layers in the same direction (and then the same number in the opposite direction) will have greatly reduced contact stresses and wire on wire movements. Other improvements in hose performance could be achieved by having a more consistent winding process which eliminates the possibility of a slack wire. Finally the introduction of a lubricant is likely to greatly increase the hoses fatigue performance, but the chemical effect on the inner core and outer cover must be considered.

6.4 References

1. Knapp, R.H. and W.H. Chan, *The Effect of Wire Indentation on Cable Rotation.* International Journal of Offshore and Polar Engineering, 1994. 4(4): p. 340-345.

2. Love, A.E.H., *A Treatise on the Mathematical Theory of Elasticity.* 1944: Dover.

3. Machida, S. and A.J. Durelli, *Response of a Strand to Axial and Torsional Displacements.* Journal of Mechanical Engineering Science, 1973. **15**(4): p. 241-251.

A. Appendix - rope and hose data

A.1 Rope data

Two ropes were used in this work: the first was a 19 mm six strand Ordinary Lay rope i.e. 6x19(9/9/1) RHOL with IWRC and the second was the same rope in Lang's Lay. The breaking load of the wires used in these rope was 1770 MPa. All the geometrical details of the rope constructions can be found in Table A.2 to Table A.4. T his data was derived from a complete strip down and measurement of a section of rope with a micrometer, angles were calculated from the winding radius and the relevant lay length. The nomenclature of the variables is given in Table A.1.

Table A.1. The nomenclature used for the rope geometry.

Term	Description
N,D and A	number, diameter and cross sectional area of a particular wire group
LL_r and LL_s	rope and strand lay lengths respectively
R_r and R_s	rope and strand winding radius.
α_r and α_s	rope and strand lay angles.

Table A.2. The details of the main strands of the rope.

rope diameter	19 2									
						strand diameter	6.3			
label	breakdown	N	D (mm)	A (mm^2)	LL_r. (mm)	LL_s (mm)	R_r (mm)	R_s (mm)	α_r (Degress)	α_s (Degress)
main wires	(6x9)	54	1.5	1.77	140	50	6.45	2.4	16.14	16.78
sub wires	(6x9)	54	0.8	0.50	140	50	6.45	1.15	16.14	8.22
king wire	(6x1)	6	1 5	1.77	140	0	6 45	0	16 14	

Table A.3. The details of the strands of the independent wire rope core (IWRC).

rope dia.	7 8									
						strand diameter	2.3			
label	breakdown	N	D (mm)	A (mm^2)	LL_r. (mm)	LL_s (mm)	R_r (mm)	R_s (mm)	α_r (Degress)	α_s (Degress)
main wire	(6x6)	36	0.75	0.44	56	16	2.55	0.775	15.97	16.93
king wire	(6x1)	6	0 8	0 50	56	0	2 55	0	15 97	0.00

Table A.4. The details of the central strand.

diameter	2 8									
label	breakdown	N	D (mm)	A (mm^2)	LL_r. (mm)	LL_s (mm)	R_r (mm)	R_s (mm)	α_r (Degress)	α_s (Degress)
main wires	6	6	0.9	0.64	0	18.8	0	0.95	0	16.78
king wire	1	1	1	0 79	0	0	0	0	0	0 00

A.2 Hose data

This section includes all the data for the various hose types modelled in Chapter 4. All the data was derived from information supplied by the manufacturer. The nomenclature used here is the same as that used in the Chapter 4. Additionally, although the data is not used in this thesis the average breaking strengths of the wires used in the various hose constructions are given in Table A.5.

Table A.5. The average strength properties of the wires used in the hose construction.

Diameter (mm)	Average Breaking strength (MPa)
0.22	3400
0.3	2900
0.35	2700
0.4	2900
0.43	3150
0.5	2600
0.56	2600
0.6	2600
0.65	2600
0.71	2600

A.2.1 Two layer hose

Table A.6. Details of all the 2 layer hose inner core properties, dimensions and the hose burst pressure, POM is a Polyoxymethylene, PA is a synthetic Polyamid and PEE is a Polyethylene.

Hose	material	R_0 (mm)	R_1 (mm)	ν_{ic}	E_{ic} (MPa)	Burst (Bar)
2004str	POM	2	2.65	0.4	2900	2950
2006st	PA12	3.15	4.15	0.47	350	2100
2006str	POM	3.15	4.05	0.4	350	2250
2008st	PA12	4.1	4.3	0.47	350	2000
2008str	POM	4	5	0.4	2900	2150
2010st	PA12	5	6.25	0.47	350	1650
2210st	PEE 5556	4.85	6.1	0.47	350	1500
2012st	PEE5556	6.4	7.55	0.47	350	1400
2020st	PA12	9.9	11.4	0.47	350	1350
2220st	PEE 5556	9 7	11.2	0 47	350	1200

Table A.7. Reinforcement layer geometry and properties of all the two layer hose constructions.

	Layer 1						Layer 2					
Hose	R_1 (mm)	N_1	A_1 (mm^2)	D_1 (mm)	E_1 (MPa)	α_1 Degrees	R_2 (mm)	N_2	A_2 (mm^2)	D_2 (mm)	E_2 (MPa)	α_2 Degrees
2004str	2.65	32	0.071	0.3	210000	56.9293	2.95	35	0.071	0.3	210000	57.3794
2006st	4.15	52	0.071	0.3	210000	54.7322	4.45	54	0.071	0.3	210000	55.9095
2006str	4.05	42	0.096	0.35	210000	56.3756	4.4	46	0.096	0.35	210000	55.9382
2008st	4.3	53	0.096	0.35	210000	48.7202	4.65	55	0.096	0.35	210000	50.5822
2008str	5	45	0.126	0.4	210000	56.5698	5.4	49	0.126	0.4	210000	56.1485
2010st	6.25	58	0.126	0.4	210000	55.0778	6.65	60	0.126	0.4	210000	56.1084
2210st	6.1	56	0.126	0.4	210000	55.5363	6.5	58	0.126	0.4	210000	56.5572
2012st	7.55	70	0.126	0.4	210000	54.8996	7.95	71	0.126	0.4	210000	56.3167
2020st	11.4	70	0.283	0.6	210000	55.1573	12	72	0.283	0.6	210000	56.0145
2220st	11 2	70	0.283	0 6	210000	54 4607	11.8	72	0 283	0 6	210000	55.3736

A.2.2 Four layer hose

Table A.8. Details of all the 4 layer hose inner core properties, dimensions and the hose burst pressure, for material abbreviations see Table A.6.

Hose	material	R_0 (mm)	R_1 (mm)	ν_{ic}	E_{ic} (MPa)	Burst (Bar)
4005st	POM	2.4	3.65	0.4	2900	4500
4006st	PA12	3.15	4.05	0.47	350	3500
4008st	POM	4	5	0.4	2900	3750
4010st	PA12	5	6.25	0.47	350	3500
4012st	PA12	6.4	7.65	0.47	350	3250
4020st	PA12	9.7	11.2	0.47	350	2500
4025st	PA12	12 5	14.5	0.47	350	2250

Table A.9. Reinforcement layer geometry and properties of the first two layers of all the four layer hose constructions.

	Layer 1						Layer 2					
Hose	R_1 (mm)	N_1	A_1 (mm^2)	D_1 (mm)	E_1 (MPa)	α_1 Degrees	R_2 (mm)	N_2	A_2 (mm^2)	D_2 (mm)	E_2 (MPa)	α_2 Degrees
4005st	3.65	37	0.096	0.35	210000	57.3954	4	39	0.096	0.35	210000	58.6442
4006st	4.05	42	0.096	0.35	210000	56.3756	4.4	46	0.096	0.35	210000	55.9382
4008st	5	44	0.126	0.4	210000	57.4063	5.4	48	0.126	0.4	210000	56.9293
4010st	6.25	42	0.246	0.56	210000	55.0228	6.81	44	0.246	0.56	210000	56.4191
4012st	7.65	48	0.283	0.6	210000	54.7910	8.25	49	0.283	0.6	210000	56.8201
4020st	11.2	84	0.332	0.65	210000	41.0619	11.85	87	0.332	0.65	210000	42.3335
4025st	14 5	74	0.396	0.71	210000	55.7428	15 21	76	0.396	0 71	210000	56 5128

Table A.10. Reinforcement layer geometry and properties of the 3rd and 4rth layers of all the four layer hose constructions.

	Layer 3						Layer 4					
Hose	R_3 (mm)	N_3	A_3 (mm^2)	D_3 (mm)	E_3 (MPa)	α_3 Degrees	R_4 (mm)	N_4	A_4 (mm^2)	D_4 (mm)	E_4 (MPa)	α_4 Degrees
4005st	4.35	53	0.071	0.3	210000	55.7817	4.65	56	0.071	0.3	210000	56.1485
4006st	4.75	49	0.096	0.35	210000	56.3434	5.1	52	0.096	0.35	210000	56.6932
4008st	5.8	51	0.126	0.4	210000	57.2396	6.2	56	0.126	0.4	210000	56.1485
4010st	7.37	51	0.196	0.5	210000	57.8184	7.87	55	0.196	0.5	210000	57.3837
4012st	8.85	64	0.246	0.56	210000	51.3350	9.41	66	0.246	0.56	210000	52.6231
4020st	12.5	89	0.283	0.6	210000	48.3963	13.1	93	0.283	0.6	210000	48.4901
4025st	15 92	84	0.332	0 65	210000	57.6612	16 57	87	0.332	0 65	210000	57 8110

A.2.3 Six layer hose

Table A.11. Details of all the 6 layer hose inner core properties and the hose burst pressure for material abbreviations see Table A.6.

Hose	material	R_0 (mm)	R_1 (mm)	ν_{ic}	E_{ic} (MPa)	Burst (Bar)
6005st	POM	2.4	3.65	0.4	2900	6250
6008st	POM	4	5	0.4	2900	5250
6012st	PA12	6.4	7.65	0.47	350	4500
6020st	PA12	9.7	11 2	0 47	350	3500

Table A.12. Reinforcement layer geometry and properties of the first two layers of all six layer hose constructions.

	Layer 1						Layer 2					
Hose	R_1 (mm)	N_1	A_1 (mm^2)	D_1 (mm)	E_1 (MPa)	α_1 Degrees	R_2 (mm)	N_2	A_2 (mm^2)	D_2 (mm)	E_2 (MPa)	α_2 Degrees
6005st	3.65	37	0.096	0.35	210000	57.3954	4	39	0.096	0.35	210000	58.6442
6008st	5	24	0.126	0.4	210000	72.9129	5.4	25	0.126	0.4	210000	73.4887
6012st	7.65	47	0.283	0.6	210000	55.6290	8.25	48	0.283	0.6	210000	57.5814
6020st	11.2	64	0 332	0 65	210000	54 9370	11.85	66	0.332	0 65	210000	55 8888

Table A.13 Reinforcement layer geometry and properties of the 3rd and 4rth layers of all six layer hose constructions.

	Layer 3						Layer 4					
Hose	R_3 (mm)	N_3	A_3 (mm^2)	D_3 (mm)	E_3 (MPa)	α_3 Degrees	R_4 (mm)	N_4	A_4 (mm^2)	D_4 (mm)	E_4 (MPa)	α_4 Degrees
6005st	4.35	53	0.071	0.3	210000	55.7817	4.65	56	0.071	0.3	210000	56.1485
6008st	5.8	61	0.126	0.4	210000	49.6669	6.2	64	0.126	0.4	210000	50.4598
6012st	8.85	62	0.246	0.56	210000	52.7537	9.41	63	0.246	0.56	210000	54.5873
6020st	12 5	74	0.283	0 6	210000	56 4909	13 1	76	0.283	0 6	210000	57 2072

Table A.14. Reinforcement layer geometry and properties of the 5th and 6th layers of all six layer hose constructions.

	Layer 5						Layer 6					
Hose	R_5 (mm)	N_5	A_1 (mm^2)	D_5 (mm)	E_5 (MPa)	α_5 Degrees	R_6 (mm)	N_6	A_6 (mm^2)	D_6 (mm)	E_6 (MPa)	α_6 Degrees
6005st	4.95	58	0.071	0.3	210000	57.1120	5.25	62	0.071	0.3	210000	56.7564
6008st	6.6	76	0.126	0.4	210000	44.6416	7	80	0.126	0.4	210000	44.9799
6012st	9.97	69	0.196	0.5	210000	57.5024	10.47	72	0.196	0.5	210000	57.6916
6020st	13.7	92	0 246	0.56	210000	54.0890	14.26	93	0 246	0 56	210000	55 2450

A.2.4 Eight layer hose

Table A.15. Inner core properties of hose 8005 and hose burst pressure.

material	R_0 (mm)	R_1 (mm)	ν_{ic}	E_{ic} (MPa)	Burst (Bar)
POM	2.25	3.5	0.4	2900	7440

Table A.16. Reinforcement layer geometry and properties of all the reinforcement layers of Hose 8005.

	R_i (mm)	N_i	A_i (mm^2)	D_i (mm)	E_i (MPa)	α_i Degrees
Layer 1	3.5	19	0.210	0.3	210000	54.5541
Layer 2	3.8	20	0.210	0.3	210000	55.6606
Layer 3	4.1	53	0.071	0.3	210000	53.4569
Layer 4	4.4	56	0.071	0.3	210000	54.0096
Layer 5	4.7	58	0.071	0.3	210000	55.1808
Layer 6	5	62	0.071	0.3	210000	54.9135
Layer 7	5.3	63	0.071	0.3	210000	56.5004
Layer 8	5.6	68	0.071	0.3	210000	55.6217